UAH/CEE-TR-97-05

October 1997

Analytical Modeling of Pressure Wall Hole Size and Maximum Tip-to-Tip Crack Length for Perforating Normal and Oblique Orbital Debris Impacts

By: William P. Schonberg
Civil & Environmental Engineering Department
University of Alabama in Huntsville
Huntsville, Alabama 35899

and

Essam Mohamed
Mechanical & Aerospace Engineering Department
University of Alabama in Huntsville
Huntsville, Alabama 35899

Final Report For: Period 01 April 1995 to 31 July 1997
Contract NCC8-28

Prepared For: NASA/Marshall Space Flight Center
Huntsville, Alabama 35812

CIVIL & ENVIRONMENTAL ENGINEERING DEPARTMENT
UNIVERSITY OF ALABAMA IN HUNTSVILLE
HUNTSVILLE, ALABAMA 35899

TABLE OF CONTENTS

LIST OF FIGURES

PREFACE

The effort described in this report was supported by the Structural Development Branch (ED52) and the Laboratory Support Branch (EH15) at the NASA/Marshall Space Flight Center in Huntsville, Alabama. The Contracting Officer's Technical Representatives for this program were Mr. Richard Dotson (ED51), Dr. Joel Williamsen (ED52), and Mr. Ben Hayashida (ED52).

ACKNOWLEDGMENTS

The authors are grateful for the support provided by the NASA/Marshall Space Flight Center that made this study possible. The authors would also like to acknowledge Dr. Joel Williamsen and Mr. Ben Hayashida for their many helpful comments and guidance during the course of this effort.

1.0 INTRODUCTION

All long-duration spacecraft in low-earth-orbit are subject to high speed impacts by meteoroids and orbital debris. As a result, the threat of damage from such high speed impacts has become a significant design consideration in the development and construction of long duration earth-orbiting spacecraft. Historically, significant amounts of resources have been devoted to developing shielding for such structures as a means of reducing the penetration potential of high speed on-orbit impacts. Many studies have concluded that the level of protection afforded a spacecraft by a dual-wall structure significantly exceeds the protection level provided by an equal weight single wall of the same material. These studies have typically focused on simply whether or not the inner (or 'pressure') walls of candidate multi-wall structural systems would be perforated. The extent of pressure wall damage following a penetration has only recently begun to be explored [1,2].

In addition to a hole, the pressure wall of a dual-wall structure impacted by a high speed particle can also experience cracking and petaling [3-5]. If such cracking were to occur on-orbit, unstable crack growth could develop which could lead to an unzipping of the impacted module [6]. Thus, it is imperative to be able to characterize the cracking phenomena associated with the penetration of the dual-wall systems being considered for the International Space Station (ISS).

This report presents the results of a study whose objective was to develop first-principles-based models of hole size and maximum tip-to-tip crack length for a spacecraft module pressure wall that has been perforated in an orbital debris particle impact. These models can be

incorporated directly into a survivability analysis (see, e.g. [7]) to determine whether or not module unzipping would occur under a specific set of impact conditions. The prediction of hole size can also be used as part of a survivability analysis to determine the time available for module evacuation prior to the onset of incapacitation due to air loss.

Preliminary empirical models of hole diameter and maximum tip-to-tip crack length were proposed by Schonberg [8] and later refined by Schonberg and Williamsen [9] for the impact of generic dual-wall systems at an impact velocity of 6.5 km/s. These studies considered the effect of pressure wall thickness and the placement of multi-layer thermal insulation (MLI) within a dual-wall system on hole diameter and crack length in the event of a pressure wall perforation. These models were subsequently extended to a variety of different ISS wall systems, but their applicability still remained limited to impact velocities of approximately 6.5 km/s [10]. Following a series of tests at the Southwest Research Institute, hole size and crack length data became available at velocities between 10.8 and 11.8 km/s. With this data, the models were then extended to impacts at 11.3 km/s for a few select ISS wall systems [11,12]. Most recently, Schonberg and Williamsen [13] presented a comprehensive series of equations that characterize the hole size and crack length associated with the penetration of the multi-wall systems being considered for the ISS.

The hole size and crack length models are developed herein by sequentially characterizing the phenomena comprising the orbital debris impact event, including the initial impact, the creation and motion of a debris cloud within the dual-wall system, the impact of the debris cloud on the pressure wall, the deformation of the pressure wall due to debris cloud impact loading prior to crack formation, pressure wall crack initiation, propagation, and arrest, and finally pressure wall deformation following crack initiation and growth.

Two types of module wall systems were considered in this study: a standard Whipple-type multi-wall system and an enhanced or 'stuffed' shielding system. In both cases, the outer wall or outer 'bumper' protects the module and its inhabitants by disrupting impacting particles. The major difference between the two multi-wall systems is the nature of the inner bumper between the outer bumper and the pressure wall. In a standard Whipple system, the inner bumper is a multi-layer thermal insulation (MLI) blanket, while in an enhanced system, the inner bumper consists of several layers of Kevlar and Nextel cloth that are added to an MLI blanket. Figure 1 depicts the normal impact of a generic multi-wall system.

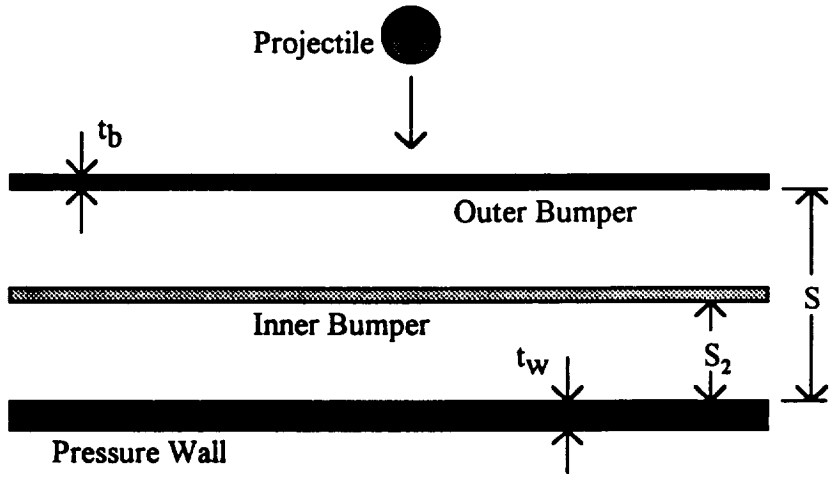

Figure 1. High Speed Normal Impact of a Generic Multi-Wall System

In this report, Section 2.0 presents the shock loading and release analysis that will be applied to the initial impact of the projectile on the bumper. The characterization and motion of the debris cloud within the dual-wall system is discussed in Section 3.0 with an emphasis on obtaining an appropriate velocity value to characterize the forward motion of the debris cloud. This is a critical value because it is eventually used as input for the pressure wall loading function,

which in turn is used to characterize the motion and deformation of the uncracked and cracked pressure wall. In Section 4.0, the form of the pressure wall loading function is developed, while Section 5.0 presents a summary of the pressure wall deformation model, including the assumptions used in its development. Section 6.0 presents the modeling of pressure wall deformation prior to crack initiation and growth. Section 7.0 discusses the initiation, propagation, and arrest of pressure wall cracks, and concludes with the method of calculating the maximum tip-to-tip crack length. Section 8.0 presents the model of pressure wall deformation following crack formation, and concludes with the method of calculating pressure wall hole diameter. Section 9.0 extends the hole size and crack length models to oblique impacts. Finally, Section 10.0 presents a comparison of the predictions of the hole size and crack length models and experimental data. Modifications to the model that are required to bring its predictions in closer agreement with the experimental results are also presented and discussed.

2.0 INITIAL IMPACT SHOCK LOADING AND RELEASE MODELING

Consider the normal hypervelocity impact of a projectile on the outer bumper of a multi-wall system as shown in Figure 1. Upon impact, shock waves are set up in the projectile and outer bumper materials. The pressures associated with these shocks typically exceed the strengths of the materials by several orders of magnitude. For example, in an 8 km/sec aluminum-on-aluminum impact, the ratio of the impact pressure (116.5 GPa=1.15 MBar) to the strength of the material (310 MPa for aluminum 6061-T6) is approximately 375, or roughly 2.5 orders of magnitude. As the shock waves propagate, the projectile and outer bumper materials are heated adiabatically and non-isentropically. The release of the shock pressures occurs isentropically through the action of rarefaction waves that are generated as the shock waves interact with the free surfaces of the projectile and the outer bumper. This process leaves the materials in high energy states and can cause either or both to fragment, melt or vaporize, depending on the material properties, geometric parameters, and the velocity of impact.

2.1 Shock Loading Due to High Speed Impact

In calculating the shock loading and subsequent release of the projectile and outer bumper materials, the shock waves are considered to be initially planar. This simplification allows one-dimensional relationships to be used for analyzing the creation and release of shock pressures. In this manner, the shock pressures, energies, etc., in the projectile and outer bumper materials are calculated using the three 1-D shock-jump conditions, a linear relationship between the shock wave velocity and particle velocity in each material, and continuity of pressure and velocity at the

projectile/outer bumper interface.

Specifically, if we consider the 1-D impact of a projectile with velocity v_O on a stationary outer bumper, conservation of mass, momentum, and energy across the shock fronts in the projectile and in the outer bumper yields

Projectile:

$$\frac{u_{sp}}{V_{op}} = \frac{u_{sp} - u_{pp}}{V_{Hp}}$$

$$P_{Hp} = P_{op} + \frac{u_{sp} u_{pp}}{V_{op}} \qquad \text{(1a-c)}$$

$$E_{Hp} = E_{op} + \frac{1}{2}(P_{Hp} + P_{op})(V_{op} - V_{Hp})$$

Outer Bumper:

$$\frac{u_{st}}{V_{ot}} = \frac{u_{st} - u_{pt}}{V_{Ht}}$$

$$P_{Ht} = P_{ot} + \frac{u_{st} u_{pt}}{V_{ot}} \qquad \text{(2a-c)}$$

$$E_{Ht} = E_{ot} + \frac{1}{2}(P_{Ht} + P_{ot})(V_{ot} - V_{Ht})$$

where $V=1/\rho$ is specific volume, u_s and u_p are shock and particle velocity, respectively; V_H,P_H,E_H and V_o,P_o,E_o are the density, pressure and energy states associated with the shocked and initial material states, respectively. In equations (1a-c) and (2a-c), the subscripts 'p', and 't' refer to projectile and outer bumper quantities, respectively. In the development of equations (1a-c) and (2a-c), the shock velocity in the projectile is taken relative to a 'stationary' projectile.

The linear shock velocity-particle velocity relationships for the projectile and outer bumper materials are taken to be in the form

$$u_s = c_o + k u_p \qquad (3)$$

where $c_o=\sqrt{(KV_o)}$ is the material bulk speed of sound, $K=E/3(1-2\nu)$ is the adiabatic bulk modulus, E and ν are Young's modulus and Poisson's ratio, respectively, and k is an empirically-derived constant. Equations (1,2) are applied to the initial impact on the outer bumper of a multi-wall system in the following manner. Upon impact, pressure equilibrium at the projectile/outer bumper interface implies that

$$P_{Hp} = P_{Ht} \tag{4}$$

while material continuity at the interface implies that

$$v_o = u_{pp} + u_{pt} \tag{5}$$

Because the outer bumper in a multi-wall system is free from any initial mechanical stress (it is merely supported at its four corners a fixed distance away from the inner pressure wall), the initial conditions ahead of the projectile and outer bumper shock waves are taken to be zero (with the exception, of course, of the initial material densities). Solving equations (1-5) simultaneously yields expressions for projectile and outer bumper particle velocities which can then be used to calculate shock velocities, pressures, internal energies, and material densities after the passage of a shock wave. For example, using this procedure to solve initially for u_{pt} yields

$$u_{pt} = \frac{b - \sqrt{\Delta}}{2a} \tag{6}$$

where

$$a = k_p - k_t\left(\frac{\rho_{ot}}{\rho_{op}}\right)$$

$$b = 2k_p v_o + c_{op} + c_{ot}\left(\frac{\rho_{ot}}{\rho_{op}}\right) \tag{7a-c}$$

$$\Delta = b^2 - 4a(c_{op}v_o + k_p v_o^2)$$

Then it follows that

$$u_{pp} = v_o - u_{pt} \tag{8a}$$

$$u_{st} = c_{ot} + k_t u_{pt} \tag{8b}$$

$$u_{sp} = c_{op} + k_p u_{pp} \tag{8c}$$

The shocked densities of the projectile and outer bumper materials are found by substituting equations (6,8a-c) into equations (1a) and (2a) to yield

$$\rho_{Hp} = \frac{1}{V_{Hp}} = \frac{u_{sp} / V_{op}}{u_{sp} - u_{pp}} \tag{9a}$$

$$\rho_{Ht} = \frac{1}{V_{Ht}} = \frac{u_{st} / V_{ot}}{u_{st} - u_{pt}} \tag{9b}$$

Finally, equations (1b,c) and (2b,c) are then used to define the pressure and energy in the projectile and outer bumper materials, respectively, associated with the passage of the shock waves created by the initial impact. This completely defines the shocked states of the projectile and outer materials due to the initial impact.

While the shock loading of a material is an irreversible process that results in an increase of the internal energy of the shocked material, the release of a shocked material occurs isentropically along an 'isentrope' or 'release adiabat'. The difference between the area under the isentrope and the energy of the shocked state is the amount of residual energy that remains in the material and can cause the material to melt or even vaporize. In order to calculate the release of the projectile and outer bumper materials from their respective shocked states (each characterized by P_H, E_H, and V_H), an appropriate equation-of-state is needed for each material. To keep the analysis relatively simple, the Mie-Gruneisen equation-of-state [14] was used in this study.

2.2 Shock Release Using the Mie-Gruneisen Equation-of-State

The Mie-Gruneisen equation-of-state (EOS) is an accurate thermodynamic description of most metals in the solid regime and is relatively easy to use. It has the form

$$P = P_H + \rho\Gamma(E - E_H) \tag{10}$$

where the time-dependent Gruneisen coefficient Γ is given for most metals as

$$\Gamma = \frac{\Gamma_o \rho_o}{\rho} \tag{11}$$

In equation (11),

$$\Gamma_o = \frac{K\beta}{\rho_o C_p} \tag{12}$$

is the ambient Gruneisen coefficient, where K is the adiabatic bulk modulus, $\beta=3\alpha$ is the volumetric coefficient of thermal expansion, and C_p is specific heat at constant pressure. Invoking the Second Law of Thermodynamics

$$dE = TdS - PdV \tag{13}$$

along with the isentropic constraint $dS=0$ for the release process allows us to construct the release isentrope in P-V space for a material referenced to the material Hugoniot in P-V space and a given initial shocked state defined by P_H, V_H, E_H. Using the procedure outlined in Reference [14], the pressure P_i at a specific position 'i' along the isentrope can be shown to be given by

$$P_i = \frac{P_{Hi} + \left(\frac{\Gamma}{V}\right)_i \left(E_{i-1} - \frac{1}{2}P_{i-1}(\Delta V) - E_{Hi}\right)}{1 + \frac{1}{2}\left(\frac{\Gamma}{V}\right)_i (\Delta V)} \tag{14}$$

where ΔV is the incremental change in volume used to create the release isentrope, and P_{Hi} and E_{Hi} are the pressure and energy along the Hugoniot corresponding to the i-th position in the

release process. The release process is continued using equation (14) until the release isentrope so determined crosses the V-axis.

It should be noted that based on its formulation, the Mie-Gruneisen EOS cannot be expected to give accurate results in a highly expanded liquid regime or in a vapor regime. This is because as impact energy increases, the assumption that the Gruneisen coefficient is a function of density alone is no longer valid. At high impact energies, the Gruneisen coefficient is a function of internal energy as well as density. Experience has shown, however, that it does yield fairly accurate end-state results even when there is a small percentage of molten material present [15].

3.0 DEBRIS CLOUD CHARACTERIZATION

Following the impact of the projectile on the outer bumper, a debris cloud is created that travels towards and eventually impacts the inner bumper. This second impact creates another debris cloud that impacts the pressure wall of the multi-wall system. These debris clouds are referred to as the "primary" and "secondary" debris clouds, respectively. This section is concerned with the means by which the masses and velocities of these debris clouds are calculated.

3.1 Primary Debris Cloud Mass Content

The mass of the primary debris cloud consists of the mass of the original impacting projectile plus the mass of the removed bumper material. No mass is considered lost to backsplash of the bumper and projectile materials; hence, since all of the mass is presumed to be directed in towards the pressure wall, the model to be developed should yield conservative results. The contribution of the bumper material to the primary debris cloud mass can be determined once the bumper hole diameter is known. This diameter can be calculated using any one of a number of empirical equations for hole diameter in a thin plate due to a high speed impact (see, e.g. [16]). The particular equation used in this study is given as follows [17]:

$$\frac{D_h}{d_p} = 3.4\left(\frac{t_b}{d_p}\right)^{0.333}\left(\frac{V_p}{C_b}\right)^{0.333}\left[1.0 - 0.0308\left(\frac{\rho_b}{\rho_p}\right)\right] \qquad (15)$$

where C_b is the speed of sound in the bumper material, d_p is the projectile diameter, V_p is the impact velocity, and ρ_b and ρ_p are the mass densities of the outer bumper and projectile materials, respectively. This equation was chosen because it is applicable over a wide range of

projectile/bumper material combinations, impact velocities, and t_b/d_p ratios. Once D_h is known, the outer bumper hole out mass is written as follows:

$$m_b = \frac{\pi}{4} D_h^2 \rho_b t_b \tag{16}$$

3.2 Primary Debris Cloud Mass Distribution

X-ray photographs of debris clouds created by hypervelocity impacts of spherical and cylindrical projectiles on thin metallic plates have shown that the primary debris cloud material is not uniformly distributed throughout the debris cloud; rather, the projectile material is typically nested within a hollow shell containing bumper material. Therefore, in order to resemble reality while remaining analytically tractable, the bumper material was assumed to be contained in a hollow spherical shell while the projectile material was assumed to be contained within a solid spherical mass. In addition, the leading edge of the projectile material is coincident with the leading edge of the spherical shell containing the bumper material (see Figure 2).

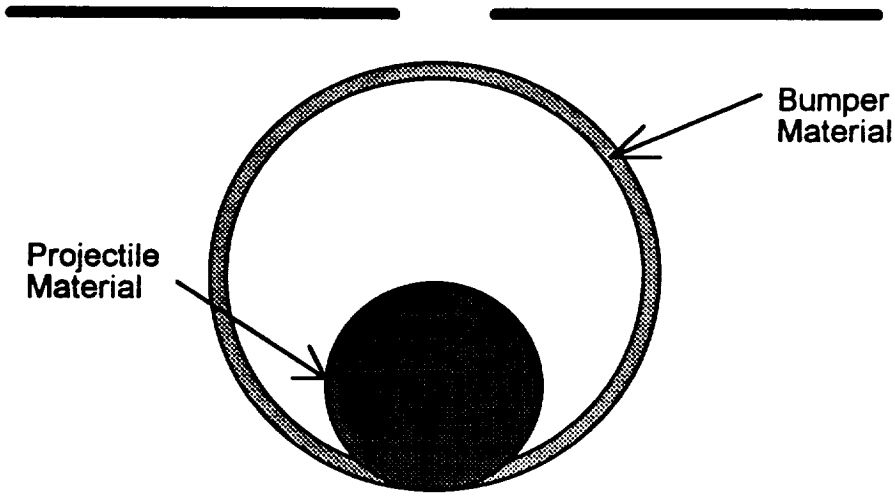

Figure 2. Generic Debris Cloud Model

The characteristic velocities of interest for the primary debris cloud are the axial and expansion velocities of the projectile and bumper material debris cloud components. These values can be determined in any number of different ways. Naturally, the various methods provide slightly different results. The 'correct' or most appropriate method is that which will provide characteristic velocity values that when used in subsequent calculations will provide pressure and temperature increases that are most consistent with experimental results. The method used in this study is based in part on that used in a preceding study in which similar quantities were determined [18]. It is based on conservation of momentum and energy before and after the impact event and is described in the following section.

3.3 Primary Debris Cloud Characteristic Velocities

To begin, we have four unknowns to determine: the axial and expansion velocities of each component of the primary debris cloud. Conservation of momentum before and after the impact on the bumper provides the first equation necessary to determine the unknowns. This equation is given as follows:

$$m_p V_p = m_p V_{ax,p} + m_b V_{ax,b} \tag{17}$$

where V_p is the impact velocity, m_p and m_b are the projectile and bumper hole-out masses, respectively, and $V_{ax,p}$ and $V_{ax,b}$ are the axial velocities of the projectile and bumper material components of the primary debris cloud, respectively.

Because the initial impact occurs at such a high velocity, momentum transfer to the bumper itself is ignored. Furthermore, because of the rapidity of the impact event, the only significant energy losses are to the accompanying light flash and the shock heating of the bumper and projectile materials. If we neglect the energy associated with the light flash, then an energy

balance before and after the initial impact provides the second necessary equation. This equation is given as follows:

$$\frac{1}{2}m_p V_p^2 = \frac{1}{2}m_p V_{ax,p}^2 + \frac{1}{2}m_p V_{exp,p}^2 + \frac{1}{2}m_b V_{ax,b}^2 + \frac{1}{2}m_b V_{exp,b}^2 + E_{sr,p}m_p + E_{sr,b}m_b \quad (18)$$

where $V_{exp,p}$ and $V_{exp,b}$ are the expansion velocities of the projectile and bumper material components of the primary debris cloud, and $E_{sr,p}$ and $E_{sr,b}$ are the waste heats per unit mass produced by the shock heating and release of the projectile and bumper hole-out materials. By neglecting energy losses such as those due to light flash, the results obtained herein should again be conservative in nature.

At this point in the development we have exhausted the tools of elementary mechanics as a means of providing equations that can be used to solve for the unknown. We turn to the debris clouds themselves and recall that we have postulated that the leading edge of the projectile component is coincident with the bumper material component. This in turn implies that the leading edge velocities of the two debris cloud components must be equal. Our next objective then is to relate the axial and expansion velocities to the leading edge velocities of the two debris cloud components. To this end, we postulate as in [18] that the leading edge velocity is merely the sum of the axial and expansion velocities for each of the material components. This provides us with the following two additional equations that can be used to solve for the unknowns:

$$V_{ax,p} + V_{exp,p} = V_{le} \quad (19a)$$

$$V_{ax,b} + V_{exp,b} = V_{le} \quad (19b)$$

However, the leading edge velocity is itself an unknown, and so while the number of equations available is now four, the number of unknowns has risen to five. A final equation is provided by assuming that the ratio of the expansion velocities of the two debris cloud

components is inversely proportional to their masses, that is,

$$\frac{V_{exp,p}}{V_{exp,b}} = \frac{m_b}{m_p} \tag{20}$$

In this manner, it is presumed that the lighter component will expand faster than the heavier one. This at last provides a system of five algebraic equations that can be used to solve for the five unknown primary debris cloud velocities.

Equations (17-20) can be solved for the unknown velocities using any number of techniques. The approach taken here is to manipulate equations (17-20) to yield the following equation for the leading edge velocity:

$$AV_{le}^2 + BV_{le} + C = 0 \tag{21}$$

where

$$A = \frac{1}{4}(m_p + m_b)\left(\frac{m_b}{m_p} + \frac{m_p}{m_b}\right) \tag{22a}$$

$$B = -\frac{1}{2}m_p V_p\left(\frac{m_b}{m_p} + \frac{m_p}{m_b}\right) \tag{22b}$$

$$C = E_{sr,t} + \frac{1}{4}m_p V_p^2\left(\frac{m_p}{m_b} - 1\right) \tag{22c}$$

where

$$E_{sr,t} = E_{sr,p}m_p + E_{sr,b}m_b \tag{23}$$

Once equation (21) is solved for V_{le}, the following relationship is used to obtain the value of the expansion velocity of the bumper component material:

$$V_{exp,b} = \frac{(m_p + m_b)V_{le} - m_p V_p}{m_p + m_b} \tag{24}$$

Next, $V_{exp,p}$ is found using equation (20), following which the two axial velocities are found using equations (19a,b). The completes the calculations required to obtain the five unknown velocity quantities that characterize the motion of the primary debris cloud.

3.4 Primary Debris Cloud Component Spread Angles

The spread of each component of the primary debris cloud (in this case the half-angles defining the spreads) can be estimated using the following relationship between the calculated primary debris cloud component expansion and axial velocities:

$$\theta_{dc,i} = \tan^{-1}\left(\frac{V_{exp,i}}{V_{ax,i}}\right), \; i = p,b \tag{25}$$

3.5 Secondary Debris Cloud Mass Content

The mass content of the secondary debris cloud is very similar to that of the primary debris cloud with the exception that it also includes the mass of the removed inner bumper material. As before, no mass is considered lost to backsplash of the bumper and projectile materials. The contribution of the inner bumper material to the secondary debris cloud mass can be determined once the bumper hole diameter is known. Unfortunately, there do not exist any equations that can be used to calculate the diameter of the hole either in an MLI blanket or a Nextel/Kevlar blanket due to a perforating impact by a debris cloud. Therefore, for the purposes of this investigation, the diameter of the hole in the inner bumper is estimated to be simply given by the diameter of the projectile material component of the primary debris cloud as it passes through the plane defining the position of the inner bumper. As such, the inner bumper hole out mass is given by

$$m_{ib} = \varepsilon_{ib}\frac{\pi}{4}\delta_h^2\lambda_{ib} \tag{26}$$

where δ_h is the inner bumper hole diameter and λ_{ib} is the inner bumper material areal density; ε_{ib} is

a user-controlled parameter that is used to adjust the calculated value of m_{ib}, if necessary.

3.6 Secondary Debris Cloud Mass Distribution

The distribution of the mass within the secondary debris cloud is analogous to that assumed for the primary debris cloud: a solid sphere of projectile material is surrounded by a hollow sphere of outer and inner bumper material. In order to maintain a parallel with the discussion concerning the primary debris cloud, the outer and inner bumper material in the hollow spherical shell is hereafter referred to simply as 'bumper' material.

3.7 Secondary Debris Cloud Characteristic Velocities

The axial and expansion velocities of the projectile and bumper components of the secondary debris cloud are calculated in a manner very similar to that used for the primary debris cloud. In fact, it is found that the equations are identical with the exception that the mass of the inner bumper hole out mass must be added to that of the outer bumper hole out mass wherever the outer bumper hole out mass term appears. That is, wherever there appears in equations (17-24) the quantity m_b, it is simply replaced by the quantity m_b+m_{ib}, where m_{ib} is the inner bumper hole-out mass as given by equation (26). In this manner, the solution of equations (17-20) using the modified bumper mass term yields the five velocity quantities that characterize the motion of the secondary debris cloud.

3.8 Identification of Dominant Debris Cloud

The next section presents the development of the function used to characterize the loads transmitted to the pressure wall that result in its subsequent deformation and perforation. Prior to the development of this function, it must be determined which of the two debris clouds discussed thus far delivers the load to the pressure wall.

In the strictest sense, based on the development of the equations used in their characterization, the primary and secondary debris clouds are tacitly assumed to emanate from a point on the outer and inner bumper, respectively, that corresponds to a "center of impact". As a result, the spread of the secondary debris cloud when it first comes into contact with the pressure wall will be much less than that of the primary debris cloud were the primary debris cloud allowed to continue unscathed through the inner bumper and impact the pressure wall. This decreased spread of the secondary debris cloud was found to give rise to many complications further in the development of the overall analytical model.

Hence, for the purposes of this investigation, it is assumed that it is the primary debris cloud that delivers the load to the pressure wall. Furthermore, the primary debris cloud will hereafter be referred to simply as "the debris cloud". However, this is not to say that the presence of the inner bumper is ignored. Only its effect on the velocities characterizing the debris cloud that delivers the load to the pressure wall is ignored. The presence of the inner bumper is taken into consideration in the calculation of the delay between the times at which the loads due to the projectile and bumper components of the primary debris cloud are applied to the pressure wall. This issue is discussed in more detail in the following section.

4.0 PRESSURE WALL LOADING FUNCTION

4.1 Load Function Characteristics

The function defining the temporal and spatial dependencies of the load on the pressure wall due to the impact of the debris cloud was developed to possess the following characteristics.

- The effect of the projectile debris cloud component begins at time t=0; the effect of the bumper material begins a short time later. This time delay is a function of the distance between the inner bumper and the pressure wall.
- The duration of the load produced by each component is calculated from the amount of time between first contact of the debris cloud component leading edge on the pressure wall and the time when the trailing edge passes through the plane defining the undeformed pressure wall.
- The combined effect of the two debris cloud components at a given instant of time is the sum of the individual component loads at that instant of time.
- The pressure wall footprint area over which the load of each debris cloud component is applied is circular and of constant radius. This footprint radius for each debris cloud component is the projection of the sphere defining each component on the pressure wall at the time of first contact with the pressure wall.

4.2 Load Function Definition

Based on the characteristics and assumptions described in the preceding section, the pressure wall loading function is taken to be in the following form:

$$p(r,t) = p_{op}R_p(r)[H(r) - H(r - R_{wp})]T_p(t)[H(t) - H(t - t_{dp})]$$

$$+ p_{ob}R_b(r)[H(r) - H(r - R_{wb})]T_b(t)[H(t - t_1) - H(t - t_1 - t_{dp})] \quad (27)$$

where $R_p(r)$ and $R_b(r)$ are dimensionless functions characterizing the pressure wall load area radii of the projectile and bumper material components of the debris cloud, $T_p(t)$ and $T_b(t)$ are dimensionless time dependent functions characterizing the position of each debris cloud component with respect to the undeformed pressure wall, p_{op} and p_{ob} are the relative maximum magnitudes of the two debris cloud component loadings, H(*) is the Heavyside Function, and t_1 is the time delay between the impact of the projectile material and bumper material components of the primary debris cloud. As discussed in Chapter 3, the phrase 'bumper material' refers to the combination of the outer and inner bumper hole-out materials. These various functions and constants are defined as follows.

4.2.1 Defining $R_p(r)$ and $R_b(r)$

Since the dimensionless functions $R_p(r)$ and $R_b(r)$ are presumed to be constant and since p_{op} and p_{ob} are as yet unknown, each of the functions $R_p(r)$ and $R_b(r)$ is set equal to unity.

4.2.2 Defining $T_p(t)$ and $T_b(t)$

In the development that follows, where appropriate, no distinction is made between projectile material debris cloud component and bumper hole-out material component quantities; it is presumed that the same arguments can be made for each both debris cloud component. Hence, all functions and variables are written without subscripts. Adding subscripts where appropriate would convert general quantities to component-specific quantities.

In developing an expression for T(t), it is assumed that the load induced by each component is zero at time t=0, steadily increases until it reaches its maximum value at a time

when the widest part of the debris cloud passes through the original horizontal plane of the undeformed pressure wall, and then steadily decreases and has a zero value when the trailing edge of the debris cloud passes through the same horizontal plane. Figure 3a shows a debris cloud component just at the instant of its impact on the pressure wall.

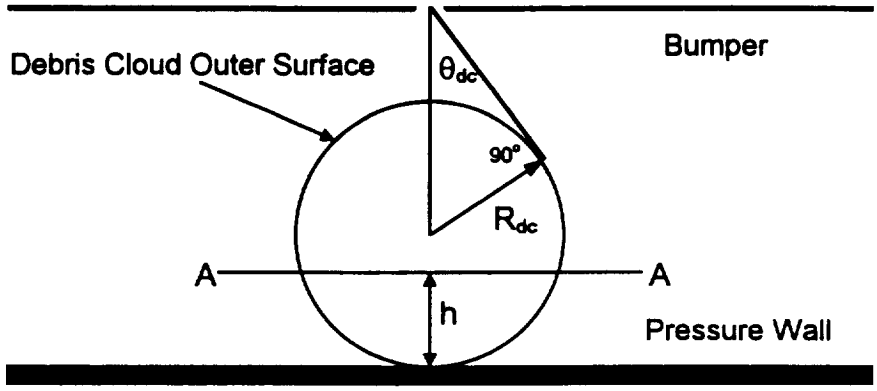

Figure 3a Debris Cloud Arrival at Pressure Wall Upper Surface

Figure 3b shows the position of the debris cloud at a short time later when Section A-A of the debris cloud, which was at a height 'h' above the pressure wall plane, arrives at the pressure wall. That is, 'h' is the depth of the debris cloud that has passed through the original horizontal pressure wall plane. In Figure 3b, r(h) is the radius of the debris cloud footprint area at that instant in time.

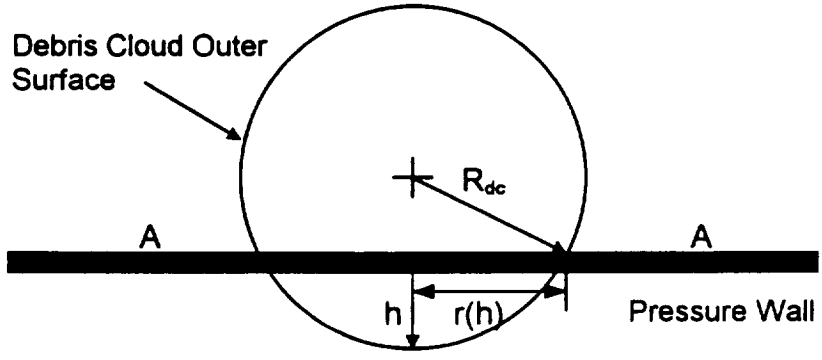

Figure 3b Debris Cloud Having Moved Through Pressure Wall Plane a Distance 'h'

While any number of functions of time can meet the conditions set forth above, it seems natural to choose the variation in r as a function of h, which is itself a function of time, as the representative function for T(t). Since T(t) must be non-dimensional, we normalize r(h) by dividing it by R_{dc}, the debris cloud radius at the instant of impact on the pressure wall. Thus, we can write

$$T(t) = \frac{r(h)}{R_{dc}} \tag{28}$$

What remains now is to determine expressions for R_{dc}, r(h), and h(t). To begin, the geometric relationship between R_{dc} and θ_{dc} as shown in Figure 3a can be used to obtain the following expression for R_{dc}:

$$R_{dc} = \frac{S \sin\theta_{dc}}{1 + \sin\theta_{dc}} \tag{29}$$

where θ_{dc} is given by equation (25). Next, the geometric relationships evident in Figure 3b provide the following expression for r(h):

$$r(h) = \sqrt{R_{dc}^2 - (R_{dc} - h)^2} \tag{30}$$

Finally, the expression for h(t) is found as follows. First, we recall that along the centerline of the debris cloud, the leading edge of the debris cloud is traveling at a velocity given by $V_{ax}+V_{exp}$, while the trailing edge is moving in the same direction at a velocity $V_{ax}-V_{exp}$. Hence, there is a variation in debris cloud velocity along the centerline of the debris cloud. Simple linear interpolation between the velocity at the leading edge and the velocity at the trailing edge tells us that at a position 'h' behind the debris cloud leading edge (see Figure 3a), the velocity is given by

$$V_{dc}(h) = V_{ax} + \frac{R_{dc} - h}{R_{dc}} V_{exp} \tag{31}$$

Second, assuming that the progress of the portion of the debris cloud that has not yet struck the pressure wall is not impeded by the portion of the debris cloud that has, the position 'h' behind the debris cloud leading edge along its centerline is reached at a time 't' according to the following relationship:

$$h(t) = \frac{1}{2} V_{dc}(h)t \tag{32}$$

where the '1/2' in equation (32) is required by the fact that $V_{dc}(h)$ is not constant but a function of time 't'. Substituting equation (31) into (32) allows us to obtain the following expression for h(t):

$$h(t) = \frac{R_{dc}\, t(V_{ax} + V_{exp})}{2R_{dc} + tV_{exp}} \tag{33}$$

Therefore, normalizing equation (30) by R_{dc} yields the following expression for the function T(t):

$$T(t) = \sqrt{1 - \left(1 - \frac{h(t)}{R_{dc}}\right)^2} \tag{34}$$

where h(t) is given by equation (33). Subsequent integrations of expressions involving this form of T(t) resulted in numerous complications, primarily due to the presence of the radical in equation (34). These difficulties ceased to exist when the radical was simply removed. Since the resulting 'radical-less' expression still possessed all of the necessary attributes, it was the one used in all subsequent calculations. That is, T(t) is given as follows:

$$T(t) = 1 - \left(1 - \frac{h(t)}{R_{dc}}\right)^2 \tag{35}$$

where h(t) is still given by equation (33).

At this point of the development, it is also possible to calculate the duration of impact for each debris cloud component. This is accomplished simply by noting that when the trailing edge

of the debris cloud passes through the horizontal plane defining the original position of the pressure wall, $h=2R_{dc}$. Substituting this value in to the left-hand-side of equation (33) and solving for time 't' yields the amount of time required for the entire debris cloud to pass through this horizontal plane, i.e. the impact duration t_d. Following this procedure results in the following expression for t_d:

$$t_d = \frac{4R_{dc}}{V_{ax} - V_{exp}} \tag{36}$$

The time delay between the impacts of the projectile and bumper material components is assumed to be given by the following relationship:

$$t_1 = \frac{S_2}{V_{exp,b}} \tag{37}$$

where S_2 is the distance between the inner bumper and the pressure wall. In effect, t_1 as given by equation (37) is a measure of time required for the bumper material component of the debris cloud to travel between the inner bumper and the pressure wall. This seems to be a natural quantity to use to offset the effects of the bumper material from those of the projectile material.

4.2.3 Calculating p_{op} and p_{ob}

The constants p_{op} and p_{ob} are each found by conserving axial momentum for the debris cloud before and after its impact on the pressure wall. The conservation equation is written as follows:

$$(m_b + m_{ib})V_{ax,b} + m_p V_{ax,p} = 2\pi\int_0^{R_{wb}} p_{ob} r dr \int_{t_1}^{t_1+t_{db}} T_b(t)dt + 2\pi\int_0^{R_{wp}} p_{op} r dr \int_0^{t_{dp}} T_p(t)dt \tag{38}$$

where m_{ib} is the inner bumper hole-out mass and is given by equation (9), $T_b(t)$ and $T_p(t)$ are given by equation (35), t_{db} and t_{dp} are the impact durations for the bumper and projectile components of

the debris cloud, respectively, and are given by equation (36), t_1 is the delay between the onset of the loads due to the projectile and bumper components of the debris cloud as given by equation (27), and R_{wb} and R_{wp} are the radii of the bumper and projectile component loading area footprints on the pressure wall. Simple geometric considerations reveal the following expression for each of the footprint radii:

$$R_w = S\tan\theta_{dc} \tag{39}$$

Performing the integrations over 'r' in equation (38) allows us to rewrite that equation as follows:

$$(m_b + m_{ib})V_{ax,b} + m_p V_{ax,p} = \pi p_{ob} R_{wb}^2 I_b + \pi p_{op} R_{wp}^2 I_p \tag{40}$$

where

$$I_b = \int_{t_1}^{t_1+t_{db}} T_b(t)dt \tag{41a}$$

$$I_p = \int_0^{t_{dp}} T_p(t)dt \tag{41b}$$

These integrations can be evaluated in closed form with the following results. First, for I_p:

$$I_p = \frac{1}{\alpha_p}\left(2 - \frac{1}{\alpha_p}\right)t_{dp} - 2\left(\frac{\gamma_p}{\alpha_p}\right)\left(1 - \frac{1}{\alpha_p}\right)\ln\left(1 + \frac{t_{dp}}{\gamma_p}\right) - \frac{1}{\alpha_p^2}\left(\frac{t_{dp}\gamma_p}{t_{dp} + \gamma_p}\right) \tag{42}$$

where

$$\alpha_p = \frac{V_{exp,p}}{V_{ax,p} + V_{exp,p}} \tag{43a}$$

and

$$\gamma_p = \frac{2R_{dcp}}{V_{exp,p}} \tag{43b}$$

Second, since the forms of T_p and T_b are identical, we note the integral for I_b can be written as

$$I_b = \int_{t_1}^{t_1+t_{d_b}} T_b(t)dt = \int_{t_1}^{t_1+t_{d_b}} T_p(t-t_1)dt = \int_0^{t_{d_b}} T_p(u)du \tag{44}$$

Hence, the expression for I_b is the same as that for I_p, but with 'b' replacing 'p' throughout equations (42) and (43a,b).

Returning to the solution of equation (40) for the two remaining unknowns, p_{ob} and p_{op}, we note that equation (40) is but one equation in two unknowns. Hence, a second equation that relates p_{ob} and p_{op} is required. To obtain this second equation, we postulate that the peak pressure delivered by each debris cloud component is directly proportional to its axial momentum, to wit:

$$\frac{p_{op}}{p_{ob}} = \frac{m_p V_{ax,p}}{(m_b + m_{ib})V_{ax,b}} \tag{45}$$

Solving equations (40) and (45) for p_{ob} and p_{op} yields the following results:

$$p_{op} = \frac{\gamma\delta}{\alpha + \beta\delta} \tag{46a}$$

$$p_{ob} = \frac{\gamma}{\alpha + \beta\delta} \tag{46b}$$

where

$$\alpha = \pi R_{wb}^2 I_b \tag{47a}$$

$$\beta = \pi R_{wp}^2 I_p \tag{47b}$$

$$\gamma = (m_b + m_{ib})V_{ax,b} + m_p V_{ax,p} \tag{47c}$$

$$\delta = \frac{m_p v_{ax,p}}{(m_b + m_{ib})v_{ax,b}} \tag{47d}$$

This completes the derivation of all the terms and quantities required to define the load on the pressure wall produced by the debris cloud impact. The following section summarizes all the

equations required to define the pressure wall load function. In the next chapter we begin the development of the pressure wall deformation model.

4.3 Load Function Summary

$$p(r,t) = p_{op}[H(r) - H(r - R_{wp})]T_p(t)[H(t) - H(t - t_{dp})]$$

$$+ p_{ob}[H(r) - H(r - R_{wb})]T_b(t)[H(t - t_1) - H(t - t_1 - t_{dp})]$$

$$p_{op} = \frac{\gamma\delta}{\alpha + \beta\delta}$$

$$p_{ob} = \frac{\gamma}{\alpha + \beta\delta}$$

$$\alpha = \pi R_{wb}^2 I_b$$

$$\beta = \pi R_{wp}^2 I_p$$

$$\gamma = (m_b + m_{ib})V_{ax,b} + m_p V_{ax,p}$$

$$\delta = \frac{m_p v_{ax,p}}{(m_b + m_{ib})v_{ax,b}}$$

$$R_{wi} = S\tan\theta_{dc,i} \ , \ i = b,p$$

$$\theta_{dc,i} = \tan^{-1}\left(\frac{v_{exp,i}}{v_{ax,i}}\right)$$

$$t_{di} = \frac{4R_{dci}}{V_{ax,i} - V_{exp,i}}$$

$$t_1 = \frac{S_2}{V_{exp,b}}$$

$$m_b = \frac{\pi}{4} D_h^2 \rho_b t_b$$

$$m_{ib} = \varepsilon_{ib} \frac{\pi}{4} \delta_h^2 \lambda_{ib}$$

$$\delta_h = 2R_{dcp}$$

$$R_{dci} = \frac{S \sin\theta_{dci}}{1 + \sin\theta_{dci}}$$

$$I_p = \frac{1}{\alpha_p}\left(2 - \frac{1}{\alpha_p}\right) t_{dp} - 2\left(\frac{\gamma_p}{\alpha_p}\right)\left(1 - \frac{1}{\alpha_p}\right) \ln\left(1 + \frac{t_{dp}}{\gamma_p}\right) - \frac{1}{\alpha_p^2}\left(\frac{t_{dp}\gamma_p}{t_{dp} + \gamma_p}\right)$$

$$\alpha_p = \frac{V_{exp,p}}{V_{ax,p} + V_{exp,p}}$$

$$\gamma_p = \frac{2R_{dcp}}{V_{exp,p}}$$

I_b , α_b , γ_b ... same as I_p , α_p , γ_p except with 'b' replacing 'p'

5.0 OVERVIEW OF PRESSURE WALL DEFORMATION MODEL

5.1 Deformation Model Features and Assumptions

Pressure wall deformation is presumed to begin at the instant the leading edge of the debris cloud strikes the pressure wall. The pressure wall deformation model developed herein contains the following features:

- pressure wall deformation prior to the onset of fracture;
- initiation of a family of radial cracks at the center of impact and their subsequent propagation;
- petalling of the pressure wall between adjacent cracks following propagation;
- calculation of the number of cracks created by the debris cloud impact;
- calculation of maximum tip-to-tip crack length; and,
- calculation of an equivalent circular hole diameter.

In modeling the response of the pressure wall to the impact of the debris cloud, the following assumptions were used to render the model analytically tractable:

- the pressure wall deformation is modeled as that of a fully clamped circular plate;
- the pressure wall is made of a rigidly plastic material;
- the material is controlled by the Tresca yield condition and the associated flow rule;
- the pressure wall starts to yield at time t=0, i.e. all elastic deformations are negligible;
- the pressure wall thickness is small enough to allow the use of thin plate theory to predict its response; and,

- the thickness of the pressure wall varies linearly from a minimum value at the center of the debris cloud impact footprint area to the outer perimeter of the footprint area where it attains its nominal constant value. This "thinning" of the pressure wall material is included to account for the erosion of the pressure wall by the grinding impacts of the many debris cloud particles.

As discussed previously, the model is developed under the assumption that the pressure wall footprint area over which the load of each debris cloud component is applied is circular and of constant radius. This footprint radius for each debris cloud component is the projection of the sphere defining each component on the pressure wall at the time of first contact with the pressure wall. The pressure wall deformation model is developed as a sequence of several discrete stages which when taken together present a complete picture of pressure wall response. An overview of these various stages is presented in the next subsection; details for each stage are given in subsequent Chapters.

5.2 Pressure Wall Deformation Model Overview

5.2.1 Stage 1: Pressure Wall Deformation Prior to Crack Initiation

Prior to the onset of crack propagation, the deformation of the pressure wall is modeled as a fully-plastic clamped circular plate under a uniform impulsive loading (see Figure 4). The theoretical development for this stage of the deformation is based on that of Florence [19,20], and Wang and Hopkins [21]. At each time-step, the velocity of the plate center and the strain at the center of the plate are calculated; the calculated strain value is compared with a material-specific critical strain value. This deformation stage ends when either 1) the velocity has dropped to zero, or 2) the strain at the plate center equals the critical strain value. In the first case, the pressure

wall is neither fractured nor perforated by the impact of the debris cloud and the final deformation of the plate consists only of plastic deformation. In the second case, the impact of the debris cloud is sufficiently powerful so as to initiate crack growth at the impact area center.

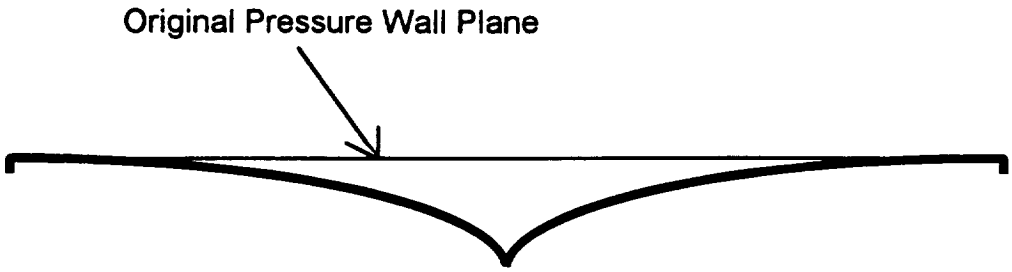

Figure 4. Pressure Wall Deformation Due to Impulsive Loading Prior to Crack Formation

5.2.2 Stage 2: Dynamic Crack Propagation and Crack Arrest

In the event that the material has ruptured at the center of the debris cloud footprint area, the model proceeds with the analysis of the propagating cracks (see Figures 5a,b). In this analysis, it is presumed that the cracks propagate at speeds far greater than that of the deforming pressure wall. Hence, the creation and growth of these cracks does not significantly affect any subsequent motion of the pressure wall and vice versa.

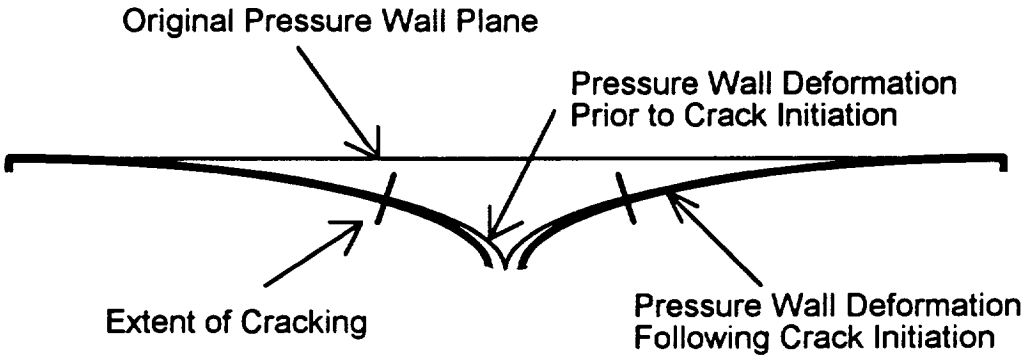

Figure 5a. Pressure Wall Deformation Following Crack Formation and Growth

The crack propagation and arrest calculations are performed using the theoretical development presented in Anderson [22]. Crack arrest occurs when the dynamic stress intensity

factor is less than the material's resistance to further dynamic crack growth. In this development all of the resulting cracks are equal in length. Thus, the maximum tip-to-tip crack length is simply twice the calculated crack length.

5.2.3 Stage 3: Pressure Wall Petalling Deformation

Following the creation of cracks in the pressure wall, the nature of the deformation of the pressure wall changes dramatically. While the portion of the pressure wall beyond the cracks may continue to deform in a manner analogous to that which preceded crack formation, the deformation of the pressure wall containing takes an entirely different nature and appearance. Specifically, the pressure wall material between two adjacent cracks begins to curl in on itself in the direction of the line of flight of the debris cloud (see Figure 5b), i.e. it begins to petal.

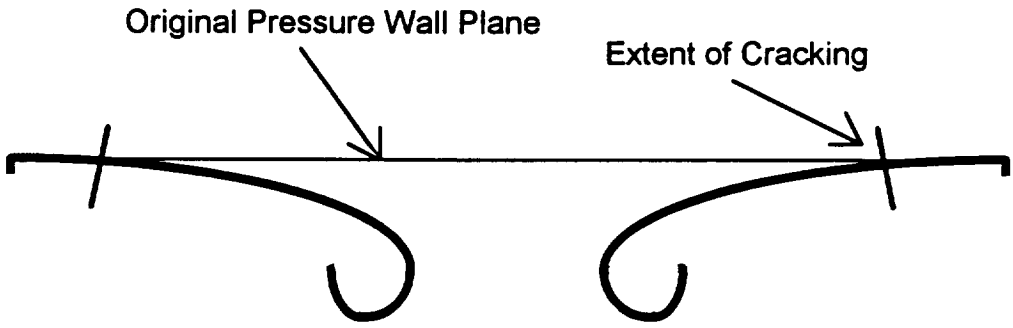

Figure 5b. Advanced Stage of Pressure Wall Cracking with Petals Shown

The shape of the pressure wall petals determined using the theoretical development in Ting [23]. The framework in Ting [23] contains a means to calculate the duration of continued deformation as well as the final deformed shape. Once the final deformed shape of the pressure wall is obtained, the total see-through area of the hole in the pressure wall is determined from the star-shaped outline of the deformed pressure wall petals. This total area is then converted into an equivalent circular hole diameter using simple geometry.

6.0 PRESSURE WALL DEFORMATION PRIOR TO CRACK FORMATION

6.1 Deformation Model Preliminaries

6.1.1 Pressure Wall Thinning Effects

In the development of the analytical pressure wall deformation model, it is assumed that the thickness of the pressure wall varies linearly from a minimum value at the center of the debris cloud impact footprint area to the outer perimeter of the footprint area where it attains its nominal constant value. Mathematically, this is stated as follows:

$$h(r) = h_o\left[\frac{r}{r^*} + \varepsilon\left(1 - \frac{r}{r^*}\right)\right] \tag{48}$$

where r^* is the radius of the pressure wall affected by the impact of the debris cloud (i.e. either R_{wp} or R_{wb}), $h_o=t_w$ is the nominal thickness of the pressure wall beyond r^*, and ε is the ratio of the thinnest pressure wall thickness value to its nominal thickness value, that is,

$$\varepsilon = \frac{h(0)}{h_o} \tag{49}$$

6.1.2 Pressure Wall Mass Per Unit Area

A quantity that will appear in subsequent expressions is the mass per unit area of the pressure wall. Since spatial integration of the expressions involving the pressure wall mass per unit area will also involve the load function developed in Chapter 4, these integration will typically have lower and upper limits of 0 and r^*. Hence, an expression for the pressure wall mass per unit area is required only in the regime $0<r<r^*$. This expression is written as follows:

$$\mu(r) = \frac{m(r)}{\pi r^2} \tag{50}$$

where m(r) is the pressure wall mass as a function of radial distance. The expression for m(r) is written as follows:

$$m(r) = \rho_w \int_0^r 2\pi r' h(r') dr' \tag{51}$$

Substituting equation (48) into equation (51), performing the indicated integration, and substituting the result into equation (50) yields the following expression for the pressure wall mass per unit area:

$$\mu(r) = 2\rho_w h_o \left[\frac{r}{3r^*} + \varepsilon\left(\frac{1}{2} - \frac{r}{3r^*}\right) \right] \tag{52}$$

6.1.3 Governing Equation of Motion

From elementary plate theory, we find that the axisymmetric dynamic response of a circular plate is governed by the following differential equation of motion:

$$\frac{\partial}{\partial r}(rM_r) - M_\theta = \int_0^r \left[\mu(r')r' \frac{\partial^2 w}{\partial t^2} - p(r', t) \right] dr' \tag{53}$$

where w(r,t) is the transverse displacement of the plate, $M_r(r,t)$ and $M_\theta(r,t)$ are the radial and circumferential bending moments in the plate, respectively, and $\mu(r)$ is given by equation (51).

6.1.4 Yield Criteria and Flow Rule

Since the plate response to the debris cloud impact is assumed to be rigid-perfectly plastic, plate yielding is assumed to be governed by the Tresca Yield Condition, which is illustrated in Figure 6 in stress space. In Figure 6, σ_o is the yield stress of the pressure wall material. This quantity is related to the maximum bending moment in the plate, M_o, as follows:

$$M_o(r) = \frac{1}{4}\sigma_o[h(r)]^2 \tag{54}$$

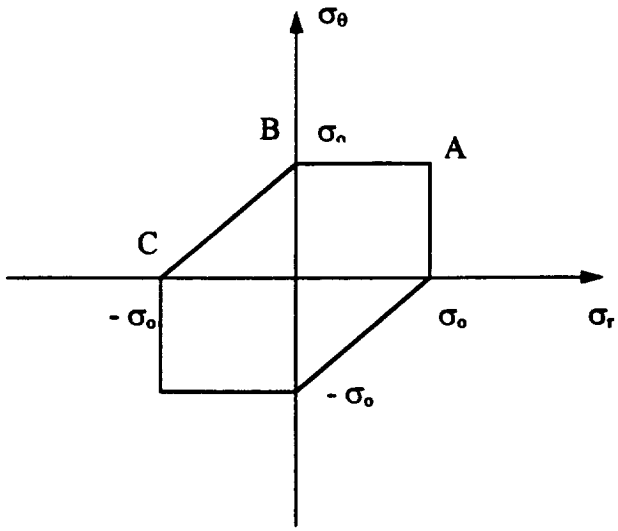

Figure 6. Tresca Yield Criterion in Stress Space

The plastic flow rule states that the flow vector with components (κ_r, κ_θ) is in the direction of the outward normal of the yield surface at the yield state (M_r, M_θ). The quantities κ_r and κ_θ are the radial and circumferential curvatures, respectively, and are related to transverse displacement as follows:

$$\kappa_r = -\frac{\partial^2 w}{\partial r^2} \quad , \qquad \kappa_\theta = -\frac{1}{r}\frac{\partial w}{\partial r} \tag{55a,b}$$

Thus, from the yield condition shown in Figure 6 and the associated flow rule described herein, the conditions on the stresses (and consequently the corresponding bending moments and curvatures) are given as follows:

Point A: $\sigma_r = \sigma_\theta = \sigma_o$, $\kappa_r \geq 0$, $\kappa_\theta \geq 0$ (56a)

Regime AB: $0 < \sigma_r < \sigma_o$, $\sigma_\theta = \sigma_o$, $\kappa_r = 0$, $\kappa_\theta \geq 0$ (56b)

Regime BC: $-\sigma_o < \sigma_r < 0$, $\sigma_\theta = \sigma_r + \sigma_o$, $\kappa_r = -\kappa_\theta > 0$ (56c)

According to Wang and Hopkins [21], during plastic deformation of clamped circular plates, the following statements can be made relating various portions of the plate to the regimes indicated in Figure 6 and mathematically characterized by equations (56a-c).

1) The center of the plate corresponds to point A. In this case, equation (56a) implies:

$$M_r = M_\theta = M_o(r = 0) \tag{57}$$

where M_o is given by equation (37).

2) The plate region $0 \le r \le r_1(t)$ corresponds to line segment AB, where $r = r_1$ defines the radial position at which $M_r = 0$, that is, r_1 defines the location of the plastic hinge. In this case, equation (56b) implies:

$$0 < M_r < M_o(r = 0)\ ,\ M_\theta = M_o(r) \tag{58}$$

3) The plate region $r_1(t) \le r \le R$ corresponds to line segment BC, where R is the radius of the plate itself. In this case, equation (56c) implies:

$$-M_o(r = R) < M_r < 0\ ,\ M_\theta = M_r + M_o(r) \tag{59}$$

6.1.5 Admissible Deformation Mechanism

Following the procedure developed by Florence [19,20], and Wang and Hopkins [21], the velocity of a plastically deforming clamped circular plate is written as follows:

$$\frac{\partial w}{\partial t}(r,t) = \begin{cases} v_o(t)\left(1 - \dfrac{\sigma r}{r_1}\right) & ,\quad 0 \le r \le r_1(t) \\ v_o(t)\sigma \ln\left(\dfrac{R}{r}\right) & ,\quad r_1(t) \le r \le R \end{cases} \tag{60a,b}$$

where

$$\frac{1}{\sigma} = \ln\left(\frac{R}{r_1}\right) + 1 \tag{61}$$

and $v_o(t)$ is the velocity of the plate center, an as yet unknown quantity. The acceleration of the plate is obtained by differentiating equation (60a,b) with respect to time and is given by the following expression:

$$\frac{\partial^2 w}{\partial t^2}(r,t) = \begin{cases} \dot{v}_o\left(1-\frac{\sigma r}{r_1}\right) - v_o\left(\frac{r_1\dot{\sigma}-\sigma\dot{r}_1}{r_1^2}\right) & , \quad 0 \le r \le r_1(t) \\ (v_o\dot{\sigma}+\sigma\dot{v}_o)\ln\left(\frac{R}{r}\right) & , \quad 0 \le r \le r_1(t) \end{cases} \tag{62a,b}$$

where a ($\dot{}$) indicates differentiation with respect to time.

We are now ready to apply the equations presented in Section 5.3 to the development of the expressions that characterize the deformation of the pressure wall prior to crack initiation as well as those that determine the moment at which crack formation commences. This will be accomplished in the next Section.

6.2 Pressure Wall Deformation Prior to Crack Formation

6.2.1 Preliminary Comments

The main objective of the development to follow is to obtain an expression for $v_o(t)$. Once this expression is obtained, equations (60a,b) can be integrated directly to yield the desired expression for pressure wall deformation prior to crack initiation, or w(r,t). To wit, if we integrate equations (56a,b) in their present form, we obtain the following expression for pressure wall deformation:

$$w(r,t) = \begin{cases} \left(1-\frac{\sigma r}{r_1}\right)\int_o^t v_o(t')dt' & , \quad 0 \le r \le r_1(t) \\ \sigma\ln\left(\frac{R}{r}\right)\int_0^t v_o(t')dt' & , \quad r_1(t) \le r \le R \end{cases} \tag{63a,b}$$

Thus, once $v_o(t)$ is known, equations (63a,b) can be used to find w(r,t).

The expression for $v_o(t)$ is ultimately found by applying the plastic hinge condition at $r = r_1$, that is, $M_r(r = r_1) = 0$. In order to apply this condition, the quantity r_1 must be defined explicitly. According to Florence [19,20], the exact value of r_1 will vary, depending on the magnitude of the applied load. From tabulated values of r_1 [19,20], it is apparent that $\lim_{p\to\infty} r_1 = a$, where 'p' is the magnitude of the applied load and 'a' is the plate radius over which the load is applied. Since our problem is concerned with very high loads, it is reasonable to assume, for the purposes of this model, that $r_1 = R_{wb}$. We have chosen R_{wb} instead of R_{wp} to define the position of the plastic hinge because the load due to the impact of the debris cloud bumper component is expected to be spread out over a larger area than the load due to the impact of the debris cloud projectile component.

We are now ready to begin the process by which we will obtain expressions for $v_o(t)$ and $w(r,t)$. We note that we must consider several possibilities. First, crack initiation may occur during the application of the debris cloud loads. Second, crack initiation may occur after the debris cloud loads have ended. Based on these possibilities, we need to develop expression for $v_o(t)$ and $w(r,t)$ while a load is being applied as well as after the applied load has been removed. Naturally, the possibility exists that the motion of the plate will cease without a crack ever having been formed. This possibility is considered as well in the development that follows.

6.2.2 Pressure Wall Deformation During Load Application

The process by which we obtain $v_o(t)$ is one in which the governing equation of motion for the plate, equation (53), is applied to the plate regimes $0 \le r \le r_1(t)$ and $r_1(t) \le r \le R$ under the conditions of plastic deformation defined by equations (58) and (59). The resulting equations for M_r are then manipulated to yield the required expression for $v_o(t)$.

$0 \le r \le r_1(t)$:

Substituting equations (52), (54), (59), and (63a) into equation (53), solving for $\partial(rM_r)/\partial r$, and integrating the result yields the following expression for $M_r(r,t)$ in this regime:

$$M_r(r,t) = \frac{\sigma_o h_o^2}{4}\left[\varepsilon^2 + \frac{\varepsilon(1-\varepsilon)}{r^*}r + \frac{(1-\varepsilon)^2}{3r^{*2}}r^2\right] + 2\rho_w h_o \dot{v}_o\left[\frac{\varepsilon r^2}{12} + (1-\varepsilon)\frac{r^3}{36r^*}\right]$$

$$- 2\rho_w h_o \dot{v}_o \frac{\sigma}{r_1}\left[\frac{\varepsilon r^3}{24} + (1-\varepsilon)\frac{r^4}{60r^*}\right] - \frac{1}{r}\int_0^r\int_0^{r'} p(r'',t)dr''dr' \qquad (64)$$

$r_1(t) \le r \le R$:

Substituting equations (52), (54), (59), and (63b) into equation (53), solving for $\partial(rM_r)/\partial r$, and integrating the result yields the following expression for $M_r(r,t)$ in this regime:

$$M_r(r,t) = \frac{\sigma_o h_o^2}{4}\left[\varepsilon^2 \ln\left(\frac{r}{r_1}\right) + \frac{2\varepsilon(1-\varepsilon)}{r^*}(r-r_1) + \frac{(1-\varepsilon)^2}{2r^{*2}}(r^2-r_1^2)\right]$$

$$+ 2\rho_w h_o \dot{v}_o \sigma\left\{\left[\frac{1-\varepsilon}{27r^*}r^3 \ln\left(\frac{R}{r}\right) + \frac{\varepsilon r^2}{8}\ln\left(\frac{R}{r}\right) + 2(1-\varepsilon)\frac{r^3-r_1^3}{81r^*}\right]\right.$$

$$+ \frac{\varepsilon}{8}(r^2-r_1^2) - \frac{1-\varepsilon}{27r^*}r_1^3 \ln\left(\frac{R}{r_1}\right) - \frac{\varepsilon r_1^3}{8}\ln\left(\frac{R}{r_1}\right)$$

$$\left. - \left[\frac{1-\varepsilon}{9r^*}r_1^3 \ln\left(\frac{R}{r_1}\right) + \frac{\varepsilon r_1^2}{4}\ln\left(\frac{R}{r_1}\right) + (1-\varepsilon)\frac{r_1^3}{27r^*} + \frac{\varepsilon r_1^2}{8}\right]\ln\left(\frac{r}{r_1}\right)\right\}$$

$$- \frac{1}{r}\int_0^r\int_0^{r'} p(r'',t)dr''dr' \qquad (65)$$

In order that these expressions for $M_r(r,t)$ satisfy kinematic admissability, it must also be true that equation (65) satisfies the plastic hinge condition at $r = r_1$, that is, $M_r(r_1,t) = 0$. Imposing this condition on equation (65), solving for $\dot{v}_o$, and integrating the result yields the following

expression for $v_o(t)$:

$$v_o(t) = \frac{1}{2\rho_w h_o r_1 \alpha} \int_0^{r_1} \int_0^{r} \int_0^{t} p(r', t')\, dt'\, dr'\, dr$$

$$- \frac{\sigma_o h_o t}{8\rho_w \alpha} \left[\varepsilon^2 + \varepsilon(1-\varepsilon)\frac{r_1}{r^*} + (1-\varepsilon)^2 \frac{r_1^2}{3r^{*2}} \right] \tag{66}$$

where

$$\alpha = \frac{r_1^3}{180 r^*}(1-\varepsilon)(5-3\sigma) + \frac{\varepsilon r_1^2}{24}(2-\sigma) \tag{67}$$

Finally then, substituting equation (66) into equations (63a,b) and performing the indicated integrations yields the expressions governing the plastic deformation of the plate during load application. These expressions are given as follows:

$0 \le r \le r_1(t)$:

$$w(r,t) = \frac{1}{2\rho_w h_o \alpha}\left(\frac{1}{r_1} - \frac{\sigma r}{r_1^2}\right) \int_0^{r_1} \int_0^{r} \int_0^{t} \int_0^{t'} p(r', t'')\, dt''\, dt'\, dr'\, dr$$

$$- \frac{\sigma_o h_o t^2}{16\rho_w \alpha}\left(1 - \frac{\sigma r}{r_1}\right) \left[\varepsilon^2 + \varepsilon(1-\varepsilon)\frac{r_1}{r^*} + (1-\varepsilon)^2 \frac{r_1^2}{3r^{*2}} \right] \tag{68}$$

$r_1(t) \le r \le R$:

$$w(r,t) = \frac{\sigma}{2\rho_w h_o \alpha r_1} \ln\left(\frac{R}{r}\right) \int_0^{r_1} \int_0^{r} \int_0^{t} \int_0^{t'} p(r', t'')\, dt''\, dt'\, dr'\, dr$$

$$- \frac{\sigma_o h_o \sigma t^2}{16\rho_w \alpha} \ln\left(\frac{R}{r}\right) \left[\varepsilon^2 + \varepsilon(1-\varepsilon)\frac{r_1}{r^*} + (1-\varepsilon)^2 \frac{r_1^2}{3r^{*2}} \right] \tag{69}$$

This completes the development of the equations required to define the motion of the pressure wall during this deformation phase.

6.2.3 Pressure Wall Deformation Following Load Removal

In this case, the process by which we obtain $v_o(t)$ is very similar to the one presented in Section 6.2.2, with one exception. Namely, the governing equation of motion for the plate, which is still given by equation (53), is applied to the plate regimes $0 \le r \le r_1(t)$ and $r_1(t) \le r \le R$ under the conditions of plastic deformation defined by equations (58) and (59). The resulting equations for M_r are again manipulated to yield the required expression for $v_o(t)$. Now, however, this process is performed under the additional condition of no load, i.e., $p(r,t) = 0$.

A point of interest is the definition of r_1 in this phase of plate deformation. Previous studies by Florence [19,20], Wang and Hopkins [21], and Krajcinovic [24] have all found that the variation of r_1 during this plate deformation phase is very small (i.e. on the order of 2%-4%) and can be neglected. Hence, for the purposes of this study, r_1 in this phase is kept constant at its previous value, that is, $r_1 = R_{wb}$.

The following is a summary of the results obtained for this phase of motion using the procedure outlined above.

$0 \le r \le r_1(t)$:

$$M_r(r,t) = \frac{\sigma_o h_o^2}{4}\left[\varepsilon^2 + \frac{\varepsilon(1-\varepsilon)}{r^*}r + \frac{(1-\varepsilon)^2}{3r^{*2}}r^2\right] + 2\rho_w h_o \dot{v}_o\left[\frac{\varepsilon r^2}{12} + (1-\varepsilon)\frac{r^3}{36r^*}\right]$$

$$- 2\rho_w h_o \dot{v}_o \frac{\sigma}{r_1}\left[\frac{\varepsilon r^3}{24} + (1-\varepsilon)\frac{r^4}{60r^*}\right] \qquad (70)$$

$r_1(t) \le r \le R$:

$$M_r(r,t) = \frac{\sigma_o h_o^2}{4}\left[\varepsilon^2 \ln\left(\frac{r}{r_1}\right) + \frac{2\varepsilon(1-\varepsilon)}{r^*}(r - r_1) + \frac{(1-\varepsilon)^2}{2r^{*2}}(r^2 - r_1^2)\right]$$

$$+2\rho_w h_o \dot{v}_o \sigma\left\{\left[\frac{1-\varepsilon}{27r^*}r^3\ln\left(\frac{R}{r}\right)+\frac{\varepsilon r^2}{8}\ln\left(\frac{R}{r}\right)+2(1-\varepsilon)\frac{r^3-r_1^3}{81r^*}\right]\right.$$

$$+\frac{\varepsilon}{8}(r^2-r_1^2)-\frac{1-\varepsilon}{27r^*}r_1^3\ln\left(\frac{R}{r_1}\right)-\frac{\varepsilon r_1^3}{8}\ln\left(\frac{R}{r_1}\right)$$

$$\left.-\left[\frac{1-\varepsilon}{9r^*}r_1^3\ln\left(\frac{R}{r_1}\right)+\frac{\varepsilon r_1^2}{4}\ln\left(\frac{R}{r_1}\right)+(1-\varepsilon)\frac{r_1^3}{27r^*}+\frac{\varepsilon r_1^2}{8}\right]\ln\left(\frac{r}{r_1}\right)\right\} \qquad (71)$$

To obtain the expression for $v_o(t)$ for this phase of pressure wall deformation, we begin by setting p(r,t) equal to zero in equation (66), differentiating with respect to time, and then integrating the result beginning at time t_o:

$$\int_{t_o}^{t} v_o(t')dt' = -\int_{t_o}^{t}\frac{\sigma_o h_o}{8\rho_w\alpha}\left[\varepsilon^2+\varepsilon(1-\varepsilon)\frac{r_1}{r^*}+(1-\varepsilon)^2\frac{r_1^2}{3r^{*2}}\right]dt' \qquad (72)$$

Performing the integrations indicated in equation (72) and applying intital conditions as appropriate results in the following expression for $v_o(t)$:

$$v_o(t)=\frac{1}{2\rho_w h_o r_1\alpha}\int_0^{r_1}\int_0^{r}\int_0^{t_o} p(r',t')dt'dr'dr$$

$$-\frac{\sigma_o h_o}{8\rho_w\alpha}\left[\varepsilon^2+\varepsilon(1-\varepsilon)\frac{r_1}{r^*}+(1-\varepsilon)^2\frac{r_1^2}{3r^{*2}}\right]t \qquad (73)$$

To obtain the expressions for w(r,t) for this plate deformation phase, we substitute equation (73) into equations (63a,b), perform the required integrations, apply appropriate initial conditions, and obtain the following results:

$0 \le r \le r_1(t)$:

$$w(r,t)=\frac{1}{2\rho_w h_o\alpha}\left(\frac{1}{r_1}-\frac{\sigma r}{r_1^2}\right)\left[\int_0^{r_1}\int_0^{r}\int_0^{t_o}\int_0^{t'} p(r',t'')dt''dt'dr'dr+(t-t_o)\int_0^{r_1}\int_0^{r}\int_0^{t_o} p(r',t')dt'dr'dr\right]$$

$$-\frac{\sigma_o h_o t^2}{16\rho_w \alpha}\left(1-\frac{\sigma r}{r_1}\right)\left[\varepsilon^2+\varepsilon(1-\varepsilon)\frac{r_1}{r^*}+(1-\varepsilon)^2\frac{r_1^2}{3r^{*2}}\right] \tag{74}$$

$r_1(t) \le r \le R$:

$$w(r,t)=\frac{\sigma}{2\rho_w h_o \alpha r_1}\ln\left(\frac{R}{r}\right)\left[\int_0^{r_1}\int_0^{r}\int_0^{t_o}\int_0^{t'} p(r',t'')dt''\,dt'\,dr'\,dr+(t-t_o)\int_0^{r_1}\int_0^{r}\int_0^{t_o} p(r',t')dt'\,dr'\,dr\right]$$

$$-\frac{\sigma_o h_o \sigma t^2}{16\rho_w \alpha}\ln\left(\frac{R}{r}\right)\left[\varepsilon^2+\varepsilon(1-\varepsilon)\frac{r_1}{r^*}+(1-\varepsilon)^2\frac{r_1^2}{3r^{*2}}\right] \tag{75}$$

This completes the development of the equations required to define the motion of the pressure wall during this deformation phase.

6.2.4 Termination of Pressure Wall Motion

The time t_m at which pressure wall motion ceases is that time at which the plate velocity equals zero, that is, when $v_o(t_m) = 0$. Making use of equation (73) results in the following expression for t_m:

$$t_m=-\frac{\dfrac{4}{\sigma_o h_o^2 r_1}\displaystyle\int_0^{r_1}\int_0^{r}\int_0^{t_o} p(r',t')dt'\,dr'\,dr}{\varepsilon^2+\varepsilon(1-\varepsilon)\dfrac{r_1}{r^*}+(1-\varepsilon)^2\dfrac{r_1^2}{3r^{*2}}} \tag{76}$$

7.0 PRESSURE WALL CRACK INITIATION, GROWTH, AND ARREST

7.1 Crack Initiation

To determine the instant of time at which crack growth begins (and hence the deformed configuration of the pressure wall at that time), we apply Gillemot's criterion of critical plastic work per unit volume [25]. This criterion states that material failure will occur when

$$\gamma_{1f}^2 + \gamma_{1f}\gamma_{2f} + \gamma_{2f}^2 = \varepsilon_{1f}^2 \tag{77}$$

where γ_{1f} and γ_{2f} are the principal in-plane strain components and ε_{1f} is the ordinate workability index of fracture strain. For our coordinate system, we have $\gamma_{1f} = \gamma_{rr}$ and $\gamma_{2f} = \gamma_{\theta\theta}$. Since we are under the assumption of axial symmetry, it follows that $\gamma_{\theta\theta} = 0$. In such a case, equation (77) reduces to the following form:

$$\gamma_{rr}^2 = \varepsilon_{1f}^2 \tag{78}$$

In cylindrical coordinates, the radial strain component γ_{rr} is written as follows:

$$\gamma_{rr} = \frac{\partial u}{\partial r} + \frac{1}{2}\left[\left(\frac{\partial u}{\partial r}\right)^2 + \left(\frac{\partial v}{\partial r}\right)^2 + \left(\frac{\partial w}{\partial r}\right)^2\right] \tag{79}$$

where 'u' and 'v' are the in-plane plate displacements. If we assume that these displacement components are small compared to 'w', the transverse plate displacement, then the radial strain component is given simply as

$$\gamma_{rr} = \frac{1}{2}\left(\frac{\partial w}{\partial r}\right)^2 \tag{80}$$

Substituting equation (80) into equation (78) and taking the square root of both sides

produces the following relationship which is used to determine the time t_c at which pressure wall crack initiation commences

$$\frac{\partial w(0,t_c)}{\partial r} = \sqrt{2\varepsilon_{1f}} \tag{81}$$

We note that implicit in equation (81) is the assumption that pressure wall cracking will commence at the center of the pressure wall loading area, i.e. at r = 0. This appears to be a reasonable assumption since it is at this point where strains attain their maximum value. Since crack initiation may occur due load application or after load removal, the form of w(r,t) to be used in equation (81) depends on whether $t < t_o$ or $t > t_o$. If $t < t_o$, then equation (68) is used; if $t < t_o$, then we use equation (74).

7.2 Initial Crack Length

While the initial extent of the failed region within the pressure wall that ultimately gives rise to crack formation and growth is undoubtedly microscopic, some finite estimate of the initial flaw size must be made in order that crack propagation and arrest theory may subsequently be used. In keeping with the first-principles-based philosophy of the model being developed, the initial crack length is estimated using the following relationship for Mode-I fracture in a thin plate under a uniformly distributed tensile load:

$$K_{IC} = S\sqrt{\pi a_o} \tag{82a}$$

where K_{IC} is the fracture toughness of the pressure wall material, a_o is the initial crack length, and 'S' is the applied tensile load. If we let $S = \sigma_o$ (i.e. the yield stress of the pressure wall material), then equation (82a) can be solved for the initial crack length a_o with the following result:

$$a_o = \frac{1}{\pi}\left(\frac{K_{Ic}}{\sigma_o}\right)^2 \tag{82b}$$

7.3 Number of Cracks

The number of cracks created by the impact of the debris cloud on the pressure wall can be estimated by considering the strain energy of the pressure wall just before and just after the cracks are created. Just before crack formation, the strain energy of the pressure wall is given as follows:

$$E_{bc} = \int_0^{t_c}\int_0^{r^*} (M_\theta \dot{\kappa}_\theta + M_r \dot{\kappa}_r) 2\pi r dr dt \tag{83}$$

Similarly, immediately after 'n' cracks, each of length a_o have formed, the energy in the pressure wall plate is given by the following expression:

$$E_{bc} = \int_0^{a_o} nG_{Ic} h(r) dr + \int_0^{t_c}\int_{a_o}^{r^*} (M_\theta \dot{\kappa}_\theta + M_r \dot{\kappa}_r) 2\pi r dr dt \tag{84}$$

where h(r) is given by equation (48), and G_{IC} is the Mode-I critical strain energy density of the pressure wall material. This quantity is related to K_{IC}, the fracture toughness of the material, as follows:

$$G_{IC} = \frac{K_{IC}^2}{E} \tag{85}$$

Equating equations (83) and (84), and noting that in equation (83), the integral from 0 to r* can be split into the sum of an integral from 0 to a_o and an integral from a_o to r*, results in the following expression for 'n':

$$nG_{Ic} \int_0^{a_o} h(r) dr = \int_0^{t_c}\int_0^{a_o} (M_\theta \dot{\kappa}_\theta + M_r \dot{\kappa}_r) 2\pi r dr dt \tag{86}$$

The integral on the right-hand side of equation (86) can be evaluated noting the following. First, according to equation (57), we have

$$M_\theta = M_o(r) \tag{87}$$

where $M_o(r)$ is given by equation (54). Next, since we are integrating in the region $0 < r < a_o < r_1$, equation (56b), together with equations (55a,b) and (60a), yields the following expression for the curvature rates $\dot{\kappa}_r$ and $\dot{\kappa}_\theta$:

$$\dot{\kappa}_r = 0 \tag{88a}$$

$$\dot{\kappa}_\theta = \left(\frac{v_o(t)\sigma}{r_1}\right)\frac{1}{r} \tag{88b}$$

Substituting equations (48), (54), (87), and (88a,b) into equation (86), performing appropriate integrations, and solving for 'n' yields the following expression for the number of cracks created by the impact of the debris cloud on the pressure wall:

$$n = \left(\frac{\pi}{2}\right)\left(\frac{\sigma}{r_1}\right)\left(\frac{\sigma_o h_o}{G_{IC}}\right)\left[\frac{6\varepsilon^2 + 6\varepsilon(1-\varepsilon)\eta + 2(1-\varepsilon)^2\eta^2}{6\varepsilon + 3(1-\varepsilon)\eta}\right]\int_0^{t_c} v_o(t)dt \tag{89a}$$

where

$$\eta = \frac{a_o}{r^*} \tag{89b}$$

The expression used for $v_o(t)$ depends on whether the crack starts before the load is removed, in which case it is given by equation (66), or after, in which case equation (73) is used.

7.4. Crack Propagation and Arrest

The governing equation for Mode I crack propagation under elasto-plastodynamic conditions is written as

$$K_I(t) = K_{ID}(V) \tag{90}$$

where $K_I(t)$ is the instantaneous dynamic stress intensity factor, K_{ID} is the dynamic material

resistance to crack propagation, and V is the velocity of crack propagation. It has been shown [22,26] that the stress intensity factor $K_I(t)$ can be written as

$$K_I(t) = \kappa(V)K_I(0) \tag{91}$$

where $\kappa(V)$ is a universal function of crack speed and $K_I(0)$ is the static Mode I stress intensity factor under elastic-plastic conditions. Thus, in order to be able to determine whether or not crack growth will occur, each of the terms $\kappa(V)$, $K_I(0)$, and $K_{ID}(V)$ must be determined.

To begin, we consider the static stress intensity factor. Using standard fracture mechanics techniques, it can be shown to be given by the expression

$$K_I(0) = \frac{\sigma\sqrt{\pi a}}{\sqrt{1 - \frac{1}{2}\left(\frac{\sigma}{\sigma_o}\right)}} \tag{92}$$

where σ is the applied tensile load and σ_o is the material yield stress. In our case, as discussed in the preceding section, $\sigma=\sigma_o$ so that for our problem, equation (92) reduces to the following form:

$$K_I(0) = 1.4142\sigma_o\sqrt{\pi a} \tag{93}$$

Next, the universal function $\kappa(V)$ was found [22] to be approximated quite well by the following expression:

$$\kappa(V) = \frac{1 - \frac{V}{C_r}}{\sqrt{1 - \xi V}} \tag{94}$$

where C_r is the Rayleigh wave speed of the material and ξ is given by the following expression:

$$\xi = \frac{2}{C_1}\left(\frac{C_2}{C_r}\right)^2\left(1 - \frac{C_2}{C_r}\right)^2 \tag{95}$$

In equation (95), C_1 and C_2 are the dilatational and shear wave speeds. These wave speeds can be

obtained using the following expressions:

$$C_1 = \sqrt{\frac{\lambda_w + 2\mu_w}{\rho_w}} \tag{96a}$$

$$C_2 = \sqrt{\frac{\mu_w}{\rho_w}} \tag{96b}$$

where ρ_w is the density of the pressure wall material. The parameters λ_w and μ_w are the Lame's constants for the pressure wall material, and are given by

$$\lambda_w = \frac{E_w \nu_w}{(1+\nu_w)(1-2\nu_w)} \tag{97a}$$

$$\mu_w = \frac{E_w}{2(1+\nu_w)} \tag{97b}$$

where E_w and ν_w are the elastic modulus and Poisson's ratio of the pressure wall material. In addition, the Rayleigh wave speed is approximately related to the shear wave speed through the following relationship:

$$C_r \cong \frac{0.862 + 1.14\nu_w}{1+\nu_w} C_2 \tag{98}$$

Finally, we consider $K_{ID}(V)$, the material resistance to dynamic crack propagation. This term is shown [22] to be given in terms of crack speed 'V' and K_{IA}, the crack arrest stress intensity factor (a material property like fracture toughness), as follows:

$$K_{ID}(V) = \frac{K_{IA}}{1 - \left(\frac{V}{V_L}\right)^m} \tag{99a}$$

where V_L is the limiting speed of crack propagation, 'm' is an empirical constant and

$$K_{IA} = \alpha_c K_{IC} \tag{99b}$$

In equation (99b), the parameter α_c is material specific; for aluminum, it has a value of 0.60.

As is evident from the above discussion, and especially in the discussion of the manner in which K_{ID} is calculated, it is necessary to possess an expression for crack propagation velocity. The following expression has been shown [27] to adequately model the speed of crack propagation in metallic materials:

$$V = 0.38C_o\left(1 - \frac{a_o}{a}\right) \tag{100}$$

where, as before, a_o is the initial crack length, 'a' is the instantaneous crack length, and C_o is the speed of sound in the material, that is,

$$C_o = \sqrt{\frac{E_w}{\rho_w}} \tag{101}$$

Based on this expression, it is easily seen that the limiting crack speed is given simply as

$$V_L = 0.38C_o \tag{102}$$

This completes the development of the equations required to determine whether or not crack propagation occurs. These equations are used in a step-by-step fashion, beginning with a crack length of a_o. The crack length is increased by a small amount Δa. For this new crack $a+\Delta a$, the quantities V, $K_I(0)$, $\kappa(V)$, and $K_{ID}(V)$ are computed using appropriate equations. If $K_I(t)$ exceeds $K_{ID}(V)$, crack propagation continues and the process is repeated with a new slightly larger crack length. If $K_I(t)$ drops below $K_{ID}(V)$, we have crack arrest.

8.0 PRESSURE WALL DEFORMATION FOLLOWING CRACK FORMATION

8.1 Introductory Comments

The shape of the pressure wall petals is determined using the theoretical development in Ting [23]. The framework in Ting [23] contains a means to calculate the large deformation of a cantilever beam as the free end of the beam experiences curling. Ting's approach was chosen because the final deformed shape of the cantilever closely resembled the final deformed shape of a pressure wall petal under debris cloud impact loading. However, whereas Ting assumed a cantilever beam with a constant-width and constant depth rectangular cross-section, pressure wall petals are typically triangular when viewed from the top or bottom. The sharpness of the petal tips at the point of crack formation resulted in singularities that, unfortunately, could not be avoided. Therefore, in order to be able to use Ting's method, each petal was modeled as a constant-width and constant-depth cantilever beam with average depth and width properties based on actual petal cross-section and width properties. When applied in such a manner, Ting's model can be said to produce the deformation of the petal centerline. The relationship between deformation of the centerline and that of parallel cross-sections is discussed in the section where the method used to calculate equivalent hole diameter is developed.

8.2 Average Petal Cross-Section Properties

Figures 7a and 7b show the top-view and side-view of a petal cross-section along its centerline. According to Figure 7a, it is easily seen that the average width of a pressure wall petal is given by

$$b_{avg} = a_{lim} \sin\left(\frac{\pi}{n}\right) \tag{103}$$

where a_{lim} and n are the length of a pressure wall crack and number of pressure wall cracks, respectively, as calculated using the procedure developed in Chapter 7.

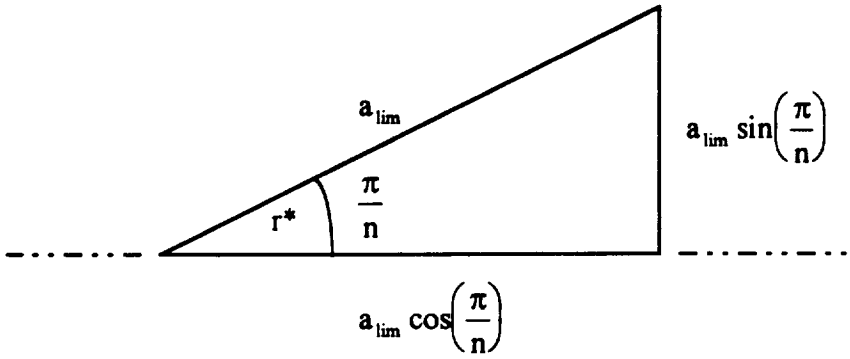

Figure 7a. Top View of Pressure Wall Petal Half

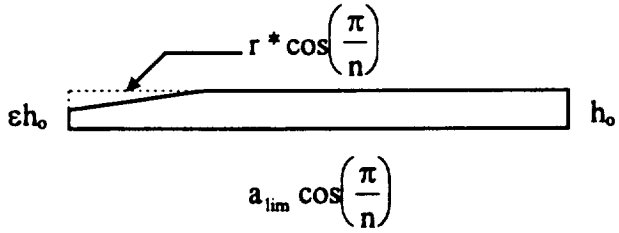

Figure 7b. Side View of Pressure Wall Petal Half Along Centerline

The average depth of a pressure wall petal is found using the information and simple geometric principles with the following result:

$$h_{avg} = h_o(1-\varepsilon)\left[1 - \frac{1}{2}\left(\frac{r^*}{a_{lim}}\right)\right] \tag{104}$$

8.3 Pressure Wall Petalling Model

As in Ting [23], we consider a cantilever beam of uniform cross-section with a mass G attached at its free end subjected to a transverse impact velocity V_o at the tip mass (see Figure 8).

The length of the beam is L, and the beam mass is mL. Figure 8 also shows a typical state of deformation at any time in which a plastic hinge appears at a distance ζ from the tip. Naturally, the position of the hinge ζ is a function of time.

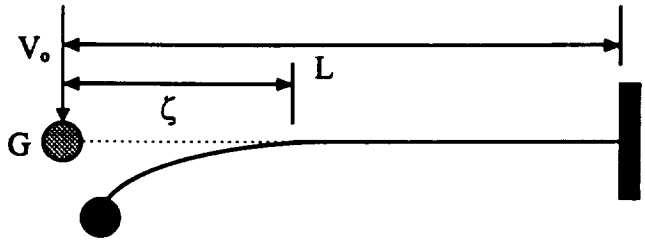

Figure 8. Typical Cantilever Beam Deformation

If we assume ζ is a one-to-one function of time, then we can take ζ as the independent variable rather than time. Thus, the slope angle $\theta(r,\zeta)$ at r when the hinge is at ζ is given by (see Figure 9):

$$\theta(r,\zeta) = \int_r^{\zeta} \kappa(\xi)d\xi \tag{105}$$

where $\kappa(\zeta)$ is the curvature of the beam at ζ.

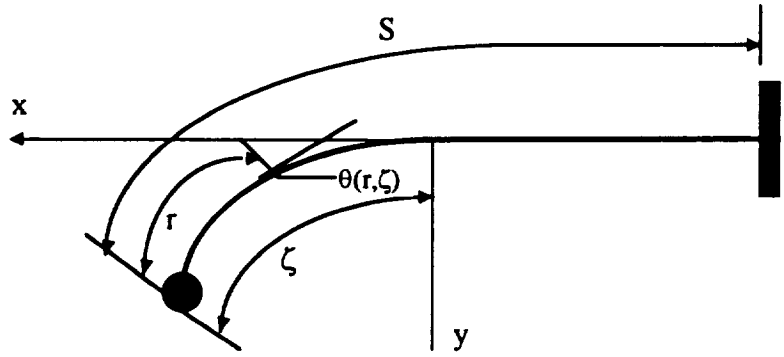

Figure 9. Coordinate and Parameter Definitions for Cantilever Beam Deformation

According to Figure 9, we can define the coordinates of a point (x,y) as follows:

$$x(r,\zeta) = \int_r^{\zeta} \cos\theta(\xi,\zeta)d\xi \tag{106a}$$

$$y(r,\zeta) = \int_{r}^{\zeta} \sin\theta(\xi,\zeta)d\xi \tag{106b}$$

Using these definitions, the first moment of the deformed portion of the beam about the x- and y-axis are given as follows:

$$I_1(\zeta) = m\int_{0}^{\zeta} x(r,\zeta)dr + Gx(0,\zeta) \tag{107a}$$

$$I_2(\zeta) = m\int_{0}^{\zeta} y(r,\zeta)dr + Gy(0,\zeta) \tag{107b}$$

respectively. Similarly, the second moment of the deformed portion of the beam about the plastic hinge is given as follows:

$$I_0(\zeta) = m\int_{0}^{\zeta} [x^2(r,\zeta) + y^2(r,\zeta)]dr + G[x^2(0,\zeta) + y^2(0,\zeta)] \tag{108}$$

Conservation of linear and angular momentum for the deformed portion of the beam are given by the relationships

$$GV_o = I_1(\zeta)\kappa(\zeta)\frac{d\zeta}{dt} \tag{109a}$$

$$t(\zeta) = \frac{GV_o}{M_o}\left[\zeta - \frac{I_o(\zeta)}{I_1(\zeta)}\right] \tag{109b}$$

respectively, while energy conservation yields the following expression

$$\int_{0}^{\zeta} \kappa(r)dr + \frac{1}{2}\left(\frac{G^2V_o^2}{M_o}\right)\left(\frac{I_o(\zeta)}{I_1(\zeta)}\right) = \frac{1}{2}\left(\frac{GV_o^2}{M_o}\right) \tag{109c}$$

After some manipulation (see [23]), equation (109c) reduces to following expression for the curvature of the beam at the location of the plastic hinge:

$$\kappa(\zeta)=\left(\frac{G^2V_o^2}{M_o}\right)\left[\frac{(G+m\zeta)I_o(\zeta)-[I_1(\zeta)]^2}{[I_1(\zeta)]^3+\left(\frac{G^2V_o^2}{M_o}\right)I_o(\zeta)I_2(\zeta)}\right] \tag{110}$$

(In passing, we note that appearing throughout these equations are the parameters G, the assumed beam tip mass, m, the mass per unit length of the beam, V_o, the impact velocity, and M_o, the beam yield moment. Further attention in defining these terms and relating them to pressure wall parameters will be discussed in a subsequent sub-section.)

When the plastic hinge reaches the fixed end $\zeta = s$, the motion of the beam is a rigid body rotation about the fixed end. Let θ_s denote the angle resulting from this rotation. Since the input energy $GV_o^2/2$ must be equal to the energy absorbed in the plastic deformation of the beam when the deformation is completed, we can write the following energy balance expression:

$$M_o\theta(0,s) + M_o\theta_s = \frac{GV_o^2}{2} \tag{111}$$

where $\theta(0,s)$ is the total rotation of the cantilever tip. If we divided both sides of equation (111) by M_o and compare the result with equation (109c), we see the following expressions for $\theta(0,s)$ and θ_s emerge:

$$\theta(0,s)=\int_0^s \kappa(r)dr \tag{112a}$$

$$\theta_s=\frac{1}{2}\left(\frac{G^2V_o^2}{M_o}\right)\left(\frac{I_o(\zeta)}{I_1(\zeta)}\right) \tag{112b}$$

The final slope along the beam is thus given as

$$\theta_f(r)=\theta_s+\theta(r,s)=\theta_s+\theta(0,s)-\theta(0,r) \tag{113}$$

According to equation (111), equation (113) reduces further to the following form:

$$\theta_f(r) = \alpha_o - \theta(0,r) \tag{114}$$

where

$$\alpha_o = \frac{GV_o^2}{2M_o} \tag{115}$$

It is interesting to note that since $\theta(0,0) = 0$, $\theta_f(0) = \alpha_o$. Thus we have the result that the final slope or rotation at the free end of the cantilever beam is simply equal to the ratio of the initial energy imparted to the beam to the yield moment of the beam. To compute the final deformed state, that is, the final x- and y- coordinates of a point along the petal centerline a distance 'r' away from the free end when the plastic hinge is at $\zeta = a_{lim}$, we use equations (106a,b) written in the following form:

$$x_f(r, a_{lim}) = \int_r^{a_{lim}} \cos\theta_f(\xi)d\xi \tag{116a}$$

$$y_f(r, a_{lim}) = \int_r^{a_{lim}} \sin\theta_f(\xi)d\xi \tag{116b}$$

where θ_f is given by equation (114).

This completes the development of the equations required to characterize the curling deformation of a cantilever beam struck at its tip. Curvatures, slopes, and displacements are computed using sequential calculations that follow from an initial value $\kappa(0)$. This initial value is found by letting $\zeta \to 0$ in equation (110) with the following result:

$$\kappa(0) = \left(\frac{m}{3}\right)\left(\frac{V_o^2}{M_o}\right) \tag{117}$$

The details of the numerical scheme, which is implemented in non-dimensional form, used can be found in Ting [23].

8.4 Values for G, M_o, m, and V_o

In keeping with the assumption of a rectangular cross-section cantilever beam, the mass per unit length and yield moment are simply defined as

$$m = \rho_w b_{avg} h_{avg} \tag{118a}$$

$$M_o = \frac{1}{4}\sigma_o b_{avg} h_{avg}^2 \tag{118b}$$

respectively. The impact velocity, V_o, is taken to be the pressure wall velocity $v_o(t=t_c)$, that is, at the time of crack initiation (see Section 7.1). Finally, the value of G is the debris cloud mass per petal, that is,

$$G = \frac{m_p + m_b + m_{ib}}{n} \tag{119}$$

However, such a simplistic form was subsequently found to yield unrealistically high values of α, the final beam tip rotation. A review of experimental evidence shows that the pressure wall petal tips rarely rotated through more than 360°, or 2π. Hence, in the event that the value of G calculated using equation (119) yielded a value of α_o in excess of 2π, it was reduced to the value that would in fact yield a value of 2π for α_o, that is, it was found by solving the equation

$$\alpha_o = 2\pi = \frac{GV_o^2}{2M_o} \tag{120}$$

8.5 Onset of Pressure Wall Petalling

In examining damaged pressure walls from a variety of different high speed impact tests, it became apparent that not all pressure walls exhibited petalling upon perforation. Rather, some perforated pressure walls holes retained their flatness and contained what may be called "cookie-cutter holes", that is, holes with jagged edges from which pressure wall material had been simply

punched out. It, therefore, became necessary to develop a means by which it would be possible to determine, a priori, whether a pressure wall perforation would be in the form of a petaled hole or a cookie-cutter hole. Further examination of damaged pressure walls revealed that the likelihood of petalling occurring increased:

- when the inner bumper was closer to the pressure wall;
- when the inner bumper was made from a relatively heavy material;
- for higher impact velocities;
- for larger projectile diameters;
- for thinner pressure walls; and,
- for normal impacts.

Based on these observations, a petalling limit function f_{pet} was developed such that if, for a given set of impact conditions and geometric parameters, its value exceeded a certain critical value f_{cr}, then pressure wall perforation would be accompanied by petalling. Alternatively, if the value of the petalling limit function was less than the critical value f_{cr}, then pressure wall perforation would be in the form of a cookie-cutter hole. The next sections addresses the form of the function f_{pet} and the manner in which f_{cr} was determined.

8.5.1 The Petalling Limit Function f_{pet}

Based on the observations in the preceding section, the functional form of f_{pet} should be such that it attain relatively large values for lower values of S_2/S, larger values of $\lambda_{ib}/\rho_w t_w$, larger values of V_p/C_w, and larger values of d_p/t_w. A natural choice for such a function is the following:

$$f_{pet} = e^{\beta\left(1-\frac{S_2}{S}\right)}\left(\frac{\lambda_{ib}}{\rho_w t_w}\right)\left(\frac{V_p}{C_w}\right)\left(\frac{d_p}{t_w}\right)\cos\theta_p \qquad (121)$$

The nature and value of the constant β will be discussed in the following section.

8.5.2 Determining the Value of f_{cr}

To assist with determining an appropriate value of f_{cr} for the multi-wall systems under considerations, a damage descriptor is required. The purpose of this descriptor is to distinguish between holes with only one or two cracks and holes with five or six cracks (a truly petaled pressure wall), and between holes in which the cracks extended only slightly beyond the pressure wall hole and holes in which the cracks extended significantly beyond the pressure wall hole (again, a truly petaled pressure wall). A function that meets these requirements can be written as follows:

$$\delta = \left(\frac{L_{tt}}{D_{eq}} \right)^{N_{cr}-2} \tag{122}$$

where L_{tt}, D_{eq}, and N_{cr} are the measured values of pressure wall maximum tip-to-tip crack length, equivalent circular hole diameter, and number of cracks. Thus, according to equation (122), a hole with only two cracks would yield a value of $\delta=1$, regardless of how long the cracks were, while a hole with 6 cracks in which the maximum tip-to-tip crack length was 5 times the equivalent diameter would yield of value of $\delta=625$.

The value of f_{cr} was determined by calculating corresponding values of δ and f_{pet} for 206 high speed impact tests. The data from these tests are presented in Appendix A. A side-by-side examination of the values of δ and f_{pet} for these tests revealed that an appropriate cut-off between petalling and non-petalling perforations occurred at a petalling limit function value of 0.22, that is $\mathbf{f_{cr} = 0.22}$. This value was obtained using a value of $\beta=2$; other values of β would naturally yield different cut-off value.

8.6 Equivalent Hole Diameter

The method for calculating equivalent hole diameter depends on whether or not the perforation was accompanied by petalling. If it was not, then the diameter of the hole created is simply taken to be some fraction of the radius of the projectile component debris cloud:

$$D_{eq} = C_D R_{wp} \tag{123}$$

However, if it was a petalling perforation, then the equivalent hole diameter is taken to be that of a circle with an area equal to the see-through area of the petaled pressure wall. This see-through area is calculated as follows. To begin, we consider the top view of half of a deformed pressure wall petal as shown in Figure 10 below.

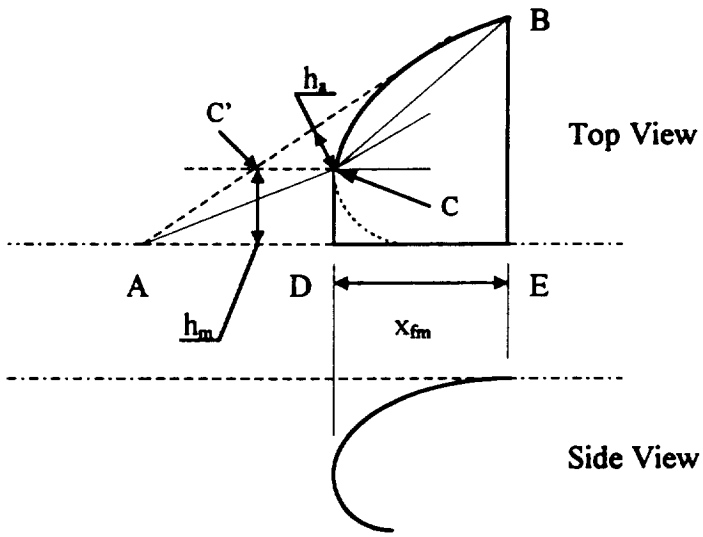

Figure 10. Top and Side Views of Deformed Pressure Wall Petal Half

As can be seen in Figure 10, the see-through area for half of a pressure wall petal can be approximated by the sum of the areas of triangles ABC and ACD. Since this actually overstimates the see-through area, the conservative nature of the model is maintained. Assuming symmetry

conditions for the other petals, the total see-through area is thus given as follows:

$$A_{tot} = 2n(A_{\Delta ABC} + A_{\Delta ACD}) \tag{124}$$

Referring back to Figures 7a,b and making use of the definitions in Figure 10, equation (124) is more explicitly written as follows:

$$A_{tot} = 2n\left\{\frac{1}{2}\left[a_{lim}\cos\left(\frac{\pi}{n}\right) - x_{fm}\right]h_m + \frac{1}{2}a_{lim}h_a\right\} \tag{125}$$

where h_a is the perpendicular distance from point C to line segment AB (i.e. the height of triangle ABC). The distances x_{fm} is calculated as part of the procedure presented in Section 8.5 while the distance h_a obtained using elementary trigonometry and is given as follows:

$$h_a = \cos\left(\frac{\pi}{n}\right)\left[a_{lim}\sin\left(\frac{\pi}{n}\right) - h_m\right] - x_{fm}\sin\left(\frac{\pi}{n}\right) \tag{126}$$

The distance h_m is obtained by noting that it is also the distance from the petal centerline to the nearest pressure wall crack along a line that is normal to the centerline and that emanates from a special point on the crack. This point lies at the intersection of the line defining the crack and a line that is parallel to the centerline and which passes through the point on the petal that is farthest away from the petal base (i.e. point C' in Figure 10).

At this point it also becomes clear that while Ting's method can be used to calculate the deformation of the petal centerline, it does not explicitly address the deformation of petal cross-sections that are parallel to the centerline. However, the centerline deformation can in fact be used to estimate that of other parallel cross-sections as follows. Consider once again the top view of a deformed petal as shown in Figure 11 below.

In Figure 11, points A, B, and C lie along the line defining the original position of the pressure wall crack adjacent to the petal; points D and E are points on the petal centerline that

correspond to points B and C, that is, points D and E are the projections of points B and C, respectively, on the petal centerline. We wish to determine the coordinates of points A', B', and C', which are the coordinates of points A, B, and C following petalling deformation. That is, we wish to calculate $x_f(r_A,z_A)$, $x_f(r_B,z_B)$, $x_f(r_C,z_C)$, and $y_f(r_A,z_A)$, $y_f(r_B,z_B)$, $y_f(r_C,z_C)$, and $z_f(r_A,z_A)$, $z_f(r_B,z_B)$, $z_f(r_C,z_C)$, where r_j and z_j define the initial positions of points A, B, C in the r-z plane (i.e. the original flat plane of the undeformed pressure wall).

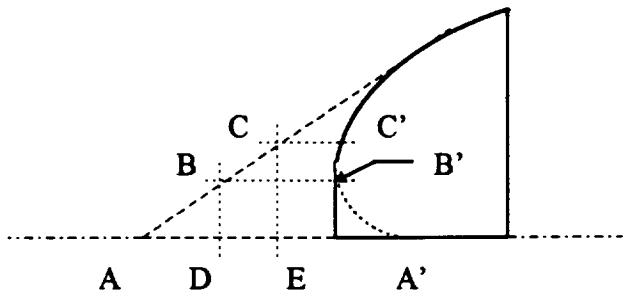

Figure 11. Top View of Deformed Pressure Wall Petal Half

The coordinates of the points A', B', and C' are determined using the following rules:

1. a point initially on the petal centerline remains on the centerline following deformation;
2. a point initially on a petal cross-section parallel to the petal centerline remains on the same parallel cross-section following deformation (i.e. parallel cross-sections remain straight and parallel);
3. the motion of a point on a cross-section parallel to the petal centerline is identical to that of the point on the centerline that is the projection of the point of interest onto the petal centerline.

Therefore, according to rules #1 and #2, point A moves to location A' according to the Ting model and remains on the centerline. Likewise points B and C move to points B' and C' and

remain on their parallel cross-sections. And, according to rule #3, the motion of point B is identical to that of point D (which is found using the Ting model since point D is on the petal centerline) while the motion of point C is the same as that of point E (which is also found using the Ting model). Thus, using this framework, the motion of any point on the pressure wall and its final position following petalling deformation can be found using the Ting model. This completes the development of the equations necessary to obtain the equivalent circular hole diameter in the event of a petaled pressure wall perforation.

9.0 APPLICATION TO OBLIQUE IMPACT

9.1 Introductory Comments

The model developed in the previous chapters is strictly applicable to normal impacts. However, the majority of orbital debris impacts will occur along non-normal trajectories. Hence, to be applicable to orbital debris impacts, it is necessary to extend the model to the case of oblique high speed impact. Consider the oblique impact of a dual-wall structure as shown in Figure 12. In Figure 12, M_1, M_2, and M_r are the masses of the 'normal", 'in-line', and 'ricochet' debris clouds. Analogously, the quantities V_1, V_2 and V_r, and θ_1, θ_2, and θ_r are the axial velocities and trajectories of the these debris clouds, respectively. We also introduce the parameter V_e (not shown in Figure 12) which is used to characterize the (assumed equal) average radial expansion velocity of each of these three debris clouds.

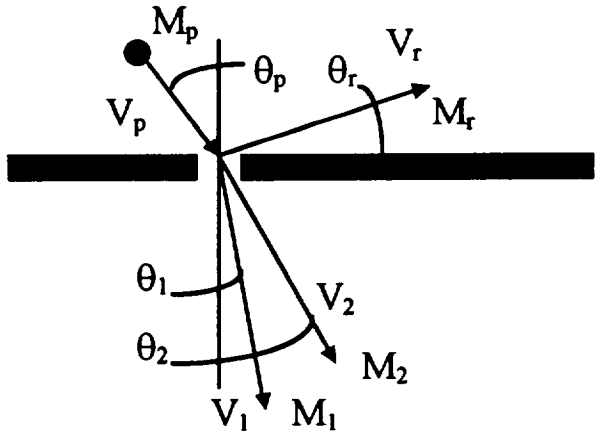

Figure 12. Oblique Hypervelocity Impact of a Flat Plate

In the following sections, a model that can be used to calculate M_i, θ_i and V_i (i=1,2 and r)

as functions of the initial impact parameters M_p, V_p, and θ_p is presented and subsequently verified by comparing its predictions with experimental results. Following verification, the model is applied to the problem of calculating crack length and hole diameter using some of the underlying principles of the normal impact model developed in the preceding chapters.

9.2 Oblique Impact Model Development

Applying conservation of momentum before and after the initial impact of the projectile on the bumper plate in the vertical and horizontal directions, we arrive at the following equations:

$$M_p V_p \cos\theta_p = M_1 V_1 \cos\theta_1 + M_2 V_2 \cos\theta_2 - M_r V_r \sin\theta_r \tag{127}$$

$$M_p V_p \sin\theta_p = M_1 V_1 \sin\theta_1 + M_2 V_2 \sin\theta_2 + M_r V_r \cos\theta_r \tag{128}$$

Assuming that no mass is lost in the initial impact, the mass conservation principle yields

$$M_p + M_f = M_1 + M_2 + M_r \tag{129}$$

where M_f is the mass of the material that is punched out in the creation of the eliptical hole in the bumper plate. This quantity is calculated by noting that for the trajectory obliquities considered, the bumper plate hole is elliptical [4]:

$$M_f = \frac{1}{4}\pi\rho_b D_{min} D_{max} t_b \tag{130}$$

The quantities D_{min} and D_{max} are the lengths of the minor and major axes of the bumper plate hole and were calculated using the following empirical equations [4]:

$$\frac{D_{min}}{d_p} = 2.698\left(\frac{V_p}{C_b}\right)^{0.689}\left(\frac{t_b}{d_p}\right)^{0.708}\cos^{0.021}\theta_p + 0.93 \tag{131a}$$

$$\frac{D_{max}}{d_p} = 2.252\left(\frac{V_p}{C_b}\right)^{0.622}\left(\frac{t_b}{d_p}\right)^{0.667}\exp(0.815\theta_p) + 1.00 \tag{131b}$$

where θ_p is in radians. We note that these equations were derived from hypervelocity impact tests in which spherical aluminum projectiles impacted thin aluminum plates. Hence, while the general methodology described herein may be valid for other materials besides aluminum, the use of empirical equations based on tests employing aluminum plates renders this specific analysis valid only for spherical aluminum projectiles impacting aluminum bumper plates.

Equations (127)-(129) constitute a system of 3 equations in 9 unknowns which must be solved for: 3 debris cloud masses, 3 axial velocities, 3 center-of-mass trajectories. An additional unknown exists in the form of the average radial expansion velocity of the debris clouds V_e, which must also be solved for. The solution process is facilitated by utilizing experimental observations from high-speed impact tests of aluminum dual-wall structures to determine several of the unknowns in equations (127)-(129). The remaining unknowns can then be determined in closed form. Once this is accomplished, an additional equation can be introduced to solve for V_e. The process by which this is done is described in the following sections.

9.3 Trajectory Angles

The angles θ_1 and θ_2 initially increase as θ_p is increased [4]. This continues until a critical value of θ_p is reached beyond which θ_1 and θ_2 decrease with continued increases in θ_p. This kind of behavior is very difficult to predict analytically without resorting to an advanced shock physics analysis. As a result, the analytical prediction of this behavior is beyond the scope of the present work. The empirical equations used to calculate values of θ_1 and θ_2 as functions of the initial impact parameters are given below [4]:

$$\frac{\theta_1}{\theta_p} = 0.471\left(\frac{V_p}{C_b}\right)^{-0.049}\left(\frac{t_b}{d_p}\right)^{-0.054}\cos^{1.134}\theta_p \qquad (132a)$$

$$\frac{\theta_2}{\theta_p} = 0.532\left(\frac{V_p}{C_b}\right)^{-0.086}\left(\frac{t_b}{d_p}\right)^{-0.478}\cos^{0.586}\theta_p \qquad (132b)$$

The angle θ_r, that is, the trajectory of the center-of-mass of the ricochet debris cloud, has been observed to decrease monotonically with increasing values of trajectory obliquity. The empirical relationship characterizing θ_r in terms of θ_p is given below [28]:

$$30^\circ < \theta_p \le 45^\circ,\ \theta_r = -\frac{10}{3}\theta_p + 160^\circ \qquad (133a)$$

$$45^\circ < \theta_p \le 60^\circ,\ \theta_r = -\frac{1}{3}\theta_p + 25^\circ \qquad (133b)$$

$$60^\circ < \theta_p \le 75^\circ,\ \theta_r = -\frac{1}{6}\theta_p + 15^\circ \qquad (133c)$$

By using equations (132a,b) and (133a-c), θ_1, θ_2, and θ_r can be treated as known quantities which reduces the number of unknowns in equations (127)-(129) to six.

9.4 Debris Cloud Masses

The three unknown debris cloud masses are calculated by systematically distributing the mass of the projectile and the mass of the bumper plate material that is punched out by the initial impact among the three debris clouds and then invoking the conservation of mass equation, equation (129). This distribution process is accomplished as follows.

First, it is noted that as θ_p increases, the amount of material in the normal and in-line debris clouds monotonically decreases while that in the ricochet debris cloud steadily increases [4]. Furthermore, it has been hypothesized that the material in the normal debris cloud is primarily bumper plate material, while the material in the in-line debris cloud is primarily projectile material [3]. The obliquity of the initial impact on the bumper plate also mandates that the in-line and

ricochet debris clouds contain a portion of the bumper plate material. Based on these observations, we postulate the following functional forms of M_1 and M_2:

$$M_1 = \overline{M_f} \cos^n \theta_p \tag{134a}$$

$$M_2 = \alpha_2 (M_f - \overline{M_f}) \cos^n \theta_p + M_p \cos^n \theta_p \tag{134b}$$

where M_f is the mass of bumper plate material that would be ejected in a normal impact at a reduced velocity $V' < V_p$, i.e. $M_f = M_f(\theta_p=0°, V_p=V')$, and α_2 is that fraction of the ejected bumper plate material in the in-line debris cloud. These forms satisfy the requirement that the debris cloud masses decrease as θ_p increases and do not violate the hypotheses regarding the origins of the material in the respective debris clouds. The values of the exponent n and the coefficient α_2 are adjusted so that the final predictions for the debris cloud spread angles based on this analysis procedure compare well with those obtained using empirical predictor equations for debris cloud spread angles [4].

The reduced velocity V' used to calculate the mass of bumper plate material in the 'normal' debris cloud is taken to be the normal component of the original impact velocity. Any material in excess of that which such a normal impact would produce is allocated to the 'in-line' and ricochet debris clouds. Therefore, the reduced velocity V' is given by

$$V' = \eta V_p \cos\theta_p \tag{135}$$

where η is a correction factor that is also adjusted so that the final predictions for debris cloud spread angles based on the analysis procedure presented herein compare well with those obtained using empirical predictor equations. Substitution of equations (134a,b) into equation (129) results in the following expression for the mass of the ricochet debris cloud:

$$M_r = (1 - \alpha_2)(M_f - \overline{M_f})\cos^n\theta_p + (M_f + M_p)(1 - \cos^n\theta_p) \quad (136)$$

These calculations and assumptions allow M_1, M_2, and M_r to be treated as known quantities which reduces the number of unknowns to three. Since one of the equations was used in the preceding analysis, we now have a system of two equations in three unknowns (V_1, V_2, V_r).

9.5 Debris Cloud Axial Velocities

Since the 'normal' debris cloud is assumed to contain only bumper plate material and the mass of that material is calculated assuming a normal impact, the method for calculating its velocity is based on a procedure currently utilized for calculating debris cloud velocities in normal impacts of thin plates. This procedure is summarized in the following paragraph.

The initial normal impact of a projectile on a thin plate produces a shock wave that undergoes reflection at the rear surface of the plate. An elementary shock wave propagation analysis indicates that the velocity of the rear surface at the moment of reflection is equal to twice the particle velocity of the plate material as the shock wave passes through the plate. For a normal impact of an aluminum projectile on an aluminum plate, particle velocity is equal to one-half of the impact velocity. Hence, a simple substitution shows that for the particular projectile and bumper plate materials under consideration, under normal impact, the velocity of the rear surface of the plate is equal to the initial normal impact velocity. Since the reflection of the shock wave from the rear surface causes the plate material to fragment and thereby creates the debris cloud, the presumption is made that the axial velocity of the debris cloud created by the normal impact is equal to the velocity of the rear surface of the plate.

Since the normal velocity assumed to create the 'normal' debris cloud is given by V', then the axial velocity of the 'normal' debris cloud is also given by V', that is,

$$V_1 = \eta V_p \cos\theta_p \tag{137}$$

We are now left with a system of two equations in two unknowns, V_2 and V_r. This system is solved explicitly with the following results:

$$V_2 = \frac{M_p V_p \cos(\theta_p - \theta_r) - V_1 \cos(\theta_1 - \theta_r)}{M_2 \cos(\theta_2 - \theta_r)} \tag{138a}$$

$$V_r = \frac{M_p V_p \sin\theta_p - M_1 V_1 \sin\theta_1 - M_2 V_2 \sin\theta_2}{M_r \cos\theta_r} \tag{138b}$$

Thus, all of the unknowns in equations (127)-(129) are now determined. The final unknown to be determined is V_e, which is found using the method presented in the next Section.

9.6 Debris Cloud Radial Expansion Velocities

If we apply the principle of energy conservation before and after the initial impact of the projectile on the bumper plate, we have the following symbolic equation:

$$K.E._{initial} = K.E._{debris} + K.E._{lost} \tag{139}$$

where the initial kinetic energy is that of the incoming projectile, the kinetic energy of the debris clouds is that due to their axial motion and expansion, and the kinetic energy that is lost is due to the irreversible processes that occur during the initial impact such as material heating, light flash, etc. If the energy that is lost is written as some fraction ξ of the initial impact energy, then writing the kinetic energy of the projectile and the debris clouds in standard form yields the following:

$$\frac{1}{2}(1-\xi) M_p V_p^2 = \frac{1}{2}(M_1 + M_2 + M_r) V_e^2 + \frac{1}{2}(M_1 V_1^2 + M_2 V_2^2 + M_r V_r^2) \tag{140}$$

The term on the left hand side of equation (138) may be regarded as the energy available for debris cloud motion and expansion. The parameter ξ is adjusted so that the final predictions for debris cloud spread angles based on the analysis procedure presented herein compare well

with those obtained using empirical predictor equations. Since the only unknown in equation (140) is V_e, the solution for the final unknown is immediate:

$$V_e = \sqrt{\frac{(1-\xi)M_p V_p^2 - (M_1 V_1^2 + M_2 V_2^2 + M_r V_r^2)}{M_1 + M_2 + M_r}} \tag{141}$$

9.7 Oblique Impact Model Verification

The validity of the proposed method of solution for the ten unknowns that characterize the debris clouds created as a result of an oblique hypervelocity impact of a thin plate (as well as all the attendant assumptions) is assessed by comparing model predictions of debris cloud spread angles with the predictions of empirically based equations for debris cloud spread angles. Model values for the spread angles of the 'normal' and 'in-line' debris clouds are given by:

$$\phi_i = 2\tan^{-1}\left(\frac{V_e}{V_i}\right) \qquad i = 1, 2 \tag{142}$$

The empirical values of debris cloud spread angles are found using the following relationships [4]:

$$\tan\phi_1 = 1.318\left(\frac{V_p}{C_b}\right)^{0.907}\left(\frac{t_b}{d_p}\right)^{0.195}\cos^{0.394}\theta_p \tag{143a}$$

$$\tan\phi_2 = 1.556\left(\frac{V_p}{C_b}\right)^{1.906}\left(\frac{t_b}{d_p}\right)^{0.345}\cos^{0.738}\theta_p \tag{143b}$$

Table 1 presents the a summary of the impact paramters used in the evaluation of the model developed herein.

Table 1. Impact Conditions Considered in Model Validation

Impact Parameter	Values Considered
Impact Velocity, V_p (km/s)	4.0, 5.5, 7.0
Trajectory Obliquity, θ_p (deg)	30, 45, 60
Projectile Diameter, d_p (cm)	0.635, 0.795, 0.953, 1.13, 1.27
Bumper Thickness, t_b (mm)	1.3, 1.6, 2.0

Tables 2a-c, 3a-c, and 4a-c present the final values of the user-controlled parameters α_2, η, ξ, and n corresponding to the impact conditions in Table 1.

Table 2a. Model Parameters α_2, η, ξ, and n for θ_p=30°, t_b=0.050 inches

V (km/s)	d_p (cm)	η	n	α_2	ξ
4.0	0.635	0.65	2.00	1.00	0.19
4.0	0.795	0.75	1.40	1.00	0.19
4.0	0.953	0.85	1.10	1.00	0.17
4.0	1.13	1.05	0.78	1.00	0.13
4.0	1.27	1.25	0.48	1.00	0.04
5.5	0.635	0.60	2.40	1.00	0.18
5.5	0.795	0.75	1.70	1.00	0.15
5.5	0.953	0.85	1.40	1.00	0.12
5.5	1.13	0.98	1.18	1.00	0.09
5.5	1.27	1.20	1.00	1.00	0.03
7.0	0.635	0.60	2.50	0.95	0.15
7.0	0.795	0.75	2.00	0.93	0.10
7.0	0.953	0.85	1.80	0.91	0.05
7.0	1.13	0.95	1.65	0.89	0.00
7.0	1.27	1.15	1.50	0.87	0.00

Table 2b. Model Parameters α_2, η, ξ, and n for θ_p=30°, t_b=0.063 inches

V (km/s)	d_p (cm)	η	n	α_2	ξ
4.0	0.635	0.65	2.00	1.00	0.25
4.0	0.795	0.75	1.40	1.00	0.22
4.0	0.953	0.85	1.10	1.00	0.20
4.0	1.13	1.05	0.78	1.00	0.16
4.0	1.27	1.25	0.48	1.00	0.10
5.5	0.635	0.60	2.40	1.00	0.25
5.5	0.795	0.75	1.70	1.00	0.18
5.5	0.953	0.85	1.40	1.00	0.14
5.5	1.13	0.98	1.18	1.00	0.11
5.5	1.27	1.20	1.00	1.00	0.03
7.0	0.635	0.60	2.50	0.95	0.25
7.0	0.795	0.75	2.00	0.93	0.12
7.0	0.953	0.85	1.80	0.91	0.07
7.0	1.13	0.95	1.65	0.89	0.02
7.0	1.27	1.15	1.50	0.87	0.00

Table 2c. Model Parameters α_2, η, ξ, and n for θ_p=30°, t_b=0.080 inches

V (km/s)	d_p (cm)	η	n	α_2	ξ
4.0	0.635	0.55	2.00	1.00	0.35
4.0	0.795	0.65	1.40	1.00	0.29
4.0	0.953	0.75	1.10	1.00	0.23
4.0	1.13	0.85	0.78	1.00	0.21
4.0	1.27	0.95	0.48	1.00	0.20
5.5	0.635	0.50	2.40	1.00	0.37
5.5	0.795	0.60	1.70	1.00	0.30
5.5	0.953	0.70	1.40	1.00	0.23
5.5	1.13	0.80	1.18	1.00	0.19
5.5	1.27	0.90	1.00	1.00	0.15
7.0	0.635	0.50	2.50	0.95	0.37
7.0	0.795	0.60	2.00	0.93	0.26
7.0	0.953	0.70	1.80	0.91	0.18
7.0	1.13	0.80	1.65	0.89	0.11
7.0	1.27	0.90	1.50	0.87	0.06

Table 3a. Model Parameters α_2, η, ξ, and n for θ_p=45°, t_b=0.050 inches

V (km/s)	d_p (cm)	η	n	α_2	ξ
4.0	0.635	1.00	2.00	1.00	0.05
4.0	0.795	1.10	1.38	1.00	0.04
4.0	0.953	1.30	1.00	1.00	0.03
4.0	1.13	1.60	0.77	1.00	0.00
4.0	1.27	1.80	0.38	1.00	0.00
5.5	0.635	1.00	2.15	1.00	0.05
5.5	0.795	1.00	1.45	1.00	0.04
5.5	0.953	1.30	1.10	1.00	0.03
5.5	1.13	1.60	0.93	1.00	0.00
5.5	1.27	1.75	0.70	1.00	0.00
7.0	0.635	1.00	2.05	0.90	0.10
7.0	0.795	1.10	1.50	0.87	0.06
7.0	0.953	1.20	1.10	0.80	0.02
7.0	1.13	1.40	0.81	0.64	0.00
7.0	1.27	1.60	0.60	0.26	0.00

Table 3b. Model Parameters α_2, η, ξ, and n for θ_p=45°, t_b=0.063 inches

V (km/s)	d_p (cm)	η	n	α_2	ξ
4.0	0.635	0.90	2.00	1.00	0.25
4.0	0.795	0.95	1.38	1.00	0.23
4.0	0.953	0.98	1.00	1.00	0.19
4.0	1.13	0.99	0.77	1.00	0.13
4.0	1.27	1.23	0.58	1.00	0.08
5.5	0.635	0.80	2.15	1.00	0.27
5.5	0.795	0.90	1.45	0.97	0.25
5.5	0.953	0.95	1.10	0.90	0.19
5.5	1.13	0.98	0.93	0.74	0.08
5.5	1.27	1.05	0.70	0.37	0.00
7.0	0.635	0.80	2.05	0.90	0.29
7.0	0.795	0.90	1.50	0.87	0.24
7.0	0.953	0.95	1.10	0.80	0.19
7.0	1.13	0.98	0.81	0.64	0.12
7.0	1.27	0.99	0.60	0.26	0.02

Table 3c. Model Parameters α_2, η, ξ, and n for θ_p=45°, t_b=0.080 inches

V (km/s)	d_p (cm)	η	n	α_2	ξ
4.0	0.635	0.75	2.00	1.00	0.42
4.0	0.795	0.80	1.38	1.00	0.38
4.0	0.953	0.85	1.00	1.00	0.34
4.0	1.13	0.90	0.77	1.00	0.29
4.0	1.27	0.95	0.58	1.00	0.25
5.5	0.635	0.65	2.15	1.00	0.44
5.5	0.795	0.70	1.45	0.97	0.41
5.5	0.953	0.75	1.10	0.90	0.35
5.5	1.13	0.80	0.93	0.74	0.25
5.5	1.27	0.85	0.70	0.37	0.15
7.0	0.635	0.55	2.05	0.90	0.46
7.0	0.795	0.60	1.50	0.87	0.40
7.0	0.953	0.75	1.10	0.80	0.35
7.0	1.13	0.80	0.81	0.64	0.28
7.0	1.27	0.85	0.60	0.26	0.18

Table 4a. Model Parameters α_2, η, ξ, and n for θ_p=60°, t_b=0.050 inches

V (km/s)	d_p (cm)	η	n	α_2	ξ
4.0	0.635	1.60	1.73	1.00	0.05
4.0	0.795	1.60	1.30	0.99	0.04
4.0	0.953	1.70	0.99	0.97	0.03
4.0	1.13	1.90	0.77	0.93	0.02
4.0	1.27	2.40	0.61	0.85	0.00
5.5	0.635	1.30	1.80	1.00	0.05
5.5	0.795	1.40	1.33	0.93	0.08
5.5	0.953	1.50	0.95	0.82	0.10
5.5	1.13	1.60	0.64	0.65	0.09
5.5	1.27	1.70	0.39	0.38	0.08
7.0	0.635	1.00	1.67	0.90	0.15
7.0	0.795	1.20	1.20	0.85	0.15
7.0	0.953	1.40	0.80	0.76	0.19
7.0	1.13	1.60	0.46	0.61	0.15
7.0	1.27	1.70	0.17	0.35	0.05

Table 4b. Model Parameters α_2, η, ξ, and n for θ_p=60°, t_b=0.063 inches

V (km/s)	d_p (cm)	η	n	α_2	ξ
4.0	0.635	1.00	1.73	1.00	0.24
4.0	0.795	1.00	1.30	0.99	0.22
4.0	0.953	1.00	0.99	0.97	0.20
4.0	1.13	1.00	0.77	0.93	0.15
4.0	1.27	1.00	0.61	0.85	0.09
5.5	0.635	0.99	1.80	1.00	0.28
5.5	0.795	1.00	1.33	0.93	0.27
5.5	0.953	1.00	0.95	0.82	0.26
5.5	1.13	1.00	0.64	0.65	0.23
5.5	1.27	1.00	0.39	0.38	0.19
7.0	0.635	0.92	1.67	0.90	0.35
7.0	0.795	0.95	1.20	0.85	0.35
7.0	0.953	0.98	0.80	0.76	0.35
7.0	1.13	0.99	0.46	0.61	0.30
7.0	1.27	1.00	0.17	0.35	0.27

Table 4c. Model Parameters α_2, η, ξ, and n for θ_p=60°, t_b=0.080 inches

V (km/s)	d_p (cm)	η	n	α_2	ξ
4.0	0.635	0.90	1.73	1.00	0.45
4.0	0.795	0.95	1.30	0.99	0.41
4.0	0.953	1.00	0.99	0.97	0.37
4.0	1.13	1.05	0.77	0.93	0.32
4.0	1.27	1.10	0.61	0.85	0.28
5.5	0.635	0.90	1.80	1.00	0.47
5.5	0.795	0.95	1.33	0.93	0.45
5.5	0.953	1.00	0.95	0.82	0.41
5.5	1.13	1.05	0.64	0.65	0.36
5.5	1.27	1.10	0.39	0.38	0.30
7.0	0.635	0.80	1.67	0.90	0.52
7.0	0.795	0.85	1.20	0.85	0.50
7.0	0.953	0.90	0.80	0.76	0.47
7.0	1.13	0.95	0.46	0.61	0.40
7.0	1.27	1.00	0.17	0.35	0.32

Finally, Table 5a-c present percent error summaries showing differences between prediction and experiment for the various bumper plate thicknesses, impact trajectories, projectile diameters, and obliquities considered. For each perforating debris cloud spread angle, the value shown is the precent difference between model prediction and empirical equation prediction. As can be seen from Table 5a-c, the values of the spread angles that result from the calculations described herein are very close to the experimental values. Naturally, the values of the parameters α_2, η, ξ, and n have been adjusted to ensure that model predictions and empirical results are closely matched.

9.8 Application to Crack Length and Hole Diameter Calculations

In order to apply the methodology developed for normal impacts to the case of an oblique impact, certain simplifying assumptions need to be made. To begin, we consider impacts with trajectory obliquities between 0° and 20° to be essentially normal impacts. Thus, for $0°<\theta_p<20°$,

the normal impact model presented in the preceding Chapters is used to determine crack lengths and hole diameters. Next, for $20° < \theta_p < 30°$, it is assumed that $\theta_p = 30°$, while if $\theta_p > 60°$, it is assumed that $\theta_p = 60°$. These are conservative assumptions: at both ends of the impact spectrum, the obliquity assumptions dictate worse conditions than the actual scenarios provide.

Table 5a. Percent Error Summaries for t_b = 1.27 mm

V_p = 4.0 km/s						
d_p	30 deg		45 deg		60 deg	
(cm)	ϕ_1	ϕ_2	ϕ_1	ϕ_2	ϕ_1	ϕ_2
0.635	9.00	-3.39	4.93	-1.94	-6.01	-7.47
0.795	1.35	3.86	2.42	11.36	-0.84	6.37
0.953	-6.76	8.62	-18.90	9.54	-4.96	16.09
1.13	-24.24	14.83	-52.53	-16.23	-28.07	2.49
1.27	-34.57	25.97	-75.60	-44.40	-58.57	-15.97
V_p = 5.5 km/s						
d_p	30 deg		45 deg		60 deg	
(cm)	ϕ_1	ϕ_2	ϕ_1	ϕ_2	ϕ_1	ϕ_2
0.635	7.55	-12.97	2.72	0.79	10.81	-11.08
0.795	0.72	0.59	10.61	10.80	0.03	-6.32
0.953	-2.38	7.90	-15.99	15.71	-9.49	-0.37
1.13	-12.43	11.60	-46.72	-7.03	-10.93	12.61
1.27	-25.42	20.14	-87.46	-75.68	-18.57	14.33
V_p = 7.0 km/s						
d_p	30 deg		45 deg		60 deg	
(cm)	ϕ_1	ϕ_2	ϕ_1	ϕ_2	ϕ_1	ϕ_2
0.635	8.86	-8.04	-6.77	4.93	17.88	-17.37
0.795	-1.69	-4.42	-8.26	8.33	9.85	0.08
0.953	-3.45	-0.05	-10.85	11.59	-11.82	6.72
1.13	-4.62	6.92	-26.86	8.78	-21.36	26.72
1.27	-28.33	-1.32	-52.90	-18.65	-28.39	35.23

Finally, we ignore the contribution of the normal debris cloud created in an oblique impact to the deformation of the pressure wall. This presumption is experience-based: in nearly all of the oblique impact tests reviewed in [4], it is the in-line debris cloud that perforates the pressure wall plate. Most of the normal debris cloud particles are trapped by the inner bumper, whether it is an

blanket of MLI or a Nextel/Kevlar blanket. Thus, it is the characteristics M_2, V_2, and V_e that dictate the response of the pressure wall plate to an oblique hypervelocity impact. Before these parameters are applied in the normal impact model developed previously, some account must be made of the effect of the inner bumper on the characteristics of the in-line debris cloud.

Table 5b. Percent Error Summaries for t_b = 1.6 mm

V_p = 4.0 km/s						
d_p	30 deg		45 deg		60 deg	
(cm)	ϕ_1	ϕ_2	ϕ_1	ϕ_2	ϕ_1	ϕ_2
0.635	-3.92	0.71	-4.34	4.28	16.81	-13.13
0.795	-7.10	7.37	-7.84	5.96	17.29	-8.68
0.953	-11.78	12.29	-5.53	8.18	9.26	-12.94
1.13	-28.03	18.49	-5.98	1.95	17.20	-7.39
1.27	-36.65	32.59	-14.32	19.36	10.43	-16.17
V_p = 5.5 km/s						
d_p	30 deg		45 deg		60 deg	
(cm)	ϕ_1	ϕ_2	ϕ_1	ϕ_2	ϕ_1	ϕ_2
0.635	-1.82	-2.92	-2.53	-1.81	13.12	-8.54
0.795	-7.21	8.61	-7.16	6.44	10.81	-8.33
0.953	-8.65	13.77	-5.18	4.99	5.78	-10.31
1.13	-16.97	16.64	1.32	0.91	8.86	-6.65
1.27	-28.22	27.34	-7.98	-9.56	13.03	-4.89
V_p = 7.0 km/s						
d_p	30 deg		45 deg		60 deg	
(cm)	ϕ_1	ϕ_2	ϕ_1	ϕ_2	ϕ_1	ϕ_2
0.635	-9.06	-3.04	-8.03	7.89	7.75	-3.56
0.795	-6.74	9.28	-9.71	9.46	3.82	-3.85
0.953	-9.59	7.73	-7.24	8.59	-6.72	-7.61
1.13	-10.18	12.11	-1.64	6.91	3.17	6.29
1.27	-31.68	4.61	-0.08	-5.02	-6.91	-3.42

9.8.1 Effect of Inner Bumper on In-line Debris Cloud

Consider the impact and perforation of the inner bumper by the in-line debris cloud created in an oblique hypervelocity impact on the outer bumper as shown in Figure 13 below.

Table 5c. Percent Error Summaries for t_b = 2.0 mm

V_p = 4.0 km/s						
d_p (cm)	30 deg		45 deg		60 deg	
	ϕ_1	ϕ_2	ϕ_1	ϕ_2	ϕ_1	ϕ_2
0.635	-5.95	3.32	-9.93	10.99	0.20	-5.87
0.795	-11.60	3.96	-10.78	11.79	0.71	1.69
0.953	-6.74	18.11	-15.05	6.65	-3.40	3.81
1.13	-14.60	20.67	-12.24	8.39	-2.21	8.40
1.27	-23.91	21.86	-10.45	11.20	-10.79	-0.44
V_p = 5.5 km/s						
d_p (cm)	30 deg		45 deg		60 deg	
	ϕ_1	ϕ_2	ϕ_1	ϕ_2	ϕ_1	ϕ_2
0.635	-4.92	1.49	-4.96	8.09	-0.70	6.99
0.795	-7.74	3.75	-5.73	8.40	-5.76	5.08
0.953	-7.44	9.48	-4.97	3.01	-6.98	9.90
1.13	-12.46	11.08	2.67	0.24	-8.70	12.86
1.27	-14.12	18.56	4.88	-5.61	-6.78	17.02
V_p = 7.0 km/s						
d_p (cm)	30 deg		45 deg		60 deg	
	ϕ_1	ϕ_2	ϕ_1	ϕ_2	ϕ_1	ϕ_2
0.635	-5.95	3.32	1.12	6.77	-4.81	9.08
0.795	-7.17	7.41	6.54	5.48	-6.31	10.71
0.953	-8.71	5.87	-6.94	8.15	-12.74	10.64
1.13	-9.33	8.69	-3.40	4.20	-18.08	11.04
1.27	-11.77	12.60	-1.57	-6.79	-19.78	12.98

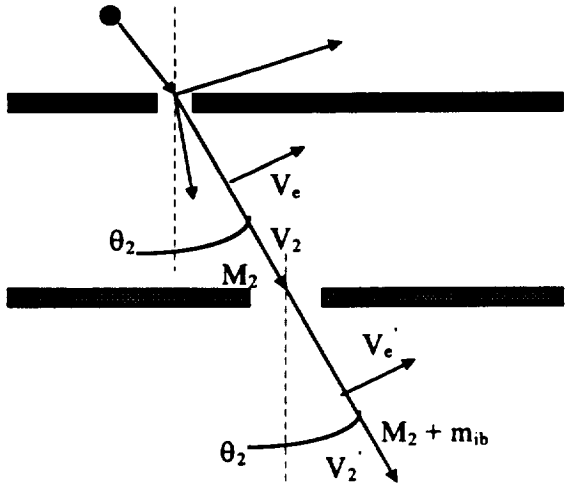

Figure 13. Perforation of Inner Bumper in an Oblique High Speed Impact

In Figure 13, the unknown quantities are V_e' and V_2', the expansion and axial velocities of the in-line debris cloud following perforation of the inner bumper, respectively. As before, m_{ib} denotes the mass of the inner bumper punched out by the in-line debris cloud. Inherent in the representation shown in Figure 13 are two assumptions regarding the nature of the perforation of the inner bumper (in addition to the entrapment of the normal debris cloud by the inner bumper as discussed previously). These assumptions are listed below.

- The direction of the in-line debris cloud following perforation of the inner bumper remains unchanged.
- None of the original in-line debris cloud mass is lost to entrappment by the inner bumper as the in-line debris cloud moves through the inner bumper.

The unknown axial and expansion velocities are calculated as follows. First, conservation of axial momentum along the line of travel for the in-line debris cloud yields the following equation:

$$M_2 V_2 = (M_2 + m_{ib}) V_2' \tag{144}$$

Thus, the axial velocity of the in-line debris cloud following inner bumper perforation can be obtained directly from equation (144):

$$V_2' = \frac{M_2 V_2}{M_2 + m_{ib}} \tag{145}$$

Conservation of energy yields the following relationship in terms of V_e':

$$\frac{1}{2} M_2 V_2^2 + \frac{1}{2} M_2 V_e^2 = \frac{1}{2} (M_2 + m_{ib})(V_2')^2 + \frac{1}{2} (M_2 + m_{ib})(V_e')^2 \tag{146}$$

Equation (146) is then solved directly for the expansion velocity following inner bumper:

$$V_e' = \sqrt{\frac{M_2}{M_2 + m_{ib}}(V_2^2 + V_e^2) - (V_2')^2} \tag{147}$$

where V_2' is given by equation (145). The inner bumper hole out mass is found using equations very similar to those developed in the preceding chapters for the case of normal impact, to wit:

$$m_{ib} = \varepsilon_{ib}\left(\frac{\pi}{4}\right)\delta_h^2 \lambda_{ib} \tag{148}$$

where ε_{ib} is a user-controlled parameter, δ_h is the inner bumper hole diameter, and λ_{ib} is the inner bumper areal density. As before, the inner bumper hole diameters is calculated using the relationship

$$\delta_h = 2R_{dcp} \tag{149a}$$

where R_{dcp} is the radius of the in-line debris cloud when it comes in contact with the inner bumper. In this case, it is given as follows:

$$R_{dcp} = \frac{(S - S_2)\sin\theta_{dcp}}{1 + \sin\theta_{dcp}} \tag{149b}$$

In equation (149b), θ_{dcp} is the angle defining the spread of the in-line debris cloud and is obained by the following relationship:

$$\theta_{dcp} = \tan^{-1}\left(\frac{V_e}{V_2}\right) \tag{149c}$$

Finally, the radius of the in-line debris cloud when it first comes in contact with the pressure wall plate is given by

$$R_{wp} = \frac{S_2 \sin\theta_{dcp}}{1 + \sin\theta_{dcp}} \tag{150}$$

9.8.2 Application of Normal Impact Equations to Oblique Impact Scenario

Now that the quantities defining the in-line debris cloud mass and velocities following inner bumper perforation have been defined, it is a rather straight-forward task to apply the equations developed for the case of normal impact to the case of oblique impact. Specifically, Table 6 below presents a summary of the oblique impact scenario values that are to be used directly in the equations developed for pressure wall deformation, cracking, etc. in the case of normal impact.

Table 6. Correspondence of Normal Impact Equation Parameters to Oblique Impact Scenario

Normal Impact Equation Parameters	Value in Oblique Impact Scenario
V_{lc}	$V_2'+V_e'$
V_{axp}	V_2'
V_{expp}	V_e'
V_{axb}	0
V_{expb}	0
θ_{dcp}	equation (149c)
θ_{dcp}	0
R_{wp}	equation (150)
R_{wb}	0
R_{dcp}	R_{dcib}
R_{dcb}	0
p_{op}	γ/β
p_{ob}	0
α	0
β	$(M_2+m_{ib})(V_2'+V_e')$
γ	$\pi R_{wp}^2 I_p$
δ	0

Of course, before the normal impact equations are used at all, it must first be verified that petalling will in fact occur in the oblique impact scenario being considered. This is done using the theory developed in Section 8.5.

10.0 MODEL CHECKOUT AND VERIFICATION

10.1 Computer Codes

The analytical hole diameter and crack length model developed in Chapters 2 through 8 was encoded in a FORTRAN program entitled "*pwcrck.for*", which is presented in its entirety in Appendix B. Input files required to run *pwcrck.for* are given in Appendix C, which Appendix D contains a sample output file obtained by running *pwcrck.for*. The oblique impact model developed in Chapter 9 was encoded in a FORTRAN program entitled "*obldata.for*", which is presented in its entirety in Appendix E. Input files required to run *obldata.for* are given in Appendix F, which Appendix G contains a sample output file obtained by running *obldata.for*. The following is a description of the various input files required to run *pwcrck.for* and *obldata.for*.

IMPDAT — input file for *pwcrck.for* and *obldata.for*. It contains material properties information for a variety of potential projectile, outer bumper, and pressure wall materials.

GPARAM — input file for *pwcrck.for*. It contains a wall system identifier (e.g. LEC or BLC) as well as pressure wall deformation, cracking, and petalling model parameter values.

GPRMOBL — input file for *obldata.for*. It contains material information and geometric parameter values.

COEF — input file for *pwcrck.for*. It contains the coefficients for the ballistic limit equations for the stuffed Whipple systems.

OBLDATA input file for *pwcrck.for*; created as an output file by *obldata.for*. It contains outer bumper hole dimensions and in-line debris cloud mass, axial velocity and radial velocity values calculated by *obldata.for* for use by *pwcrck.for*.

WALDAT input file for *pwcrck.for*. It contains geometric parameter values for the BLC, ELC, and LEC wall systems.

REGDAT input file for *pwcrck.for*. It contains the coefficient values for the empirical predictor equations for hole diameter and crack length for the BLC, ELC, and LEC wall systems.

CDCLELC input file for *pwcrck.for*. It contains the coefficient values for the C_D and C_L functions for the ELC wall system.

CDCLLEC input file for *pwcrck.for*. It contains the coefficient values for the C_D and C_L functions for the LEC wall system.

CDCLBLC input file for *pwcrck.for*. It contains the coefficient values for the C_D and C_L functions for the BLC wall system.

10.2 Model Checkout

Prior to verifying the hole diameter and crack length model developed in the previous sections, a parametric study was performed to characterize the effects of the various user-controlled parameters within the model on model predictions. Table 7 below contains a summary of the various user-controlled parameters that were found to significantly affect hole diameter and crack length calculations. This table presents the definition of each user-controlled parameter and the model output quantity it most strongly affects.

Table 7. Summary of User-Controlled Parameters and Affected Model Components

Model Parameter	Parameter Definition	Model Component Affected
α_c	Ratio of Crack Arrest Stress Intensity Factor to Critical Stress Intensity Factor	Final crack length
ε_{1f}	Critical Failure Strain	Crack initiation
ε_{ib}	Inner Bumper Hole Out Mass Factor	Secondary debris cloud velocities, spread angles, footprint radii, etc
ε	Ratio of Pressure Wall Thickness at Impact Center to Nominal Pressure Wall Thickness	Time of crack initiation, plate velocity at crack formation, etc
m	Empirical Exponent	Final crack length

Of note was the effect of the parameter ε_{ib} on the characteristics of the secondary debris cloud. If ε_{ib} was too small, then a likely result was that the expansion velocity of the bumper material component in the secondary debris cloud exceeded the axial velocity. Using the assumed definition for the debris cloud trailing edge velocity, a negative value would result. A direct consequence of a negative trailing edge velocity value was a negative value for impact duration, which is physically not possible. If ε_{ib} was too large, then the projectile material component was affected in a similar manner. Hence, model users are cautioned with regard to the adverse effects resulting from cavalier selection of user-controlled parameter values. Table 8 presents summarizes the effect of changes in the values of the user-controlled parameters listed in Table 7 on the results of the model developed herein.

Table 8. Results of Parametric Study: Effect of User-Controlled Parameters on Model Output

Output Result	User-Controlled Parameter				
	ε_{1f} ↑	ε_{ib} ↑	ε ↑	α_c ↑	m ↑
t_c	↑	↓	↑	—	—
V_c	↑	↑	↓	—	—
N_{cr}	↑	↑	↑	—	—
a_{lim}	—	—	—	↓	↑
D_{eq}	↓	↓	↑	↓	↑

10.3 Model Verification

10.3.1 Multi-wall System Configurations and Impact Test Parameters

The predictions of the model developed herein are compared against the predictions of empirically-based equations for hole diameters and maximum tip-to-tip crack length for three International Space Station (ISS) wall configurations. The ISS wall systems used for model verification are the baseline US Lab Cylinder (BLC), the enhanced US Lab Cylinder (ELC), and the US Lab Endcone (LEC). Table 9 below presents a summary of the geometric parameters for these three wall configurations; Table 10 following presents a summary of the impact parameters for the impact tests performed to support the development of the empirical predictor equations.

Table 9. Multi-wall System Geometric Parameters

WALL SYSTEM	t_b (mm)	INNER WALL	S (cm)	S_2 (cm)	t_w (mm)
BLC[1]	1.27	MLI[3]	11.43	5.72	4.78
LEC[2]	1.91	MLI[3]	22.15	18.33	4.78
ELC[2]	2.03	6N+6K[4]	11.43	5.72	4.78

[1]Tested with full-scale and 2/3-scale test specimens
[2]Tested using only 2/3-scale test specimens
[3]20 layers of multi-layer thermal insulation
[4]6 layers of Nextel AF62 cloth backed with 6 layers of Kevlar 710 cloth

In some instances, sub-scale versions of the actual wall systems were occasionally used to allow the modeling of such systems under the impact of projectiles that are considerably larger than those which could be tested. All dimensions presented in Table 9 are full-scale values; superscripts are used to indicate which wall systems were tested using sub-scale configurations.

Table 10. Summary of Impact Test Parameters

WALL SYSTEM	V_p (km/s)	θ_p (deg)	M_p (gm)	Number of Tests
BLC	6.3 to 11.7	0, 45	1.2 to 5.7	14
LEC	6.4 to 11.4	0, 45	2.4 to 6.6	8
ELC	6.0 to 11.7	0, 45	2.9 to 8.0	18

In Table 10, V_p, M_p and θ_p are the velocity, mass and obliquity of the impacting projectile; aluminum was used as the projectile material in all of the tests. Tests were performed using spherical projectiles at impact velocities of 6.5 ± 0.3 km/sec with a two-stage light gas gun and at 11.3 ± 0.5 km/sec using an inhibited shaped charge launcher (ISCL). Due to the physics involved in using an ISCL, the projectiles in the tests performed at 11.3 ± 0.5 km/sec were typically elongated hollow cylinders with a length-to-diameter ratio of approximately 1.5. In all of the tests, the technique used to hold the MLI was identical as was the manner in which the pressure walls were mounted and secured.

The empirical equations for effective pressure wall hole diameter and maximum tip-to-tip crack length were all in the following format:

$$X = Af(\theta_p)g(V_p)\{1-e^{-C(M_p/M_{BL}-1)}\} \tag{151}$$

where, for example, $X=D_{eq}$ for effective hole diameter and $X=L_{tt}$ for maximum tip-to-tip crack length, respectively. In equation (151), M_{BL} is the ballistic limit mass at a velocity of interest for the particular system under consideration under a θ_p-degree impact. The constants A and C and the impact velocity dependent function $g(V_p)$ for each of the three multi-wall systems considered in this study can be found in Reference [13].

10.3.2 Comparison of Model Predictions with Experimental Results

A series of runs using the analytical model developed herein was performed to generate theoretical predictions of hole diameter and crack length for each of the three multi-wall systems described above. These predicted values were subsequently compared against the values generated by the empirical equations. These runs were performed at two projectile trajectory obliquities: 0° and 45°.

For the 0° impacts, three impact velocities were considered: 6, 9, and 12 km/s. For each impact velocity, three projectile diameters were considered. The smallest was just above the ballistic limit diameter at the impact velocity being considered. The largest was 1.91 cm, which corresponds to a mass of approximately 10 gms, the upper limit of the projectile mass values in the experimental test program. Finally, the third diameter was chosen as that being midway between the smallest and largest values.

For the 45° impacts, we note that the values for the user-controlled parameters in Tables 2 through 4 do not exist for impact velocities in excess of 7 km/s. Hence, the 45° runs were performed only at an impact velocity of 6 km/s. In order to determine corresponding parameter values for impact velocities above 7 km/s, additional tests would have to be performed at the higher velocities of interest on the wall system configurations of interest, but without any inner bumper. Pressure wall damage area data from such tests would then be used to back out debris cloud spread angle values at the higher impact velocities. This data would then be combined with existing spread angle data and used to obtain empirical debris cloud spread angle predictor equations similar to equations (143a,b), but valid at the higher impact velocities. Once these equations were available, then the oblique impact model in Chapter 9 could be run at higher impact velocities, and appropriate values of the user-controlled parameters could be determined.

The projectile diameters for the oblique runs were chosen similarly to the manner in which the diameters were selected for the normal impact runs. However, for the 45° runs, the largest projectile diameter considered was 1.27 cm, the upper limit of the oblique impact model developed in Chapter 9. If a projectile diameter in excess of 1.27 cm were to be used, the oblique impact model developed in Chapter 9 would yield spurious results (e.g. negative debris cloud mass and velocity values, etc. Review of the results obtained in these initial runs revealed several

interesting trends in the predictions of the analytical model.

First, when the projectile diameter was less than the petalling limit diameter, the predictions of the analytical model greatly exceeded the empirical equation values. Thus, the use of the debris cloud projectile component diameter to calculate the diameter of the resulting hole in the pressure wall greatly overestimated actual hole diameter values. Second, when the projectile diameter exceeded the petalling limit diameter, the predictions of the analytical model ranged from being fairly close to the empirical predictions to being significantly lower than the empirical predictions. Thus, depending on the multi-wall system configuration, in most of the cases where petalling occurs, the pressure wall petals do not sufficiently open up during the curling process which in turn results in underpredicted pressure wall hole diameters.

10.3.3 Analytical Model Modifications

Based on the results discussed in the preceding section, it appears that some adjustment of the analytical model is required to bring it more in line with experimental results. Two possibilities arose regarding the approach that would render the analytical model more accurate in its predictive capability. The first was to determine particular combinations of the empirical constants contained within the model (e.g. failure strain, etc.) that would render the results of specific model runs to be in agreement with the predictions of the empirical equations. The result of such an effort would be that every combination of impact parameters would need to possess its own set of empirical constants in order for the model to have predictive accuracy. All physical meaning of the empirical parameters would be lost as the values they would take on would have cease to have any basis in reality.

Alternatively, the second approach was to introduce modifications functions to the model that would take on appropriate values for a given multi-wall system geometry and for a specific

set of impact parameters. In this manner, adjustment factors for other impact conditions would be automatically calculated without the need for performing an inordinately large number of model run comparisons. Given the broader model applicability that results from this approach, it is this method that is chosen to modify the analytical model in an attempt to improve its predictive accuracy. Naturally, the specific functional forms of the correcting factors used depended on the multi-wall system and were functions of projectile diameter, trajectory obliquity, and impact velocity. These functions are summarized below, where C_D is the correction factor for pressure wall hole diameter and C_L is the correction factor for maximum tip-to-tip crack length.

Baseline Lab Cylinder (BLC)

$$\theta_p = 0^\circ,\ V_p = 6\ km/s \quad C_D = \begin{cases} A_1\left(\frac{d_p}{d_{BL}}\right) + B_1 & ,\quad d_p < 1.18cm \\ A_2\left(\frac{d_p}{d_{BL}}\right) + B_2 & ,1.18cm < d_p < 1.33cm \\ A_3\left(\frac{d_p}{d_{BL}}\right)^2 + B_3\left(\frac{d_p}{d_{BL}}\right) + C_3 & ,1.33cm < d_p \end{cases} \qquad (152a\text{-}c)$$

$$\theta_p = 0^\circ,\ V_p = 9\ km/s \quad C_D = \begin{cases} A_1\left(\frac{d_p}{d_{BL}}\right) + B_1 & ,\quad d_p < 0.89cm \\ A_3\left(\frac{d_p}{d_{BL}}\right)^2 + B_3\left(\frac{d_p}{d_{BL}}\right) + C_3 & ,0.89cm < d_p \end{cases} \qquad (152d,e)$$

$$\theta_p = 0^\circ,\ V_p = 12\ km/s \quad C_D = \begin{cases} A_1\left(\frac{d_p}{d_{BL}}\right) + B_1 & ,\quad d_p < 0.79cm \\ A_3\left(\frac{d_p}{d_{BL}}\right)^2 + B_3\left(\frac{d_p}{d_{BL}}\right) + C_3 & ,0.79cm < d_p \end{cases} \qquad (152f,g)$$

$$\theta_p = 45^\circ,\ V_p = 6\ km/s \quad C_L = D_1\left(\frac{d_p}{d_{BL}} - 1\right)^{E_1}\left(\frac{d_p}{d_{BL}}\right)^{F_1} \qquad (153)$$

Enhanced Lab Cylinder (ELC)

$\theta_p = 0°,\ V_p = 6,9,12\ km/s \qquad C_D = A_1\left(\frac{d_p}{d_{BL}} - 1\right)^{B_1}\left(\frac{d_p}{d_{BL}}\right)^{C_1}$ (154a)

$\theta_p = 45°,\ V_p = 6\ km/s \qquad C_D = A_1\left(\frac{d_p}{d_{BL}} - 1\right)\exp\left[B_1\left(\frac{d_p}{d_{BL}} - 1\right)^2\right]$ (154b)

$\theta_p = 0°,\ V_p = 6,9,12\ km/s \qquad C_L = D_1\left(\frac{d_p}{d_{BL}} - 1\right)^{E_1}\left(\frac{d_p}{d_{BL}}\right)^{F_1}$ (155a)

$\theta_p = 45°,\ V_p = 6\ km/s \qquad C_L = D_1\left(\frac{d_p}{d_{BL}} - 1\right)^{E_1}\left(\frac{d_p}{d_{BL}}\right)^{F_1}$ (155b)

US Lab Endcone (LEC)

$\theta_p = 0°,\ V_p = 6,9,12\ km/s \qquad C_D = A_1\left(\frac{d_p}{d_{BL}} - 1\right)^{B_1}\left(\frac{d_p}{d_{BL}}\right)^{C_1}$ (156a)

$\theta_p = 45°,\ V_p = 6\ km/s \qquad C_D = A_1\left(\frac{d_p}{d_{BL}} - 1\right)^{B_1}\left(\frac{d_p}{d_{BL}}\right)^{C_1}$ (156b)

$\theta_p = 0°,\ V_p = 6,9,12\ km/s \qquad C_L = D_1\left(\frac{d_p}{d_{BL}} - 1\right)^{E_1}\left(\frac{d_p}{d_{BL}}\right)^{F_1}$ (157a)

$\theta_p = 45°,\ V_p = 6\ km/s \qquad C_L = D_1\left(\frac{d_p}{d_{BL}} - 1\right)^{E_1}\left(\frac{d_p}{d_{BL}}\right)^{F_1}$ (157b)

Tables 11, 12, and 13 below provide a summary of the values of the various parameters in equations (152) through (157) above for 6, 9, and 12 km/s impacts, respectively. These values were obtained by ensuring that the predictions of the analytical model matched the predictions of the empirical hole diameter and crack length equations at the various projectile diameters, trajectory obliquities, and impact velocities considered. Since the oblique impact mass partitioning

model was developed only for impact velocities up to 7 km/s, the correction factor equation parameters for 45-deg impacts are given only for V_p =6 km/s.

Table 11. Correction Factor Equation Parameters, V_p = 6 km/s

Wall System	θ_p (deg)	Equation Parameters											
		A1	B1	C1	A2	B2	C2	A3	B3	C3	D1	E1	F1
BLC	0	1.099	0.00364	—	7.068	-3.501	—	1.721	-4.215	4.267	2.998	1.134	-1.732
	45	0.346	0.804	1.624	—	—	—	—	—	—	0.473	0.798	2.364
ELC	0	10.01	0.812	-0.0208	—	—	—	—	—	—	11.75	0.936	-3.081
	45	117.8	49.98	—	—	—	—	—	—	—	23.52	1.009	-4.609
LEC	0	1.059	1.154	-1.815	—	—	—	—	—	—	3.239	1.117	-1.926
	45	1.177	1.145	-1.321	—	—	—	—	—	—	2.366	1.132	-1.636

Table 12. Correction Factor Equation Parameters, V_p = 9 km/s

Wall System	θ_p (deg)	Equation Parameters											
		A1	B1	C1	A2	B2	C2	A3	B3	C3	D1	E1	F1
BLC	0	21.95	-0.216	—	—	—	—	4.523	-9.489	5.973	2.483	1.117	-1.703
ELC	0	49.48	1.135	-1.062	—	—	—	—	—	—	18.94	0.919	-3.179
LEC	0	0.272	0.867	1.978	—	—	—	—	—	—	1.888	0.999	-0.308

Table 13. Correction Factor Equation Parameters, V_p = 12 km/s

Wall System	θ_p (deg)	Equation Parameters											
		A1	B1	C1	A2	B2	C2	A3	B3	C3	D1	E1	F1
BLC	0	16.85	0.837	—	—	—	—	3.809	-11.33	9.057	3.173	1.382	-2.179
ELC	0	90.59	1.197	-1.379	—	—	—	—	—	—	21.74	0.897	-2.694
LEC	0	0.227	0.822	1.834	—	—	—	—	—	—	1.872	0.983	-0.574

10.3.4 Comparison of Modified Model Predictions with Experimental Results

10.3.4.1 Comparison Against Empirical Holde Size and Crack Length Equation Predictions

Tables 14-16 contain a summary of the comparisons between the predictions of the modified analytical model and those of the empirical equations. In these tables, entries in the d_h and L_{tt} columns are the ratios of empirical prediction equation values to modified analytical model values of pressure wall hole diameter and maximum tip-to-tip crack length, respectively. Review of the information in these tables reveals that the predictive accuracy of the modified analytical

model is significantly improved when compared to that of the original analytical model.

However, it can also be seen that there will still occasionally exist significant differences between the predictions of the modified analytical model and the predictions of the empirical equations. This is especially true for normal impacts of the BLC wall system at impact velocities of 9 km/s and above. In these cases, additional modifications to the model will have to be made.

10.3.4.2 Comparison Against Empirical Hole Size and Crack Length Data

Further validation of the analytical model developed herein was obtained by comparing its predictions against actual empirical hole diameter and crack length data. Model predictions were obtained for nine (9) impact scenarios, three (3) for each of the BLC, ELC, and LEC wall systems. For each wall system, model predictions were obtained for two 0° impacts and one 45° impacts. For the 0° impacts, model predictions were obtained for impact velocities near 6.5 km/s and near 11 km/s; for the oblique impacts, model predictions were obtained at impact velocities near 6.5 km/s only.

Table 17 contains the experimental and model values of hole diameter and crack length for the nine impact scenarios considered. Also shown in Table 17 are the hole diameter and crack length values predicted by the empirical equations. As can be seen from Table 17, the predictions of the modified analytical model, in general, compare rather favorably with actual experimental data values. However, there do occasionally exist instances where the model predictions and empirical data are somewhat divergent. Of some concern is the discrepancy between the predicted and experimental values of hole diameter and crack length for Test No. 1722. Analysis of the data for tests conducted under similar impact conditions revealed that the damage sustained by the pressure wall in this test was anomalous.

Table 14. Ratios Of Empirical To Modified Analytical Model Predictions For LEC Wall System

θ_p=0-deg				θ_p=45-deg			
	d_p (cm)	D_{eq} Ratio	L_{tt} Ratio		d_p (cm)	D_{eq} Ratio	L_{tt} Ratio
V_p=6 km/s	0.92	1.194	1.184	V_p=6 km/s	0.71	1.176	1.172
	1.16	0.987	1.027		0.85	0.971	0.987
	1.41	1.006	1.002		0.99	1.005	1.003
	1.66	0.891	0.876		1.13	0.998	0.985
	1.91	1.001	1.001		1.27	1.003	1.001
V_p=9 km/s	0.93	1.166	1.188	V_p=9 km/s	(1)	(1)	(1)
	1.17	1.012	1.008		(1)	(1)	(1)
	1.41	0.594	0.764		(1)	(1)	(1)
	1.66	1.180	1.275		(1)	(1)	(1)
	1.91	1.006	1.003		(1)	(1)	(1)
V_p=12 km/s	0.77	1.108	1.129	V_p=12 km/s	(1)	(1)	(1)
	1.03	1.009	1.005		(1)	(1)	(1)
	1.33	1.049	1.592		(1)	(1)	(1)
	1.62	0.958	1.208		(1)	(1)	(1)
	1.91	1.004	1.001		(1)	(1)	(1)

(1) Impact velocity exceeds maximum allowable value.

Table 15. Ratios Of Empirical To Modified Analytical Model Predictions For BLC Wall System

θ_p=0-deg				θ_p=45-deg			
	d_p (cm)	D_{eq} Ratio	L_{tt} Ratio		d_p (cm)	D_{eq} Ratio	L_{tt} Ratio
V_p=6 km/s	0.75	1.001	1.013	V_p=6 km/s	0.64	0.998	1.001
	1.03	1.159	1.141		0.78	1.238	1.216
	1.33	1.001	0.999		0.94	1.001	0.999
	1.62	0.999	1.041		1.11	0.826	0.830
	1.91	1.000	1.028		1.27	0.999	1.000
V_p=9 km/s	0.75	0.503	0.951	V_p=9 km/s	(1)	(1)	(1)
	1.03	0.633	0.814		(1)	(1)	(1)
	1.32	1.002	0.999		(1)	(1)	(1)
	1.61	1.532	1.039		(1)	(1)	(1)
	1.91	0.997	1.026		(1)	(1)	(1)
V_p=12 km/s	0.64	1.004	1.013	V_p=12 km/s	(1)	(1)	(1)
	0.95	0.529	0.911		(1)	(1)	(1)
	1.27	0.998	0.999		(1)	(1)	(1)
	1.59	2.396	0.989		(1)	(1)	(1)
	1.91	1.003	1.000		(1)	(1)	(1)

(1) Impact velocity exceeds maximum allowable value.

Table 16. Ratios Of Empirical To Modified Analytical Model Predictions For ELC Wall System

θ_p=0-deg				θ_p=45-deg			
	d_p (cm)	R_D Ratio	R_L Ratio		d_p (cm)	R_D Ratio	R_L Ratio
V_p=6 km/s	1.21	1.082	1.109	V_p=6 km/s	1.09	0.935	1.003
	1.38	0.806	1.113		1.13	0.718	0.999
	1.55	1.004	1.001		1.18	1.001	1.000
	1.73	1.057	0.969		1.22	0.728	0.999
	1.91	1.002	0.999		1.27	1.000	1.000
V_p=9 km/s	1.25	1.022	1.014	V_p=9 km/s	(1)	(1)	(1)
	1.41	0.933	1.082		(1)	(1)	(1)
	1.57	1.001	1.000		(1)	(1)	(1)
	1.74	1.019	0.973		(1)	(1)	(1)
	1.91	1.000	1.001		(1)	(1)	(1)
V_p=12 km/s	1.14	1.119	1.086	V_p=12 km/s	(1)	(1)	(1)
	1.32	0.916	1.138		(1)	(1)	(1)
	1.52	1.002	1.001		(1)	(1)	(1)
	1.71	0.995	0.969		(1)	(1)	(1)
	1.91	1.001	0.999		(1)	(1)	(1)

(1) Impact velocity exceeds maximum allowable value.

Table 17. Comparison of Modified Model Predictions and Actual Empirical Data

Wall System	Test No.	θ_p (deg)	V_p (km/s)	d_p (cm)	D_{eq} (cm)			L_{tt} (cm)		
					Exp. Res.	Model Pred.	Emp. Eqn.	Exp. Res.	Model Pred.	Emp. Eqn.
BLC	HS-11	0	6.41	0.95	3.25	7.69	2.70	5.66	3.50	3.34
	7698-1	0	11.70	1.47	3.96	1.81	4.05	10.29	10.97	10.94
	HS-15	45	6.40	1.11	2.74	3.39	3.05	3.63	6.98	6.67
ELC	1722	0	6.78	1.42	11.20	3.98	3.43	32.39	8.79	10.04
	7698-3	0	11.64	1.32	22.17	22.91	20.79	41.91	39.35	45.11
	n/a	45	All diameters tested exceeded maximum model allowable limit of 1.27 cm							
LEC	1699	0	6.67	1.42	7.12	6.46	5.93	18.67	19.59	18.76
	7698-7	0	11.37	1.32	6.25	4.04	7.68	13.72	14.15	23.49
	1691	45	6.62	1.18	1.22	4.81	4.80	9.91	8.49	8.44

11.0 SUMMARY AND RECOMMENDATIONS

11.1 Summary

This report presents the results of a study whose objective was to develop first-principles-based models of hole size and maximum tip-to-tip crack length for a spacecraft module pressure wall that has been perforated in an orbital debris particle impact. The hole size and crack length models are developed by sequentially characterizing the phenomena comprising the orbital debris impact event, including the initial impact, the creation and motion of a debris cloud within the dual-wall system, the impact of the debris cloud on the pressure wall, the deformation of the pressure wall due to debris cloud impact loading prior to crack formation, pressure wall crack initiation, propagation, and arrest, and finally pressure wall deformation following crack initiation and growth.

The model development has been accomplished through the application of elementary shock physics and thermodynamic theory, as well as the principles of mass, momentum, and energy conservation. The predictions of the model developed herein are compared against the predictions of empirically-based equations for hole diameters and maximum tip-to-tip crack length for three International Space Station wall configurations. The ISS wall systems considered are the baseline U.S. Lab Cylinder, the enhanced U.S. Lab Cylinder, and the U.S. Lab Endcone. The empirical predictor equations were derived from experimentally obtained hole diameters and crack length data. The original model predictions did not compare favorably with the experimental data, especially for cases in which pressure wall petalling did not occur. Several modifications were

made to the original model to bring its predictions closer in line with the experimental results. Following the adjustment of several empirical constants, the predictions of the modified analytical model were in much closer agreement with the experimental results.

11.2 Recommendations

Following a review of the methodology used to develop the pressure wall hole size and crack length models presented herein, the following recommendations are offered as suggestions for improving the robustness of the model as well as for improving its ability to model the phenomena associated with the high speed impact of a pressurized module. These recommendations are grouped according to the part of the model that would be affected by their implementation.

Outer Bumper Impact

1) Include the effects of backsplash due to the impact of the projectile on the outer bumper. This would have the effect of decreasing the mass of the primary debris cloud, but, due to momentum conservation, *increasing* its center-of-mass velocity (the so-called "momentum enhancement effect"). Since the energy of the debris cloud is proportional to the square of the velocity, this could have a significant impact on the subsequent effects produced by the primary debris cloud.

2) Include the effects of light flash in the energy balance for the initial impact on the outer bumper. This would have the effect of producing more accurate primary debris cloud velocities.

Inner Bumper Impact

1) Develop a more suitable equation for the diameter of the hole in the inner bumper produced by the impact of the primary debris cloud. The present approximation is at best an order-of-magnitude estimate. A more appropriate hole-out equation would produce a more

accurate mass value for this component of the secondary debris cloud. This in turn would have some effect on the magnitude of the velocity imparted to the pressure wall by the impact of this component of the secondary debris cloud.

2) Include the effects of inner bumper burning and/or melting. This may be a significant energy absorbing mechanism and may have a significant influence on the energy balance that is applied to the system before and after the impact of the primary debris cloud on the inner bumper.

Pressure Wall Impact

1) Modify the cantilever beam curling model to include a tapered beam width. A sharper beam tip would affect the rate at which curling occurs, which would affect the diameter of the hole created in the pressure wall.

2) Consider the motion of the debris cloud exiting the pressure wall. This would serve as a check on the motion of the pressure wall petals and the kinetic energy absorbed therein.

3) Include the effects of pressure wall curvature and internal stress. This would increase the applicability of the model developed to on-orbit pressurized spacecraft modules.

12.0 REFERENCES

1. W. P. Schonberg, Cracking Characteristics of a Habitable Module Pressure Wall Following Orbital Debris Penetration, Final Report, NASA/ASEE Summer Faculty Fellowship Program, Marshall Space Flight Center, Alabama, 1994.

2. B. E .P. Lutz and C. J. Goodwin, Catastrophic Failure Modes Assessment of the International Space Station Alpha, NASA CR-4720, Marshall Space Flight Center, Alabama, 1996.

3. G. T. Burch, Multi-plate Damage Study, AFATL-TR-67-116, Eglin Air Force Base, Florida, 1967.

4. W. P. Schonberg, A. J. Bean and K. Darzi, Hypervelocity Impact Physics, NASA CR-4343, Washington, D.C.. 1991.

5. W. P. Schonberg, "Aluminum 2219-T87 vs. 5456-H116: A Comparative Study of Pressure Wall Materials in Dual-Wall Structures Under Hypervelocity Impact," *Acta Astronautica*, Vol. 26, 1992, pp. 799-812.

6. SSFPO, Common Module Shell Unzipping Due to Meteoroid/Orbital Debris Strikes, Space Station Freedom Program Office, Report No. GSS-40.05-RPT-6-001, Reston, Virginia, 1994.

7. J. E. Williamsen, Vulnerability of Manned Spacecraft to Crew Loss from Orbital Debris Penetration, NASA TM-108452, Marshall Space Flight Center, Alabama, 1994.

8. W. P. Schonberg, Pressure Wall Hole Size and Maximum Tip-to-Tip Crack Length Following Orbital Debris Penetration, Final Report, NASA/ASEE Summer Faculty Fellowship Program, Marshall Space Flight Center, Alabama, 1995.

9. W. P. Schonberg and J. E. Williamsen, "Cracking Characteristics of Multi-Wall Pressure Vessels Following Hypervelocity Projectile Impact," Proceedings of the 1996 ASME Conference on Structures Under Extreme Loading Conditions, (edited by Y. S. Shin and J. A. Zukas), Montreal, Canada, AMSE-PVP-Vol. 325, 1996.

10. W. P. Schonberg and J. E. Williamsen, "Space Station Module Wall Hole Size and Crack Length Following an Orbital Debris Penetration at 6.5 km/s," Proceedings of the SPACE 96/Comet Day II Symposium, Vol. 1, (edited by S. E. Johnson), pp. 1-7, Albuquerque, New Mexico, 1996.

11. W. P. Schonberg and J. E. Williamsen, "Hole Size and Crack Length Following Orbital Debris Penetration of Space Station Module Walls at 6.5 and 11.3 km/s," Proceedings of the 20th

International Symposium on Space Technology and Science, (ed. Y. Arakawa), Paper No. 96-m-20v, Gifu, Japan, 1996.

12. J. E. Williamsen, D. J. Grosch and W. P. Schonberg, "Empirical Prediction Models for Hole and Crack Size in Space Station Shielding from 6 to 12 km/s," Proceedings of the SPIE Symposium on Orbital Debris Impact Modeling and Penetration Effects, Paper No. 2813-20, Denver, Colorado, 1996.

13. W.P. Schonberg, and J.E. Williamsen, "Empirical Hole Size and Crack Length Models for Dual-Wall Systmes Under Hypervelocity Projectile Impact," *International Journal of Impact Engineering*, to appear, 1997.

14. M.H. Rice, R.G. McQueen, and J.M. Walsh, "Compression of Solids by Strong Shock Waves," Solid State Physics, Volume VI, (ed. F. Seitz and D. Turnbull), Academic Press, New York, 1958.

15. C.A. Anderson, T.G. Trucano, and S.A. Mullin, "Debris Cloud Dynamics," *International Journal of Impact Engineering*, Vol. 9, No. 1, 1990, pp. 89-113.

16. W. Jolly and W.P. Schonberg, "Analytical Prediction of Hole Diameter in Thin Plates Due to Hypervelocity Impact of Spherical Projectiles", *Shock and Vibration*, to appear, 1998.

17. J.F. Lundeberg, P.H. Stern, and R.J. Bristow, Meteoroid Protection for Spacecraft Structures, NASA CR-54201, Washington, D.C., 1965.

18. J. Serrano, D. Liquornik, and W.P. Schonberg, Vulnerability of Space Station Freedom Modules: A Study of the Effects of Module Perforation on Crew and Equipment, NASA CR-4716, Marshall Space Flight Center, Alabama, 1996.

19. A.L. Florence, "Clamped Circular Rigid-Plastic Plates Under Blast Loading," *Journal of Applied Mechanics*, Vol. 33, No. 2, 1966, pp. 256-260.

20. A.L. Florence, "Clamped Circular Rigid-Plastic Plates Under Central Blast Loading," *International Journal of Solids and Structures*, Vol. 2, 1966, pp. 319-335.

21. A.J. Wang and H.G. Hopkins, "On the Plastic Deformation of Built-in Circular Plates Under Impulsive Load", *Journal of the Mechanics and Physics of Solids*, Vol. 3, 1954, pp. 22-37.

22. T.L. Anderson, Fracture Mechanics: Fundamentals and Applications, CRC Press, New York, 1991.

23. T.C.T. Ting, "Large Deformation of a Rigid Ideally Plastic Cantilever Beam," *Journal of Applied Mechanics*, Vol. 32, No. 2, 1965, pp. 295-302.

24. D. Krajcinovic, "Dynamic Analysis of Clamped Plastic Circular Plates", *International Journal of Mechanical Sciences*, Vol. 14., 1972, pp. 225-234.

25. A. Atkins, Elastic Plastic Fracture, John Wiley and Sons, New York, 1985.

26. M.F. Kanninen and C.H. Popelar, Advanced Fracture Mechanics, Oxford University Press, Oxford, England, 1985.

27. D.K. Roberts and A.A. Wells, "The Velocity of Brittle Fracture", *Engineering*, Vol. 178, 1954, pp. 820-821.

28. W.P. Schonberg and F. Yang, "Response of Structures to Orbital Debris Particle Impact", *International Journal of Impact Engineering*, Vol. 14, 1993, pp. 647-658.

APPENDIX A

EXPERIMENTAL HOLE SIZE AND CRACK LENGTH DATA

Table A.1 High Speed Impact Test Parameters and Experimental Data

Test No.	D_p (cm)	D_{ML} (cm)	V_p (kms)	θ_b (deg)	t_b (cm)	λ_{ML} (gm/cm^2)	L_{ML} (cm)	S (cm)	S_2 (cm)	D_{perf} (cm)	L_{ML} (cm)	N_{cr}	Δ	f_{pen}
T2-7A	0.795	0.310	3.21	0	0.16	0.107	0.32	10.16	0.00	1.60	8.00	6	625.00	1.46
UAH-13	1.588	1.372	6.52	0	0.16	1.170	0.48	11.43	2.25	7.11	25.15	7	552.67	10.56
UAH-9	1.588	1.328	6.21	0	0.16	1.170	0.48	11.43	2.25	8.26	22.61	8	421.74	10.06
3402C	0.795	0.569	6.17	0	0.16	0.107	0.32	10.16	2.00	0.45	7.26	4	261.09	1.04
3401B	0.795	0.622	7.09	0	0.16	0.072	0.32	10.16	2.00	1.40	8.92	5	258.50	0.80
3011B	0.795	0.605	6.75	0	0.10	0.107	0.32	10.16	0.00	6.08	20.32	6	256.00	3.08
3402B	0.795	0.622	7.10	0	0.16	0.107	0.32	10.16	2.00	0.88	5.51	5	246.69	1.19
3404D	0.953	0.503	5.50	0	0.16	0.107	0.32	10.16	2.00	4.57	13.23	7	203.72	1.11
3401C	0.795	0.551	6.12	0	0.16	0.072	0.32	10.16	2.00	0.61	8.61	4	199.52	0.69
3404C	0.953	0.564	6.23	0	0.16	0.107	0.32	10.16	2.00	4.75	17.68	6	191.90	1.25
1698	0.953	0.683	6.61	0	0.13	0.033	0.32	11.43	2.25	6.58	18.29	7	166.02	0.41
339	0.953	0.470	6.49	45	0.10	0.107	0.32	10.16	0.00	4.37	22.30	5	133.01	2.51
UAH-1	1.270	0.826	6.70	0	0.16	0.033	0.48	11.43	2.25	5.84	15.24	7	120.81	0.24
3227A	0.953	0.610	6.80	0	0.16	0.107	0.32	10.16	0.00	9.27	30.73	6	120.77	3.72
3401D	0.795	0.478	5.25	0	0.16	0.072	0.32	10.16	2.00	0.57	6.15	4	116.72	0.59
3401A	0.795	0.615	7.22	0	0.16	0.072	0.32	10.16	2.00	2.01	9.07	5	91.93	0.82
3402A	0.795	0.617	7.18	0	0.16	0.107	0.32	10.16	2.00	0.82	7.72	4	88.58	1.20
3403C	0.795	0.561	6.20	0	0.16	0.107	0.32	10.16	3.80	1.76	7.72	5	84.42	0.43
3402D	0.795	0.462	5.02	0	0.16	0.107	0.32	10.16	2.00	0.54	4.70	4	75.44	0.84
3020A	0.795	0.599	6.65	0	0.16	0.107	0.32	10.16	0.00	2.62	22.28	4	72.50	3.03
3011A	0.795	0.627	7.02	0	0.10	0.107	0.32	10.16	0.00	6.55	18.72	6	66.59	3.20
1691	1.193	1.006	6.62	0	0.19	0.033	0.48	22.15	7.22	1.22	9.91	4	66.02	0.12
UAH-PT1	1.430	1.285	6.00	0	0.16	1.170	0.48	11.43	2.25	2.34	18.80	4	64.70	8.76
PREH2	0.795	0.617	6.88	0	0.16	0.107	0.32	10.16	0.00	5.05	20.24	5	64.24	3.14
EH-M4	0.795	0.620	6.92	0	0.16	0.107	0.32	10.16	0.00	2.03	15.95	4	61.62	3.16
7698-22	0.884	0.820	11.36	45	0.13	0.033	0.32	11.43	2.25	2.18	17.02	4	60.69	0.46
3404B	0.953	0.615	6.85	0	0.16	0.107	0.32	10.16	2.00	6.76	15.24	7	58.28	1.38
338	0.795	0.493	6.98	45	0.10	0.107	0.32	10.16	0.00	2.44	9.30	5	55.42	2.25
T2-5	0.795	0.348	3.94	0	0.10	0.107	0.32	10.16	0.00	2.13	5.82	6	55.24	1.80
EH2A	0.795	0.627	6.99	0	0.16	0.107	0.32	10.16	0.00	3.58	26.57	4	55.03	3.19
7139-15	1.749	1.382	11.01	45	0.20	0.800	0.48	11.43	2.25	26.47	71.12	6	52.14	9.50
WS-77	1.588	1.468	6.47	45	0.18	0.800	0.48	11.43	2.25	6.30	22.86	5	47.79	5.07
1699	1.429	1.024	6.67	0	0.19	0.033	0.48	22.15	7.22	7.12	18.67	6	47.14	0.14
EH2E	0.795	0.602	6.70	0	0.16	0.107	0.32	10.16	0.00	6.88	17.93	6	46.06	3.06

P33B1	0.635	0.470	5.26	0	0.10	0.107	0.32	10.16	0.00	0.64	4.19	4	43.56	1.92
PREH1	0.795	0.627	6.99	0	0.16	0.107	0.32	10.16	0.00	2.79	18.29	4	42.84	3.19
003A	0.795	0.470	6.51	45	0.10	0.107	0.32	10.16	0.00	3.43	11.99	5	42.74	2.10
HS-19	0.795	0.693	6.34	0	0.13	0.033	0.41	11.43	2.25	0.53	3.38	4	40.11	0.20
7698-2	1.386	0.777	11.38	0	0.19	0.033	0.48	22.15	7.22	6.78	22.02	5	34.24	0.24
EH4A	0.795	0.554	6.13	0	0.16	0.107	0.32	10.16	0.00	2.21	12.70	4	33.03	2.80
7698-20	1.269	0.785	11.40	45	0.13	0.033	0.48	11.43	2.25	8.76	20.96	6	32.70	0.29
7698-5	1.348	0.511	11.80	0	0.13	0.033	0.32	11.43	2.25	15.24	30.48	7	32.00	1.04
1783	1.669	1.494	6.65	45	0.20	0.800	0.48	11.43	2.25	10.33	24.00	6	29.21	5.48
3404A	0.953	0.815	6.85	0	0.16	0.107	0.32	10.16	2.00	8.05	24.38	5	27.80	1.38
HS-21	1.113	0.691	6.32	0	0.13	0.033	0.41	11.43	2.25	4.55	10.41	6	27.52	0.28
1716	1.193	1.176	6.74	0	0.13	0.800	0.32	11.43	2.25	6.44	32.39	4	25.30	12.69
7698-9	1.321	0.815	11.40	45	0.13	0.033	0.32	11.43	2.25	22.10	49.53	6	25.24	0.69
7698-21	1.214	1.151	11.30	0	0.20	0.800	0.48	11.43	2.25	7.62	22.23	5	24.81	9.57
1722	1.429	1.361	6.78	0	0.20	0.800	0.48	11.43	2.25	11.20	32.39	5	24.17	6.76
1792	1.669	0.973	6.41	0	0.19	0.033	0.48	22.15	7.22	9.03	25.91	5	23.62	0.16
UAH-5	1.588	1.379	6.58	0	0.16	1.170	0.48	11.43	2.25	13.41	24.89	7	22.03	10.66
EH2C	0.795	0.592	6.58	0	0.16	0.107	0.32	10.16	0.00	1.04	22.66	3	21.78	3.00
7698-19	1.105	0.790	11.30	45	0.13	0.033	0.48	11.43	2.25	3.24	15.08	4	21.69	0.25
WS-63	1.748	1.486	6.61	45	0.18	0.800	0.48	11.43	2.25	10.95	30.48	5	21.58	5.70
1725	1.429	1.278	6.69	45	0.13	0.800	0.32	11.43	2.25	12.38	26.67	6	21.52	10.67
7698-4	1.307	0.785	11.40	45	0.13	0.033	0.48	11.43	2.25	6.55	28.58	4	19.01	0.30
337	0.795	0.488	6.90	45	0.10	0.107	0.32	10.16	0.00	2.13	8.92	4	17.46	2.23
7139-9	1.279	1.161	11.00	0	0.20	0.800	0.48	11.43	2.25	20.80	41.91	6	16.47	9.81
T2-17	0.953	0.429	4.62	0	0.16	0.107	0.32	10.16	0.00	8.31	16.66	6	16.20	2.53
1721	1.429	1.176	6.74	0	0.13	0.800	0.32	11.43	2.25	17.34	27.43	8	15.70	15.20
EH4B	0.795	0.602	6.70	0	0.16	0.107	0.32	10.16	0.00	4.06	10.16	5	15.63	3.06
3034A	0.795	0.432	4.50	0	0.20	0.107	0.32	10.16	0.00	0.53	7.77	3	14.57	2.05
1790	1.669	1.240	6.38	45	0.13	0.800	0.32	11.43	2.25	21.79	41.91	6	13.68	11.88
1777	1.669	1.153	6.31	0	0.13	0.800	0.32	11.43	2.25	21.95	41.91	6	13.30	16.62
7698-3	1.330	1.110	11.64	0	0.20	0.800	0.48	11.43	2.25	22.17	41.91	6	12.76	10.80
3006A	0.795	0.488	7.01	45	0.08	0.107	0.32	10.16	0.00	1.68	5.84	4	12.14	2.26
336	0.635	0.376	4.47	45	0.10	0.107	0.32	10.16	0.00	0.99	3.33	4	11.28	1.15
WS-47	1.588	1.374	6.66	0	0.18	0.800	0.48	11.43	2.25	16.10	25.40	7	9.76	7.37
1780	1.905	1.618	6.01	65	0.13	0.800	0.32	11.43	2.25	14.14	43.82	4	9.61	7.64
T2-15	0.953	0.445	4.98	0	0.10	0.107	0.32	10.16	0.00	8.74	15.34	6	9.50	2.72
3034C	0.795	0.518	5.60	0	0.20	0.107	0.32	10.16	0.00	1.57	14.53	3	9.23	2.55
002B	0.795	0.495	6.51	45	0.16	0.107	0.32	10.16	0.00	0.48	4.24	3	8.79	2.10
3034B	0.795	0.363	3.63	0	0.20	0.107	0.32	10.16	0.00	0.79	6.12	3	7.77	1.66
WS-44	1.588	1.379	6.58	0	0.18	0.800	0.48	11.43	2.25	16.94	25.40	7	7.57	7.29
102D	0.762	0.378	3.83	0	0.20	0.107	0.32	10.16	0.00	0.51	3.81	3	7.50	1.67
WS-78	1.588	1.468	6.47	45	0.18	0.800	0.48	11.43	2.25	7.09	19.05	4	7.23	5.07
HS-10	0.795	0.787	6.40	0	0.13	0.033	0.48	11.43	2.25	0.23	1.65	3	7.22	0.15
EH2D	0.795	0.602	6.62	0	0.16	0.107	0.32	10.16	0.00	3.23	23.04	3	7.14	3.02
1779	1.669	1.623	6.44	65	0.13	0.800	0.32	11.43	2.25	3.31	15.24	3	4.60	7.17
3227B	0.953	0.602	6.70	0	0.16	0.107	0.32	10.16	0.00	9.50	19.86	4	4.37	3.66
7139-1	0.956	0.635	11.30	0	0.13	0.033	0.48	11.43	2.25	2.87	5.84	4	4.14	0.31

211D	0.889	0.508	6.84	45	0.16	0.107	0.32	10.16	0.00	2.79	5.61	4	4.04	2.47
7139-10	1.779	1.156	11.19	0	0.20	0.800	0.48	11.43	2.25	44.25	58.42	7	4.01	13.89
1762	1.669	1.372	6.49	0	0.20	0.800	0.48	11.43	2.25	18.48	34.67	4	3.52	7.56
1764	1.113	0.648	6.34	0	0.13	0.033	0.32	11.43	2.25	10.41	18.80	4	3.26	0.46
WS-64	1.748	1.379	6.58	0	0.18	0.800	0.48	11.43	2.25	18.11	24.13	6	3.16	8.02
306	0.953	0.569	6.25	45	0.16	0.107	0.41	10.16	0.00	3.89	9.98	3	2.57	1.47
T219B	0.795	0.300	2.90	0	0.16	0.107	0.32	10.16	0.00	1.75	3.94	3	2.25	1.32
UAH-6	1.588	0.803	6.50	0	0.16	0.033	0.48	11.43	2.25	6.35	14.22	3	2.24	0.30
HS-11	0.953	0.787	6.41	0	0.13	0.033	0.48	11.43	2.25	3.25	5.66	3	1.74	0.18
T219A	0.795	0.295	2.96	0	0.16	0.107	0.32	10.16	0.00	1.27	2.16	3	1.70	1.35
HS-20	0.953	0.693	6.35	0	0.13	0.033	0.41	11.43	2.25	4.65	7.62	3	1.64	0.24
3403D	0.795	0.462	5.03	0	0.16	0.107	0.32	10.16	3.80	2.16	3.30	3	1.53	0.35
UAH-10	1.588	0.815	6.63	0	0.16	0.033	0.48	11.43	2.25	6.60	9.65	3	1.46	0.30
P33B	0.635	0.432	4.85	0	0.10	0.107	0.32	10.16	0.00	2.11	2.11	1	1.00	1.77
201D	0.635	0.526	7.69	45	0.10	0.107	0.32	10.16	0.00	1.24	1.24	1	1.00	1.96
4113C	0.635	0.602	6.30	60	0.20	0.107	0.32	10.16	3.80	0.24	0.24	1	1.00	0.18
P33B	0.635	0.432	4.85	0	0.10	0.107	0.32	10.16	0.00	2.11	2.11	1	1.00	1.77
215A	0.889	0.549	4.66	0	0.10	0.107	0.48	10.16	0.00	1.45	1.45	1	1.00	1.05
3024B	0.795	0.627	7.02	0	0.16	0.107	0.32	10.16	0.00	0.46	17.37	2	1.00	3.20
320	0.795	0.503	3.03	45	0.16	0.107	0.32	10.16	0.00	0.03	0.64	2	1.00	0.98
3002A	0.635	0.627	6.99	0	0.08	0.107	0.32	10.16	0.00	0.23	4.42	2	1.00	2.55
1690	0.795	0.671	6.50	0	0.13	0.033	0.32	11.43	2.25	0.58	10.16	2	1.00	0.34
3020B	0.795	0.627	7.05	0	0.16	0.107	0.32	10.16	0.00	2.36	25.70	2	1.00	3.22
001B	0.795	0.513	6.56	45	0.20	0.107	0.32	10.16	0.00	0.79	3.86	2	1.00	2.12
325	0.795	0.411	4.14	45	0.16	0.107	0.32	10.16	0.00	1.12	2.97	2	1.00	1.34
3028A	0.795	0.516	7.01	45	0.16	0.107	0.32	10.16	0.00	1.40	3.68	2	1.00	2.26
7698-1	1.475	0.620	11.70	0	0.13	0.033	0.48	11.43	2.25	3.96	10.29	2	1.00	0.50
7698-7	1.330	0.980	11.37	45	0.19	0.033	0.48	22.15	7.22	6.25	13.72	2	1.00	0.16
3002B	0.635	0.610	7.33	0	0.08	0.107	0.32	10.16	0.00	3.53	5.99	2	1.00	2.67
UAH-3	1.588	0.790	6.42	0	0.16	0.033	0.48	11.43	2.25	6.10	8.64	2	1.00	0.29
MD-TA	0.475	0.361	2.15	0	0.16	0.107	0.32	10.16	0.00	0.81	0.81	1	1.00	0.59
T2-1	0.475	0.292	2.55	0	0.10	0.107	0.32	10.16	0.00	0.71	0.71	1	1.00	0.69
P07	0.635	0.297	2.93	0	0.16	0.107	0.32	10.16	0.00	0.91	0.91	1	1.00	1.07
P08	0.635	0.295	2.96	0	0.16	0.107	0.32	10.16	0.00	0.99	0.99	1	1.00	1.08
T2-3	0.635	0.292	2.99	0	0.16	0.107	0.32	10.16	0.00	0.41	0.41	1	1.00	1.09
229B	0.795	0.409	3.07	0	0.20	0.107	0.48	10.16	0.00	1.22	1.22	1	1.00	0.62
205E	0.635	0.490	3.15	45	0.16	0.107	0.32	10.16	0.00	0.89	0.89	1	1.00	0.81
229C	0.795	0.462	3.56	0	0.20	0.107	0.48	10.16	0.00	0.76	0.76	1	1.00	0.72
203G	0.889	0.772	4.70	65	0.10	0.107	0.32	10.16	0.00	0.38	0.38	1	1.00	1.01
205C	0.635	0.447	5.30	45	0.16	0.107	0.32	10.16	0.00	0.97	0.97	1	1.00	1.37
215B	0.889	0.645	5.48	0	0.10	0.107	0.48	10.16	0.00	0.84	0.84	1	1.00	1.24
201B	0.635	0.424	5.51	45	0.10	0.107	0.32	10.16	0.00	1.17	1.17	1	1.00	1.42
210B	0.889	0.762	5.67	65	0.16	0.107	0.32	10.16	0.00	0.33	0.33	1	1.00	1.22
P21D	0.762	0.531	5.85	0	0.16	0.107	0.32	10.16	0.00	2.62	2.62	1	1.00	2.56
218B	0.889	0.617	6.40	45	0.10	0.107	0.48	10.16	0.00	1.78	1.78	1	1.00	1.02
207B	0.762	0.701	6.47	65	0.16	0.107	0.32	10.16	0.00	0.36	0.36	1	1.00	1.20
210D	0.889	0.665	7.05	65	0.16	0.107	0.32	10.16	0.00	0.81	0.81	1	1.00	1.52

203G	0.889	0.772	4.70	65	0.10	0.107	0.32	10.16	0.00	0.38	0.38	1	1.00	1.01
205C	0.635	0.447	5.30	45	0.16	0.107	0.32	10.16	0.00	0.97	0.97	1	1.00	1.37
201B	0.635	0.424	5.51	45	0.10	0.107	0.32	10.16	0.00	1.17	1.17	1	1.00	1.42
210B	0.889	0.762	5.67	65	0.16	0.107	0.32	10.16	0.00	0.33	0.33	1	1.00	1.22
P21D	0.762	0.531	5.85	0	0.16	0.107	0.32	10.16	0.00	2.62	2.62	1	1.00	2.56
207B	0.762	0.701	6.47	65	0.16	0.107	0.32	10.16	0.00	0.36	0.36	1	1.00	1.20
210D	0.889	0.665	7.05	65	0.16	0.107	0.32	10.16	0.00	0.81	0.81	1	1.00	1.52
218B	0.889	0.617	6.40	45	0.10	0.107	0.48	10.16	0.00	1.76	1.76	1	1.00	1.02
7139-13	1.000	0.820	10.70	45	0.13	0.033	0.48	11.43	2.25	1.27	1.27	1	1.00	0.22
4001A	0.795	0.523	3.15	45	0.20	0.107	0.32	10.16	3.80	1.14	1.14	1	1.00	0.15
4114D	0.795	0.607	7.40	60	0.20	0.107	0.32	10.16	3.80	0.53	0.53	1	1.00	0.26
3403B	0.795	0.622	7.10	0	0.16	0.107	0.32	10.16	3.80	2.02	2.03	1	0.99	0.50
3303D	0.475	0.483	5.65	45	0.20	0.107	0.32	10.16	3.80	0.15	0.15	1	0.98	0.17
3306C	0.635	0.625	7.05	0	0.16	0.072	0.32	10.16	3.80	0.47	0.48	1	0.97	0.26
321	0.795	0.546	2.97	45	0.20	0.107	0.32	10.16	0.00	0.79	0.81	1	0.97	0.96
1816	1.429	0.991	6.42	65	0.13	0.033	0.58	22.15	7.22	2.29	2.36	1	0.97	0.04
3306D	0.635	0.625	6.98	0	0.16	0.072	0.32	10.16	3.80	0.27	0.28	1	0.96	0.26
1771	1.905	0.942	6.30	65	0.19	0.033	0.48	22.15	7.22	3.92	4.19	1	0.94	0.08
207A	0.762	0.747	5.86	65	0.16	0.107	0.32	10.16	0.00	0.36	0.38	1	0.93	1.08
3304A	0.635	0.500	6.20	45	0.20	0.107	0.32	10.16	3.80	0.64	0.69	1	0.93	0.24
207A	0.762	0.747	5.86	65	0.16	0.107	0.32	10.16	0.00	0.36	0.38	1	0.93	1.08
218A	0.889	0.584	5.82	45	0.10	0.107	0.48	10.16	0.00	1.68	1.80	1	0.93	0.93
303A	0.795	0.523	3.65	45	0.16	0.107	0.41	10.16	0.00	1.57	1.70	1	0.93	0.72
1756	0.953	0.838	6.65	65	0.13	0.033	0.48	11.43	0.00	1.22	1.32	1	0.92	0.21
1773	1.113	0.843	6.57	65	0.13	0.033	0.48	11.43	0.00	0.58	0.64	1	0.92	0.24
1755	1.429	0.658	6.57	65	0.19	0.033	0.48	22.15	7.22	1.75	1.91	1	0.92	0.06
WS-76	1.270	0.813	6.63	0	0.13	0.033	0.48	11.43	3.50	4.90	5.33	1	0.92	0.14
1770	1.669	0.925	6.49	65	0.19	0.033	0.48	22.15	7.22	2.10	2.29	1	0.92	0.07
1759	1.113	0.762	6.21	0	0.13	0.033	0.48	11.43	0.00	4.09	4.62	1	0.88	0.54
1768	1.270	0.640	6.10	65	0.13	0.033	0.32	11.43	2.25	2.59	2.95	1	0.88	0.21
1825	0.953	0.787	6.39	0	0.13	0.033	0.48	11.43	0.00	3.58	4.14	1	0.87	0.48
3304C	0.635	0.523	6.84	45	0.20	0.107	0.32	10.16	3.80	1.52	1.78	1	0.85	0.27
HS-12	1.113	0.777	6.32	0	0.13	0.033	0.48	11.43	2.25	5.11	5.99	1	0.85	0.20
212B	0.762	0.490	6.38	45	0.16	0.107	0.32	10.16	0.00	1.57	1.85	1	0.85	1.97
201A	0.635	0.371	4.33	45	0.10	0.107	0.32	10.16	0.00	0.84	1.02	1	0.83	1.12
HS-17	0.953	0.853	6.47	65	0.13	0.033	0.48	11.43	2.25	0.58	0.71	1	0.82	0.07
3308B	0.635	0.483	6.21	45	0.16	0.107	0.32	10.16	3.80	1.04	1.27	1	0.82	0.25
201C	0.635	0.503	7.21	45	0.10	0.107	0.32	10.16	0.00	0.33	0.41	1	0.81	1.86
WS-34	0.953	0.828	6.72	0	0.13	0.033	0.48	11.43	3.50	2.06	2.54	1	0.81	0.11
205B	0.635	0.422	4.62	45	0.16	0.107	0.32	10.16	0.00	0.43	0.53	1	0.81	1.19
1798	1.669	1.120	6.48	0	0.13	0.033	0.58	22.15	7.22	6.93	8.57	1	0.81	0.11
335	0.635	0.376	4.07	45	0.10	0.107	0.32	10.16	0.00	0.97	1.19	1	0.81	1.05
1772	1.113	0.643	6.57	45	0.13	0.033	0.48	11.43	0.00	3.33	4.14	1	0.80	0.40
7698-13	0.901	0.780	11.50	45	0.13	0.033	0.48	11.43	2.25	1.42	1.78	1	0.80	0.21
4003C	0.795	0.488	3.18	45	0.16	0.107	0.32	10.16	3.80	1.27	1.60	1	0.79	0.16
326	0.795	0.437	4.22	45	0.20	0.107	0.32	10.16	0.00	1.37	1.75	1	0.78	1.36
HS-18	1.113	0.853	6.46	65	0.13	0.033	0.48	11.43	2.25	2.26	2.90	1	0.78	0.09

1753	0.959	0.846	6.62	65	0.13	0.033	0.32	11.43	2.25	0.99	1.27	1	0.78	0.17
4002C	0.795	0.762	6.30	75	0.20	0.107	0.32	10.16	3.80	0.41	0.53	1	0.77	0.11
HS-23	0.953	0.554	6.28	45	0.13	0.033	0.41	11.43	2.25	2.21	2.90	1	0.76	0.17
1712	0.795	0.643	6.56	45	0.13	0.033	0.48	11.43	0.00	1.93	2.54	1	0.76	0.29
1817	1.193	1.100	6.40	0	0.13	0.033	0.58	22.15	7.22	2.25	2.97	1	0.76	0.08
HS-15	1.113	0.635	6.40	45	0.13	0.033	0.48	11.43	2.25	2.74	3.63	1	0.76	0.14
4003A	0.795	0.465	3.43	45	0.16	0.107	0.32	10.16	3.80	1.53	2.03	1	0.75	0.17
HS-14	0.953	0.630	6.35	45	0.13	0.033	0.48	11.43	2.25	2.39	3.18	1	0.75	0.12
1766	1.113	0.650	6.33	45	0.13	0.033	0.32	11.43	2.25	3.10	4.17	1	0.74	0.32
HS-24	1.113	0.556	6.33	45	0.13	0.033	0.41	11.43	2.25	2.77	3.76	1	0.74	0.20
4111A	0.795	0.556	2.85	45	0.20	0.107	0.32	10.16	3.80	0.69	0.94	1	0.74	0.14
211B	0.889	0.470	5.88	45	0.16	0.107	0.32	10.16	0.00	2.13	2.92	1	0.73	2.12
1709	0.795	0.653	6.42	45	0.13	0.033	0.32	11.43	2.25	1.85	2.54	1	0.73	0.23
1769	1.669	0.752	6.51	45	0.19	0.033	0.48	22.15	7.22	6.36	8.76	1	0.73	0.11
1767	1.113	0.841	6.53	65	0.13	0.033	0.32	11.43	2.25	1.30	1.80	1	0.72	0.20
1815	1.429	0.831	6.50	45	0.13	0.033	0.58	22.15	7.22	4.53	6.32	1	0.72	0.07
4003B	0.795	0.485	6.29	45	0.16	0.107	0.32	10.16	3.80	1.80	2.54	1	0.71	0.31
4004B	0.795	0.777	6.08	75	0.20	0.107	0.32	10.16	3.80	0.27	0.38	1	0.71	0.11
1735	0.953	0.648	6.60	45	0.13	0.033	0.48	11.43	0.00	2.69	3.81	1	0.71	0.35
1726	0.953	0.660	6.58	45	0.13	0.033	0.32	11.43	2.25	2.87	4.06	1	0.71	0.29
319	0.795	0.462	2.93	45	0.10	0.107	0.32	10.16	0.00	1.83	2.59	1	0.71	0.95
4001B	0.795	0.434	4.29	45	0.20	0.107	0.32	10.16	3.80	1.60	2.29	1	0.70	0.21
205A	0.635	0.409	4.20	45	0.16	0.107	0.32	10.16	0.00	0.23	0.33	1	0.69	1.08
4003D	0.795	0.500	6.22	45	0.20	0.107	0.32	10.16	3.80	1.30	1.91	1	0.68	0.31
3403A	0.795	0.620	7.15	0	0.16	0.107	0.32	10.16	3.80	2.05	3.07	1	0.67	0.50
HS-13	0.795	0.635	6.40	45	0.13	0.033	0.48	11.43	2.25	0.91	1.37	1	0.67	0.10
1814	1.429	1.140	6.60	0	0.13	0.033	0.58	22.15	7.22	4.38	6.67	1	0.66	0.09
4001C	0.795	0.498	6.12	45	0.20	0.107	0.32	10.16	3.80	1.33	2.03	1	0.66	0.30
1727	1.429	0.762	6.59	45	0.19	0.033	0.48	22.15	7.22	4.19	6.48	1	0.65	0.10
1818	1.193	0.820	6.40	45	0.13	0.033	0.58	22.15	7.22	3.39	5.26	1	0.64	0.05
4111B	0.795	0.455	3.94	45	0.20	0.107	0.32	10.16	3.80	0.95	1.47	1	0.64	0.19
324	0.795	0.376	4.05	45	0.10	0.107	0.32	10.16	0.00	1.80	3.00	1	0.60	1.31
218C	0.889	0.645	6.88	45	0.10	0.107	0.48	10.16	0.00	1.85	3.10	1	0.60	1.10
1796	1.905	1.024	6.10	65	0.13	0.033	0.58	22.15	7.22	3.51	6.21	1	0.56	0.05
1711	1.193	0.770	6.65	45	0.19	0.033	0.48	22.15	7.22	3.01	5.72	1	0.53	0.08
1800	1.669	0.975	6.60	65	0.13	0.033	0.58	22.15	7.22	1.49	2.86	1	0.52	0.05
4111C	0.795	0.493	5.97	45	0.20	0.107	0.32	10.16	3.80	1.41	2.79	1	0.50	0.30
1799	1.669	0.833	6.49	45	0.13	0.033	0.58	22.15	7.22	3.85	8.12	1	0.47	0.08
HS-28	0.953	0.787	6.28	65	0.13	0.033	0.41	11.43	2.25	1.85	4.11	1	0.45	0.10
1774	1.270	0.876	6.21	65	0.13	0.033	0.48	11.43	0.00	0.71	1.60	1	0.44	0.26
HS-22	0.795	0.559	6.37	45	0.13	0.033	0.41	11.43	2.25	1.40	3.15	1	0.44	0.14
4111D	0.795	0.521	6.81	45	0.20	0.107	0.32	10.16	3.80	0.82	1.91	1	0.43	0.34
HS-27	1.113	0.754	6.41	65	0.13	0.033	0.41	11.43	2.25	1.32	4.47	1	0.30	0.12
4001D	0.795	0.518	6.71	45	0.20	0.107	0.32	10.16	3.80	1.09	3.81	1	0.29	0.33
T2-7	0.795	0.312	3.24	0	0.16	0.107	0.32	10.16	0.00	1.42	7.11	1	0.20	1.48

APPENDIX B

FORTRAN PROGRAM PWCRCK.FOR

```
$DEBUG
      PROGRAM PWCRCK
      IMPLICIT DOUBLE PRECISION (A-H,O-Z)
      DOUBLE PRECISION KSB,KSP,KB,KP,KT,NUB,NUP,NUT,MB,MIB,MBT,MP,NCR
      DOUBLE PRECISION KIOJ,KAPJ,KJ,KJ1G,KIJ,KIDJ,KSI,LTT,MY,MPL,M2
      DOUBLE PRECISION PRP(500),PRB(500),XF(2001),YF(2001)
      CHARACTER*1 DET,MPLOPT,MYOPT,MODE
      CHARACTER*2 BID,PID,TID,BIDCHK,PIDCHK,TIDCHK
      CHARACTER*3 IB,WSID,WSCHK
      CHARACTER*10 BMAT,PMAT,TMAT,IBMAT
      CHARACTER*21 WTYPE
C
      OPEN(1,FILE='IMPDAT')
      OPEN(2,FILE='IMPOUT')
C        OPEN(3,FILE='PRPLOT')
      OPEN(4,FILE='GPARAM')
C        OPEN(5,FILE='XYPLOT')
C        OPEN(6,FILE='TGINFO')
C        OPEN(7,FILE='TPLOT')
      OPEN(8,FILE='COEFF')
      OPEN(9,FILE='OBLDATA')
      OPEN(10,FILE='WALDAT')
      OPEN(11,FILE='REGDAT')
      OPEN(12,FILE='CDCLNEC')
      OPEN(13,FILE='CDCLELC')
      OPEN(14,FILE='CDCLBLC')
        OPEN(15,FILE='CDCLLEC')
C
      PI=3.141592
C
C.....  READ PROJECTILE, BUMPER, AND PRESSURE WALL MATERIAL PROPERTIES.
C.....  THE PARAMETERS MUST BE IN THE FOLLOWING UNITS:
C.....
C.....          BID,PID,TID,IB ......... MATERIAL ID CODES
C.....              NOTE: IB = AA0 ..... MLI INNER BUMPER
C.....                    IB = BB1 ..... ENHANCED US LAB CONFIGURATION
C.....                    IB = BB2 ..... ENHANCED JEM WALL CONFIGURATION
C.....          BMAT,PMAT,TMAT,IBMAT ... MATERIALS
C.....          COB,COP,COT.............. BULK SOUND SPEED, KM/S
C.....          RB,RP,RT ................ AMBIENT MATL DENSITY, GM/CUCM
C.....          RIBA .................... INNER BMPR AREAL DNSTY,GM/SQCM
C.....          KB,KP,KT ................ SLOPE OF US-UP LINE
C.....          EB,EP,ET................. ELASTIC MODULUS, LBS/SQ.IN.
C.....          ALFAB,ALFAP,ALFAT ...... LINEAR COEFF OF TERMAL EXP, 1/C
C.....          CPSB,CPSP,CPST ......... SPECIFIC HEAT (SOLID), CAL/GM-C
```

```
C.....          CPLB,CPLP,CPLT ......... SPECIFIC HEAT (LIQD), CAL/GM/C
C.....          TMB,TMP,TMT ............ MELT TEMPERATURE, C
C.....          TVB,TVP,TVT ............ VAPORIZATION TEMPERATURE, C
C.....          HFB,HFP,HFT ............ LATENT HEAT OF FUSION, CAL/GM
C.....          HVB,HVP,HVT ............ LATENT HEAT OF VPRZTN, CAL/GM
C
      READ(4,5) PID,BID,TID,MODE
    5 FORMAT(3A2,A1)
      READ(4,109) WSID
  109 FORMAT(A3)
C
      REWIND 1
      READ(1,4)
    4 FORMAT(////)
C
   99 READ(1,1) PIDCHK
    1 FORMAT(A2)
      IF (PID.EQ.PIDCHK) THEN
      READ(1,10) PMAT,COP,KP,RP,GPI
   10 FORMAT(A10,4F10.5)
      READ(1,100) EP,NUP,ALPHAP,CPSP,CPLP
  100 FORMAT(2(E10.3,F10.5),F10.5)
      READ(1,102) TMP,TVP,HFP,HVP
  102 FORMAT(4F10.5)
      ENDIF
      IF (PID.NE.PIDCHK) THEN
      IF (PIDCHK.EQ.'XX') THEN
      WRITE (*,17)
   17 FORMAT(' PROJECTILE MATERIAL NOT FOUND IN MATERIAL LIBRARY.',/,
     $' PLEASE CHECK DEBRIS CLOUD MATERIAL ID CODE AND BEGIN AGAIN.')
      STOP
      ENDIF
      IF (PIDCHK.NE.'XX') THEN
      READ (1,2)
    2 FORMAT(///)
      GOTO 99
      ENDIF
      ENDIF
C
      REWIND 1
      READ(1,4)
  999 READ(1,1) BIDCHK
      IF (BID.EQ.BIDCHK) THEN
      READ(1,10) BMAT,COB,KB,RB,GBI
      READ(1,100) EB,NUB,ALPHAB,CPSB,CPLB
      READ(1,102) TMB,TVB,HFB,HVB
      ENDIF
      IF (BID.NE.BIDCHK) THEN
      IF (BIDCHK.EQ.'XX') THEN
      WRITE (*,117)
  117 FORMAT(' BUMPER MATERIAL NOT FOUND IN MATERIAL LIBRARY.',/,' PLEAS
     $E CHECK BUMPER MATERIAL ID CODE AND BEGIN AGAIN.')
      STOP
      ENDIF
      IF (BIDCHK.NE.'XX') THEN
```

```
      READ (1,2)
      GOTO 999
      ENDIF
      ENDIF
C
      REWIND 1
      READ(1,4)
 9999 READ(1,1) TIDCHK
      IF (TID.EQ.TIDCHK) THEN
      READ(1,10) TMAT,COT,KT,RT,GTI
      READ(1,100) ET,NUT,ALPHAT,CPST,CPLT
      READ(1,102) TMT,TVT,HFT,HVT
      ENDIF
      IF (TID.NE.TIDCHK) THEN
      IF (TIDCHK.EQ.'XX') THEN
      WRITE (*,1117)
 1117 FORMAT(' PRESSURE WALL MATERIAL NOT FOUND IN MATERIAL LIBRARY.',/
     $,' PLEASE CHECK PRESSURE WALL MATERIAL ID CODE AND BEGIN AGAIN.')
      STOP
      ENDIF
      IF (TIDCHK.NE.'XX') THEN
      READ (1,2)
      GOTO 9999
      ENDIF
      ENDIF
C
C.....  READ GEOMETRIC PARAMETERS AND ASSUMPTIONS
C.....
C.....          DPE ... PROJECTILE DIAMETER, IN
C.....          THP ... TRAJECTORY OBLIQUITY, DEG
C.....          TS .... BUMPER THICKNESS, CM
C.....          TW .... PRESSURE WALL THICKNESS, CM
C.....          S ..... BUMPER-TO-PRESSURE WALL STAND-OFF DISTANCE, CM
C.....          S2 .... INNER BUMPER-TO-PRESSURE WALL DISTANCE, CM
C.....          SY .... PRESSURE WALL YIELD STRESS, MPa
C
      READ (4,113) THP,SY,DPE,EPS1,EPS2
  113 FORMAT(3F10.5,/,2F10.5)
C
      IF (THP.NE.0.0.AND.THP.NE.45.0) THEN
      WRITE (2,1019)
      WRITE (*,1019)
 1019 FORMAT(/,' WARNING --- PROGRAM RUNNING IN NON-VALIDATED MODE')
      ENDIF
  110 READ (10,114) WSCHK
  114 FORMAT(A3)
      IF (WSCHK.EQ.WSID) THEN
      READ (10,115) WTYPE,TS,TW,S,S2,IB
  115 FORMAT(A21,/,4F10.5,A3)
      ENDIF
      IF (WSCHK.NE.WSID) THEN
      IF (WSCHK.EQ.'EOF') THEN
      WRITE (*,116)
  116 FORMAT(' WALL SYSTEM NOT FOUND IN LIBRARY.',/,' PLEASE CHECK WALL
     $ SYSTEM ID CODE AND BEGIN AGAIN.')
```

```
      STOP
      ENDIF
      IF (WSCHK.NE.'EOF') THEN
      READ (10,118)
  118 FORMAT(/)
      GOTO 110
      ENDIF
      ENDIF
C
      WRITE (*,119) WTYPE
  119 FORMAT(/,' ********************************************************
     $*****',/,' * PERFORMING HOLE SIZE AND CRACK LENGTH CALCULATIONS FO
     $R A *',/,' * ',11X,A21,1X,'WALL SYSTEM',12X,' *',/,' *************
     $*********************************************',/)
      IF (IB.EQ.'AA0') THEN
      IBMAT='MLI-BLNKT'
      RIBA=0.033
      ENDIF
      IF (IB.EQ.'BB1'.OR.IB.EQ.'BB2') THEN
      IBMAT='6K/6N'
      RIBA=0.80
      ENDIF
C
      IF (THP.GT.60.0) THEN
      WRITE (2,112) THP
  112 FORMAT(/,' INPUT IMPACT OBLIQUITY (',F4.1,'-DEG) > 60-DEG.  PROGRA
     $M STOP.')
      WRITE (*,112) THP
      STOP
      ENDIF
C
      IF (DPE.GT.0.75.OR.DPE.LT.0.25) THEN
      WRITE (2,111) DPE
  111 FORMAT(/,' INPUT PROJECTILE DIAMETER (',F5.3,' IN) OUTSIDE ALLOWAB
     $LE',/,' VALUE RANGE (0.25 TO 0.75 IN). PROGRAM STOP.')
      WRITE (*,111) DPE
      STOP
      ENDIF
C
      DP=DPE*2.54
C
C.....  READ PROJECTILE IMPACT VELOCITY IN KM/S
C
      WRITE(*,29)
   29 FORMAT(' INPUT PROJECTILE IMPACT VELOCITY IN KM/SEC (F5.2) AND HIT
     $ ENTER')
      READ(*,30) VP
   30 FORMAT(F5.2)
C
C.....  COMPUTE BALLISTIC LIMIT DIAMETER FOR GIVEN GEOMETRY AND VELOCITY
C
      IF (IB.EQ.'AA0') CALL BLCALC1(VP,THP,TS,S,TW,SY,RP,RB,RT,DCN)
      IF (IB.EQ.'BB1'.OR.IB.EQ.'BB2') CALL BLCALC2(IB,VP,THP,DCN)
C
      WRITE(2,40) THP,PMAT,BMAT,IBMAT,TMAT
```

```
   40 FORMAT(F4.1,'-DEG IMPACT OF A ',A10,' PROJ ON A DUAL-WALL SYSTEM W
     $ITH A',/,A10,' BUMPER, A ',A10,' INNER BUMPER, AND A ',A10,' PRESS
     $ WALL')
      RTHP=THP*PI/180.0
C
      IF (DCN.GT.DP) THEN
      WRITE (2,31) DCN,DP
   31 FORMAT(/,'BL DIAM (',F7.4,' CM) > PROJ DIAM (',F7.4,' CM)',/,3X,
     $' ---> PRESS WALL PERFORATION UNLIKELY',/,' ---> PROGRAM STOP')
      WRITE (*,31) DCN,DP
      STOP
      ENDIF
      IF (DCN.LE.DP) THEN
      WRITE (2,32) DCN,DP
   32 FORMAT(/,'BL DIAM (',F7.4,' CM) < PROJ DIAM (',F7.4,' CM)',/,3X,
     $' ---> PRESS WALL PERFORATION LIKELY')
      ENDIF
C
      EB=EB*68947.0
      BETAB=3.0*ALPHAB
      IF (NUB.LT.0.5) THEN
      KSB=EB/3.0/(1.0-2.0*NUB)
      COBC=DSQRT((KSB/10.0)/(RB*1000.0))/1000.0
      CBC=DSQRT((EB/10.0)/(RB*1000.0))/1000.0
      ENDIF
      IF (NUB.EQ.0.5) THEN
      KSB=-1.0
      COBC=-1.0
      ENDIF
      IF (NUB.LT.0.5) GB=2.3885E-08*KSB*BETAB/CPSB/RB
      IF (NUB.EQ.0.5) GB=GBI
      GRB=GB*RB*1000.0
C
      EP=EP*68947.0
      BETAP=3.0*ALPHAP
      IF (NUP.LT.0.5) THEN
      KSP=EP/3.0/(1.0-2.0*NUP)
      COPC=DSQRT((KSP/10.0)/(RP*1000.0))/1000.0
      CPC=DSQRT((EB/10.0)/(RB*1000.0))/1000.0
      ENDIF
      IF (NUP.EQ.0.5) THEN
      KSP=-1.0
      COPC=-1.0
      ENDIF
      IF (NUP.LT.0.5) GP=2.3885E-08*KSP*BETAP/CPSP/RP
      IF (NUP.EQ.0.5) GP=GPI
      GRP=GP*RP*1000.0
C
      C=CBC
C
C.....  CALCULATE PROJECTILE AND BUMPER HOLE-OUT MASSES (IN KG)
C
      MP=(PI/6.0)*(DP/100.0)*(DP/100.0)*(DP/100.0)*(RP*1000.0)
C
      IF (THP.GT.0.0) THEN
```

```
      READ (9,44) DMN,DMX
   44 FORMAT(2F10.5)
C        DMN=DN(VP,C,TS,DP,RTHP)
C        DMX=DX(VP,C,TS,DP,RTHP)
      MB=EPS1*(PI/4.0)*(DMN/100.0)*(DMX/100.0)*(TS/100.0)*(RB*1000.0)
      ENDIF
C
      IF (THP.EQ.0.0) THEN
      R1=VP/COB
      R2=TS/DP
      R3=RB/RP
      DBDP=3.4*(R2**0.33333)*(R1**0.33333)*(1.0-0.0308*R3)
      DB=DP*DBDP
      MB=EPS1*(PI/4.0)*(DB/100.0)*(DB/100.0)*(TS/100.0)*(RP*1000.0)
      DMN=DB
      DMX=DB
      ENDIF
C
      WRITE (2,45) PMAT,COP,KP,RP,DP,MP*1000.0,VP,BMAT,COT,KT,RT,TS,
     $             DMN,DMX,EPS1,MB*1000.0,S
   45 FORMAT(/,'PROJECTILE PROPERTIES ...',/,3X,'MAT = ',A10,/,3X,
     $'CO  = ',F6.3,' KM/S',/,3X,'K   = ',F6.3,/,3X,'RHO = ',F6.3,' GM/C
     $U.CM.',/,3X,'DP  = ',F6.3,' CM',/,3X,'MP  = ',F6.3,' GMS',/,3X,
     $'VP  = ',F6.3,' KM/S',//,'OUTER BUMPER PROPERTIES ...',/,3X,
     $'MAT = ',A10,/,3X,'CO  = ',F6.3,' KM/S',/,3X,'K   = ',F6.3,/,3X,
     $'RHO = ',F6.3,' GM/CU.CM.',/,3X,'TS  = ',F6.3,' CM',/,3X,'DMN = ',
     $F6.3,' CM',/,3X,'DMX = ',F6.3,' CM',/,3X,'EPS1= ',F6.3,4X,' (INITI
     $AL VALUE)',/,3X,'MB  = ',F6.3,' GMS (INITIAL VALUE)',/,3X,'S   = '
     $,F6.3,' CM')
C
C.....  CALCULATE PARTICLE AND SHOCK WAVE VELOCITIES AND HUGONIOT
C.....  PRESSURE DUE TO PROJECTILE IMPACT
C
      V=VP
      IF (BMAT.EQ.PMAT) GOTO 35
      A=KP-KB*(RB/RP)
      B=2.0*KP*V+COP+COB*(RB/RP)
      C=COP*V+KP*V*V
      D=B*B-4.0*A*C
      UBP=(B-SQRT(D))/(2.0*A)
      GOTO 38
   35   UBP=V/2.0
   38   UPP=V-UBP
      UBS=COB+KB*UBP
      UPS=COP+KP*UPP
      PP=RP*UPS*UPP
      PB=RB*UBS*UBP
C
C.....  PROJECTILE AND BUMPER SHOCK LOADING RESPONSE AND RELEASE
C.....  CALCULATION PHASE
C
      WRITE(*,5080)
 5080 FORMAT(/,' BEGIN PROJECTILE AND BUMPER SHOCK LOADING RESPONSE AND'
     $,/,' RELEASE CALCULATIONS')
      WRITE(2,509)
```

```
  509 FORMAT(/,'**** PROJECTILE AND BUMPER SHOCK LOADING RESPONSE AND RE
     $LEASE CALCULATIONS ****')
      WRITE(2,6011) VP,UPP,UPS,PP,UBP,UBS,PB
 6011 FORMAT(/,'PROJECTILE IMPACT VELOCITY .... VP = ',F7.3,' KM/S',/,
     $'PROJ MATL PARTICLE VELOCITY ... UP = ',F7.3,' KM/S',/,'PROJ MATL
     $SHOCK WAVE SPEED .... US = ',F7.3,' KM/S',/,'HUGONIOT IMPACT PRESS
     $URE ...... PH = ',F7.3,' GPA',/,'BMPR MATL PARTICLE VELOCITY ... U
     $P = ',F7.3,' KM/S',/,'BMPR MATL SHOCK WAVE SPEED .... US = ',F7.3,
     $' KM/S',/,'HUGONIOT IMPACT PRESSURE ...... PH = ',F7.3,' GPA')
C
      VPO=1.0/RP
      VP1=RP*UPS/(UPS-UPP)
      VP1=1.0/VP1
C
      PH=PP*1.0E09
C
      WRITE(2,705) EP/10.0,NUP,KSP/10.0,ALPHAP,CPSP,CPLP
  705 FORMAT(/,'PARAMETERS REQUIRED FOR CALCULATING PROJECTILE MATERIAL
     $RESPONSE AND',/,'RELEASE FROM SHOCKED STATE USING THE MIE-GRUNEISE
     $N E-O-S:',/,3X,'ELASTIC MODULUS ..... E    =',E10.4,' N/SQ
     $.M.',/,3X,'POISSON RATIO ..... NU   =',F10.3,/,3X,'BULK
     $MODULUS ..... K    =',E10.4,' N/SQ.M.',/,3X,'LIN. COEF.
     $ OF THERM. EXP. ... ALFA =',E10.4,' /DEG-C',/,3X,'SP HEAT (SOLID)
     $..... CPS  =',F10.3,' CAL/GM/DEG-C',/,3X,'SP HEAT (LIQUID)
     $ ..... CPL  =',F10.3,' CAL/GM/DEG-C')
      PHMB=PH/100.0E+09
      WRITE(2,800) PH,PHMB,VPO,VP1,GP,GPI
  800 FORMAT(3X,'HUGON IMP PRESS (PA,MBAR) ... PH   =',E10.4,',',F5.3,/,
     $3X,'SP VOL AT REST ..... VO   =',F10.3,' CU.CM./GM',/,3X,
     $'SP VOL AT IMPACT ..... V1   =',F10.3,' CU.CM./GM',/,3X,'AM
     $B M-GRUN COEF (CAL,INP) ... GAM0 =',F10.3,',',F5.3)
      WRITE(2,805) TMP,TVP,HFP,HVP
  805 FORMAT(3X,'MELT TEMPERATURE ..... TM   =',F10.2,' DEG-C',/,
     $3X,'VAPOR TEMPERATURE ..... TV   =',F10.2,' DEG-C',/,3X,'HEA
     $T OF FUSION ..... HF   =',F10.2,' CAL/GM',/,3X,'HEAT OF V
     $APORIZATION ..... HV   =',F10.2,' CAL/GM')
C
C.....  CALCULATE RELEASE OF PROJECTILE MATERIAL UP UNTIL ZERO PRESSURE
C.....  IS REACHED
C
      WRITE (2,1701)
 1701 FORMAT(/,'RELEASE OF SHOCKED PROJECTILE MATERIAL ...')
      PFIN=0.0
      CALL RELS(COP,KP,RP,GRP,VPO,VP1,PH,EXTP,UPP,PFIN,VFP)
C
C.....  CALCULATE TEMPERATURE INCREASE IN PROJECTILE MATERIAL
C
      CALL TINC(CPSP,CPLP,TMP,TVP,HFP,HVP,EXTP)
C
      PELOST=EXTP*MP
C
      VBO=1.0/RB
      VB1=RB*UBS/(UBS-UBP)
      VB1=1.0/VB1
C
```

```
      PH=PB*1.0E+09
C
      WRITE(2,7051) EB/10.0,NUB,KSB/10.0,ALPHAB,CPSB,CPLB
 7051 FORMAT(/,'PARAMETERS REQUIRED FOR CALCULATING BUMPER MATERIAL RESP
     $ONSE AND',/,'RELEASE FROM SHOCKED STATE USING THE MIE-GRUNEISEN E-
     $O-S:',/,3X,'ELASTIC MODULUS ..... E    =',E10.4,' N/SQ.M.'
     $,/,3X,'POISSON RATIO ..... NU   =',F10.3,/,3X,'BULK MODU
     $LUS ..... K    =',E10.4,' N/SQ.M.',/,3X,'LIN. COEF. OF
     $THERM. EXP. ... ALFA =',E10.4,' /DEG-C',/,3X,'SP HEAT (SOLID) ....
     $..... CPS  =',F10.3,' CAL/GM/DEG-C',/,3X,'SP HEAT (LIQUID) ...
     $..... CPL  =',F10.3,' CAL/GM/DEG-C')
      PHMB=PH/100.0E+09
      WRITE(2,8001) PH,PHMB,VBO,VB1,GB,GBI
 8001 FORMAT(3X,'HUGON IMP PRESS (PA,MBAR) ... PH   =',E10.4,',',F5.3,/,
     $3X,'SP VOL AT REST ..... V0   =',F10.3,' CU.CM./GM',/,3X,
     $'SP VOL AT IMPACT ..... V1   =',F10.3,' CU.CM./GM',/,3X,'AM
     $B M-GRUN COEF (CAL,INP) ... GAM0 =',F10.3,',',F5.3)
      WRITE(2,8051) TMB,TVB,HFB,HVB
 8051 FORMAT(3X,'MELT TEMPERATURE ..... TM   =',F10.2,' DEG-C',/,
     $3X,'VAPOR TEMPERATURE ..... TV   =',F10.2,' DEG-C',/,3X,'HEA
     $T OF FUSION ..... HF   =',F10.2,' CAL/GM',/,3X,'HEAT OF V
     $APORIZATION ..... HV   =',F10.2,' CAL/GM')
C
C.....  CALCULATE RELEASE OF BUMPER MATERIAL UP UNTIL ZERO PRESSURE IS
C.....  REACHED
C
      WRITE (2,1703)
 1703 FORMAT(/,'RELEASE OF SHOCKED BUMPER MATERIAL ...')
      PFIN=0.0
      CALL RELS(COB,KB,RB,GRB,VBO,VB1,PH,EXTB,UBP,PFIN,VFB)
C
C.....  CALCULATE TEMPERATURE INCREASE IN BUMPER MATERIAL
C
      CALL TINC(CPSB,CPLB,TMB,TVB,HFB,HVB,EXTB)
C
      BELOST=EXTB*MB
C
      TKELOST=PELOST+BELOST
      TKEINIT=0.5*MP*(VP*1000.0)*(VP*1000.0)
      FRLOST=TKELOST/TKEINIT
      WRITE (2,1706) TKEINIT,TKELOST,FRLOST
 1706 FORMAT(/,'TOTAL KINETIC ENERGY DUE TO INITIAL IMPACT ...',E10.4,
     $' JOULES',/,'TOTAL KINETIC ENERGY LOST TO SH HTNG & REL ...',
     $E10.4,' JOULES',/'FRACTION OF INITIAL K.E. LOST ... ',F5.3)
C
      IF (THP.EQ.0.0) GOTO 9090
      IF (THP.GT.0.0) THEN
      READ (9,1753) M2,V2,VRD
 1753 FORMAT(3F10.5)
      READ (4,590) E1RF
      READ (4,591) E2RF
      READ (4,592) IDDC
      THDCIB=ATAN(VRD/V2)
      THDEGIB=180.0*THDCIB/PI
      RDCIB=(S-S2)*DSIN(THDCIB)/(1.0+DSIN(THDCIB))
```

```
      DH2=2.0*RDCIB
      MIB=EPS2*(PI/4.0)*DH2*DH2*RIBA/1000.0
      AMIB=MIB
      CALL VCALCS0(M2,AMIB,EPS2,FEPS2,FMIB,V2,VRD,E2RF,VLE,VAXP,VEXPP
     $                  ,VAXB,VEXPB,THDCP,THDEGP,THDCB,THDEGB)
      MIB=FMIB
      RWP=S2*DTAN(THDCP)
      RWB=0.0
      RDCP=S2*DSIN(THDCP)/(1.0+DSIN(THDCP))
      RDCB=0.0
C
      WRITE (2,1900) IBMAT,RIBA,DH2,EPS2,MIB*1000.0,S2
 1900 FORMAT(/,'INNER BUMPER PROPERTIES ...',/,3X,'MAT = ',A10,/,3X,
     $'RHO = ',F6.3,' GM/SQ.CM.',/,3X,'DH  = ',F6.3,' CM',/,3X,'EPS2= ',
     $F6.3,4X,' (INITIAL VALUE)',/,3X,'MIB = ',F6.3,' GMS (INITIAL VALUE
     $)',/,3X,'S2  = ',F6.3,' CM')
C
      WRITE (2,2101) M2*1000.0,V2+VRD,V2,VRD,THDEGIB,MBT*1000.0,
     $                  VLE,VAXP,VEXPP,THDEGP,RDCP,RWP
 2101 FORMAT(/,'IN-LINE DEBRIS CLOUD CHARACTERISTICS ...',/,3X,'PRIOR TO
     $INNER BMPR IMPACT ... ',/,5X,'MATERIAL MASS ..... ',F10.5,
     $' GMS',/,5X,'LEADING EDGE VELOCITY ..... ',F10.5,' KM/S',/,5X,'CEN
     $TER-OF-MASS VELOCITY ... ',F10.5,' KM/S',/,5X,'EXPANSION VELOCITY
     $..... ',F10.5,' KM/S',/,5X,'1/2-ANGLE SPREAD ..... ',F10.5
     $,' DEG',/,3X,'AFTER INNER BMPR IMPACT ... ',/,5X,'MATERIAL MASS ..
     $..... ',F10.5,' GMS',/,5X,'LEADING EDGE VELOCITY ..... ',
     $F10.5,' KM/S',/,5X,'CENTER-OF-MASS VELOCITY ... ',F10.5,' KM/S',/,
     $5X,'EXPANSION VELOCITY ..... ',F10.5,' KM/S',/,5X,'1/2-ANGLE SP
     $READ ..... ',F10.5,' DEG',/,5X,'DEB CLD RAD @ PR-WALL ..... '
     $,F10.5,' CM',/,5X,'PR WALL FOOTPRINT RAD ..... ',F10.5,' CM')
      GOTO 9000
      ENDIF
C
 9090 READ (4,590) E1RF
  590 FORMAT(F10.5)
C
C        IF (S2.EQ.S) GOTO 2010
C
      WRITE(*,58)
   58 FORMAT(/,' BEGIN PRIMARY DEBRIS CLOUD CHARACTERIZATION')
C
C.....  CALCULATE AXIAL AND EXPANSION VELOCITIES AND SEMI-CONE ANGLES
C.....  FOR PRIMARY DEBRIS CLOUD PROJECTILE AND BUMPER COMPONENTS
C
      AMB=MB
      CALL VCALCS1(EXTP,EXTB,MP,EPS1,AMB,FEPS1,FMB,MBT,VP,VLE,VAXP,
     $          VEXPP,VAXB,VEXPB,THDCP,THDEGP,THDCB,THDEGB,E1RF)
      MB=FMB
C
C.....  CALCULATE FOOTPRINT RADII AT INNER BUMPER IMPACT
C
      RIP=(S-S2)*DTAN(THDCP)
      RIB=(S-S2)*DTAN(THDCB)
C
C.....  CALCULATE DEBRIS CLOUD RADII AT INNER BUMPER IMPACT
```

```
C
      RDCP=(S-S2)*DSIN(THDCP)/(1.0+DSIN(THDCP))
      RDCB=(S-S2)*DSIN(THDCB)/(1.0+DSIN(THDCB))
C
C.....  PRINT PRIMARY DEBRIS CLOUD CHARACTERISTICS
C
      WRITE (2,2000) MP*1000.0,VLE,VAXP,VEXPP,THDEGP,RDCP,RIP,
     $                  MB*1000.0,FEPS1,VLE,VAXB,VEXPB,THDEGB,RDCB,RIB
 2000 FORMAT(/,'PRIMARY DEBRIS CLOUD CHARACTERISTICS ...',/,3X,'PROJECTI
     $LE COMPONENT ... ',/,5X,'MATERIAL MASS ..... ',F10.5,' GMS
     $',/,5X,'LEADING EDGE VELOCITY ..... ',F10.5,' KM/S',/,5X,'CENTER-O
     $F-MASS VELOCITY ... ',F10.5,' KM/S',/,5X,'EXPANSION VELOCITY .....
     $... ',F10.5,' KM/S',/,5X,'1/2-ANGLE SPREAD ..... ',F10.5,' DE
     $G',/,5X,'DEB CLD RAD @ INN-BMPR .... ',F10.5,' CM',/,5X,'INN-BMPR
     $FOOTPRINT RAD .... ',F10.5,' CM',/,3X,'BUMPER COMPONENT ..... ',
     $/,5X,'MATERIAL MASS (FIN VAL) ... ',F10.5,' GMS',/,7X,'EPS1 (FIN V
     $AL) ... ',F10.5,/,5X,'LEADING EDGE VELOCITY ..... ',F10.5,' KM/S',
     $/,5X,'CENTER-OF-MASS VELOCITY ... ',F10.5,' KM/S',/,5X,'EXPANSION
     $VELOCITY ..... ',F10.5,' KM/S',/,5X,'1/2-ANGLE SPREAD .....
     $. ',F10.5,' DEG',/,5X,'DEB CLD RAD @ INN-BMPR .... ',F10.5,' CM',
     $/,5X,'INN-BMPR FOOTPRINT RAD .... ',F10.5,' CM')
C
 2010 WRITE(*,59)
   59 FORMAT(/,' BEGIN SECONDARY DEBRIS CLOUD CHARACTERIZATION')
C
      IF (S2.EQ.S) THEN
      DH2=DB
      ENDIF
      IF (S2.LT.S) THEN
      IF (2.0*RDCP.LE.DB) DH2=DB
      IF (2.0*RDCP.GT.DB) DH2=2.0*RDCP
      ENDIF
      MIB=EPS2*(PI/4.0)*DH2*DH2*RIBA/1000.0
C
      WRITE (2,1900) IBMAT,RIBA,DH2,EPS2,MIB*1000.0,S2
C
C.....  CALCULATE AXIAL AND EXPANSION VELOCITIES AND SEMI-CONE ANGLES
C.....  FOR PRIMARY DEBRIS CLOUD PROJECTILE AND BUMPER COMPONENTS
C
      READ (4,591) E2RF
  591 FORMAT(F10.5)
      AMB=MB
      AMIB=MIB
      CALL VCALCS2(EXTP,EXTB,MP,EPS2,AMB,AMIB,FEPS2,FMB,FMIB,MBT,VP,
     $VLET,VAXPT,VEXPPT,VAXBT,VEXPBT,THDCPT,THDEGPT,THDCBT,THDEGBT,E2RF)
      MB=FMB
      MIB=FMIB
C
C.....  DETERMINE DOMINATING DEBRIS CLOUD
C
      READ (4,592) IDDC
  592 FORMAT(I2)
      IF (IDDC.EQ.2) THEN
      VLE=VLET
      VAXP=VAXPT
```

```
      VEXPP=VEXPPT
      VAXB=VAXBT
      VEXPB=VEXPBT
      THDCP=THDCPT
      THDEGP=THDEGPT
      THDCB=THDCBT
      THDEGB=THDEGBT
      RWP=S2*DTAN(THDCP)
      RWB=S2*DTAN(THDCB)
      RDCP=S2*DSIN(THDCP)/(1.0+DSIN(THDCP))
      RDCB=S2*DSIN(THDCB)/(1.0+DSIN(THDCB))
      WRITE (2,1901)
 1901 FORMAT(/,'SECONDARY DEBRIS CLOUD DELIVERS LOAD TO PRESSURE WALL')
C
C.....  PRINT SECONDARY DEBRIS CLOUD CHARACTERISTICS
C
      WRITE (2,2100) MP*1000.0,VLE,VAXP,VEXPP,THDEGP,RDCP,RWP,
     $                MBT*1000.0,MB*1000.0,MIB*1000.0,FEPS2,VLE,VAXB,
     $                VEXPB,THDEGB,RDCB,RWB
 2100 FORMAT(/,'SECONDARY DEBRIS CLOUD CHARACTERISTICS ...',/,3X,'PROJEC
     $TILE COMPONENT ... ',/,5X,'MATERIAL MASS ............. ',F10.5,
     $' GMS',/,5X,'LEADING EDGE VELOCITY ..... ',F10.5,' KM/S',/,5X,'CEN
     $TER-OF-MASS VELOCITY ... ',F10.5,' KM/S',/,5X,'EXPANSION VELOCITY
     $........ ',F10.5,' KM/S',/,5X,'1/2-ANGLE SPREAD .......... ',F10.5
     $,' DEG',/,5X,'DEB CLD RAD @ PR-WALL ..... ',F10.5,' CM',/,5X,
     $'PR WALL FOOTPRINT RAD ..... ',F10.5,' CM',/,3X,'BUMPER COMPONENT
     $....... ',/,5X,'MATERIAL MASS (TOTAL) ..... ',F10.5,' GMS',/,7X,
     $'OUTR-BMPR COMPONENT ..... ',F10.5,' GMS',/,7X,'INNR-BMPR COMPONEN
     $T ..... ',F10.5,' GMS (FIN VAL)',/,9X,'EPS2 (FINAL VALUE) .... ',
     $F10.5,/,5X,'LEADING EDGE VELOCITY ..... ',F10.5,' KM/S',/,5X,'CENT
     $ER-OF-MASS VELOCITY ... ',F10.5,' KM/S',/,5X,'EXPANSION VELOCITY .
     $....... ',F10.5,' KM/S',/,5X,'1/2-ANGLE SPREAD .......... ',F10.5,
     $' DEG',/,5X,'DEB CLD RAD @ PR-WALL ..... ',F10.5,' CM',/,5X,'PR WA
     $LL FOOTPRINT RAD ..... ',F10.5,' CM')
      ENDIF
C
      IF (IDDC.EQ.1) THEN
      RWP=S*DTAN(THDCP)
      RWB=S*DTAN(THDCB)
      RDCP=S*DSIN(THDCP)/(1.0+DSIN(THDCP))
      RDCB=S*DSIN(THDCB)/(1.0+DSIN(THDCB))
      WRITE (2,1903)
 1903 FORMAT(/,'PRIMARY DEBRIS CLOUD DELIVERS LOAD TO PRESSURE WALL')
C
C.....  PRINT REPRINT DEBRIS CLOUD CHARACTERISTICS AT PRESSURE WALL
C
      WRITE (2,2011) MP*1000.0,VLE,VAXP,VEXPP,THDEGP,RDCP,RWP,
     $                MB*1000.0,FEPS1,VLE,VAXB,VEXPB,THDEGB,RDCB,RWB
 2011 FORMAT(/,'PRIMARY DEBRIS CLOUD CHARACTERISTICS AT PRESSURE WALL ..
     $.',/,3X,'PROJECTILE COMPONENT ... ',/,5X,'MATERIAL MASS ..........
     $... ',F10.5,' GMS',/,5X,'LEADING EDGE VELOCITY ..... ',F10.5,' KM/
     $S',/,5X,'CENTER-OF-MASS VELOCITY ... ',F10.5,' KM/S',/,5X,'EXPANSI
     $ON VELOCITY ........ ',F10.5,' KM/S',/,5X,'1/2-ANGLE SPREAD ......
     $.... ',F10.5,' DEG',/,5X,'DEB CLD RAD AT PR WALL .... ',F10.5,' CM
     $',/,5X,'PR WALL FOOTPRINT RAD .... ',F10.5,' CM',/,3X,'BUMPER COMP
```

```
     $ONENT ....... ',/,5X,'MATERIAL MASS (FIN VAL) ... ',F10.5,' GMS',/
     $,7X,'EPS1 (FIN VAL) ... ',F10.5,/,5X,'LEADING EDGE VELOCITY .....
     $',F10.5,' KM/S',/,5X,'CENTER-OF-MASS VELOCITY ... ',F10.5,' KM/S',
     $/,5X,'EXPANSION VELOCITY ........ ',F10.5,' KM/S',/,5X,'1/2-ANGLE
     $SPREAD .......... ',F10.5,' DEG',/,5X,'DEB CLD RAD AT PR WALL ....
     $ ',F10.5,' CM',/,5X,'PR WALL FOOTPRINT RAD .... ',F10.5,' CM')
      ENDIF
C
C.....  DETERMINE WHETHER OR NOT PETALING WILL OCCUR
C
 9000 READ(4,2151) F2CRIT
 2151 FORMAT(F5.3)
C
C.....  CALCULATE ADJUSTMENT FACTORS
C
      IF (MODE.EQ.'U') THEN
      CD=1.0
      CL=1.0
      GOTO 9001
      ENDIF
      IF (WSID.EQ.'NEC') CALL NECNTRP(DPE,DCN,THP,CD,CL)
      IF (WSID.EQ.'ELC') CALL ELCNTRP(DPE,DCN,THP,VP,CD,CL)
        IF (WSID.EQ.'BLC') CALL BLCNTRP(DPE,DCN,THP,VP,TS,S,TW,SY,RP,RB,
     $                                  RT,CD,CL)
        IF (WSID.EQ.'LEC') CALL LECNTRP(DPE,DCN,THP,VP,CD,CL)
        IF (WSID.NE.'NEC'.AND.WSID.NE.'ELC'.AND.WSID.NE.'BLC'.AND.WSID.
     $      NE.'LEC') THEN
      CD=1.0
      CL=1.0
      ENDIF
C
 9001 ARG=THP*PI/190.0
      F2=DEXP(2.0*(1-S2/S))*(RIBA/(RT*TW))*(VP/COB)*(DP/TW)*DCOS(ARG)
      IF (F2.GE.F2CRIT) THEN
      WRITE (2,2156) F2,F2CRIT
 2156 FORMAT(/,'F2 = ',F6.3,' >= ',F6.3,' = F2,CRIT',/,3X,'---> PETALING
     $ WILL LIKELY OCCUR')
      GOTO 2155
      ENDIF
      IF (F2.LT.F2CRIT) THEN
      DEQ2=2.0*RWP/100.0
      DH=CD*DEQ2
      ALIM=RWP
      LTT=CL*2.0*ALIM
      WRITE (2,2157) F2,F2CRIT,DH*100.0,LTT
 2157 FORMAT(/,'F2 = ',F6.3,' < ',F6.3,' = F2,CRIT',/,3X,'---> PETALING
     $WILL LIKELY NOT OCCUR',//,'DEQ = ',F6.3,' CM',/,'LTT = ',F6.3,
     $' CM')
      GOTO 3025
      ENDIF
C
 2155 WRITE (*,60)
   60 FORMAT(/,' BEGIN TIME-PHASING AND PRESSURE COEFFICIENT CALCULATION
     $S')
C
```

```
      IF (THP.EQ.0.0) T1=(S2/100.0)/(VAXB*1000.0)
      IF (THP.GT.0.0) T1=0.0
C
C.....  CALCULATE IMPACT DURATIONS OF PROJECTILE AND BUMPER COMPONENTS
C
      TDP=4.0*(RDCP/100.0)/(VAXP*1000.0-VEXPP*1000.0)
      IF (THP.EQ.0.0) TDB=4.0*(RDCB/100.0)/(VAXB*1000.0-VEXPB*1000.0)
      IF (THP.GT.0.0) TDB=0.0
C
C.....  CALCULATE TIME OF PEAK PRESSURES
C
      TSTP=2.0*(RDCP/100.0)/(VAXP*1000.0)
      IF (THP.EQ.0.0) TSTB=T1+2.0*(RDCB/100.0)/(VAXB*1000.0)
      IF (THP.GT.0.0) TSTB=0.0
C
C.....  PRINT TIME-PHASING INFORMATION FOR PRESSURE WALL IMPACT BY
C.....  DEBRIS CLOUD
C
      TO=0.0
      WRITE (2,2200) TO,TSTP,TDP,TDP
      IF (THP.EQ.0.0) WRITE (2,2201) T1,T1,TSTB,TDB,T1+TDB
 2200 FORMAT(/,'TIME-PHASING INFORMATION FOR PRESSURE WALL DEBRIS CLOUD
     $IMPACT ...',/,3X,'BEGINNING OF PROJ COMP IMPACT EVENT ..... ',
     $F11.9,' SECS',/,3X,'TIME OF PEAK PROJ COMP PRESSURE ......... ',
     $F11.9,' SECS'/,3X,'DURATION OF PROJ COMP IMPACT EVENT ...... ',
     $F11.9,' SECS',/,3X,'COMPLETION OF PROJ COMP IMPACT EVENT .... ',
     $F11.9,' SECS')
 2201 FORMAT(/,3X,'DELAY BET BEGIN PR & BEGIN BPR EVENTS ... ',F11.9,
     $' SECS',//,3X,'BEGINNING OF BMPR COMP IMPACT EVENT ..... ',F11.9,
     $' SECS',/,3X,'TIME OF PEAK BMPR COMP PRESSURE ......... ',F11.9,
     $' SECS',/,3X,'DURATION OF BMPR COMP IMPACT EVENT ...... ',F11.9,
     $' SECS',/,3X,'COMPLETION OF BMPR COMP IMPACT EVENT .... ',F11.9,
     $' SECS')
C
C.....  CALCULATE PRESSURE DISTRIBUTION COEFFICIENTS
C
      READ (4,2250) NPT
 2250 FORMAT(I5)
      AIP=AIFCN(TDP,RDCP,VAXP,VEXPP)
      IF (THP.EQ.0.0) AIB=AIFCN(TDB,RDCB,VAXB,VEXPB)
      IF (THP.GT.0.0) AIB=0.0
      ALFA=PI*(RWB/100.0)*(RWB/100.0)*AIB
      BETA=PI*(RWP/100.0)*(RWP/100.0)*AIP
      GAMA=(MB+MIB)*(VLE*1000.0)+MP*(VLE*1000.0)
      DELTA=(MP*VLE)/(MB+MIB)/VLE
      POP=(GAMA*DELTA)/(ALFA+BETA*DELTA)
      IF (THP.EQ.0.0) POB=POP/DELTA
      IF (THP.GT.0.0) POB=0.0
C
      WRITE (2,2300) POP,POB
 2300 FORMAT(/,'PRESSURE DISTRIBUTION COEFFICIENTS ... ',/,3X,'PROJ COMP
     $ ... ',E10.3,' N/SQ.M.',/,3X,'BMPR COMP ... ',E10.3,' N/SQ.M.')
C
C.....  CALCULATE PRESSURE HISTORIES, ETC AS A FUNCTION OF TIME
C
```

```
      IF (THP.EQ.0.0) DELT=(T1+TDB)/NPT
      IF (THP.GT.0.0) DELT=TDP/NPT
      T=0.0
      DO 2500 I=1,NPT
      T=T+DELT
      IF (T.LE.TDP) THEN
      HP=H(VAXP,VEXPP,RDCP,T)
      DIFF=RDCP-HP*100.0
      COEF=DIFF/DABS(DIFF)
      IF (DABS(DIFF).GT.RDCP) DIFF=COEF*RDCP
      RADP=DSQRT(RDCP*RDCP-DIFF*DIFF)
      PRP(I)=POP*(RADP/RDCP)*(RADP/RDCP)
      ENDIF
      IF (T.GT.TDP) THEN
      PRP(I)=0.0
      HP=0.0
      RADP=0.0
      ENDIF
      IF (T.LE.T1) THEN
      PRB(I)=0.0
      HB=0.0
      RADB=0.0
      ENDIF
      IF (THP.EQ.0.0) THEN
      IF (T.GT.T1.AND.T.LE.T1+TDB) THEN
      HB=H(VAXB,VEXPB,RDCB,T-T1)
      DIFF=RDCB-HB*100.0
      COEF=DIFF/DABS(DIFF)
      IF (DABS(DIFF).GT.RDCB) DIFF=COEF*RDCB
      RADB=DSQRT(RDCB*RDCB-DIFF*DIFF)
      PRB(I)=POB*(RADB/RDCB)*(RADB/RDCB)
      ENDIF
      IF (T.GT.T1+TDB) THEN
      PRB(I)=0.0
      HB=0.0
      RADB=0.0
      ENDIF
      ENDIF
      IF (THP.GT.0.0) PRB(I)=0.0
      PT=PRP(I)+PRB(I)
C        WRITE (3,2400) T,PRP(I)/1.0E+09,PRB(I)/1.0E+09,PT/1.0E+09,
C     $                  HP*100.0,RADP,HB*100.0,RADB
 2400 FORMAT(4E11.4,4F7.3)
 2500 CONTINUE
C
      WRITE (*,61)
   61 FORMAT(/,' BEGIN PLATE MOTION CALCULATIONS')
C
C....   CALCULATE TIME OF PLATE MOTION CESSATION
C
      READ (4,2600) ETA,R,EPSF,SIF,AC,AM
 2600 FORMAT(F5.2,5F5.2)
      ET=ET*6894.7
      GT=ET/2.0/(1.0+NUT)
      ALAM=ET*NUT/(1.0+NUT)/(1.0-2.0*NUT)
```

```
      ANUM=ALAM+2.0*GT
      C0T=DSQRT(ET/(RT*1000.0))/1000.0
      C1T=DSQRT(ANUM/(RT*1000.0))/1000.0
      C2T=DSQRT(GT/(RT*1000.0))/1000.0
      CRT=(0.862+1.14*NUT)*C2T/(1.0+NUT)
      WRITE (2,2601) TMAT,ET,NUT,GT,S,RT,R,ETA,EPSF,SY,SIF,
     $AC*SIF,AM,TW
 2601 FORMAT(/,'PRESSURE WALL PROPERTIES ...',/,3X,'MAT  = ',A10,/,
     $3X,'EMOD = ',E10.3,' N/SQ.M.',/,3X,'NU   = ',F6.3,/,3X,'SMOD = ',
     $E10.3,' N/SQ.M.',/,3X,'S    = ',F6.3,' CM',/,3X,'RHO  = ',F6.3,
     $' GM/CU.CM.',/,3X,'RAD  = ',F6.3,' CM',/,3X,'ETA  = ',F6.3,/,3X,
     $'EPSF = ',F6.3,/,3X,'SIGY = ',F6.1,' MPA',/,3X,'SIF  = ',F6.3,
     $' MPA-/M',/,3X,'SIFA = ',F6.3,' MPA-/M',/,3X,'MEXP = ',F6.3,/,3X,
     $'TW   = ',F6.3,' CM')
      WRITE (2,2602) C0T,C1T,C2T,CRT
 2602 FORMAT(3X,'C0   = ',F6.3,' KM/S',/,3X,'CL   = ',F6.3,' KM/S',/,3X,
     $'CT   = ',F6.3,' KM/S',/,3X,'CR   = ',F6.3,' KM/S')
      IF (THP.EQ.0.0) THEN
      R1=RWB
      RSTAR=RWB
      ENDIF
      IF (THP.GT.0.0) THEN
      R1=RWP
      RSTAR=RWP
      ENDIF
      EPSFCN=ETA*ETA+ETA*(1.0-ETA)*(R1/RSTAR)+(1.0-ETA)*(1.0-ETA)*
     $          (R1/RSTAR)*(R1/RSTAR)/3.0
      COEF=4.0/(SY*1.0E06)/(TW/100.0)/(TW/100.0)/(R1/100.0)
      CALL AINT12(RDCP,VAXP,VEXPP,TDP,AIPR)
      IF (THP.EQ.0.0) CALL AINT12(RDCB,VAXB,VEXPB,TDB,AIBR)
      IF (THP.GT.0.0) AIBR=0.0
      AI12=POP*(RWP/100.0)*(RWP/100.0)*(RWP/100.0)*AIPR/6.0 +
     $           POB*(RWB/100.0)*(RWB/100.0)*(RWB/100.0)*AIBR/6.0
      ANUM=COEF*AI12
      TM=ANUM/EPSFCN
C
      WRITE (*,62)
   62 FORMAT(/,' CALCULATE TIME OF CRACK INITIATION')
C
C....   CALCULATE TIME OF CRACK INITIATION
C
      DTP=TDP/100.0
      IF (THP.EQ.0.0) DTB=TDB/100.0
      IF (THP.GT.0.0) DTB=0.0
      IF (THP.EQ.0.0) DTM=(TM-(T1+TDB))/100.0
      IF (THP.GT.0.0) DTM=(TM-TDP)/100.0
      SIG=1.0/(DLOG(R/R1)+1.0)
      ALF1=(R1/100.0)*(R1/100.0)*(R1/100.0)/(180.0*RSTAR/100.0)*(1.0-
     $           ETA)*(5.0-3.0*SIG)
      ALF2=ETA*(R1/100.0)*(R1/100.0)*(2.0-SIG)/24.0
      ALF=ALF1+ALF2
      C11=(SY*1.0E06)*(TW/100.0)/16.0/(RT*1000.0)/ALF
      C12=SIG/(R1/100.0)
      C1=C11*C12*EPSFCN
      C21=1.0/2.0/(RT*1000.0)/(TW/100.0)/ALF
```

```
      C22=SIG/(R1/100.0)/(R1/100.0)
      C2=C21*C22
 2698   T=0.0
      DO 2700 I=1,5000
C
      IF (THP.EQ.0.0) THEN
      IF (T.LE.T1+TDB) THEN
      IF (T.LE.TDP.AND.T.LE.T1) THEN
      T=T+DTP
      CALL AINT56(RDCP,VAXP,VEXPP,T,AJPR)
      AJBR=0.0
      ENDIF
      IF (T.LE.TDP.AND.T.GT.T1.AND.T.LE.T1+TDB) THEN
      T=T+DTP
      CALL AINT56(RDCP,VAXP,VEXPP,T,AJPR)
      CALL AINT56(RDCB,VAXB,VEXPB,T,AJBR)
      ENDIF
      IF (T.GT.TDP.AND.T.GT.T1.AND.T.LE.T1+TDB) THEN
      T=T+DTB
      CALL AINT56(RDCP,VAXP,VEXPP,TDP,AJPR)
      CALL AINT56(RDCB,VAXB,VEXPB,T,AJBR)
      ENDIF
      AI56=POP*(RWP/100.0)*(RWP/100.0)*(RWP/100.0)*AJPR/6.0 +
     $          POB*(RWB/100.0)*(RWB/100.0)*(RWB/100.0)*AJBR/6.0
      DWDR=C1*T*T-C2*AI56
      ENDIF
      IF (T.GT.T1+TDB) THEN
      T=T+DTM
      CALL AINT34(RDCP,VAXP,VEXPP,TDP,AFPR)
      CALL AINT34(RDCB,VAXB,VEXPB,TDB,AFBR)
      AI34=POP*(RWP/100.0)*(RWP/100.0)*(RWP/100.0)*AFPR/6.0 +
     $          POB*(RWB/100.0)*(RWB/100.0)*(RWB/100.0)*AFBR/6.0
      DWDR=C1*T*T-C2*AI34+(T-(T1+TDB))*AI12
      ENDIF
      ENDIF
C
      IF (THP.GT.0.0) THEN
      IF (T.LE.TDP) THEN
      T=T+DTP
      CALL AINT56(RDCP,VAXP,VEXPP,T,AJPR)
      AI56=POP*(RWP/100.0)*(RWP/100.0)*(RWP/100.0)*AJPR/6.0
      DWDR=C1*T*T-C2*AI56
      ENDIF
      IF (T.GT.TDP) THEN
      T=T+DTM
      CALL AINT34(RDCP,VAXP,VEXPP,TDP,AFPR)
      AI34=POP*(RWP/100.0)*(RWP/100.0)*(RWP/100.0)*AFPR/6.0
      DWDR=C1*T*T-C2*AI34+(T-TDP)*AI12
      ENDIF
      ENDIF
C
      COMP=DSQRT(2.0*EPSF)
C        WRITE (3,2699) T,DWDR,COMP
C 2699 FORMAT(3E11.4)
      IF (DWDR+COMP.LT.0.0) THEN
```

```
      TC=T
      WRITE (2,2712) EPSF
 2712 FORMAT(/,3X,'EPSF-FINAL = ',F6.3)
      GOTO 2649
      ENDIF
 2700 CONTINUE
      IF (TC.EQ.0.0) THEN
      EPSF=EPSF-0.1
      GOTO 2698
      IF (EPSF.LE.0.0) WRITE (2,2711)
 2711 FORMAT(' ERROR IN TIME OF CRACK INITIATION CALCULATION.',/,' CHECK
     $ VALUE OF EPS-1F.',/,' PROGRAM STOP.')
      WRITE (*,2711)
      STOP
      ENDIF
C
C.....  CALCULATE V0(T) UNTIL PLATE MOTION STOPS
C
 2649 SIG=1.0/(DLOG(R/R1)+1.0)
      ALF1=(R1/100.0)*(R1/100.0)*(R1/100.0)/(180.0*RSTAR/100.0)*(1.0-
     $          ETA)*(5.0-3.0*SIG)
      ALF2=ETA*(R1/100.0)*(R1/100.0)*(2.0-SIG)/24.0
      ALF=ALF1+ALF2
      COEF1=1.0/2.0/(RT*1000.0)/(TW/100.0)/(R1/100.0)/ALF
      COEF2=(SY*1.0E06)*(TW/100.0)/8.0/(RT*1000.0)/ALF
      DTP=TDP/100.0
      IF (THP.EQ.0.0) DTB=TDB/100.0
      IF (THP.GT.0.0) DTB=0.0
      IF (THP.EQ.0.0) DTM=(TM-(T1+TDB))/100.0
      IF (THP.GT.0.0) DTM=(TM-TDP)/100.0
      T=0.0
      VINT=0.0
      DO 2625 I=1,5000
C
      IF (THP.EQ.0.0) THEN
      IF (T.LE.T1+TDB) THEN
      IF (T.LE.TDP.AND.T.LE.T1) THEN
      T=T+DTP
      CALL AINT12(RDCP,VAXP,VEXPP,T,AIPR)
      AIBR=0.0
      DT=DTP
      ENDIF
      IF (T.LE.TDP.AND.T.GT.T1.AND.T.LE.T1+TDB) THEN
      T=T+DTP
      CALL AINT12(RDCP,VAXP,VEXPP,T,AIPR)
      CALL AINT12(RDCB,VAXB,VEXPB,T,AIBR)
      DT=DTP
      ENDIF
      IF (T.GT.TDP.AND.T.GT.T1.AND.T.LE.T1+TDB) THEN
      T=T+DTB
      CALL AINT12(RDCP,VAXP,VEXPP,TDP,AIPR)
      CALL AINT12(RDCB,VAXB,VEXPB,T,AIBR)
      DT=DTB
      ENDIF
      AI12=POP*(RWP/100.0)*(RWP/100.0)*(RWP/100.0)*AIPR/6.0 +
```

```
     $          POB*(RWB/100.0)*(RWB/100.0)*(RWB/100.0)*AIBR/6.0
      ENDIF
      IF (T.GT.T1+TDB) THEN
      T=T+DTM
      CALL AINT12(RDCP,VAXP,VEXPP,TDP,AIPR)
      CALL AINT12(RDCB,VAXB,VEXPB,TDB,AIBR)
      AI12=POP*(RWP/100.0)*(RWP/100.0)*(RWP/100.0)*AIPR/6.0 +
     $          POB*(RWB/100.0)*(RWB/100.0)*(RWB/100.0)*AIBR/6.0
      DT=DTM
      ENDIF
      ENDIF
C
      IF (THP.GT.0.0) THEN
      IF (T.LE.TDP) THEN
      T=T+DTP
      CALL AINT12(RDCP,VAXP,VEXPP,T,AIPR)
      DT=DTP
      ENDIF
      IF (T.GT.TDP) THEN
      T=T+DTM
      CALL AINT12(RDCP,VAXP,VEXPP,TDP,AIPR)
      T=T+DTM
      ENDIF
      AI12=POP*(RWP/100.0)*(RWP/100.0)*(RWP/100.0)*AIPR/6.0
      ENDIF
C
      VOT=COEF1*AI12-COEF2*EPSFCN*T
      VINT=VINT+VOT*DT
      IF (T.EQ.TC) VOTC=VOT
C        WRITE (3,2624) T,VOT
C 2624 FORMAT(2E11.4)
      IF (T.GT.TM) GOTO 2626
 2625 CONTINUE
C
 2626 IF (TC.LT.TM) WRITE (2,2650) TC,TM,VOTC/1000.0
 2650 FORMAT(/,'TIME OF CRACK INITIATION ... ',F11.9,' SECS (< TM = ',
     $F11.9,' S)',//,'PLATE CTR VELOCITY AT T=TC ... ',F6.3,' KM/S')
      IF (TC.GT.TM) WRITE (2,2651) TM,TC
 2651 FORMAT(/,'TIME OF PLATE MOTION CESSATION ... ',F11.9,' SECS (> TC
     $= ',F11.9,' S)')
C
C.....  CALCULATE INITIAL CRACK LENGTH
C
      AO=100.0*(1.0/PI)*(SIF/SY)*(SIF/SY)
C
      WRITE (*,63)
   63 FORMAT(/,' CALCULATE NUMBER OF CRACKS')
C
C.....  CALCULATE NUMBER OF CRACKS
C
      GIC=(SIF*1.0E06)*(SIF*1.0E06)/ET
      C1=(PI/2.0)*SIG/(R1/100.0)*(SY*1.0E06)*(TW/100.0)/GIC
      ETO=AO/RSTAR
      C2D=6.0*ETA+3.0*(1.0-ETA)*ETO
      C2N=6.0*ETA*ETA+6.0*ETA*(1.0-ETA)*ETO+
```

```
     $                  2.0*(1.0-ETA)*(1.0-ETA)*ETO*ETO
      C2=C2N/C2D
      V02=(SY*1.0E06)*(TW/100.0)/8.0/(RT*1000.0)/ALF
      V01=1.0/2.0/(RP*1000.0)/(TW/100.0)/ALF/(R1/100.0)
C
      IF (THP.EQ.0.0) THEN
      IF (TC.LE.T1+TDB) THEN
      IF (TC.LE.T1) THEN
      CALL AINT34(RDCP,VAXP,VEXPP,TC,AFPR)
      AFBR=0.0
      AINT=POP*(RWP/100.0)*(RWP/100.0)*(RWP/100.0)*AFPR/6.0 +
     $          POB*(RWB/100.0)*(RWB/100.0)*(RWB/100.0)*AFBR/6.0
      ENDIF
      IF (TC.GT.T1.AND.TC.LE.TDP) THEN
      CALL AINT34(RDCP,VAXP,VEXPP,TC,AFPR)
      CALL AINT34(RDCB,VAXB,VEXPB,TC,AFBR)
      AINT=POP*(RWP/100.0)*(RWP/100.0)*(RWP/100.0)*AFPR/6.0 +
     $          POB*(RWB/100.0)*(RWB/100.0)*(RWB/100.0)*AFBR/6.0
      ENDIF
      IF (TC.GT.TDP.AND.TC.LE.T1+TDB) THEN
      CALL AINT34(RDCP,VAXP,VEXPP,TDP,AFPR)
      CALL AINT34(RDCB,VAXB,VEXPB,TC,AFBR)
      AINT=POP*(RWP/100.0)*(RWP/100.0)*(RWP/100.0)*AFPR/6.0 +
     $          POB*(RWB/100.0)*(RWB/100.0)*(RWB/100.0)*AFBR/6.0
      ENDIF
      C3=V01*AINT-V02*EPSFCN*TC*TC/2.0
      ENDIF
      IF (TC.GT.T1+TDB) THEN
      CALL AINT12(RDCP,VAXP,VEXPP,TDP,AIPR)
      CALL AINT12(RDCB,VAXB,VEXPB,TDB,AIBR)
      AINT=POP*(RWP/100.0)*(RWP/100.0)*(RWP/100.0)*AIPR/6.0 +
     $          POB*(RWB/100.0)*(RWB/100.0)*(RWB/100.0)*AIBR/6.0
      C3=TC*V01*AINT-V02*EPSFCN*TC*TC/2.0
      ENDIF
      ENDIF
C
      IF (THP.GT.0.0) THEN
      IF (TC.LE.TDP) THEN
      CALL AINT34(RDCP,VAXP,VEXPP,TC,AFPR)
      AINT=POP*(RWP/100.0)*(RWP/100.0)*(RWP/100.0)*AFPR/6.0
      C3=V01*AINT-V02*EPSFCN*TC*TC/2.0
      ENDIF
      IF (TC.GT.TDP) THEN
      CALL AINT12(RDCP,VAXP,VEXPP,TDP,AIPR)
      AINT=POP*(RWP/100.0)*(RWP/100.0)*(RWP/100.0)*AIPR/6.0
      C3=TC*V01*AINT-V02*EPSFCN*TC*TC/2.0
      ENDIF
      ENDIF
C
      NCR=C1*C2*C3
      NCR=DFLOAT(DINT(NCR))+1.0
C
      WRITE (*,64)
   64 FORMAT(/,' CALCULATE CRACK LENGTHS')
C
```

```
C.....  CALCULATE CRACK LENGTHS
C
      VL=0.38*C0T
      SIFA=AC*SIF
      DELTA=A0/10.0
      KSI=(2.0/C1T)*(C2T/CRT)*(C2T/CRT)*(1.0-C2T/C1T)*(1.0-C2T/C1T)
      J=0
 2800 J=J+1
      AJ=A0+J*DELTA
      VJ=VL*(1.0-A0/AJ)
      KI0J=1.4142*(SY*1.0E06)*DSQRT(PI*AJ/100.0)
      KAPJ=(1-VJ/CRT)/DSQRT(1.0-KSI*VJ)
      KIJ=KAPJ*KI0J
      KIDJ=(SIFA*1.0E06)/(1.0-(VJ/VL)**AM)
      IF (J.EQ.1000) THEN
      WRITE (2,2749)
 2749 FORMAT('*** PROGRAM STOP. MAX ITERATIONS EXCEEDED IN CALCULATING A
     $LIM ***')
      STOP
      ENDIF
      IF (KIJ.GE.KIDJ) GOTO 2800
      ALIM=A0+(J-1)*DELTA
      LTT=CL*2.0*ALIM
C
C        WRITE (2,2750) NCR,A0,ALIM,2.0*ALIM
C 2750 FORMAT(/,'PRESSURE WALL CRACKING CHARACTERISTICS ...',/,3X,'NUMBER
C     $ OF CRACKS ........ ',F6.1,/,3X,'INITIAL CRACK LENGTH .... ',F6.3,
C     $' CM',/,3X,'FINAL CRACK LENGTH ...... ',F6.3,' CM',/,3X,'MAX TIP-T
C     $O-TIP CR LEN ... ',F6.3,' CM')
C
      WRITE (2,2750) LTT
 2750 FORMAT(/,'PRESSURE WALL CRACKING CHARACTERISTICS ...',/,3X,'MAXIMU
     $M TIP-TO-TIP CRACK LENGTH ... ',F6.3,' CM')
C
        IF (NCR.LT.3.0) NCR=3.0
C        IF (NCR.LT.3.0) THEN
C        WRITE (2,2751)
C 2751 FORMAT(' NUMBER OF CRACKS LESS THAN 3; PROGRAM STOP')
C        WRITE (*,2751)
C        STOP
C        ENDIF
C
      WRITE (*,65)
   65 FORMAT(/,' BEGIN PETAL DEFORMATION CALCULATIONS')
C
      WRITE (2,66)
   66 FORMAT(/,'RESULTS OF PETAL DEFORMATION CALCULATIONS ...',/)
C
C.....  CALCULATE PETAL DEFORMATIONS
C
      READ (4,2899) NZPTS,NITPTS,DET,IPRT,MPLOPT,MYOPT
 2899 FORMAT(I6,I4,A1,I3,2A1)
      G=(MP+MBT)/NCR
      BAVG=ALIM*DSIN(PI/NCR)
      IF (ALIM.GE.RSTAR) HAVG=TW*(1.0-0.5*(RSTAR/ALIM)*(1.0-ETA))
```

```
      IF (ALIM.LE.RSTAR) HAVG=(TW/2.0)*(2.0*ETA+ALIM/RSTAR)
      AMY=(SY*1.0E+06)*(BAVG/100.0)*(HAVG/100.0)*(HAVG/100.0)/4.0
      AMPL=(RT*1000.0)*(BAVG/100.0)*(HAVG/100.0)
      TM1=(RT*1000.0)*(TW/100.0)*2.0*PI/NCR
      ALIM2=(ALIM/100.0)*(ALIM/100.0)
      IF (ALIM.LE.RSTAR) THEN
      BMPL=TM1*(0.5*ETA*ALIM2 +
     $          (1.0-ETA)*(ALIM/100.0)*ALIM2/(RSTAR/100.0)/3.0)
      ENDIF
      IF (ALIM.GT.RSTAR) THEN
      BMPL=TM1*((ETA-1.0)*(RSTAR/100.0)*(RSTAR/100.0)/3.0 + ALIM2)
      ENDIF
      BMPL=BMPL/(ALIM/100.0)
      RAT1=ALIM/RSTAR
      RAT2=RSTAR/ALIM
      TM2=PI*(SY*1.0E+06)*(TW/100.0)*(TW/100.0)*(ALIM/100.0)/NCR/2.0
      IF (ALIM.LE.RSTAR) THEN
      BMY=TM2*(0.5*ETA*ETA+(2.0*ETA/3.0)*(1.0-ETA)*RAT1 +
     $          0.25*(1.0-ETA)*(1.0-ETA)*RAT1*RAT1)
      ENDIF
      IF (ALIM.GT.RSTAR) THEN
      BMY=TM2*((ETA*ETA+2.0*ETA-9.0)*RAT2*RAT2/12.0 + 1.0)
      ENDIF
      IF (MPLOPT.EQ.'A') MPL=AMPL
      IF (MPLOPT.EQ.'B') MPL=BMPL
      IF (MYOPT.EQ.'A') MY=AMY
      IF (MYOPT.EQ.'B') MY=BMY
      ALFAC=G*V0TC*V0TC/2.0/MY
      ALFAM=2.0*PI
      IF (ALFAC.GE.ALFAM) THEN
      ALFA=ALFAM
      GC=G
      G=ALFA*(2.0*MY)/(V0TC*V0TC)
      ENDIF
      IF (ALFAC.LE.ALFAM) THEN
      ALFA=ALFAC
      GC=G
      ENDIF
      ZMAX=(MPL/G)*(ALIM/100.0)*DCOS(PI/NCR)
      DZ=ZMAX/NZPTS
      IF (DZ.LT.0.05) THEN
   11 NZPTS=NZPTS-10.0
      DZ=ZMAX/NZPTS
      IF (DZ.LT.0.05) GOTO 11
      IPRT=NZPTS/10
      ENDIF
      WRITE (2,67) MP,MBT,GC,G,BAVG,HAVG,MY,MPL,ALFAC,ALFA,ZMAX,NZPTS,
     $                  NITPTS,DZ
   67 FORMAT('TIP MASS PARAMETERS ...',/,5X,'MP  = ',E10.3,' KG',/,5X,
     $'MBT = ',E10.3,' KG',/,5X,'GC  = ',E10.3,' KG',/,5X,'G   = ',E10.3
     $,' KG',//,'EQUIVALENT BEAM PARAMETERS ...',/,5X,'B-AVG = ',F6.4,
     $' CM',/,5X,'H-AVG = ',F6.4,' CM',/,5X,'M-YLD = ',E10.4,' N-M',/,5X
     $,'MPL   = ',E10.4,' KG/SQM',/,5X,'ALFAC = ',E10.4,/,5X,'ALFA  = ',
     $F6.3,//,'ITERATION PARAMETERS ...',/,5X,'ZMAX   = ',E10.4,/,5X,
     $'NZPTS  = ',I5,/,5X,'NITPTS = ',I5,/,5X,'DZ (ND) = ',E10.4,//,
```

```
     $'RESULTS OF PETAL DEFORMATION CALCULATIONS ...',/)
      J=0
      ZJ=0.0
      KJ=2.0*ALFA/3.0
      AI1J=0.0
      AI2J=0.0
      AI0J=0.0
      DTH=0.0
      THETA=0.0
      THF=ALFA
      TZ=0.0
C
      DO 2901 I=1,NZPTS+1
      XF(I)=0.0
      YF(I)=0.0
 2901 CONTINUE
      XFM=0.0
      YFM=0.0
 2900 J=J+1
      THETA=THETA+DTH
      IF (DFLOAT(J-1)/DFLOAT(IPRT)-DINT((J-1)/IPRT).EQ.0) THEN
C        WRITE (6,2925) ZJ,AI1J,AI2J,AI0J,KJ,THETA,THF,TZ
C 2925 FORMAT('Z=',E10.4,2X,'I1=',E10.4,2X,'I2=',E10.4,2X,'I0=',E10.4,2X,
C     $'K=',E10.4,2X,'TH0=',E10.4,2X,'THF=',E10.4,2X,'TZ=',E10.4)
      ENDIF
      IF (J.EQ.NZPTS) THEN
      Z=0.0
      DO 2927 I=1,NZPTS+1
      IF (XF(I).GT.XFM) THEN
      XFM=XF(I)
      HFM=(I-1)*DZ*DTAN(PI/NCR)*(G/MPL)
      ENDIF
      IF (YF(I).GT.YFM) THEN
      YFM=YF(I)
      ENDIF
      IF (DFLOAT(I-1)/DFLOAT(IPRT)-DINT((I-1)/IPRT).EQ.0) THEN
      DELZ=ZMAX-Z
C        WRITE (5,2926) (Z*G/MPL)*100.0,(DELZ*G/MPL)*100.0,XF(I)*100.0,
C     $                  (DELZ*G/MPL-XF(I))*100.0,YF(I)*100.0
C 2926 FORMAT('Z=',E10.4,2X,'X-ORIG=',E10.4,2X,'X-FINL=',E10.4,2X,'DELX=',
C     $E10.4,2X,'DELY=',E10.4)
      ENDIF
      Z=Z+DZ
 2927 CONTINUE
      GOTO 3000
      ENDIF
      ZJ1=ZJ+DZ
      KJ1G=0.99*KJ
      DO 2950 I=1,NITPTS
      DTH=DZ*(KJ1G+KJ)/2.0
      AI1J1=AI1J-DTH*AI2J+(1.0+ZJ1-0.5*DZ)*DZ
      AI2J1=AI2J+DTH*AI1J+0.5*DTH*DZ*(1.0+ZJ1-(2.0/3.0)*DZ)
      AI0J1=AI0J+2.0*DZ*AI1J-DTH*DZ*AI2J+DZ*DZ*(1.0+ZJ1-(2.0/3.0)*DZ)
      ANT1=(1.0+ZJ1)*AI0J1
      ANT2=AI1J1*AI1J1
```

```
      ANUM=ANT1-ANT2
      ADT1=AI1J1*AI1J1*AI1J1
      ADT2=2.0*ALFA*AI0J1*AI2J1
      ADENOM=ADT1+ADT2
      Q=KJ1G-2.0*ALFA*ANUM/ADENOM
C
      IF (DET.EQ.'Y'.AND.J.LE.3) THEN
      WRITE (2,301) DTH,DZ,AI1J1,AI2J1,AI0J1
  301 FORMAT(3X,'DTH = ',E16.10,3X,'DZ  = ',E16.10,/,3X,'AI1 = ',E16.10,
     $3X,'AI2 = ',E16.10,3X,'AI0 = ',E16.10)
      WRITE (2,311) ANT1,ANT2,ANUM
  311 FORMAT(3(3X,E16.10))
      WRITE (2,331) ADT1,ADT2,ADENOM
  331 FORMAT(3(3X,E16.10))
      WRITE (2,401) KJ1G,Q
  401 FORMAT(3X,'KG  = ',E16.10,3X,'Q   = ',E16.10)
      ENDIF
C
      IF (DABS(Q).GT.0.001) THEN
      AN=2.0*AI1J1*AI2J1+3.0*KJ1G*AI1J1*AI1J1*AI2J1 -
     $          2.0*ALFA*KJ1G*AI0J1*AI1J1
      AD=AI1J1*AI1J1*AI1J1+2.0*ALFA*AI0J1*AI0J1
      DQDK=1.0-ALFA*DZ*AN/AD
      KJ1G=KJ1G-Q/DQDK
      ENDIF
      IF (DABS(Q).LE.0.001) THEN
      AI1J=AI1J1
      AI2J=AI2J1
      AI0J=AI0J1
      THF=ALFA*AI0J/AI1J/AI1J
      TZ=ZJ1-AI0J/AI1J
      IF (KJ1G.GE.KJ) THEN
        WRITE (2,402) J
  402 FORMAT('*** ERROR OCCURED IN ',I4,'-TH CURVATURE CALCUATION ***')
C       STOP
      ENDIF
      KJ=KJ1G
      ZJ=ZJ1
      DO 501 JJ=1,J
      XF(JJ)=XF(JJ)+DCOS(THF)*DZ*(G/MPL)
      YF(JJ)=YF(JJ)+DSIN(THF)*DZ*(G/MPL)
  501 CONTINUE
      GOTO 2900
      ENDIF
 2950 CONTINUE
      IF (J.LE.NZPTS) THEN
        WRITE (2,2951) J
 2951 FORMAT(//,3X,'*** CONVERGENCE ERROR OCCURED IN ',I2,'-TH CURVATURE
     $ CALCULATION ***')
      STOP
      ENDIF
C
 3000   DO 3007 I=1,NZPTS+1
      ZX=(I-1)*DZ*(G/MPL)
      ZZ=ZX*DTAN(PI/NCR)
```

```
      IF (DFLOAT(I-1)/DFLOAT(IPRT)-DINT((I-1)/IPRT).EQ.0) THEN
C        WRITE (7,3005) I,ZX*100.0,ZZ*100.0,XF(I)*100.0,ZZ*100.0
C 3005 FORMAT(I5,4F10.5)
      ENDIF
 3007 CONTINUE
C
C.....  CACULATE EQUIVALENT CIRCULAR HOLE DIAMETER
C
      ARG=PI/NCR
C
C.....  POLYGON APPROXIMATION
C
C        XF0=(ALIM/100.0)*DCOS(ARG)-XFM
C        DEQ1=2.0*XF0*DSQRT(DTAN(ARG)/ARG)
C        WRITE (2,3010) DEQ1*100.0,XF0*100.0,YFM*100.0
C 3010 FORMAT(3X,'POLYGON APPROXIMATION ...',/,5X,'EQUIVALENT SNGL HOLE D
C     $IAMETER  = ',F10.5,' CM',/,5X,'MIN DISTANCE TO PETAL TANGENT  = ',
C     $F10.5,' CM',/,5X,'MAX DEPTH OF PETAL DEFORMATION = ',F10.5,' CM'
C     $,/)
C
C.....  STAR PATTERN APPROXIMATION
C
      XF0=(ALIM/100.0)*DCOS(ARG)-XFM
      AL1=(ALIM/100.0)*DSIN(ARG)-HFM
      AL2=(ALIM/100.0)*DCOS(ARG)-XFM
      HA=DABS(DCOS(ARG)*AL1-XFM*DSIN(ARG))
      AONE=0.5*(AL2)*HFM
      ATWO=0.5*(ALIM/100.0)*HA
      ATOT=(AONE+ATWO)*2.0*NCR
      DEQ2=DSQRT(ATOT*4.0/PI)
      DH=CD*DEQ2
      WRITE (2,3020) DH*100.0,XF0*100.0,2.0*HFM*100.0,YFM*100.0
 3020 FORMAT(3X,'STAR PATTERN APPROXIMATION ...',/,5X,'EQUIVALENT SNGL H
     $OLE DIAMETER  = ',F10.5,' CM',/,5X,'MIN DISTANCE TO PETAL TANGENT
     $ = ',F10.5,' CM',/,5X,'WIDTH OF FLAT PORTION OF PETAL = ',F10.5,
     $' CM',/,5X,'MAX DEPTH OF PETAL DEFORMATION = ',F10.5,' CM')
C
C.....  COMPUTE EMPIRICAL PREDICTIONS IF APPROPRIATE
C
 3025 IF (WSID.EQ.'BLC'.OR.WSID.EQ.'ELC'.OR.WSID.EQ.'NEC'.OR.WSID.EQ.
     $         'LEC') THEN
        IF (WSID.EQ.'NEC'.AND.VP.GT.6.5) STOP
      WRITE (*,3026)
 3026 FORMAT(/,' COMPARING MODEL PREDICTIONS WITH EXPERIMENTAL RESULTS')
      CALL EMPCHK(WSID,DP,DCN,THP,COB,RP,VP,DHEMP,CREMP)
      WRITE (2,3027) DHEMP,CREMP
 3027 FORMAT(/,'PREDICTIONS OF EMPIRICALLY-BASED REGRESSION EQUATIONS ..
     $.',/,3X,'EQUIVALENT HOLE DIAMETER ..... ',F10.5,' CM',/,3X,'MAX T
     $IP-TO-TIP CRACK LENGTH ... ',F10.5,' CM')
      DHRAT=DHEMP/(DH*100.0)
      CRRAT=CREMP/LTT
      WRITE (2,3030) DHRAT,CRRAT
 3030 FORMAT(/,' COMPARISON OF EMPIRICAL VALUES TO MODEL PREDICTIONS ...
     $',/,3X,'DH,EXP/DH,MODEL ..... ',F10.5,/,3X,'LTT,EXP/LTT,MODEL ...
     $',F10.5)
```

```
        WRITE (*,3030) DHRAT,CRRAT
       ENDIF
C
       STOP
       END
C
       FUNCTION DN(VP,C,TB,DP,RTHP)
       IMPLICIT DOUBLE PRECISION (A-H,O-Z)
       DN=(2.698*((VP/C)**0.689)*((TB/DP)**0.708)*(COS(RTHP)**0.021)
      $          +0.93)*DP
       RETURN
       END
C
       FUNCTION DX(VP,C,TB,DP,RTHP)
       IMPLICIT DOUBLE PRECISION (A-H,O-Z)
       DX=(2.252*((VP/C)**0.622)*((TB/DP)**0.667)*(EXP(0.815*RTHP))
      $          +1.00)*DP
       RETURN
       END
C
       SUBROUTINE BLCALC1(VP,THP,TS,S,TW1,SY,RP,RB,RW,DCN)
       IMPLICIT DOUBLE PRECISION (A-H,O-Z)
C
       PI=3.141592
C
       SYW=SY*(1.0E+06)*(1.4504E-04)/1000.0
       TW=TW1+0.033/RW
       TB=TS
       IF (THP.GT.65.0) TH1=65.0
       IF (THP.LE.65.0) TH1=THP
       TH=TH1*PI/180.0
       V=VP
       VN=VP*DCOS(TH)
C
       IF (VN.LE.3.0) THEN
       T1=TW*DSQRT(SYW/40.0)+TB
       T2=0.6*(DCOS(TH)**1.66666)*DSQRT(RP)*(V**0.66666)
       DCN=(T1/T2)**(18.0/19.0)
       ENDIF
C
       IF (VN.GT.3.0.AND.VN.LT.7.0) THEN
       TA1=TW*DSQRT(SYW/40.0)+TB
       TA2=1.248*DCOS(TH)*DSQRT(RP)
       TA=(1.75-0.25*V*DCOS(TH))*((TA1/TA2)**(18.0/19.0))
       TZ1=1.071*(TW**0.66666)*(S**0.33333)*((SYW/70.0)**0.33333)/
      $(RP**0.33333)/(RB**0.11111)
       TZ2=0.25*V*DCOS(TH)-0.75
       TZ=TZ1*TZ2
       DCN=TA+TZ
       ENDIF
C
       IF (VN.GE.7.0) THEN
       DCN=3.918*(TW**0.66666)*(S**0.33333)*((SYW/70.0)**0.33333)/
      $(RP**0.33333)/(RB**0.11111)/((V*DCOS(TH))**0.66666)
       ENDIF
```

```
C
      RETURN
      END
C
      SUBROUTINE BLCALC2(IB,VP,THP,DCN)
      IMPLICIT DOUBLE PRECISION (A-H,O-Z)
      DOUBLE PRECISION CF(4,2)
      CHARACTER*3 IB
      INTEGER COPT
C
      PI=3.141592
C
      DO 30 I=1,2
      READ (8,25) (CF(I,J),J=1,2)
   25 FORMAT(4F10.5)
   30 CONTINUE
      IF (IB.EQ.'BB1') COPT=1
      IF (IB.EQ.'BB2') COPT=2
      CH=CF(1,COPT)
      CHI=CF(2,COPT)
      CLI=CF(3,COPT)
      CL=CF(4,COPT)
C
C.....  COMPUTE BALLISTIC LIMIT DIAMETER DATA USING JSC (1995) EQUATIONS
C
      IF (THP.GT.65.0) TH1=65.0
      IF (THP.LE.65.0) TH1=THP
      TH=TH1*PI/180.0
      V=VP
      ARG=DCOS(TH)
      VN1=2.7/(ARG**0.5)
      VN2=6.5/(ARG**0.33333)
      DEN=VN2-VN1
C
      IF (V.LE.VN1) THEN
      DCN=CL/(V**0.66666)/(ARG**1.66666)
      ENDIF
C
      IF (V.GT.VN1.AND.V.LT.VN2) THEN
      T1=(CHI/(ARG**(7.0/18.0)))*(V-VN1)/DEN
      T2=(CLI/(ARG**(4.0/3.00)))*(VN2-V)/DEN
      DCN=T1+T2
      ENDIF
C
      IF (V.GE.VN2) THEN
      DCN=CH/(V**0.33333)/(ARG**0.5)
      ENDIF
C
      REWIND (8)
      RETURN
      END
C
      SUBROUTINE RELS(CO,K,R,G,VO,V1,PHO,EX,UP,PHA,VF)
      IMPLICIT DOUBLE PRECISION (A-H,O-Z)
      DOUBLE PRECISION K,PH(201),EH(201),V(201),P(201),E(201)
```

```
C
C.....  THIS SUBROUTINE CALCULATES THE RELEASE OF A SHOCKED MATERIAL
C.....  USING THE MIE-GRUNHEISEN EQUATION OF STATE.  INCLUDED IS A
C.....  CALCULATION OF THE FINAL SPECIFIC VOLUME AND THE WASTE HEAT
C.....  GENERATED BY THE RELEASE PROCESS.  WHEN THE PRESSURE ALONG THE
C.....  ISENTROPE DROPS BELOW THE REFLECTED PRESSURE ARE CALCULATED BY
C.....  THE IMPEDANCE MATCH PROCESS, THE RELEASE PROCESS IS TERMINATED
C
      V(1)=V1
      PH(1)=PHO
      EH(1)=0.5*PH(1)*(VO-V1)/1000.0
      DV=(VO-V1)/50.0
      DE=0.0
      DV2=DV/1000.0
      E(1)=EH(1)
      P(1)=PH(1)
      DEN1=1.0+G*DV2*0.5
C
      II=0
      UR=0.0
      DO 10 I=2,201
      V(I)=V(I-1)+DV
      PH(I)=CO**2*R*1000.0*(1.0-V(I)/VO)/(1.0-K*(1.0-V(I)/VO))**2
      PH(I)=PH(I)*1.0E06
      EH(I)=0.5*PH(I)*(VO-V(I))/1000.0
      P(I)=(PH(I)+G*(E(I-1)-EH(I)-0.5*P(I-1)*DV2))/DEN1
      E(I)=E(I-1)-0.5*(P(I)+P(I-1))*DV2
      DP=P(I)-P(I-1)
      DUR=DSQRT(-DP*(DV/1000.0))
      UR=UR+DUR/1000.0
      II=II+1
      IF (P(I).GE.0.0) DE=DE+0.5*DV2*(P(I)+P(I-1))
      IF (P(I).LT.0.0) GOTO 15
      IF (P(I).LE.PHA) GOTO 15
   10 CONTINUE
C
   15 Q=P(II)/(P(II)-P(II+1))
      DE=DE+0.5*Q*DV2*P(II)
      EX=EH(1)-DE
      VF=V(II)+Q*(V(II+1)-V(II))
      UFS1=UP+UR
      UFS2=2.0*UP
C
      WRITE(2,20) VF,EH(1),DE,EX
   20 FORMAT(/,'SPECIFIC VOL AFTER RELEASE ..... VF =',F5.3,
     $' CU.CM./GM',/,'ENERGY DUE TO DEB CLD IMPACT .... ',E10.4,
     $' JOULES/KG',/,'ENERGY RECOVERED BY RELEASE ..... ',E10.4,
     $' JOULES/KG',/,'WASTE HEAT GENERATED ............ ',E10.4,
     $' JOULES/KG')
C
      RETURN
      END
C
      SUBROUTINE TINC(SHS,SHL,TM,TV,HF,HV,EXH)
      IMPLICIT DOUBLE PRECISION (A-H,O-Z)
```

```
      DOUBLE PRECISION IME,IVE
C
C.....  THIS SUBROUTINE CALCULATES THE RESIDUAL TEMPERATURE INCREASE
C.....  IN A MATERIAL THAT HAS BEEN RELEASED FROM THE SHOCKED STATE
C.....  ESTIMATES THE PERCENTAGE OF VAPORIZED, MELTED, AND SOLID
C.....  MATERIAL DUE TO THE RELEASE PROCESS
C
      SHS=SHS*4186.0
      SHL=SHL*4186.0
      HF=HF*4186.0
      HV=HV*4186.0
C
C.....  CALCULATE ENERGIES REQUIRED TO INITIATE MATERIAL MELT AND
C.....  VAPORIZATION.
C
      IME=TM*SHS
      IVE=IME+HF+(TV-TM)*SHL
C
C.....  IF WASTE HEAT IS LESS THAN THE ENERGY REQ'D TO START MELT,
C.....  CALCULATE TEMPERATURE RISE USING W.H.=S.H.*(TEMP.INCR.)
C
      IF (EXH.LT.IME) THEN
      DT=EXH/SHS
      TR=DT
      DEL=0.0
      WRITE(2,50) IME,DEL,EXH
   50 FORMAT('ENERGY REQ, INCIPIENT MELT ... ',E10.4,' JOULES/KG',/,
     $'ENERGY AVAILABLE FOR MELT .... ',E10.4,' JOULES/KG',/,
     $'EXCESS ENERGY AVAILABLE ..... ',E10.4,' JOULES/KG')
      PV=0.0
      PL=0.0
      PS=100.0
      GOTO 100
      ENDIF
C
C.....  IF WASTE HEAT EXCEEDS THE ENERGY REQ'D TO START MELT, BUT IS
C.....  LESS THAN THAT REQ'D TO COMPLETE MELT, RESET THE VALUE OF THE
C.....  ENERGY AVAILABLE FROM THE WASTE HEAT VALUE TO THE VALUE REQ'D
C.....  TO START MELT.  THIS IMPLIES THAT SOME ENERGY IS AVAILABLE FOR
C.....  MELTING A PORTION OF THE MATERIAL.  NOTE: THE TEMPERATURE RISE
C.....  EQUALS THE MELT TEMPERATURE OF THE MATERIAL.
C
      IF (EXH.GE.IME.AND.EXH.LT.IME+HF) THEN
      TR=TM
      DEL=EXH-IME
      REQM=IME+HF
      WRITE(2,60) IME,REQM,DEL
   60 FORMAT('ENERGY REQ, INCIPIENT MELT ... ',E10.4,' JOULES/KG',/,
     $'ENERGY REQ, COMPLETE MELT .... ',E10.4,' JOULES/KG',/,
     $'ENERGY AVAILABLE FOR MELT .... ',E10.4,' JOULES/KG')
      PV=0.0
      PL=100.0*DEL/HF
      PS=100.0-PL
      GOTO 100
      ENDIF
```

```
C
C.....  IF THE WASTE HEAT EXCEEDS THE ENERGY REQ'D TO COMPLETELY MELT
C.....  THE MATERIAL, BUT IS LESS THAN THAT REQ'D TO START VAPORIZA-
C.....  TION, COMPUTE THE TEMPERATURE INCREASE CAUSED BY THE EXCESS
C.....  ENERGY AND ADD IT TO THE MELT TEMPERATURE OF THE MATERIAL.
C
      IF (EXH.GE.IME+HF.AND.EXH.LT.IVE) THEN
      DEL=EXH-IME-HF
      DT=DEL/SHL
      TR=TM+DT
      REQM=IME+HF
      WRITE(2,70) IME,REQM,DEL
   70 FORMAT('ENERGY REQ, INCIPIENT MELT ... ',E10.4,' JOULES/KG',/,
     $'ENERGY REQ, COMPLETE MELT .... ',E10.4,' JOULES/KG',/,
     $'EXCESS ENERGY AVAILABLE ..... ',E10.4,' JOULES/KG')
      PV=0.0
      PL=100.0
      PS=100.0-PL
      GOTO 100
      ENDIF
C
      IF (EXH.GE.IVE.AND.EXH.LT.IVE+HV) THEN
      DEL=EXH-IVE
      REQV=IVE+HV
      TR=TV
      WRITE(2,80) IVE,REQV,DEL
   80 FORMAT('ENERGY REQ, INCIPIENT VAP .... ',E10.4,' JOULES/KG',/,
     $'ENERGY REQ, COMPLETE VAP ..... ',E10.4,' JOULES/KG',/,
     $'EXCESS ENERGY AVAILABLE ..... ',E10.4,' JOULES/KG')
      PV=100.0*DEL/HV
      PL=100.0-PV
      PS=100.0-PL
      GOTO 100
      ENDIF
C
      IF (EXH.GE.IVE+HV) THEN
      ECVAP=IVE+HV
      PV=100.0
      PL=0.0
      PS=0.0
      WRITE (2,90) ECVAP
   90 FORMAT('ENERGY REQ, COMPLETE VAP .... ',E10.4,' JOULES/KG',/,
     $'*** THE MATERIAL IS COMPLETELY VAPORIZED ***')
      GOTO 120
      ENDIF
C
  100 WRITE(2,110) TR,PS,PL,PV
  110 FORMAT('RESIDUAL MATERIAL TEMP ..... ',F10.3,' DEG-C',//,'PERCEN
     $T SHKD AND REL PRESS WALL MATERIAL ...',/,3X,'IN SOLID STATE ... '
     $,F6.2,'%',/,3X,'IN MOLTEN FORM ... ',F6.2,'%',/,3X,'IN VAPOR FORM
     $.... ',F6.2,'%')
C
  120 RETURN
      END
C
```

```
      SUBROUTINE INTEG(NPT,DELT,VAX,VEXP,T1,RDC,AI)
      IMPLICIT DOUBLE PRECISION (A-H,O-Z)
C
      AI=0.0
      DO 10 I=1,NPT
      T=T1+I*DELT
      AI=AI+FCN(VAX,VEXP,RDC,T,T1)*DELT
   10 CONTINUE
C
      RETURN
      END
C
      DOUBLE PRECISION FUNCTION FCN(VAX,VEXP,RDC,T,T1)
      IMPLICIT DOUBLE PRECISION (A-H,O-Z)
      HDST=H(VAX,VEXP,RDC,T-T1)
      DIFF=RDC-HDST*100.0
      COEF=DIFF/DABS(DIFF)
      IF (DABS(DIFF).GT.RDC) DIFF=COEF*RDC
      TM=RDC*RDC-DIFF*DIFF
      FCN=TM/(RDC*RDC)
      RETURN
      END
C
      DOUBLE PRECISION FUNCTION H(VAX,VEXP,RDC,T)
      IMPLICIT DOUBLE PRECISION (A-H,O-Z)
      AN=(RDC/100.0)*T*(VAX*1000.0+VEXP*1000.0)
      AD=2.0*RDC/100.0+(T*VEXP*1000.0)
      H=AN/AD
      RETURN
      END
C
      DOUBLE PRECISION FUNCTION AIFCN(TD,RDC,VAX,VEXP)
      IMPLICIT DOUBLE PRECISION (A-H,O-Z)
      ALFA=VEXP/(VAX+VEXP)
      GAMA=2.0*(RDC/100.0)/(VEXP*1000.0)
      T1=(1.0/ALFA)*(2.0-1.0/ALFA)*TD
      T2=2.0*(GAMA/ALFA)*(1.0-1.0/ALFA)*DLOG(1.0+TD/GAMA)
      T3=(1.0/ALFA)*(1.0/ALFA)*TD*GAMA/(TD+GAMA)
      AIFCN=T1-T2-T3
      RETURN
      END
C
      SUBROUTINE AINT12(RDC,VAX,VEXP,TD,AI)
      IMPLICIT DOUBLE PRECISION (A-H,O-Z)
      GAMA=2.0*(RDC/100.0)/(VEXP*1000.0)
      ALFA=VEXP/(VAX+VEXP)
      T1=(2.0-1.0/ALFA)*TD/ALFA
      T2=2.0*(GAMA/ALFA)*(1.0-1.0/ALFA)*DLOG(1.0+TD/GAMA)
      T3=TD*GAMA/(TD+GAMA)/(ALFA*ALFA)
      AI=T1-T2-T3
      RETURN
      END
C
      SUBROUTINE AINT34(RDC,VAX,VEXP,TD,AF)
      IMPLICIT DOUBLE PRECISION (A-H,O-Z)
```

```
      GAMA=2.0*(RDC/100.0)/(VEXP*1000.0)
      ALFA=VEXP/(VAX+VEXP)
      T1=(2.0-1.0/ALFA)*TD*TD/2.0/ALFA
      T21=(GAMA*GAMA/ALFA)*DLOG(1.0+TD/GAMA)
      T22=2.0*(1.0-1.0/ALFA)*(1.0+TD/GAMA)-1.0/ALFA
      T2=T21*T22
      T3=GAMA*TD/ALFA/ALFA
      AF=T1-T2-T3
      RETURN
      END
C
      SUBROUTINE AINT56(RDC,VAX,VEXP,T,AJ)
      IMPLICIT DOUBLE PRECISION (A-H,O-Z)
      GAMA=2.0*(RDC/100.0)/(VEXP*1000.0)
      ALFA=VEXP/(VAX+VEXP)
      T1=(2.0-1.0/ALFA)*T*T/2.0/ALFA
      T21=(GAMA*GAMA/ALFA)*DLOG(1.0+T/GAMA)
      T22=2.0*(1.0-1.0/ALFA)*(1.0+T/GAMA)-1.0/ALFA
      T2=T21*T22
      T3=GAMA*T/ALFA/ALFA
      AJ=T1-T2-T3
      RETURN
      END
C
      DOUBLE PRECISION FUNCTION AMAX(A,B)
      IMPLICIT DOUBLE PRECISION (A-H,O-Z)
      IF (A.GT.B) AMAX=A
      IF (B.GT.A) AMAX=B
      RETURN
      END
C
      SUBROUTINE VCALCS0(M2,MIBI,EPSI,EPSF,MIBF,V2,VRD,ERF,VLE,VAXP,
     $                         VEXPP,VAXB,VEXPB,THDCP,THDEGP,THDCB,THDEGB)
      IMPLICIT DOUBLE PRECISION (A-H,O-Z)
      DOUBLE PRECISION M2,MIB,MIBI,MIBF,MBT
      PI=3.141592
C
      EPS=EPSI
      MIB=MIBI
      ICNTR=0
C
   10 MBT=M2+MIB
      V2P=M2*V2/MBT
      T1=M2/MBT
      VRDP=DSQRT(T1*(V2*V2+VRD*VRD)-V2P*V2P)
      VLE=V2P+VRDP
      VAXP=V2P
      VEXPP=VRDP
      VAXB=0.0
      VEXPB=0.0
C
      IF (VAXP.LE.0.0) THEN
      MIB=MIB/EPS
      EPS=ERF*EPS
      MIB=EPS*MIB
```

```
      ICNTR=ICNTR+1
      IF (ICNTR.GT.500) GOTO 20
      GOTO 10
      ENDIF
C
      THDCP=ATAN(VRDP/V2P)
      THDEGP=180.0*THDCP/PI
      THDCB=0.0
      THDEGB=0.0
C
C.....  VERIFY THAT CONE ANGLES ARE LESS THAN 45-DEG. IF NOT, ADJUST
C.....  EPS TO MAKE IT SO.
C
      IF (THDEGP.GE.45.0) THEN
      MIB=MIB/EPS
      EPS=ERF*EPS
      MIB=EPS*MIB
      ICNTR=ICNTR+1
      IF (ICNTR.GT.500) GOTO 20
      GOTO 10
      ENDIF
C
   20 EPSF=EPS
      MIBF=MIB
C
      RETURN
      END
C
      SUBROUTINE VCALCS1(EXTP,EXTB,MP,EPSI,MBI,EPSF,MBF,MBT,VP,VLE,
     $             VAXP,VEXPP,VAXB,VEXPB,THDCP,THDEGP,THDCB,THDEGB,E1)
      IMPLICIT DOUBLE PRECISION (A-H,O-Z)
      DOUBLE PRECISION MB,MBF,MBI,MBT,MP
C
      PI=3.141592
      EPS=EPSI
C
      MB=MBI
      ICNTR=0
   10 MBT=MB
      CALL DEBCLD(EXTP,EXTB,MP,MB,MBT,VP,VLE,VAXP,VEXPP,VAXB,VEXPB)
C
      IF (VAXP.LE.0.0) THEN
      MB=MB/EPS
      EPS=E1*EPS
      MB=EPS*MB
      ICNTR=ICNTR+1
      IF (ICNTR.GT.500) GOTO 20
      GOTO 10
      ENDIF
C
      IF (VAXB.LE.0.0) THEN
      MB=MB/EPS
      EPS=(1.0/E1)*EPS
      MB=EPS*MB
      ICNTR=ICNTR+1
```

```
      IF (ICNTR.GT.500) GOTO 20
      GOTO 10
      ENDIF
C
C.....  CALCULATE PRIMARY DEBRIS CLOUD 1/2-ANGLE SPREADS
C
      THDCP=ATAN(VEXPP/VAXP)
      THDEGP=180.0*THDCP/PI
      THDCB=ATAN(VEXPB/VAXB)
      THDEGB=180.0*THDCB/PI
C
C.....  VERIFY THAT SEMI-CONE ANGLES ARE LESS THAN 45-DEG; IF NOT,
C.....  ADJUST EPS TO MAKE IT SO
C
      IF (THDEGP.GE.45.0) THEN
      MB=MB/EPS
      EPS=E1*EPS
      MB=EPS*MB
      ICNTR=ICNTR+1
      IF (ICNTR.GT.500) GOTO 20
      GOTO 10
      ENDIF
C
      IF (THDEGB.GE.45.0) THEN
      MB=MB/EPS
      EPS=(1.0/E1)*EPS
      MB=EPS*MB
      ICNTR=ICNTR+1
      IF (ICNTR.GT.500) GOTO 20
      GOTO 10
      ENDIF
C
      IF (THDEGP.GE.THDEGB) THEN
      MB=MB/EPS
      EPS=E1*EPS
      MB=EPS*MB
      ICNTR=ICNTR+1
      IF (ICNTR.GT.500) GOTO 20
      GOTO 10
      ENDIF
C
   20 EPSF=EPS
      MBF=MB
C
      RETURN
      END
C
      SUBROUTINE VCALCS2(EXTP,EXTB,MP,EPSI,MBI,MIBI,EPSF,MBF,MIBF,MBT,
     $        VP,VLE,VAXP,VEXPP,VAXB,VEXPB,THDCP,THDEGP,THDCB,THDEGB,E2)
      IMPLICIT DOUBLE PRECISION (A-H,O-Z)
      DOUBLE PRECISION MB,MBF,MBI,MBT,MIB,MIBI,MIBF,MP
C
      PI=3.141592
      EPS=EPSI
C
```

```
      MB=MBI
      MIB=MIBI
      ICNTR=0
   10 MBT=MB+MIB
      CALL DEBCLD(EXTP,EXTB,MP,MB,MBT,VP,VLE,VAXP,VEXPP,VAXB,VEXPB)
C
      IF (VAXP.LE.0.0) THEN
      MIB=MIB/EPS
      EPS=E2*EPS
      MIB=EPS*MIB
      ICNTR=ICNTR+1
      IF (ICNTR.GT.500) GOTO 20
      GOTO 10
      ENDIF
C
      IF (VAXB.LE.0.0) THEN
      MIB=MIB/EPS
      EPS=(1.0/E2)*EPS
      MIB=EPS*MIB
      ICNTR=ICNTR+1
      IF (ICNTR.GT.500) GOTO 20
      GOTO 10
      ENDIF
C
C.....  CALCULATE PRIMARY DEBRIS CLOUD 1/2-ANGLE SPREADS
C
      THDCP=ATAN(VEXPP/VAXP)
      THDEGP=180.0*THDCP/PI
      THDCB=ATAN(VEXPB/VAXB)
      THDEGB=180.0*THDCB/PI
C
C.....  VERIFY THAT SEMI-CONE ANGLES ARE LESS THAN 45-DEG; IF NOT,
C.....  ADJUST EPS TO MAKE IT SO
C
      IF (THDEGP.GE.45.0) THEN
      MIB=MIB/EPS
      EPS=E2*EPS
      MIB=EPS*MIB
      ICNTR=ICNTR+1
      IF (ICNTR.GT.500) GOTO 20
      GOTO 10
      ENDIF
C
      IF (THDEGB.GE.45.0) THEN
      MIB=MIB/EPS
      EPS=(1.0/E2)*EPS
      MIB=EPS*MIB
      ICNTR=ICNTR+1
      IF (ICNTR.GT.500) GOTO 20
      GOTO 10
      ENDIF
C
      IF (THDEGP.GE.THDEGB) THEN
      MIB=MIB/EPS
      EPS=E2*EPS
```

```
      MIB=EPS*MIB
      ICNTR=ICNTR+1
      IF (ICNTR.GT.500) GOTO 20
      GOTO 10
      ENDIF
C
   20 EPSF=EPS
      MBF=MB
      MIBF=MIB
C
      RETURN
      END
C
      SUBROUTINE DEBCLD(EP,EB,MP,MB1,MB,VP,VLE,VAXP,VEXPP,VAXB,VEXPB)
      IMPLICIT DOUBLE PRECISION (A-H,O-Z)
      DOUBLE PRECISION MP,MB,MB1
C
      ESRT=EP*MP+EB*MB1
      R1=MP/MB
      R2=MB/MP
      AA=0.25*(MP+MB)*(R1+R2)
      BB=-0.5*MP*(VP*1000.0)*(R1+R2)
      CC=ESRT+0.25*MP*(VP*1000.0)*(VP*1000.0)*(R1-1.0)
      VLE=(-BB+DSQRT(BB*BB-4.0*AA*CC))/(2.0*AA)/1000.0
      VEXPB=((MP+MB)*VLE-MP*VP)/(2.0*MB)
      VEXPP=R2*VEXPB
      VAXB=VLE-VEXPB
      VAXP=VLE-VEXPP
C
      RETURN
      END
C
      SUBROUTINE NECNTRP(DPE,DBL,THP,CD,CL)
      IMPLICIT DOUBLE PRECISION (A-H,O-Z)
C
C.....  POWER LAW INTERPOLATIONS
C
      IF (THP.EQ.0.0) THEN
      READ (12,10) TH,AA,BB,CC
   10 FORMAT(10X,4F10.5)
      T1=DPE*2.54/DBL
      T2=DPE*2.54/DBL-1.0
      CD=AA*(T1**CC)*(T2**BB)
      READ (12,11) TH,AA,BB,CC
   11 FORMAT(10X,4F10.5)
      T1=DPE*2.54/DBL
      T2=DPE*2.54/DBL-1.0
      CL=AA*(T1**CC)*(T2**BB)
      ENDIF
C
      IF (THP.EQ.45.0) THEN
      READ (12,20) TH,AA,BB,CC
   20 FORMAT(//,10X,4F10.5)
      T1=DPE*2.54/DBL
      T2=DPE*2.54/DBL-1.0
```

```
      CD=AA*(T1**CC)*(T2**BB)
      READ (12,21) TH,AA,BB,CC
   21 FORMAT(10X,4F10.5)
      T1=DPE*2.54/DBL
      T2=DPE*2.54/DBL-1.0
      CL=AA*(T1**CC)*(T2**BB)
      ENDIF
C
      RETURN
      END
C
      SUBROUTINE ELCNTRP(DPE,DBL,THP,VP,CD,CL)
      IMPLICIT DOUBLE PRECISION (A-H,O-Z)
C
      IF (THP.EQ.0.0) THEN
C
        IF (VP.EQ.6.0) THEN
      READ (13,10) TH,V,AA,BB,CC
   10 FORMAT(10X,5F10.5)
      T1=DPE*2.54/DBL
      T2=DPE*2.54/DBL-1.0
      CD=AA*(T1**CC)*(T2**BB)
      READ (13,11) TH,V,AA,BB,CC
   11 FORMAT(10X,5F10.5)
      T1=DPE*2.54/DBL
      T2=DPE*2.54/DBL-1.0
      CL=AA*(T1**CC)*(T2**BB)
      ENDIF
C
      IF (VP.GT.6.0.AND.VP.LT.9.0) THEN
      RATIO=DPE*2.54/DBL
      V1=6.0
      V2=9.0
      TH1=0.0
      CALL BLCALC2('BB1',V1,TH1,DBL6)
      DP6=RATIO*(DBL6/2.54)
      CALL BLCALC2('BB1',V2,TH1,DBL9)
      DP9=RATIO*(DBL9/2.54)
      READ (13,110) TH,V,AA,BB,CC
  110 FORMAT(10X,5F10.5)
      T1=RATIO
      T2=RATIO-1.0
      CD6=AA*(T1**CC)*(T2**BB)
      READ (13,111) TH,V,AA,BB,CC
  111 FORMAT(10X,5F10.5)
      T1=RATIO
      T2=RATIO-1.0
      CL6=AA*(T1**CC)*(T2**BB)
      READ (13,120) TH,V,AA,BB,CC
  120 FORMAT(10X,5F10.5)
      T1=RATIO
      T2=RATIO-1.0
      CD9=AA*(T1**CC)*(T2**BB)
      READ (13,121) TH,V,AA,BB,CC
  121 FORMAT(10X,5F10.5)
```

```
      T1=RATIO
      T2=RATIO-1.0
      CL9=AA*(T1**CC)*(T2**BB)
      VR=(VP-6.0)/(VP-9.0)
      CD=(CD6-CD9*VR)/(1.0-VR)
      CL=(CL6-CL9*VR)/(1.0-VR)
      ENDIF
C
      IF (VP.EQ.9.0) THEN
      READ (13,20) TH,V,AA,BB,CC
   20 FORMAT(//,10X,5F10.5)
      T1=DPE*2.54/DBL
      T2=DPE*2.54/DBL-1.0
      CD=AA*(T1**CC)*(T2**BB)
      READ (13,21) TH,V,AA,BB,CC
   21 FORMAT(10X,5F10.5)
      T1=DPE*2.54/DBL
      T2=DPE*2.54/DBL-1.0
      CL=AA*(T1**CC)*(T2**BB)
      ENDIF
C
      IF (VP.GT.9.0.AND.VP.LT.12.0) THEN
      RATIO=DPE*2.54/DBL
      V1=9.0
      V2=12.0
      TH1=0.0
      CALL BLCALC2('BB1',V1,TH1,DBL9)
      DP9=RATIO*(DBL9/2.54)
      CALL BLCALC2('BB1',V2,TH1,DBL12)
      DP12=RATIO*(DBL12/2.54)
      READ (13,210) TH,V,AA,BB,CC
  210 FORMAT(//,10X,5F10.5)
      T1=RATIO
      T2=RATIO-1.0
      CD9=AA*(T1**CC)*(T2**BB)
      READ (13,211) TH,V,AA,BB,CC
  211 FORMAT(10X,5F10.5)
      T1=RATIO
      T2=RATIO-1.0
      CL9=AA*(T1**CC)*(T2**BB)
      READ (13,220) TH,V,AA,BB,CC
  220 FORMAT(10X,5F10.5)
        T1=RATIO
      T2=RATIO-1.0
      CD12=AA*(T1**CC)*(T2**BB)
      READ (13,221) TH,V,AA,BB,CC
  221 FORMAT(10X,5F10.5)
      T1=RATIO
      T2=RATIO-1.0
      CL12=AA*(T1**CC)*(T2**BB)
      VR=(VP-9.0)/(VP-12.0)
      CD=(CD9-CD12*VR)/(1.0-VR)
      CL=(CL9-CL12*VR)/(1.0-VR)
      ENDIF
C
```

```
      IF (VP.EQ.12.0) THEN
      READ (13,30) TH,V,AA,BB,CC
   30 FORMAT(////,10X,5F10.5)
      T1=DPE*2.54/DBL
      T2=DPE*2.54/DBL-1.0
      CD=AA*(T1**CC)*(T2**BB)
      READ (13,31) TH,V,AA,BB,CC
   31 FORMAT(10X,5F10.5)
      T1=DPE*2.54/DBL
      T2=DPE*2.54/DBL-1.0
      CL=AA*(T1**CC)*(T2**BB)
      ENDIF
C
        ENDIF
C
      IF (THP.EQ.45.0) THEN
      READ (13,40) TH,V,AA,BB
   40 FORMAT(//////,10X,4F10.5)
      X=DPE*2.54/DBL-1.0
      CD=AA*X*DEXP(-BB*X*X)
      READ (13,41) TH,V,AA,BB,CC
   41 FORMAT(10X,5F10.5)
      T1=DPE*2.54/DBL
      T2=DPE*2.54/DBL-1.0
      CL=AA*(T1**CC)*(T2**BB)
      ENDIF
C
      RETURN
      END
C
        SUBROUTINE BLCNTRP(DPE,DBL,THP,VP,TS,S,TW,SY,RP,RB,RW,CD,CL)
      IMPLICIT DOUBLE PRECISION (A-H,O-Z)
C
      IF (THP.EQ.0.0) THEN
C
        IF (VP.EQ.6.0) THEN
        READ (14,9) TH,V,AAL1,BBL1,AAL2,BBL2
    9 FORMAT(10X,6F10.5)
        READ (14,10) TH,V,AA,BB,CC
   10 FORMAT(10X,5F10.5)
        T1=DPE*2.54/DBL-1.0
        IF (DPE.LT.0.465) CD=AAL1*T1+BBL1
        IF (DPE.GE.0.465.AND.DPE.LT.0.522) CD=AAL2*T1+BBL2
        IF (DPE.GE.0.522) CD=AA*T1*T1+BB*T1+CC
        READ (14,11) TH,V,AA,BB,CC
   11 FORMAT(10X,5F10.5)
      T1=DPE*2.54/DBL
      T2=DPE*2.54/DBL-1.0
      CL=AA*(T1**CC)*(T2**BB)
        ENDIF
C
      IF (VP.GT.6.0.AND.VP.LT.9.0) THEN
      RATIO=DPE*2.54/DBL
      V1=6.0
      V2=9.0
```

```
      TH1=0.0
        CALL BLCALC1(V1,TH1,TS,S,TW,SY,RP,RB,RW,DBL6)
      DP6=RATIO*(DBL6/2.54)
        CALL BLCALC1(V2,TH1,TS,S,TW,SY,RP,RB,RW,DBL9)
      DP9=RATIO*(DBL9/2.54)
        READ (14,109) TH,V,AAL1,BBL1,AAL2,BBL2
  109 FORMAT(10X,6F10.5)
        READ (14,110) TH,V,AA,BB,CC
  110 FORMAT(10X,5F10.5)
        T1=RATIO-1.0
        IF (DP6.LT.0.465) CD6=AAL1*T1+BBL1
        IF (DP6.GE.0.465.AND.DP6.LT.0.522) CD6=AAL2*T1+BBL2
        IF (DP6.GE.0.522) CD6=AA*T1*T1+BB*T1+CC
        READ (14,111) TH,V,AA,BB,CC
  111 FORMAT(10X,5F10.5)
      T1=RATIO
      T2=RATIO-1.0
      CL6=AA*(T1**CC)*(T2**BB)
        READ (14,119) TH,V,AAL1,BBL1
  119 FORMAT(10X,4F10.5)
        READ (14,120) TH,V,AA,BB,CC
  120 FORMAT(10X,5F10.5)
        T1=RATIO-1.0
        IF (DP9.LT.0.350) CD9=AAL1*T1+BBL1
        IF (DP9.GE.0.350) CD9=AA*T1*T1+BB*T1+CC
        READ (14,121) TH,V,AA,BB,CC
  121 FORMAT(10X,5F10.5)
      T1=RATIO
      T2=RATIO-1.0
      CL9=AA*(T1**CC)*(T2**BB)
      VR=(VP-6.0)/(VP-9.0)
      CD=(CD6-CD9*VR)/(1.0-VR)
      CL=(CL6-CL9*VR)/(1.0-VR)
      ENDIF
C
      IF (VP.EQ.9.0) THEN
        READ (14,19) TH,V,AAL1,BBL1
   19 FORMAT(///,10X,4F10.5)
        READ (14,20) TH,V,AA,BB,CC
   20 FORMAT(10X,5F10.5)
        T1=DPE*2.54/DBL-1.0
        IF (DPE.LT.0.350) CD=AAL1*T1+BBL1
        IF (DPE.GE.0.350) CD=AA*T1*T1+BB*T1+CC
        READ (14,21) TH,V,AA,BB,CC
   21 FORMAT(10X,5F10.5)
      T1=DPE*2.54/DBL
      T2=DPE*2.54/DBL-1.0
      CL=AA*(T1**CC)*(T2**BB)
        ENDIF
C
      IF (VP.GT.9.0.AND.VP.LT.12.0) THEN
      RATIO=DPE*2.54/DBL
      V1=9.0
      V2=12.0
      TH1=0.0
```

```
        CALL BLCALC1(V1,TH1,TS,S,TW,SY,RP,RB,RW,DBL9)
        DP9=RATIO*(DBL9/2.54)
        CALL BLCALC1(V2,TH1,TS,S,TW,SY,RP,RB,RW,DBL12)
        DP12=RATIO*(DBL12/2.54)
        READ (14,209) TH,V,AAL1,BBL1
  209 FORMAT(///,10X,4F10.5)
        READ (14,210) TH,V,AA,BB,CC
  210 FORMAT(10X,5F10.5)
        T1=RATIO-1.0
        IF (DP9.LT.0.350) CD9=AAL1*T1+BBL1
        IF (DP9.GE.0.350) CD9=AA*T1*T1+BB*T1+CC
        READ (14,211) TH,V,AA,BB,CC
  211 FORMAT(10X,5F10.5)
      T1=RATIO
      T2=RATIO-1.0
      CL9=AA*(T1**CC)*(T2**BB)
        READ (14,219) TH,V,AAL1,BBL1
  219 FORMAT(10X,4F10.5)
        READ (14,220) TH,V,AA,BB,CC
  220 FORMAT(10X,5F10.5)
        T1=RATIO-1.0
        IF (DP12.LT.0.313) CD12=AAL1*T1+BBL1
        IF (DP12.GE.0.313) CD12=AA*T1*T1+BB*T1+CC
        READ (14,221) TH,V,AA,BB,CC
  221 FORMAT(10X,5F10.5)
      T1=RATIO
      T2=RATIO-1.0
      CL12=AA*(T1**CC)*(T2**BB)
      VR=(VP-9.0)/(VP-12.0)
      CD=(CD9-CD12*VR)/(1.0-VR)
      CL=(CL9-CL12*VR)/(1.0-VR)
        ENDIF
C
      IF (VP.EQ.12.0) THEN
        READ (14,29) TH,V,AAL1,BBL1
   29 FORMAT(//////,10X,4F10.5)
        READ (14,30) TH,V,AA,BB,CC
   30 FORMAT(10X,5F10.5)
        T1=DPE*2.54/DBL-1.0
        IF (DPE.LT.0.313) CD=AAL1*T1+BBL1
        IF (DPE.GE.0.313) CD=AA*T1*T1+BB*T1+CC
        READ (14,31) TH,V,AA,BB,CC
   31 FORMAT(10X,5F10.5)
      T1=DPE*2.54/DBL
      T2=DPE*2.54/DBL-1.0
      CL=AA*(T1**CC)*(T2**BB)
      ENDIF
C
        ENDIF
C
      IF (THP.EQ.45.0) THEN
      READ (14,40) TH,V,AA,BB,CC
   40 FORMAT(/////////,10X,5F10.5)
      T1=DPE*2.54/DBL
      T2=DPE*2.54/DBL-1.0
```

```
      CD=AA*(T1**CC)*(T2**BB)
      READ (14,41) TH,V,AA,BB,CC
   41 FORMAT(10X,5F10.5)
      T1=DPE*2.54/DBL
      T2=DPE*2.54/DBL-1.0
      CL=AA*(T1**CC)*(T2**BB)
      ENDIF
C
      RETURN
      END
C
        SUBROUTINE LECNTRP(DPE,DBL,THP,VP,CD,CL)
      IMPLICIT DOUBLE PRECISION (A-H,O-Z)
C
      IF (THP.EQ.0.0) THEN
C
        IF (VP.EQ.6.0) THEN
        READ (15,10) TH,V,AA,BB,CC
   10 FORMAT(10X,5F10.5)
      T1=DPE*2.54/DBL
      T2=DPE*2.54/DBL-1.0
      CD=AA*(T1**CC)*(T2**BB)
        READ (15,11) TH,V,AA,BB,CC
   11 FORMAT(10X,5F10.5)
      T1=DPE*2.54/DBL
      T2=DPE*2.54/DBL-1.0
      CL=AA*(T1**CC)*(T2**BB)
      ENDIF
C
      IF (VP.GT.6.0.AND.VP.LT.9.0) THEN
      RATIO=DPE*2.54/DBL
      V1=6.0
      V2=9.0
      TH1=0.0
      CALL BLCALC2('BB1',V1,TH1,DBL6)
      DP6=RATIO*(DBL6/2.54)
      CALL BLCALC2('BB1',V2,TH1,DBL9)
      DP9=RATIO*(DBL9/2.54)
        READ (15,110) TH,V,AA,BB,CC
  110 FORMAT(10X,5F10.5)
      T1=RATIO
      T2=RATIO-1.0
      CD6=AA*(T1**CC)*(T2**BB)
        READ (15,111) TH,V,AA,BB,CC
  111 FORMAT(10X,5F10.5)
      T1=RATIO
      T2=RATIO-1.0
      CL6=AA*(T1**CC)*(T2**BB)
        READ (15,120) TH,V,AA,BB,CC
  120 FORMAT(10X,5F10.5)
      T1=RATIO
      T2=RATIO-1.0
      CD9=AA*(T1**CC)*(T2**BB)
        READ (15,121) TH,V,AA,BB,CC
  121 FORMAT(10X,5F10.5)
```

```
      T1=RATIO
      T2=RATIO-1.0
      CL9=AA*(T1**CC)*(T2**BB)
      VR=(VP-6.0)/(VP-9.0)
      CD=(CD6-CD9*VR)/(1.0-VR)
      CL=(CL6-CL9*VR)/(1.0-VR)
      ENDIF
C
      IF (VP.EQ.9.0) THEN
        READ (15,20) TH,V,AA,BB,CC
   20 FORMAT(//,10X,5F10.5)
      T1=DPE*2.54/DBL
      T2=DPE*2.54/DBL-1.0
      CD=AA*(T1**CC)*(T2**BB)
        READ (15,21) TH,V,AA,BB,CC
   21 FORMAT(10X,5F10.5)
      T1=DPE*2.54/DBL
      T2=DPE*2.54/DBL-1.0
      CL=AA*(T1**CC)*(T2**BB)
      ENDIF
C
      IF (VP.GT.9.0.AND.VP.LT.12.0) THEN
      RATIO=DPE*2.54/DBL
      V1=9.0
      V2=12.0
      TH1=0.0
      CALL BLCALC2('BB1',V1,TH1,DBL9)
      DP9=RATIO*(DBL9/2.54)
      CALL BLCALC2('BB1',V2,TH1,DBL12)
      DP12=RATIO*(DBL12/2.54)
        READ (15,210) TH,V,AA,BB,CC
  210 FORMAT(//,10X,5F10.5)
      T1=RATIO
      T2=RATIO-1.0
      CD9=AA*(T1**CC)*(T2**BB)
        READ (15,211) TH,V,AA,BB,CC
  211 FORMAT(10X,5F10.5)
      T1=RATIO
      T2=RATIO-1.0
      CL9=AA*(T1**CC)*(T2**BB)
        READ (15,220) TH,V,AA,BB,CC
  220 FORMAT(10X,5F10.5)
        T1=RATIO
      T2=RATIO-1.0
      CD12=AA*(T1**CC)*(T2**BB)
        READ (15,221) TH,V,AA,BB,CC
  221 FORMAT(10X,5F10.5)
      T1=RATIO
      T2=RATIO-1.0
      CL12=AA*(T1**CC)*(T2**BB)
      VR=(VP-9.0)/(VP-12.0)
      CD=(CD9-CD12*VR)/(1.0-VR)
      CL=(CL9-CL12*VR)/(1.0-VR)
      ENDIF
C
```

```
      IF (VP.EQ.12.0) THEN
        READ (15,30) TH,V,AA,BB,CC
   30 FORMAT(////,10X,5F10.5)
      T1=DPE*2.54/DBL
      T2=DPE*2.54/DBL-1.0
      CD=AA*(T1**CC)*(T2**BB)
        READ (15,31) TH,V,AA,BB,CC
   31 FORMAT(10X,5F10.5)
      T1=DPE*2.54/DBL
      T2=DPE*2.54/DBL-1.0
      CL=AA*(T1**CC)*(T2**BB)
      ENDIF
C
        ENDIF
C
      IF (THP.EQ.45.0) THEN
        READ (15,40) TH,V,AA,BB,CC
   40 FORMAT(//////,10X,5F10.5)
      T1=DPE*2.54/DBL
      T2=DPE*2.54/DBL-1.0
      CD=AA*(T1**CC)*(T2**BB)
        READ (15,41) TH,V,AA,BB,CC
   41 FORMAT(10X,5F10.5)
      T1=DPE*2.54/DBL
      T2=DPE*2.54/DBL-1.0
      CL=AA*(T1**CC)*(T2**BB)
      ENDIF
C
      RETURN
      END
C
      SUBROUTINE EMPCHK(WSID,DP,DCN,THP,COB,RP,VP,DE,CE)
      IMPLICIT DOUBLE PRECISION (A-H,O-Z)
        DOUBLE PRECISION DCOEF(4,5),LCOEF(4,5)
      CHARACTER*3 WSID
      PI=3.141592
      RTHP=PI*THP/180.0
      AMP=(PI/6.0)*DP*DP*DP*RP
      AMBL=(PI/6.0)*DCN*DCN*DCN*RP
      AMR=AMP/AMBL
        DO 10 I=1,4
      READ (11,5) (DCOEF(I,J),J=1,5)
    5 FORMAT(5F10.5)
   10 CONTINUE
        DO 20 I=1,4
      READ (11,15) (LCOEF(I,J),J=1,5)
   15 FORMAT(5F10.5)
   20 CONTINUE
      IF (WSID.EQ.'BLC') IR=1
      IF (WSID.EQ.'ELC') IR=2
      IF (WSID.EQ.'NEC') IR=3
        IF (WSID.EQ.'LEC') IR=4
C
C.....  COMPUTE EMPRICAL HOLE DIAMETER
C
```

```
      T1=DCOEF(IR,1)
      TT3=DEXP(-DCOEF(IR,3)*(AMR-1.0))
      T3=1.0-TT3
      T4=(VP/COB)**DCOEF(IR,4)
        IF (WSID.EQ.'ELC'.OR.WSID.EQ.'NEC'.OR.WSID.EQ.'LEC') THEN
        T2=DCOS(RTHP)**DCOEF(IR,2)
        ENDIF
      IF (WSID.EQ.'BLC') THEN
      EXPON=DCOEF(IR,2)*(DCOEF(IR,5)-VP)/COB
      T2=DCOS(RTHP)**EXPON
      ENDIF
      DE=T1*T2*T3*T4
C
C.....  COMPUTE EMPRICAL TIP-TO-TIP CRACK LENGTH
C
      T1=LCOEF(IR,1)
      TT3=DEXP(-LCOEF(IR,3)*(AMR-1.0))
      T3=1.0-TT3
      T4=(VP/COB)**LCOEF(IR,4)
        IF (WSID.EQ.'ELC'.OR.WSID.EQ.'NEC'.OR.WSID.EQ.'LEC') THEN
        T2=DCOS(RTHP)**LCOEF(IR,2)
        ENDIF
      IF (WSID.EQ.'BLC') THEN
      EXPON=LCOEF(IR,2)*(LCOEF(IR,5)-VP)/COB
      T2=DCOS(RTHP)**EXPON
      ENDIF
      CE=T1*T2*T3*T4
C
      RETURN
      END
```

APPENDIX C

REQUIRED INPUT FILES FOR PWCRCK.FOR

Input File IMPDAT

---MAT'L---	----C0---	----K----	---RHO---	--GAM0---
--EL.MOD.-	----NU---	--ALFA---	---CPS---	---CPL---
--T.MELT--	--T.VAP--	--H.FUS--	--H.VAP--	
AL				
ALUMINUM	5.380	1.340	2.712	2.130
0.103E+08	0.35	0.240E-04	0.235	0.255
660.0	2450.0	95.0	2450.0	
A1				
2XXX ALUM	5.350	1.340	2.800	2.000
0.106E+08	0.33	0.209E-04	0.212	0.242
640.0	2450.0	85.0	2450.0	
A2				
5XXX ALUM	5.310	1.340	2.670	2.000
0.101E+08	0.33	0.225E-04	0.215	0.245
641.0	2450.0	85.0	2450.0	
A3				
6XXX ALUM	5.380	1.340	2.700	2.000
0.100E+08	0.33	0.233E-04	0.212	0.242
652.0	2450.0	85.0	2450.0	
A4				
7XXX ALUM	5.290	1.340	2.810	2.000
0.103E+08	0.33	0.221E-04	0.217	0.245
636.0	2450.0	85.0	2450.0	
BE				
BERYLLIUM	7.975	1.124	1.820	1.160
0.419E+08	0.08	0.140E-04	0.570	0.832
1281.0	2884.0	260.0	8195.0	
CD				
CADMIUM	2.307	1.640	8.640	2.270
0.672E+07	0.33	0.343E-04	0.058	0.063
321.0	765.0	13.5	212.0	
CU				
COPPER	3.940	1.489	8.930	2.000
0.190E+08	0.34	0.170E-04	0.097	0.114

```
    1083.0     2590.0       49.0     1150.0
-------------------------------------------------
EP
EPOXY           3.020      1.520      1.180      0.800
 0.650E+06       0.50 0.500E-04      0.250      0.285
     350.0       -1.0       -1.0       -1.0
-------------------------------------------------
FE
IRON            4.580      1.490      7.870      1.570
 0.290E+08       0.30 0.120E-04      0.120      0.150
    1539.0     3035.0       65.0     1591.0
-------------------------------------------------
PB
LEAD            2.030      1.470     11.340      2.770
 0.200E+07       0.45 0.293E-04      0.031      0.036
     327.0     1740.0        6.0      210.0
-------------------------------------------------
LX
LEXAN           2.750      1.480      1.180      0.860
 0.345E+06       0.50 0.650E-04      0.290      0.315
     225.0       -1.0       -1.0       -1.0
-------------------------------------------------
MO
MOLYBDENUM      5.173      1.220     10.200      1.520
 0.460E+08       0.31 0.061E-04      0.079      0.104
    2610.0     5555.0       70.0     1242.0
-------------------------------------------------
NI
NICKEL          4.667      1.530      8.860      1.800
 0.330E+08       0.30 0.143E-04      0.130      0.157
    1454.0     2865.0       74.0     1523.0
-------------------------------------------------
PT
PLATINUM        3.680      1.500     21.370      2.940
 0.277E+08       0.39 0.110E-04      0.037      0.042
    1769.0     4349.0       26.0      632.0
-------------------------------------------------
S1
304 STEEL       4.590      1.550      7.910      1.670
 0.284E+08       0.28 0.112E-04      0.110      0.125
    1425.0     3035.0       65.0     1590.0
-------------------------------------------------
S2
430 STEEL       4.680      1.550      7.830      1.670
 0.299E+08       0.29 0.104E-04      0.110      0.125
    1470.0     3035.0       65.0     1590.0
-------------------------------------------------
S3
4340 STEEL      4.570      1.550      7.830      1.670
 0.290E+08       0.30 0.112E-04      0.110      0.125
    1510.0     3070.0       65.0     1590.0
-------------------------------------------------
TA
TANTALUM        3.374      1.201     16.650      1.690
 0.260E+08       0.35 0.065E-04      0.033      0.039
```

```
    2996.0     5425.0       38.0     1007.0
-------------------------------------------------
SN
TIN              2.560      1.520      7.280      1.850
 0.603E+07        0.33 0.269E-04      0.058      0.062
     235.0     2450.0       14.0      580.0
-------------------------------------------------
TI
TITANIUM         4.786      1.049      4.512      1.100
 0.180E+08        0.30 0.100E-04      0.150      0.167
    1676.0     3260.0       99.0     2182.0
-------------------------------------------------
W
TUNGSTEN         4.150      1.237     19.170      1.480
 0.590E+08        0.30 0.040E-04      0.035      0.046
    3410.0     5900.0       53.0     1054.0
-------------------------------------------------
ZN
ZINC             3.042      1.500      7.140      2.150
 0.108E+08        0.33 0.274E-04      0.100      0.115
     420.0      907.0       25.0      420.0
-------------------------------------------------
AU
GOLD             3.060      1.570     19.240      3.100
 0.124E+08        0.42 0.161E-04      0.034      0.038
    1063.0     2960.0       16.0      413.0
-------------------------------------------------
AG
SILVER           3.230      2.500     10.490      2.500
 0.120E+08        0.37 0.211E-04      0.062      0.071
     961.0     2210.0       25.0      554.0
-------------------------------------------------
MG
MAGNESIUM        4.490      1.240      1.740      1.500
 0.640E+07        0.29 0.300E-04      0.295      0.336
     650.0     1110.0       88.0     1326.0
-------------------------------------------------
XX
-------------------------------------------------
```

Input File GPARAM

```
ALALALM
LEC
     00.00      358.0      0.556
      2.00       0.50
      0.90
      0.90
 2
 0.20
  500
  0.0 30.0 1.00 40.0 0.60  5.0
  2000 200N 20BB
```

Input File COEF

```
 2.584     2.219     1.427     1.336
 1.385     1.189     0.765     0.716
 0.636     0.503     0.418     0.356
 1.233     0.975     0.810     0.691
   0.0      45.0      65.0
```

Input File OBLDATA

```
1.47255   2.02818
    .00059   5.09485   2.15233
```

Input File WALDAT

```
BLC
BASELINE LAB CYLINDER
      0.13      0.48     11.43      5.72AA0
ELC
ENHANCED LAB CYLINDER
      0.20      0.48     11.43      5.72BB1
NEC
ISSA NODE END-CONE
      0.13      0.58     22.15     18.34AA0
LEC
ISSA LAB END-CONE
      0.19      0.48     22.15     18.34AA0
XXX
GENERIC DUAL-WALL SYS
      0.16      0.48     11.43      5.72AA0
EOF
```

Input File REGDAT

```
 8.61      4.48      0.66     -0.97      9.2     BLC-DH
19.90      0.41      1.17      1.03      0.0     ELC-DH
 7.27      1.31      4.11      0.00      0.0     NEC-DH
 8.14      1.19      0.83    -0.014      0.0     LEC-DH
15.30      4.88      0.38     -0.42      8.1     BLC-LTT
22.10     -0.69      3.44      1.14      0.0     ELC-LTT
 9.77      0.97      4.29      0.00      0.0     NEC-LTT
22.60      2.72      1.07     0.078      0.0     LEC-LTT
```

Input File CDCLNEC

```
  CD     .00000   2.46702   1.00456  -3.53041
  CL     .00000   3.34527   1.00456  -3.53041
  CD   45.00000    .36587    .53151   1.58059
  CL   45.00000    .55978    .53151   1.58059
```

Input File CDCLELC

```
CD     .00000    6.00000   10.00995     .81186    -.02083
CL     .00000    6.00000   11.75406     .93593   -3.08149
CD     .00000    9.00000   49.47987    1.13548   -1.06262
CL     .00000    9.00000   18.93908     .91881   -3.17900
CD     .00000   12.00000   90.59812    1.19686   -1.37908
CL     .00000   12.00000   21.73896     .89736   -2.69372
CD   45.00000    6.00000  117.77013   49.97815
CL   45.00000    6.00000   23.52283    1.00885   -4.60904
```

Input File CDCLBLC

```
CD     .00000    6.00000    1.09936     .00364    7.06798  -3.50012
CD     .00000    6.00000    1.72081   -4.21527    4.26737
CL     .00000    6.00000    2.99842    1.13434   -1.73170
CD     .00000    9.00000   21.95076    -.21550
CD     .00000    9.00000    4.52326   -9.48852    5.97285
CL     .00000    9.00000    2.48254    1.11739   -1.70276
CD     .00000   12.00000   16.85333     .83678
CD     .00000   12.00000    3.80878  -11.33089    9.05710
CL     .00000   12.00000    3.17268    1.38218   -2.17896
CD   45.00000    6.00000     .34570     .80399    1.62360
CL   45.00000    6.00000     .47288     .79811    2.36358
```

Input File CDCLLEC

```
CD     .00000    6.00000    1.05951    1.15394   -1.81505
CL     .00000    6.00000    3.23949    1.11675   -1.92639
CD     .00000    9.00000     .27237     .86739    1.97813
CL     .00000    9.00000    1.88837     .99889    -.30810
CD     .00000   12.00000     .22726     .82193    1.83412
CL     .00000   12.00000    1.87153     .98289    -.57366
CD   45.00000    6.00000    1.17701    1.14479   -1.32090
CL   45.00000    6.00000    2.36591    1.13197   -1.63608
```

APPENDIX D

SAMPLE OUTPUT FILE FOR PWCRCK.FOR

```
  .0-DEG IMPACT OF A ALUMINUM   PROJ ON A DUAL-WALL SYSTEM WITH A
ALUMINUM   BUMPER, A MLI-BLNKT  INNER BUMPER, AND A ALUMINUM   PRESS WALL

BL DIAM (  .7603 CM) < PROJ DIAM ( 1.4122 CM)
    ---> PRESS WALL PERFORATION LIKELY

PROJECTILE PROPERTIES ...
   MAT = ALUMINUM
   CO  =  5.380 KM/S
   K   =  1.340
   RHO =  2.712 GM/CU.CM.
   DP  =  1.412 CM
   MP  =  4.000 GMS
   VP  = 12.000 KM/S

OUTER BUMPER PROPERTIES ...
   MAT = ALUMINUM
   CO  =  5.380 KM/S
   K   =  1.340
   RHO =  2.712 GM/CU.CM.
   TS  =   .190 CM
   DMN =  3.116 CM
   DMX =  3.116 CM
   EPS1=  2.000     (INITIAL VALUE)
   MB  =  7.857 GMS (INITIAL VALUE)
   S   = 22.150 CM

PROJECTILE AND BUMPER SHOCK LOADING RESPONSE AND RELEASE CALCULATIONS

PROJECTILE IMPACT VELOCITY .... VP =  12.000 KM/S
PROJ MATL PARTICLE VELOCITY ... UP =   6.000 KM/S
PROJ MATL SHOCK WAVE SPEED .... US =  13.420 KM/S
HUGONIOT IMPACT PRESSURE ...... PH = 218.370 GPA
BMPR MATL PARTICLE VELOCITY ... UP =   6.000 KM/S
BMPR MATL SHOCK WAVE SPEED .... US =  13.420 KM/S
HUGONIOT IMPACT PRESSURE ...... PH = 218.370 GPA

PARAMETERS REQUIRED FOR CALCULATING PROJECTILE MATERIAL RESPONSE AND
RELEASE FROM SHOCKED STATE USING THE MIE-GRUNEISEN E-O-S:
   ELASTIC MODULUS ............. E    = .7102E+11 N/SQ.M.
   POISSON RATIO ............... NU   =      .350
   BULK MODULUS ................ K    = .7891E+11 N/SQ.M.
   LIN. COEF. OF THERM. EXP. ... ALFA = .2400E-04 /DEG-C
   SP HEAT (SOLID) ............. CPS  =      .235 CAL/GM/DEG-C
```

```
   SP HEAT (LIQUID) ..... CPL  =      .255 CAL/GM/DEG-C
   HUGON IMP PRESS (PA,MBAR) ... PH   = .2184E+12,2.184
   SP VOL AT REST ..... VO   =      .369 CU.CM./GM
   SP VOL AT IMPACT ..... V1   =      .204 CU.CM./GM
   AMB M-GRUN COEF (CAL,INP) ... GAM0 =     2.129,2.130
   MELT TEMPERATURE ..... TM   =    660.00 DEG-C
   VAPOR TEMPERATURE ..... TV   =   2450.00 DEG-C
   HEAT OF FUSION ..... HF   =     95.00 CAL/GM
   HEAT OF VAPORIZATION ..... HV   =   2450.00 CAL/GM

RELEASE OF SHOCKED PROJECTILE MATERIAL ...

SPECIFIC VOL AFTER RELEASE ..... VF = .487 CU.CM./GM
ENERGY DUE TO DEB CLD IMPACT ....  .1800E+08 JOULES/KG
ENERGY RECOVERED BY RELEASE .....  .1514E+08 JOULES/KG
WASTE HEAT GENERATED .....  .2862E+07 JOULES/KG
ENERGY REQ, INCIPIENT MELT ...  .6492E+06 JOULES/KG
ENERGY REQ, COMPLETE MELT ....  .1047E+07 JOULES/KG
EXCESS ENERGY AVAILABLE .....  .1815E+07 JOULES/KG
RESIDUAL MATERIAL TEMP .....   2360.310 DEG-C

PERCENT SHKD AND REL PRESS WALL MATERIAL ...
   IN SOLID STATE ...    .00%
   IN MOLTEN FORM ... 100.00%
   IN VAPOR FORM ....    .00%

PARAMETERS REQUIRED FOR CALCULATING BUMPER MATERIAL RESPONSE AND
RELEASE FROM SHOCKED STATE USING THE MIE-GRUNEISEN E-O-S:
   ELASTIC MODULUS ..... E    = .7102E+11 N/SQ.M.
   POISSON RATIO ..... NU   =      .350
   BULK MODULUS ..... K    = .7891E+11 N/SQ.M.
   LIN. COEF. OF THERM. EXP. ... ALFA = .2400E-04 /DEG-C
   SP HEAT (SOLID) ..... CPS  =      .235 CAL/GM/DEG-C
   SP HEAT (LIQUID) ..... CPL  =      .255 CAL/GM/DEG-C
   HUGON IMP PRESS (PA,MBAR) ... PH   = .2184E+12,2.184
   SP VOL AT REST ..... VO   =      .369 CU.CM./GM
   SP VOL AT IMPACT ..... V1   =      .204 CU.CM./GM
   AMB M-GRUN COEF (CAL,INP) ... GAM0 =     2.129,2.130
   MELT TEMPERATURE ..... TM   =    660.00 DEG-C
   VAPOR TEMPERATURE ..... TV   =   2450.00 DEG-C
   HEAT OF FUSION ..... HF   =     95.00 CAL/GM
   HEAT OF VAPORIZATION ..... HV   =   2450.00 CAL/GM

RELEASE OF SHOCKED BUMPER MATERIAL ...

SPECIFIC VOL AFTER RELEASE ..... VF = .487 CU.CM./GM
ENERGY DUE TO DEB CLD IMPACT ....  .1800E+08 JOULES/KG
ENERGY RECOVERED BY RELEASE .....  .1514E+08 JOULES/KG
WASTE HEAT GENERATED .....  .2862E+07 JOULES/KG
ENERGY REQ, INCIPIENT MELT ...  .6492E+06 JOULES/KG
ENERGY REQ, COMPLETE MELT ....  .1047E+07 JOULES/KG
EXCESS ENERGY AVAILABLE .....  .1815E+07 JOULES/KG
RESIDUAL MATERIAL TEMP .....   2360.310 DEG-C

PERCENT SHKD AND REL PRESS WALL MATERIAL ...
```

```
   IN SOLID STATE ...     .00%
   IN MOLTEN FORM ... 100.00%
   IN VAPOR FORM ....     .00%

TOTAL KINETIC ENERGY DUE TO INITIAL IMPACT ... .2880E+06 JOULES
TOTAL KINETIC ENERGY LOST TO SH HTNG & REL ... .3393E+05 JOULES
FRACTION OF INITIAL K.E. LOST ...  .118

PRIMARY DEBRIS CLOUD CHARACTERISTICS ...
   PROJECTILE COMPONENT ...
     MATERIAL MASS .............    3.99957 GMS
     LEADING EDGE VELOCITY .....   11.68069 KM/S
     CENTER-OF-MASS VELOCITY ...    6.35269 KM/S
     EXPANSION VELOCITY ........    5.32800 KM/S
     1/2-ANGLE SPREAD ..........   39.98655 DEG
     DEB CLD RAD @ INN-BMPR ....    1.49052 CM
     INN-BMPR FOOTPRINT RAD ....    3.19544 CM
   BUMPER COMPONENT .......
     MATERIAL MASS (FIN VAL) ...    3.75804 GMS
       EPS1 (FIN VAL) ...     .95659
     LEADING EDGE VELOCITY .....   11.68069 KM/S
     CENTER-OF-MASS VELOCITY ...    6.01026 KM/S
     EXPANSION VELOCITY ........    5.67043 KM/S
     1/2-ANGLE SPREAD ..........   43.33356 DEG
     DEB CLD RAD @ INN-BMPR ....    1.55054 CM
     INN-BMPR FOOTPRINT RAD ....    3.59458 CM

INNER BUMPER PROPERTIES ...
   MAT = MLI-BLNKT
   RHO =   .033 GM/SQ.CM.
   DH  =  3.116 CM
   EPS2=   .500     (INITIAL VALUE)
   MIB =   .126 GMS (INITIAL VALUE)
   S2  = 18.340 CM

SECONDARY DEBRIS CLOUD DELIVERS LOAD TO PRESSURE WALL

SECONDARY DEBRIS CLOUD CHARACTERISTICS ...
   PROJECTILE COMPONENT ...
     MATERIAL MASS .............    3.99957 GMS
     LEADING EDGE VELOCITY .....   11.59687 KM/S
     CENTER-OF-MASS VELOCITY ...    6.16778 KM/S
     EXPANSION VELOCITY ........    5.42909 KM/S
     1/2-ANGLE SPREAD ..........   41.35530 DEG
     DEB CLD RAD @ PR-WALL .....    7.29664 CM
     PR WALL FOOTPRINT RAD .....   16.14347 CM
   BUMPER COMPONENT .......
     MATERIAL MASS (TOTAL) .....    3.88384 GMS
       OUTR-BMPR COMPONENT .....    3.75804 GMS
       INNR-BMPR COMPONENT .....     .12580 GMS (FIN VAL)
         EPS2 (FINAL VALUE) ....     .50000
     LEADING EDGE VELOCITY .....   11.59687 KM/S
     CENTER-OF-MASS VELOCITY ...    6.00601 KM/S
     EXPANSION VELOCITY ........    5.59086 KM/S
     1/2-ANGLE SPREAD ..........   42.94982 DEG
```

```
      DEB CLD RAD @ PR-WALL .....     7.43215 CM
      PR WALL FOOTPRINT RAD .....    17.07231 CM

F2 =    .235 >=    .200 = F2,CRIT
   ---> PETALING WILL LIKELY OCCUR

TIME-PHASING INFORMATION FOR PRESSURE WALL DEBRIS CLOUD IMPACT ...
   BEGINNING OF PROJ COMP IMPACT EVENT .....  .000000000 SECS
   TIME OF PEAK PROJ COMP PRESSURE .........  .000023660 SECS
   DURATION OF PROJ COMP IMPACT EVENT ......  .000395108 SECS
   COMPLETION OF PROJ COMP IMPACT EVENT ....  .000395108 SECS

   DELAY BET BEGIN PR & BEGIN BPR EVENTS ...  .000030536 SECS

   BEGINNING OF BMPR COMP IMPACT EVENT .....  .000030536 SECS
   TIME OF PEAK BMPR COMP PRESSURE .........  .000055285 SECS
   DURATION OF BMPR COMP IMPACT EVENT ......  .000716104 SECS
   COMPLETION OF BMPR COMP IMPACT EVENT ....  .000746640 SECS

PRESSURE DISTRIBUTION COEFFICIENTS ...
   PROJ COMP ...    .351E+07 N/SQ.M.
   BMPR COMP ...    .340E+07 N/SQ.M.

PRESSURE WALL PROPERTIES ...
   MAT  = ALUMINUM
   EMOD =    .710E+11 N/SQ.M.
   NU   =    .350
   SMOD =    .263E+11 N/SQ.M.
   S    = 22.150 CM
   RHO  =  2.712 GM/CU.CM.
   RAD  = 30.000 CM
   ETA  =    .000
   EPSF =  1.000
   SIGY =  358.0 MPA
   SIF  = 40.000 MPA-/M
   SIFA = 24.000 MPA-/M
   MEXP =  5.000
   TW   =    .480 CM
   CO   =  5.117 KM/S
   CL   =  6.483 KM/S
   CT   =  3.114 KM/S
   CR   =  2.909 KM/S

   EPSF-FINAL =    .700

TIME OF CRACK INITIATION ...  .000717355 SECS (< TM =  .006900005 S)

PLATE CTR VELOCITY AT T=TC ...    .327 KM/S

PRESSURE WALL CRACKING CHARACTERISTICS ...
   MAXIMUM TIP-TO-TIP CRACK LENGTH ... 16.404 CM

RESULTS OF PETAL DEFORMATION CALCULATIONS ...

TIP MASS PARAMETERS ...
```

```
      MP  =    .400E-02 KG
      MBT =    .388E-02 KG
      GC  =    .263E-02 KG
      G   =    .167E-02 KG

EQUIVALENT BEAM PARAMETERS ...
      B-AVG = 6.2978 CM
      H-AVG =  .1022 CM
      M-YLD =  .1425E+02 N-M
      MPL   =  .2815E+00 KG/SQM
      ALFAC =  .9870E+01
      ALFA  =  6.283

ITERATION PARAMETERS ...
      ZMAX   =  .6119E+01
      NZPTS  =   120
      NITPTS =   200
      DZ (ND) =  .5099E-01

RESULTS OF PETAL DEFORMATION CALCULATIONS ...

   STAR PATTERN APPROXIMATION ...
     EQUIVALENT SNGL HOLE DIAMETER  =    5.83088 CM
     MIN DISTANCE TO PETAL TANGENT  =    3.63601 CM
     WIDTH OF FLAT PORTION OF PETAL =     .00000 CM
     MAX DEPTH OF PETAL DEFORMATION =     .80387 CM

PREDICTIONS OF EMPIRICALLY-BASED REGRESSION EQUATIONS ...
   EQUIVALENT HOLE DIAMETER ......    7.95865 CM
   MAX TIP-TO-TIP CRACK LENGTH ...   23.98550 CM

 COMPARISON OF EMPIRICAL VALUES TO MODEL PREDICTIONS ...
   DH,EXP/DH,MODEL .....    1.36491
   LTT,EXP/LTT,MODEL ...    1.46217
```

APPENDIX E

FORTRAN PROGRAM OBLDATA.FOR

```
$DEBUG
      PROGRAM OBLDATA
      IMPLICIT DOUBLE PRECISION (A-H,O-Z)
      DOUBLE PRECISION KSB,KSP,KB,KP,KT,NUB,NUP,NUT,MB,MP
      DOUBLE PRECISION MB1,MB2,MBE,M1,M2,MBR,MR
      DOUBLE PRECISION PARAM(3,27,6)
      CHARACTER*2 BID,PID,TID,BIDCHK,PIDCHK,TIDCHK
      CHARACTER*3 IB
      CHARACTER*10 BMAT,PMAT,TMAT,IBMAT
C
      OPEN(1,FILE='IMPDAT')
      OPEN(2,FILE='OBLOUT')
      OPEN(3,FILE='OBLDATA')
      OPEN(4,FILE='GPRMOBL')
C
      PI=3.141592
C
C.....  READ PROJECTILE, BUMPER, AND PRESSURE WALL MATERIAL PROPERTIES.
C.....  THE PARAMETERS MUST BE IN THE FOLLOWING UNITS:
C.....
C.....          BID,PID,TID,IB ......... MATERIAL ID CODES
C.....              NOTE: IB = AA0 ..... MLI INNER BUMPER
C.....                    IB = BB1 ..... ENHANCED US LAB CONFIGURATION
C.....                    IB = BB2 ..... ENHANCED JEM WALL CONFIGURATION
C.....          BMAT,PMAT,TMAT,IBMAT ... MATERIALS
C.....          COB,COP,COT.............. BULK SOUND SPEED, KM/S
C.....          RB,RP,RT ................ AMBIENT MATL DENSITY, GM/CUCM
C.....          RIBA .................... INNER BMPR AREAL DNSTY,GM/SQCM
C.....          KB,KP,KT ................ SLOPE OF US-UP LINE
C.....          EB,EP,ET................. ELASTIC MODULUS, LBS/SQ.IN.
C.....          ALFAB,ALFAP,ALFAT ...... LINEAR COEFF OF TERMAL EXP, 1/C
C.....          CPSB,CPSP,CPST ......... SPECIFIC HEAT (SOLID), CAL/GM-C
C.....          CPLB,CPLP,CPLT ......... SPECIFIC HEAT (LIQD), CAL/GM/C
C.....          TMB,TMP,TMT ............ MELT TEMPERATURE, C
C.....          TVB,TVP,TVT ............ VAPORIZATION TEMPERATURE, C
C.....          HFB,HFP,HFT ............ LATENT HEAT OF FUSION, CAL/GM
C.....          HVB,HVP,HVT ............ LATENT HEAT OF VPRZTN, CAL/GM
C
      READ(4,5) PID,BID,TID
    5 FORMAT(3A2)
      READ(4,109) IB
  109 FORMAT(A3)
      IF (IB.EQ.'AA0') THEN
      IBMAT='MLI-BLNKT'
      RIBA=0.033
```

```
      ENDIF
      IF (IB.EQ.'BB1'.OR.IB.EQ.'BB2') THEN
      IBMAT='6K/6N'
      RIBA=0.80
      ENDIF
C
      REWIND 1
      READ(1,4)
    4 FORMAT(////)
C
   99 READ(1,1) PIDCHK
    1 FORMAT(A2)
      IF (PID.EQ.PIDCHK) THEN
      READ(1,10) PMAT,COP,KP,RP,GPI
   10 FORMAT(A10,4F10.5)
      READ(1,100) EP,NUP,ALPHAP,CPSP,CPLP
  100 FORMAT(2(E10.3,F10.5),F10.5)
      READ(1,102) TMP,TVP,HFP,HVP
  102 FORMAT(4F10.5)
      ENDIF
      IF (PID.NE.PIDCHK) THEN
      IF (PIDCHK.EQ.'XX') THEN
      WRITE (*,17)
   17 FORMAT(' PROJECTILE MATERIAL NOT FOUND IN MATERIAL LIBRARY.',/,
     $' PLEASE CHECK DEBRIS CLOUD MATERIAL ID CODE AND BEGIN AGAIN.')
      STOP
      ENDIF
      IF (PIDCHK.NE.'XX') THEN
      READ (1,2)
    2 FORMAT(///)
      GOTO 99
      ENDIF
      ENDIF
C
      REWIND 1
      READ(1,4)
  999 READ(1,1) BIDCHK
      IF (BID.EQ.BIDCHK) THEN
      READ(1,10) BMAT,COB,KB,RB,GBI
      READ(1,100) EB,NUB,ALPHAB,CPSB,CPLB
      READ(1,102) TMB,TVB,HFB,HVB
      ENDIF
      IF (BID.NE.BIDCHK) THEN
      IF (BIDCHK.EQ.'XX') THEN
      WRITE (*,117)
  117 FORMAT(' BUMPER MATERIAL NOT FOUND IN MATERIAL LIBRARY.',/,' PLEAS
     $E CHECK BUMPER MATERIAL ID CODE AND BEGIN AGAIN.')
      STOP
      ENDIF
      IF (BIDCHK.NE.'XX') THEN
      READ (1,2)
      GOTO 999
      ENDIF
      ENDIF
C
```

```
      REWIND 1
      READ(1,4)
 9999 READ(1,1) TIDCHK
      IF (TID.EQ.TIDCHK) THEN
      READ(1,10) TMAT,COT,KT,RT,GTI
      READ(1,100) ET,NUT,ALPHAT,CPST,CPLT
      READ(1,102) TMT,TVT,HFT,HVT
      ENDIF
      IF (TID.NE.TIDCHK) THEN
      IF (TIDCHK.EQ.'XX') THEN
      WRITE (*,1117)
 1117 FORMAT(' PRESSURE WALL MATERIAL NOT FOUND IN MATERIAL LIBRARY.',/
     $,' PLEASE CHECK PRESSURE WALL MATERIAL ID CODE AND BEGIN AGAIN.')
      STOP
      ENDIF
      IF (TIDCHK.NE.'XX') THEN
      READ (1,2)
      GOTO 9999
      ENDIF
      ENDIF
C
C.....  READ PROJECTILE, IMPACT, AND GEOMETRIC PARAMETERS
C.....
C.....          DPE ... PROJECTILE DIAMETER, IN
C.....          THP ... TRAJECTORY OBLIQUITY,DEG
C.....          TS .... BUMPER THICKNESS, CM
C
      WRITE (*,1112)
 1112 FORMAT(' ENTER DP (INCHES,F10.5), THP (DEG,F10.5), AND TS (CM,F10.
     $5) ...')
      READ (*,113) DPE,THP,TS
  113 FORMAT(F10.5,/,F10.5,/,F10.5)
C
      EPS1=1.0
      IF (THP.GT.60.0) THEN
      WRITE (2,112) THP
  112 FORMAT(/,' INPUT IMPACT OBLIQUITY (',F4.1,'-DEG) > 60-DEG.  PROGRA
     $M STOP.')
      WRITE (*,112) THP
      STOP
      ENDIF
C
      IF (DPE.GT.0.75.OR.DPE.LT.0.25) THEN
      WRITE (2,111) DPE
  111 FORMAT(/,' INPUT PROJECTILE DIAMETER (',F5.3,' IN) OUTSIDE ALLOWAB
     $LE',/,' VALUE RANGE (0.25 TO 0.75 IN). PROGRAM STOP.')
      WRITE (*,111) DPE
      STOP
      ENDIF
C
      TS1=TS/0.13+0.01
      TS2=TS/0.16+0.01
      TS3=TS/0.20+0.01
      CHK1=DFLOAT(DINT((DFLOAT(DINT(TS1*100.0))/100.0)*10.0))/10.0
      CHK2=DFLOAT(DINT((DFLOAT(DINT(TS2*100.0))/100.0)*10.0))/10.0
```

```
      CHK3=DFLOAT(DINT((DFLOAT(DINT(TS3*100.0))/100.0)*10.0))/10.0
      IF (CHK1.EQ.1.0) THEN
      OPEN(5,FILE='PRM30050')
      OPEN(6,FILE='PRM45050')
      OPEN(7,FILE='PRM60050')
      ENDIF
      IF (CHK2.EQ.1.0) THEN
      OPEN(5,FILE='PRM30063')
      OPEN(6,FILE='PRM45063')
      OPEN(7,FILE='PRM60063')
      ENDIF
      IF (CHK3.EQ.1.0) THEN
      OPEN(5,FILE='PRM30080')
      OPEN(6,FILE='PRM45080')
      OPEN(7,FILE='PRM60080')
      ENDIF
C
      DP=DPE*2.54
C
C.....  READ PROJECTILE IMPACT VELOCITY IN KM/S
C
      WRITE(*,29)
   29 FORMAT(' INPUT PROJECTILE IMPACT VELOCITY IN KM/SEC (F5.2) AND HIT
     $ ENTER')
      READ(*,30) VP
   30 FORMAT(F5.2)
C
      WRITE(2,40) THP,PMAT,BMAT,IBMAT,TMAT
   40 FORMAT(F4.1,'-DEG IMPACT OF A ',A10,' PROJ ON A DUAL-WALL SYSTEM W
     $ITH A',/,A10,' BUMPER, A ',A10,' INNER BUMPER, AND A ',A10,' PRESS
     $ WALL')
      RTHP=THP*PI/180.0
C
      EB=EB*68947.0
      BETAB=3.0*ALPHAB
      IF (NUB.LT.0.5) THEN
      KSB=EB/3.0/(1.0-2.0*NUB)
      COBC=DSQRT((KSB/10.0)/(RB*1000.0))/1000.0
      CBC=DSQRT((EB/10.0)/(RB*1000.0))/1000.0
      ENDIF
      IF (NUB.EQ.0.5) THEN
      KSB=-1.0
      COBC=-1.0
      ENDIF
      IF (NUB.LT.0.5) GB=2.3885E-08*KSB*BETAB/CPSB/RB
      IF (NUB.EQ.0.5) GB=GBI
      GRB=GB*RB*1000.0
C
      EP=EP*68947.0
      BETAP=3.0*ALPHAP
      IF (NUP.LT.0.5) THEN
      KSP=EP/3.0/(1.0-2.0*NUP)
      COPC=DSQRT((KSP/10.0)/(RP*1000.0))/1000.0
      CPC=DSQRT((EB/10.0)/(RB*1000.0))/1000.0
      ENDIF
```

```
      IF (NUP.EQ.0.5) THEN
      KSP=-1.0
      COPC=-1.0
      ENDIF
      IF (NUP.LT.0.5) GP=2.3885E-08*KSP*BETAP/CPSP/RP
      IF (NUP.EQ.0.5) GP=GPI
      GRP=GP*RP*1000.0
C
      C=CBC
C
C.....  CALCULATE PROJECTILE AND BUMPER HOLE-OUT MASSES (IN KG)
C
      MP=(PI/6.0)*(DP/100.0)*(DP/100.0)*(DP/100.0)*(RP*1000.0)
C
      DMN=DN(VP,C,TS,DP,RTHP)
      DMX=DX(VP,C,TS,DP,RTHP)
      MB=EPS1*(PI/4.0)*(DMN/100.0)*(DMX/100.0)*(TS/100.0)*(RB*1000.0)
C
      WRITE (2,45) PMAT,COP,KP,RP,DP,MP*1000.0,VP,BMAT,COT,KT,RT,TS,
     $                DMN,DMX,EPS1,MB*1000.0
   45 FORMAT(/,'PROJECTILE PROPERTIES ...',/,3X,'MAT = ',A10,/,3X,
     $'CO  = ',F6.3,' KM/S',/,3X,'K   = ',F6.3,/,3X,'RHO = ',F6.3,' GM/C
     $U.CM.',/,3X,'DP  = ',F6.3,' CM',/,3X,'MP  = ',F6.3,' GMS',/,3X,
     $'VP  = ',F6.3,' KM/S',//,'OUTER BUMPER PROPERTIES ...',/,3X,
     $'MAT = ',A10,/,3X,'CO  = ',F6.3,' KM/S',/,3X,'K   = ',F6.3,/,3X,
     $'RHO = ',F6.3,' GM/CU.CM.',/,3X,'TS  = ',F6.3,' CM',/,3X,'DMN = ',
     $F6.3,' CM',/,3X,'DMX = ',F6.3,' CM',/,3X,'EPS1= ',F6.3,4X,' (INITI
     $AL VALUE)',/,3X,'MB  = ',F6.3,' GMS (INITIAL VALUE)')
C
C.....  CALCULATE PARTICLE AND SHOCK WAVE VELOCITIES AND HUGONIOT
C.....  PRESSURE DUE TO PROJECTILE IMPACT
C
      V=VP
      IF (BMAT.EQ.PMAT) GOTO 35
      A=KP-KB*(RB/RP)
      B=2.0*KP*V+COP+COB*(RB/RP)
      C=COP*V+KP*V*V
      D=B*B-4.0*A*C
      UBP=(B-SQRT(D))/(2.0*A)
      GOTO 38
   35   UBP=V/2.0
   38   UPP=V-UBP
      UBS=COB+KB*UBP
      UPS=COP+KP*UPP
      PP=RP*UPS*UPP
      PB=RB*UBS*UBP
C
C.....  PROJECTILE AND BUMPER SHOCK LOADING RESPONSE AND RELEASE
C.....  CALCULATION PHASE
C
      WRITE(*,5080)
 5080 FORMAT(/,' BEGINNING PROJECTILE AND BUMPER SHOCK LOADING RESPONSE
     $AND',/,' RELEASE CALCULATIONS')
      WRITE(2,509)
  509 FORMAT(/,'**** PROJECTILE AND BUMPER SHOCK LOADING RESPONSE AND RE
```

```
     $LEASE CALCULATIONS ****')
      WRITE(2,6011) VP,UPP,UPS,PP,UBP,UBS,PB
 6011 FORMAT(/,'PROJECTILE IMPACT VELOCITY .... VP = ',F7.3,' KM/S',/,
     $'PROJ MATL PARTICLE VELOCITY ... UP = ',F7.3,' KM/S',/,'PROJ MATL
     $SHOCK WAVE SPEED .... US = ',F7.3,' KM/S',/,'HUGONIOT IMPACT PRESS
     $URE ..... PH = ',F7.3,' GPA',/,'BMPR MATL PARTICLE VELOCITY ... U
     $P = ',F7.3,' KM/S',/,'BMPR MATL SHOCK WAVE SPEED .... US = ',F7.3,
     $' KM/S',/,'HUGONIOT IMPACT PRESSURE ..... PH = ',F7.3,' GPA')
C
      VPO=1.0/RP
      VP1=RP*UPS/(UPS-UPP)
      VP1=1.0/VP1
C
      PH=PP*1.0E09
C
      WRITE(2,705) EP/10.0,NUP,KSP/10.0,ALPHAP,CPSP,CPLP
  705 FORMAT(/,'PARAMETERS REQUIRED FOR CALCULATING PROJECTILE MATERIAL
     $RESPONSE AND',/,'RELEASE FROM SHOCKED STATE USING THE MIE-GRUNEISE
     $N E-O-S:',/,3X,'ELASTIC MODULUS ..... E    =',E10.4,' N/SQ
     $.M.',/,3X,'POISSON RATIO ..... NU   =',F10.3,/,3X,'BULK
     $MODULUS ..... K    =',E10.4,' N/SQ.M.',/,3X,'LIN. COEF.
     $ OF THERM. EXP. ... ALFA =',E10.4,' /DEG-C',/,3X,'SP HEAT (SOLID)
     $..... CPS  =',F10.3,' CAL/GM/DEG-C',/,3X,'SP HEAT (LIQUID)
     $ ..... CPL  =',F10.3,' CAL/GM/DEG-C')
      PHMB=PH/100.0E+09
      WRITE(2,800) PH,PHMB,VPO,VP1,GP,GPI
  800 FORMAT(3X,'HUGON IMP PRESS (PA,MBAR) ... PH   =',E10.4,',',F5.3,/,
     $3X,'SP VOL AT REST ..... V0   =',F10.3,' CU.CM./GM',/,3X,
     $'SP VOL AT IMPACT ..... V1   =',F10.3,' CU.CM./GM',/,3X,'AM
     $B M-GRUN COEF (CAL,INP) ... GAM0 =',F10.3,',',F5.3)
      WRITE(2,805) TMP,TVP,HFP,HVP
  805 FORMAT(3X,'MELT TEMPERATURE ..... TM   =',F10.2,' DEG-C',/,
     $3X,'VAPOR TEMPERATURE ..... TV   =',F10.2,' DEG-C',/,3X,'HEA
     $T OF FUSION ..... HF   =',F10.2,' CAL/GM',/,3X,'HEAT OF V
     $APORIZATION ..... HV   =',F10.2,' CAL/GM')
C
C.....  CALCULATE RELEASE OF PROJECTILE MATERIAL UP UNTIL ZERO PRESSURE
C.....  IS REACHED
C
      WRITE (2,1701)
 1701 FORMAT(/,'RELEASE OF SHOCKED PROJECTILE MATERIAL ...')
      PFIN=0.0
      CALL RELS(COP,KP,RP,GRP,VPO,VP1,PH,EXTP,UPP,PFIN,VFP)
C
C.....  CALCULATE TEMPERATURE INCREASE IN PROJECTILE MATERIAL
C
      CALL TINC(CPSP,CPLP,TMP,TVP,HFP,HVP,EXTP)
C
      PELOST=EXTP*MP
C
      VBO=1.0/RB
      VB1=RB*UBS/(UBS-UBP)
      VB1=1.0/VB1
C
      PH=PB*1.0E+09
```

```
C
      WRITE(2,7051) EB/10.0,NUB,KSB/10.0,ALPHAB,CPSB,CPLB
 7051 FORMAT(/,'PARAMETERS REQUIRED FOR CALCULATING BUMPER MATERIAL RESP
     $ONSE AND',/,'RELEASE FROM SHOCKED STATE USING THE MIE-GRUNEISEN E-
     $O-S:',/,3X,'ELASTIC MODULUS ..... E    =',E10.4,' N/SQ.M.'
     $,/,3X,'POISSON RATIO ..... NU   =',F10.3,/,3X,'BULK MODU
     $LUS ..... K    =',E10.4,' N/SQ.M.',/,3X,'LIN. COEF. OF
     $THERM. EXP. ... ALFA =',E10.4,' /DEG-C',/,3X,'SP HEAT (SOLID) ....
     $..... CPS  =',F10.3,' CAL/GM/DEG-C',/,3X,'SP HEAT (LIQUID) ...
     $..... CPL  =',F10.3,' CAL/GM/DEG-C')
      PHMB=PH/100.0E+09
      WRITE(2,8001) PH,PHMB,VBO,VB1,GB,GBI
 8001 FORMAT(3X,'HUGON IMP PRESS (PA,MBAR) ... PH   =',E10.4,',',F5.3,/,
     $3X,'SP VOL AT REST ..... V0   =',F10.3,' CU.CM./GM',/,3X,
     $'SP VOL AT IMPACT ..... V1   =',F10.3,' CU.CM./GM',/,3X,'AM
     $B M-GRUN COEF (CAL,INP) ... GAM0 =',F10.3,',',F5.3)
      WRITE(2,8051) TMB,TVB,HFB,HVB
 8051 FORMAT(3X,'MELT TEMPERATURE ..... TM   =',F10.2,' DEG-C',/,
     $3X,'VAPOR TEMPERATURE ..... TV   =',F10.2,' DEG-C',/,3X,'HEA
     $T OF FUSION ..... HF   =',F10.2,' CAL/GM',/,3X,'HEAT OF V
     $APORIZATION ..... HV   =',F10.2,' CAL/GM')
C
C.....  CALCULATE RELEASE OF BUMPER MATERIAL UP UNTIL ZERO PRESSURE IS
C.....  REACHED
C
      WRITE (2,1703)
 1703 FORMAT(/,'RELEASE OF SHOCKED BUMPER MATERIAL ...')
      PFIN=0.0
      CALL RELS(COB,KB,RB,GRB,VBO,VB1,PH,EXTB,UBP,PFIN,VFB)
C
C.....  CALCULATE TEMPERATURE INCREASE IN BUMPER MATERIAL
C
      CALL TINC(CPSB,CPLB,TMB,TVB,HFB,HVB,EXTB)
C
      WRITE(*,5081)
 5081 FORMAT(//,' PROJECTILE AND BUMPER SHOCK LOADING RESPONSE RELEASE',
     $/,' CALCULATIONS COMPLETE')
C
      BELOST=EXTB*MB
C
      TKELOST=PELOST+BELOST
      TKEINIT=0.5*MP*(VP*1000.0)*(VP*1000.0)
      FRLOST=TKELOST/TKEINIT
      WRITE (2,1706) TKEINIT,TKELOST,FRLOST
 1706 FORMAT(/,'TOTAL KINETIC ENERGY DUE TO INITIAL IMPACT ...',E10.4,
     $' JOULES',/,'TOTAL KINETIC ENERGY LOST TO SH HTNG & REL ...',
     $E10.4,' JOULES',/'FRACTION OF INITIAL K.E. LOST ... ',F5.3)
C
      DO 919 I=1,3
      DO 919 J=1,27
      READ (I+4,918) (PARAM(I,J,K),K=1,6)
  918 FORMAT(6F8.2)
  919 CONTINUE
C
      CALL INTERP(DPE,VP,THP,PARAM,ETA,EN,A2,AR,ELF)
```

```
C
      WRITE (2,41)
   41 FORMAT('IMPACT MODEL INPUT PARAMETER VALUES ...')
      WRITE (2,51) ETA,EN,A2,AR,ELF
   51 FORMAT(5X,'V1-FACTOR (ETA) = ',F4.2,/,5X,'M1-POWER (EN) =  ',1X,
     $F4.2,/,5X,'M1 EXCESS MULTIPLIER FOR M2 (A2) = ',F4.2,/,5X,'M1 EXCE
     $SS MULTIPLIER FOR MR (AR) = ',F4.2,/,5X,'ENERGY LOSS FACTOR (EL) =
     $ ',F4.2,/)
C
C....   CALCULATE RICOCHET ANGLE
C
      IF (THP.GE.30.0.AND.THP.LT.45.0) THR=-(10.0/3.0)*THP+160.0
      IF (THP.GE.45.0.AND.THP.LT.60.0) THR=-(1.0/3.0)*THP+25.0
      IF (THP.GE.60.0.AND.THP.LT.90.0) THR=-(1.0/6.0)*THP+15.0
      RTHR=THR*PI/180.0
C
C....   CALCULATE PREDICTED PERFORATION DEBRIS CLOUD TRAJECTORIES
C
      TH1=T1(VP,C,TS,DP,THP,RTHP)
      TH2=T2(VP,C,TS,DP,THP,RTHP)
      RTH1=TH1*PI/180.0
      RTH2=TH2*PI/180.0
C
C....   CALCULATE V1
C
      V1=ETA*VP*COS(RTHP)
C
      WRITE (2,6) TH1,V1,TH2,THR
    6 FORMAT('EXPER. NORMAL DEBRIS CLOUD TRAJECTORY (TH1) = ',5X,F4.1,
     $' DEG',/,'PREDICTED NORMAL DEBRIS CLOUD VELOCITY (V1) = ',5X,F4.1,
     $' KM/SEC',/,'EXPER. IN-LINE DEBRIS CLOUD TRAJECTORY (TH2) = ',4X,
     $F4.1,' DEG',/,'PREDICTED RICOCHET DEBRIS CLOUD TRAJECTORY (THR) =
     $',F4.1,' DEG',/)
C
C....   CALCULATE DISTRIBUTION OF BUMPER HOLE AND PROJECTILE MASS AMONG
C....   NORMAL, IN-LINE, AND RICOCHET DEBRIS CLOUD MASSES
C
      ANG=0.0
      D1=DN(V1,C,TS,DP,ANG)
      D2=DX(V1,C,TS,DP,ANG)
      MB1=(PI/4.0)*(D1/100.0)*(D2/100.0)*(TS/100.0)*(RP*1000.0)
      FR1=MB1/MB
      M1=MB1*(COS(RTHP)**EN)
      MBE=MB-MB1
      MB2=A2*MBE
      MBR=AR*MBE
      FR2=MB2/MB
      FR3=MBR/MB
      M2=MP*(COS(RTHP)**EN)+MB2*(COS(RTHP)**EN)
      MR=(1.0-COS(RTHP)**EN)*(MB+MP)+MBR*(COS(RTHP)**EN)
      TM=MB+MP
      F1=M1/TM
      F2=M2/TM
      F3=MR/TM
C
```

```
      WRITE (2,7) MP*1000.0,DMN,DMX,MB*1000.0,D1,D2,MB1*1000.0,
     $                  MB1*1000.0,FR1,MB2*1000.0,FR2,MBR*1000.0,FR3
    7 FORMAT('IMPACTING PROJECTILE MASS (MP) = ',3X,F10.6,' GMS',/,
     $'BUMPER PLATE HOLE DIMENSIONS ...',/,5X,'DMIN = ',F6.4,' CM',/,5X,
     $'DMAX = ',F6.4,' CM',/,'BUMPER PLATE DEBRIS MASS (MB) = ',F10.6,
     $' GMS',/,'BUMPER PLATE HOLE SIZE UNDER NORMAL IMPACT AT V1 ...',/,
     $5X,'D1 = ',F6.4,' CM',/,5X,'D2 = ',F6.4,' CM',/,'NORMAL IMPACT HOL
     $E MASS (MB1) = ',F10.6,' GMS',/,'AMOUNT OF ACTUAL HOLE MASS APPORT
     $IONED TO M1 = ',F10.6,' GMS (',F4.2,' %)',/,'AMOUNT OF ACTUAL HOLE
     $ MASS APPORTIONED TO M2 = ',F10.6,' GMS (',F4.2,' %)',/,'AMOUNT OF
     $ ACTUAL HOLE MASS APPORTIONED TO MR = ',F10.6,' GMS (',F4.2,' %)',
     $/)
C
      WRITE (2,8) M1*1000.0,F1,M2*1000.0,F2,MR*1000.0,F3
    8 FORMAT('PREDICTED NORMAL DEBRIS CLOUD MASS (M1) =   ',F8.6,' GMS (
     $',F4.2,' % OF MP+MB)',/,'PREDICTED IN-LINE DEBRIS CLOUD MASS (M2)
     $=  ',F8.6,' GMS (',F4.2,' % OF MP+MB)',/,'PREDICTED RICOCHET DEBRI
     $S CLOUD MASS (MR) = ',F8.6,' GMS (',F4.2,' % OF MP+MB)',/)
C
C....   CALCULATE CONSTANTS FOR V2 AND VR CALCULATIONS
C
      C1=+MP*VP*COS(RTHP-RTHR)
      C2=-M1*V1*COS(RTH1-RTHR)
      C3=+M2*COS(RTH2-RTHR)
C
C....   CALCULATE IN-LINE AND RICOCHET DEBRIS CLOUD VELOCITIES BASED ON
C....   MOMENTUM BALANCE
C
      V2=(C1+C2)/C3
      C4=+MP*VP*SIN(RTHP)
      C5=-M1*V1*SIN(RTH1)
      C6=-M2*V2*SIN(RTH2)
      C7=+MR*COS(RTHR)
      VR=(C4+C5+C6)/C7
C
      WRITE (2,14) V2,VR
   14 FORMAT('PREDICTED IN-LINE DEBRIS CLOUD VELCOTIY (V2) = ',1X,F5.1,
     $' KM/SEC',/,'PREDICTED RICOCHET DEBRIS CLOUD VELOCITY (VR) = ',
     $F5.1,' KM/SEC',/)
C
      CALL VRAD(MP,VP,M1,V1,M2,V2,MR,VR,TS,DP,RTHP,C,PI,ELF,THR,VRD)
C
      WRITE (3,909) DMN,DMX,M2,V2,VRD
  909 FORMAT(2F10.5,/,3F10.5)
C
      CLOSE (1)
      CLOSE (2)
      CLOSE (3)
      CLOSE (4)
      STOP
      END
C
      FUNCTION DN(VP,C,TB,DP,RTHP)
      IMPLICIT DOUBLE PRECISION (A-H,O-Z)
      DN=(2.698*((VP/C)**0.689)*((TB/DP)**0.708)*(COS(RTHP)**0.021)
```

```
     $          +0.93)*DP
      RETURN
      END
C
      FUNCTION DX(VP,C,TB,DP,RTHP)
      IMPLICIT DOUBLE PRECISION (A-H,O-Z)
      DX=(2.252*((VP/C)**0.622)*((TB/DP)**0.667)*(EXP(0.815*RTHP))
     $          +1.00)*DP
      RETURN
      END
C
      FUNCTION T1(VP,C,TB,DP,THP,RTHP)
      IMPLICIT DOUBLE PRECISION (A-H,O-Z)
      T1=(0.471*((VP/C)**(-0.049))*((TB/DP)**(-0.054))*(COS(RTHP)**
     $          1.143))*THP
      RETURN
      END
C
      FUNCTION T2(VP,C,TB,DP,THP,RTHP)
      IMPLICIT DOUBLE PRECISION (A-H,O-Z)
      T2=(0.532*((VP/C)**(-0.086))*((TB/DP)**(-0.478))*(COS(RTHP)**
     $          0.586))*THP
      RETURN
      END
C
      SUBROUTINE VRAD(AMP,VP,AM1,V1,AM2,V2,AMR,VR,TB,DP,RTHP,C,PI,ELF,
     $                    THR,VRD)
      IMPLICIT DOUBLE PRECISION (A-H,O-Z)
      EA=1.0-ELF
      EAP=100.0*EA
      EPR=0.5*AMP*(VP*1000.0)*(VP*1000.0)
      EPROJ=EA*0.5*AMP*(VP*1000.0)*(VP*1000.0)
      E1=0.5*AM1*(V1*1000.0)*(V1*1000.0)
      E2=0.5*AM2*(V2*1000.0)*(V2*1000.0)
      ER=0.5*AMR*(VR*1000.0)*(VR*1000.0)
      DIFF=EPROJ-(E1+E2+ER)
      WRITE (2,1) EPR,EPROJ,EAP,E1,E2,ER,DIFF
    1 FORMAT('INITIAL PROJECTILE IMPACT ENERGY = ',14X,F10.2,' J',/,
     $'PROJ. ENERGY AVAIL. FOR DEBRIS CLOUD SPREAD = ',3X,F10.2,' J  (',
     $F5.1,' %)',/,'NORMAL DEBRIS CLOUD KINETIC ENERGY = ',12X,F10.2,
     $' J',/,'IN-LINE DEBRIS CLOUD KINETIC ENERGY = ',11X,F10.2,' J',/,
     $'RICOCHET DEBRIS CLOUD KINETIC ENERGY = ',10X,F10.2,' J',/,
     $'ENERGY DIFFERENCE (INITIAL - DEBRIS CLOUD SUM) = ',F10.2,' J')
      IF (DIFF.LE.0.0) THEN
      WRITE (2,2)
    2 FORMAT(/,'*** INSUFFICIENT KINETIC ENERGY REMAINING FOR DEBRIS CLO
     $UD EXPANSION ***')
      WRITE (*,2)
      GOTO 7
      ENDIF
      IF (DIFF.GT.0.0) THEN
      EG1=G1(VP,C,TB,DP,RTHP)*180.0/PI
      EG2=G2(VP,C,TB,DP,RTHP)*180.0/PI
      TM=AM1+AM2+AMR
      VRD=SQRT(2.0*DIFF/TM)/1000.0
```

```
      PG1=2.0*ATAN(VRD/V1)*180.0/PI
      PG2=2.0*ATAN(VRD/V2)*180.0/PI
      A99=THR+ATAN(VRD/VR)*180.0/PI
      WRITE (2,3) VRD
    3 FORMAT(/,'IF RADIAL EXPANSION VELOCITIES ARE EQUAL FOR ALL THREE D
     $EBRIS CLOUDS ...',/,3X,'DEBRIS CLOUD RADIAL EXPANSION VELOCITY ...
     $ VE =',F10.5,' KM/SEC')
      E1=100.0*(PG1-EG1)/EG1
      E2=100.0*(PG2-EG2)/EG2
      WRITE (2,4) EG1,PG1,E1,EG2,PG2,E2
    4 FORMAT(3X,'DEBRIS CLOUD CONE ANGLES ...',/,5X,'EXPER. NORMAL DEBRI
     $S CLOUD CONE ANGLE ... G1 = ',1X,F5.1,' DEG',/,5X,'MODEL NORMAL DE
     $BRIS CLOUD CONE ANGLE ... G1 = ',2X,F5.1,' DEG',2X,'(',F6.2,1X,'%)
     $',/,5X,'EXPER. IN-LINE DEBRIS CLOUD CONE ANGLE ... G2 = ',F5.1,' D
     $EG',/,5X,'MODEL IN-LINE DEBRIS CLOUD CONE ANGLE ... G2 = ',1X,F5.1
     $,' DEG',2X,'(',F6.2,1X,'%)')
      WRITE (*,4) EG1,PG1,E1,EG2,PG2,E2
      ENDIF
    7 RETURN
      END
C
      FUNCTION G1(VP,C,TB,DP,RTHP)
      IMPLICIT DOUBLE PRECISION (A-H,O-Z)
      TG1=1.318*((VP/C)**0.907)*((TB/DP)**0.195)*(COS(RTHP)**0.394)
      G1=ATAN(TG1)
      RETURN
      END
C
      FUNCTION G2(VP,C,TB,DP,RTHP)
      IMPLICIT DOUBLE PRECISION (A-H,O-Z)
      TG2=1.556*((VP/C)**1.096)*((TB/DP)**0.345)*(COS(RTHP)**0.738)
      G2=ATAN(TG2)
      RETURN
      END
C
      SUBROUTINE INTERP(DPE,VP,THP,PARAM,ETA,EN,A2,AR,ELF)
      IMPLICIT DOUBLE PRECISION (A-H,O-Z)
      DOUBLE PRECISION PINT(7,4),PARAM(3,27,6)
C
      IT=INT(THP/15.0)-1
      IV=INT((VP-4.0)/1.5)+1
      IF (DPE.EQ.0.750) THEN
      ID=9
      GOTO 12
      ENDIF
      DO 11 K=1,9
      IF (DPE.GE.PARAM(1,K,2).AND.DPE.LT.PARAM(1,K+1,2)) THEN
      ID=K
      GOTO 12
      ENDIF
   11 CONTINUE
C
   12 CONTINUE
      IF (IT.LT.3) IT1=IT+1
      IF (IT.EQ.3) IT1=IT
```

```
      IF (IV.LT.3) IV1=IV+1
      IF (IV.EQ.3) IV1=IV
      IF (ID.LT.9) ID1=ID+1
      IF (ID.EQ.9) ID1=ID
C
      DP=DPE*2.54
      DPJ=PARAM(1,ID,2)*2.54
      DPJ1=PARAM(1,ID1,2)*2.54
C
      VPJ=(IV-1)*1.5+4.0
      VPJ1=(IV1-1)*1.5+4.0
      THPJ=(IT+1)*15.0
      THPJ1=(IT1+1)*15.0
C
      IJ=(IV-1)*9+ID
      IJD1=(IV-1)*9+ID1
      IJV1=(IV1-1)*9+ID
      IJVD1=(IV1-1)*9+ID1
      IF (DPJ1.EQ.DPJ) FRDP=0.0
      IF (DPJ1.NE.DPJ) FRDP=(DP-DPJ)/(DPJ1-DPJ)
      IF (VPJ1.EQ.VPJ) FRVP=0.0
      IF (VPJ1.NE.VPJ) FRVP=(VP-VPJ)/(VPJ1-VPJ)
      IF (THPJ1.EQ.THPJ) FRTHP=0.0
      IF (THPJ1.NE.THPJ) FRTHP=(THP-THPJ)/(THPJ1-THPJ)
C
      DO 10 K=1,4
      PINT(1,K)=PARAM(IT,IJ,K+2) +
     $                  FRDP*(PARAM(IT,IJD1,K+2)-PARAM(IT,IJ,K+2))
   10 CONTINUE
C
      DO 20 K=1,4
      PINT(2,K)=PARAM(IT,IJV1,K+2) +
     $                  FRDP*(PARAM(IT,IJVD1,K+2)-PARAM(IT,IJV1,K+2))
   20 CONTINUE
C
      DO 30 K=1,4
      PINT(3,K)=PINT(1,K)+FRVP*(PINT(2,K)-PINT(1,K))
   30 CONTINUE
C
      DO 40 K=1,4
      PINT(4,K)=PARAM(IT1,IJ,K+2) +
     $                  FRDP*(PARAM(IT1,IJD1,K+2)-PARAM(IT1,IJ,K+2))
   40 CONTINUE
C
      DO 50 K=1,4
      PINT(5,K)=PARAM(IT1,IJV1,K+2) +
     $                  FRDP*(PARAM(IT1,IJVD1,K+2)-PARAM(IT1,IJV1,K+2))
   50 CONTINUE
C
      DO 60 K=1,4
      PINT(6,K)=PINT(4,K)+FRVP*(PINT(5,K)-PINT(4,K))
   60 CONTINUE
C
      DO 70 K=1,4
      PINT(7,K)=PINT(3,K)+FRTHP*(PINT(6,K)-PINT(3,K))
```

```
   70 CONTINUE
C
      ETA=PINT(7,1)
      EN=PINT(7,2)
      A2=PINT(7,3)
      AR=1.0-A2
      ELF=PINT(7,4)
C
      RETURN
      END
C
      SUBROUTINE RELS(CO,K,R,G,VO,V1,PHO,EX,UP,PHA,VF)
      IMPLICIT DOUBLE PRECISION (A-H,O-Z)
      DOUBLE PRECISION K,PH(201),EH(201),V(201),P(201),E(201)
C
C.....  THIS SUBROUTINE CALCULATES THE RELEASE OF A SHOCKED MATERIAL
C.....  USING THE MIE-GRUNHEISEN EQUATION OF STATE.  INCLUDED IS A
C.....  CALCULATION OF THE FINAL SPECIFIC VOLUME AND THE WASTE HEAT
C.....  GENERATED BY THE RELEASE PROCESS.  WHEN THE PRESSURE ALONG THE
C.....  ISENTROPE DROPS BELOW THE REFLECTED PRESSURE ARE CALCULATED BY
C.....  THE IMPEDANCE MATCH PROCESS, THE RELEASE PROCESS IS TERMINATED
C
      V(1)=V1
      PH(1)=PHO
      EH(1)=0.5*PH(1)*(VO-V1)/1000.0
      DV=(VO-V1)/50.0
      DE=0.0
      DV2=DV/1000.0
      E(1)=EH(1)
      P(1)=PH(1)
      DEN1=1.0+G*DV2*0.5
C
      II=0
      UR=0.0
      DO 10 I=2,201
      V(I)=V(I-1)+DV
      PH(I)=CO**2*R*1000.0*(1.0-V(I)/VO)/(1.0-K*(1.0-V(I)/VO))**2
      PH(I)=PH(I)*1.0E06
      EH(I)=0.5*PH(I)*(VO-V(I))/1000.0
      P(I)=(PH(I)+G*(E(I-1)-EH(I)-0.5*P(I-1)*DV2))/DEN1
      E(I)=E(I-1)-0.5*(P(I)+P(I-1))*DV2
      DP=P(I)-P(I-1)
      DUR=DSQRT(-DP*(DV/1000.0))
      UR=UR+DUR/1000.0
      II=II+1
      IF (P(I).GE.0.0) DE=DE+0.5*DV2*(P(I)+P(I-1))
      IF (P(I).LT.0.0) GOTO 15
      IF (P(I).LE.PHA) GOTO 15
   10 CONTINUE
C
   15 Q=P(II)/(P(II)-P(II+1))
      DE=DE+0.5*Q*DV2*P(II)
      EX=EH(1)-DE
      VF=V(II)+Q*(V(II+1)-V(II))
      UFS1=UP+UR
```

```
      UFS2=2.0*UP
C
      WRITE(2,20) VF,EH(1),DE,EX
   20 FORMAT(/,'SPECIFIC VOL AFTER RELEASE ..... VF =',F5.3,
     $' CU.CM./GM',/,'ENERGY DUE TO DEB CLD IMPACT .... ',E10.4,
     $' JOULES/KG',/,'ENERGY RECOVERED BY RELEASE ..... ',E10.4,
     $' JOULES/KG',/,'WASTE HEAT GENERATED ..... ',E10.4,
     $' JOULES/KG')
C
      RETURN
      END
C
      SUBROUTINE TINC(SHS,SHL,TM,TV,HF,HV,EXH)
      IMPLICIT DOUBLE PRECISION (A-H,O-Z)
      DOUBLE PRECISION IME,IVE
C
C.....  THIS SUBROUTINE CALCULATES THE RESIDUAL TEMPERATURE INCREASE
C.....  IN A MATERIAL THAT HAS BEEN RELEASED FROM THE SHOCKED STATE
C.....  ESTIMATES THE PERCENTAGE OF VAPORIZED, MELTED, AND SOLID
C.....  MATERIAL DUE TO THE RELEASE PROCESS
C
      SHS=SHS*4186.0
      SHL=SHL*4186.0
      HF=HF*4186.0
      HV=HV*4186.0
C
C.....  CALCULATE ENERGIES REQUIRED TO INITIATE MATERIAL MELT AND
C.....  VAPORIZATION.
C
      IME=TM*SHS
      IVE=IME+HF+(TV-TM)*SHL
C
C.....  IF WASTE HEAT IS LESS THAN THE ENERGY REQ'D TO START MELT,
C.....  CALCULATE TEMPERATURE RISE USING W.H.=S.H.*(TEMP.INCR.)
C
      IF (EXH.LT.IME) THEN
      DT=EXH/SHS
      TR=DT
      DEL=0.0
      WRITE(2,50) IME,DEL,EXH
   50 FORMAT('ENERGY REQ, INCIPIENT MELT ... ',E10.4,' JOULES/KG',/,
     $'ENERGY AVAILABLE FOR MELT .... ',E10.4,' JOULES/KG',/,
     $'EXCESS ENERGY AVAILABLE ..... ',E10.4,' JOULES/KG')
      PV=0.0
      PL=0.0
      PS=100.0
      GOTO 100
      ENDIF
C
C.....  IF WASTE HEAT EXCEEDS THE ENERGY REQ'D TO START MELT, BUT IS
C.....  LESS THAN THAT REQ'D TO COMPLETE MELT, RESET THE VALUE OF THE
C.....  ENERGY AVAILABLE FROM THE WASTE HEAT VALUE TO THE VALUE REQ'D
C.....  TO START MELT.  THIS IMPLIES THAT SOME ENERGY IS AVAILABLE FOR
C.....  MELTING A PORTION OF THE MATERIAL.  NOTE: THE TEMPERATURE RISE
C.....  EQUALS THE MELT TEMPERATURE OF THE MATERIAL.
```

```
C
      IF (EXH.GE.IME.AND.EXH.LT.IME+HF) THEN
      TR=TM
      DEL=EXH-IME
      REQM=IME+HF
      WRITE(2,60) IME,REQM,DEL
   60 FORMAT('ENERGY REQ, INCIPIENT MELT ... ',E10.4,' JOULES/KG',/,
     $'ENERGY REQ, COMPLETE MELT .... ',E10.4,' JOULES/KG',/,
     $'ENERGY AVAILABLE FOR MELT .... ',E10.4,' JOULES/KG')
      PV=0.0
      PL=100.0*DEL/HF
      PS=100.0-PL
      GOTO 100
      ENDIF
C
C.....  IF THE WASTE HEAT EXCEEDS THE ENERGY REQ'D TO COMPLETELY MELT
C.....  THE MATERIAL, BUT IS LESS THAN THAT REQ'D TO START VAPORIZA-
C.....  TION, COMPUTE THE TEMPERATURE INCREASE CAUSED BY THE EXCESS
C.....  ENERGY AND ADD IT TO THE MELT TEMPERATURE OF THE MATERIAL.
C
      IF (EXH.GE.IME+HF.AND.EXH.LT.IVE) THEN
      DEL=EXH-IME-HF
      DT=DEL/SHL
      TR=TM+DT
      REQM=IME+HF
      WRITE(2,70) IME,REQM,DEL
   70 FORMAT('ENERGY REQ, INCIPIENT MELT ... ',E10.4,' JOULES/KG',/,
     $'ENERGY REQ, COMPLETE MELT .... ',E10.4,' JOULES/KG',/,
     $'EXCESS ENERGY AVAILABLE ..... ',E10.4,' JOULES/KG')
      PV=0.0
      PL=100.0
      PS=100.0-PL
      GOTO 100
      ENDIF
C
      IF (EXH.GE.IVE.AND.EXH.LT.IVE+HV) THEN
      DEL=EXH-IVE
      REQV=IVE+HV
      TR=TV
      WRITE(2,80) IVE,REQV,DEL
   80 FORMAT('ENERGY REQ, INCIPIENT VAP .... ',E10.4,' JOULES/KG',/,
     $'ENERGY REQ, COMPLETE VAP ..... ',E10.4,' JOULES/KG',/,
     $'EXCESS ENERGY AVAILABLE ..... ',E10.4,' JOULES/KG')
      PV=100.0*DEL/HV
      PL=100.0-PV
      PS=100.0-PL
      GOTO 100
      ENDIF
C
      IF (EXH.GE.IVE+HV) THEN
      ECVAP=IVE+HV
      PV=100.0
      PL=0.0
      PS=0.0
      WRITE (2,90) ECVAP
```

```
   90 FORMAT('ENERGY REQ, COMPLETE VAP .... ',E10.4,' JOULES/KG',/,
     $'*** THE MATERIAL IS COMPLETELY VAPORIZED ***')
      GOTO 120
      ENDIF
C
  100 WRITE(2,110) TR,PS,PL,PV
  110 FORMAT('RESIDUAL MATERIAL TEMP ..... ',F10.3,' DEG-C',//,'PERCEN
     $T SHKD AND REL PRESS WALL MATERIAL ...',/,3X,'IN SOLID STATE ... '
     $,F6.2,'%',/,3X,'IN MOLTEN FORM ... ',F6.2,'%',/,3X,'IN VAPOR FORM
     $.... ',F6.2,'%')
C
  120 RETURN
      END
```

APPENDIX F

REQUIRED INPUT FILE FOR OBLDATA.FOR

Input File GPRMOBL

```
ALALAL
AA0
     45.00       0.500       0.13        1.00
```

APPENDIX G

SAMPLE OUTPUT FILES FOR OBLDATA.FOR

Output File OBLOUT

```
45.0-DEG IMPACT OF A ALUMINUM   PROJ ON A DUAL-WALL SYSTEM WITH A
ALUMINUM   BUMPER, A MLI-BLNKT  INNER BUMPER, AND A ALUMINUM   PRESS WALL

PROJECTILE PROPERTIES ...
   MAT = ALUMINUM
   CO  =  5.380 KM/S
   K   =  1.340
   RHO =  2.712 GM/CU.CM.
   DP  =   .795 CM
   MP  =   .714 GMS
   VP  =  7.000 KM/S

OUTER BUMPER PROPERTIES ...
   MAT = ALUMINUM
   CO  =  5.380 KM/S
   K   =  1.340
   RHO =  2.712 GM/CU.CM.
   TS  =   .130 CM
   DMN =  1.473 CM
   DMX =  2.028 CM
   EPS1=  1.000     (INITIAL VALUE)
   MB  =   .827 GMS (INITIAL VALUE)

PROJECTILE AND BUMPER SHOCK LOADING RESPONSE AND RELEASE CALCULATIONS

PROJECTILE IMPACT VELOCITY .... VP =   7.000 KM/S
PROJ MATL PARTICLE VELOCITY ... UP =   3.500 KM/S
PROJ MATL SHOCK WAVE SPEED .... US =  10.070 KM/S
HUGONIOT IMPACT PRESSURE ...... PH =  95.584 GPA
BMPR MATL PARTICLE VELOCITY ... UP =   3.500 KM/S
BMPR MATL SHOCK WAVE SPEED .... US =  10.070 KM/S
HUGONIOT IMPACT PRESSURE ...... PH =  95.584 GPA

PARAMETERS REQUIRED FOR CALCULATING PROJECTILE MATERIAL RESPONSE AND
RELEASE FROM SHOCKED STATE USING THE MIE-GRUNEISEN E-O-S:
   ELASTIC MODULUS ............. E    = .7102E+11 N/SQ.M.
   POISSON RATIO ............... NU   =      .350
   BULK MODULUS ................ K    = .7891E+11 N/SQ.M.
   LIN. COEF. OF THERM. EXP. ... ALFA = .2400E-04 /DEG-C
   SP HEAT (SOLID) ............. CPS  =      .235 CAL/GM/DEG-C
   SP HEAT (LIQUID) ............ CPL  =      .255 CAL/GM/DEG-C
```

```
   HUGON IMP PRESS (PA,MBAR) ... PH   = .9558E+11, .956
   SP VOL AT REST ..... VO   =      .369 CU.CM./GM
   SP VOL AT IMPACT ..... V1   =      .241 CU.CM./GM
   AMB M-GRUN COEF (CAL,INP) ... GAMO =     2.129,2.130
   MELT TEMPERATURE ..... TM   =    660.00 DEG-C
   VAPOR TEMPERATURE ..... TV   =   2450.00 DEG-C
   HEAT OF FUSION ..... HF   =     95.00 CAL/GM
   HEAT OF VAPORIZATION ..... HV   =   2450.00 CAL/GM

RELEASE OF SHOCKED PROJECTILE MATERIAL ...

SPECIFIC VOL AFTER RELEASE ..... VF = .403 CU.CM./GM
ENERGY DUE TO DEB CLD IMPACT ....  .6125E+07 JOULES/KG
ENERGY RECOVERED BY RELEASE .....  .5035E+07 JOULES/KG
WASTE HEAT GENERATED .....  .1090E+07 JOULES/KG
ENERGY REQ, INCIPIENT MELT ...  .6492E+06 JOULES/KG
ENERGY REQ, COMPLETE MELT ....  .1047E+07 JOULES/KG
EXCESS ENERGY AVAILABLE .....  .4313E+05 JOULES/KG
RESIDUAL MATERIAL TEMP .....    700.405 DEG-C

PERCENT SHKD AND REL PRESS WALL MATERIAL ...
   IN SOLID STATE ...    .00%
   IN MOLTEN FORM ... 100.00%
   IN VAPOR FORM ....    .00%

PARAMETERS REQUIRED FOR CALCULATING BUMPER MATERIAL RESPONSE AND
RELEASE FROM SHOCKED STATE USING THE MIE-GRUNEISEN E-O-S:
   ELASTIC MODULUS ..... E    = .7102E+11 N/SQ.M.
   POISSON RATIO ..... NU   =      .350
   BULK MODULUS ..... K    = .7891E+11 N/SQ.M.
   LIN. COEF. OF THERM. EXP. ... ALFA = .2400E-04 /DEG-C
   SP HEAT (SOLID) ..... CPS  =      .235 CAL/GM/DEG-C
   SP HEAT (LIQUID) ..... CPL  =      .255 CAL/GM/DEG-C
   HUGON IMP PRESS (PA,MBAR) ... PH   = .9558E+11, .956
   SP VOL AT REST ..... VO   =      .369 CU.CM./GM
   SP VOL AT IMPACT ..... V1   =      .241 CU.CM./GM
   AMB M-GRUN COEF (CAL,INP) ... GAMO =     2.129,2.130
   MELT TEMPERATURE ..... TM   =    660.00 DEG-C
   VAPOR TEMPERATURE ..... TV   =   2450.00 DEG-C
   HEAT OF FUSION ..... HF   =     95.00 CAL/GM
   HEAT OF VAPORIZATION ..... HV   =   2450.00 CAL/GM

RELEASE OF SHOCKED BUMPER MATERIAL ...

SPECIFIC VOL AFTER RELEASE ..... VF = .403 CU.CM./GM
ENERGY DUE TO DEB CLD IMPACT ....  .6125E+07 JOULES/KG
ENERGY RECOVERED BY RELEASE .....  .5035E+07 JOULES/KG
WASTE HEAT GENERATED .....  .1090E+07 JOULES/KG
ENERGY REQ, INCIPIENT MELT ...  .6492E+06 JOULES/KG
ENERGY REQ, COMPLETE MELT ....  .1047E+07 JOULES/KG
EXCESS ENERGY AVAILABLE .....  .4313E+05 JOULES/KG
RESIDUAL MATERIAL TEMP .....    700.405 DEG-C

PERCENT SHKD AND REL PRESS WALL MATERIAL ...
   IN SOLID STATE ...    .00%
```

```
   IN MOLTEN FORM ... 100.00%
   IN VAPOR FORM ....    .00%

TOTAL KINETIC ENERGY DUE TO INITIAL IMPACT ... .1748E+05 JOULES
TOTAL KINETIC ENERGY LOST TO SH HTNG & REL ... .1679E+04 JOULES
FRACTION OF INITIAL K.E. LOST ...  .096
IMPACT MODEL INPUT PARAMETER VALUES ...
     V1-FACTOR (ETA) = 1.10
     M1-POWER (EN) =   1.50
     M1 EXCESS MULTIPLIER FOR M2 (A2) =  .87
     M1 EXCESS MULTIPLIER FOR MR (AR) =  .13
     ENERGY LOSS FACTOR (EL) =  .06

EXPER. NORMAL DEBRIS CLOUD TRAJECTORY (TH1) =      15.5 DEG
PREDICTED NORMAL DEBRIS CLOUD VELOCITY (V1) =       5.4 KM/SEC
EXPER. IN-LINE DEBRIS CLOUD TRAJECTORY (TH2) =     45.2 DEG
PREDICTED RICOCHET DEBRIS CLOUD TRAJECTORY (THR) = 10.0 DEG

IMPACTING PROJECTILE MASS (MP) =       .713547 GMS
BUMPER PLATE HOLE DIMENSIONS ...
     DMIN = 1.4726 CM
     DMAX = 2.0282 CM
BUMPER PLATE DEBRIS MASS (MB) =    .826990 GMS
BUMPER PLATE HOLE SIZE UNDER NORMAL IMPACT AT V1 ...
     D1 = 1.3605 CM
     D2 = 1.3511 CM
NORMAL IMPACT HOLE MASS (MB1) =    .509000 GMS
AMOUNT OF ACTUAL HOLE MASS APPORTIONED TO M1 =    .509000 GMS ( .62 %)
AMOUNT OF ACTUAL HOLE MASS APPORTIONED TO M2 =    .276651 GMS ( .33 %)
AMOUNT OF ACTUAL HOLE MASS APPORTIONED TO MR =    .041339 GMS ( .05 %)

PREDICTED NORMAL DEBRIS CLOUD MASS (M1) =    .302654 GMS ( .20 % OF MP+MB)
PREDICTED IN-LINE DEBRIS CLOUD MASS (M2) =   .588775 GMS ( .38 % OF MP+MB)
PREDICTED RICOCHET DEBRIS CLOUD MASS (MR) =  .649108 GMS ( .42 % OF MP+MB)

PREDICTED IN-LINE DEBRIS CLOUD VELCOTIY (V2) =    5.1 KM/SEC
PREDICTED RICOCHET DEBRIS CLOUD VELOCITY (VR) =   1.5 KM/SEC

INITIAL PROJECTILE IMPACT ENERGY =                 17481.89 J
PROJ. ENERGY AVAIL. FOR DEBRIS CLOUD SPREAD =      16432.98 J  ( 94.0 %)
NORMAL DEBRIS CLOUD KINETIC ENERGY =                4486.08 J
IN-LINE DEBRIS CLOUD KINETIC ENERGY =               7641.55 J
RICOCHET DEBRIS CLOUD KINETIC ENERGY =               737.06 J
ENERGY DIFFERENCE (INITIAL - DEBRIS CLOUD SUM) =    3568.29 J

IF RADIAL EXPANSION VELOCITIES ARE EQUAL FOR ALL THREE DEBRIS CLOUDS ...
   DEBRIS CLOUD RADIAL EXPANSION VELOCITY ... VE =   2.15233 KM/SEC
   DEBRIS CLOUD CONE ANGLES ...
     EXPER. NORMAL DEBRIS CLOUD CONE ANGLE ... G1 =   47.0 DEG
     MODEL NORMAL DEBRIS CLOUD CONE ANGLE ... G1 =    43.1 DEG  ( -8.26 %)
     EXPER. IN-LINE DEBRIS CLOUD CONE ANGLE ... G2 =  42.3 DEG
     MODEL IN-LINE DEBRIS CLOUD CONE ANGLE ... G2 =   45.8 DEG  (  8.33 %)
```

Output File OBLDATA

```
1.47255    2.02818
 .00059    5.09485    2.15233
```

APPENDIX H

GENERAL EMPIRICAL HOLE DIAMETER AND CRACK LENGTH EQUATIONS

Reference [12] presents a series of empirical equations for pressure wall hole diameter and maximum tip-to-tip crack length for thirteen ISS wall configurations. These equations are all in the following format:

$$X = Af(\theta_p)g(V_p)\left[1 - e^{-C(M_p/M_{BL}-1)}\right] \qquad (H.1)$$

where X represents either hole diameter or crack length, and V_p, M_p, and θ_p are the velocity, mass, and obliquity, respectively, of the impacting projectile. The quantity M_{BL} is the projectile ballistic limit mass at velocity V_p for a particular system under a θ_p-degree impact.

The use of projectile mass and ballistic limit mass in equation (H.1) was motivated by the desire to pool together two sets of data. The first set consisted of light gas gun test data in which spherical projectiles were fired at velocities near 6.5 km/s. The second set consisted of Inhibited Shaped Charge Launcher (ISCL) test data in which cylindrical projectiles with an aspect ratio of approximately 1.5 were fired at approx. 11.3 km/s. Because projectile mass and ballistic limit mass were used in equation (H.1), shape effects were not considered in the development of the hole diameter and crack length equations in Reference [13].

The forms of the functions $f(\theta_p)$ and $g(V_p)$ in equation (H.1) depended on the particular wall system and the nature of the data obtained for that system. For example, if data for a particular wall system were available only at 6.5 km/s, then a velocity dependence was not needed in the equations for that system; hence, in that particular case, $g(V_p)=1$ and the equations

developed would be valid only for V_p=6.5 km/s. For wall systems where test data were available at both 6.5 km/s and 11.3 km/s, the velocity dependence in equation (H.1) was taken to be in the following form:

$$g(V_p) = (V_p/C_b)^D \tag{H.2}$$

where C_b is the speed of sound in the bumper plate material.

The form of the $f(\theta_p)$ term, for all wall configurations except the baseline US Lab Cylinder (BLC) and the baseline JEM Cylinder (BJC) systems, was given by

$$f(\theta_p) = \cos^B\theta_p \tag{H.3}$$

For the BLC and the BJC wall systems, the form of the $f(\theta_p)$ term was given by

$$f(\theta_p) = \cos^{B\left(\frac{V_c - V_p}{C_b}\right)}\theta_p \tag{H.4}$$

This form of the $f(\theta_p)$ for the BLC and BJC wall systems was motivated by the following considerations.

At an impact velocity of 6.5 km/s, the response of these two wall systems was similar to that of the other wall systems: when trajectory obliquity was increased, hole diameter and crack length decreased. However, at an impact velocity of 11.3 km/s, the response of the BLC and BJC wall systems was *un*like that of the other wall systems at 11.3 km/s: when trajectory obliquity was increased, hole diameter and crack length unexpectedly *increased*. Thus, what was needed for these two wall systems was a cosine term whose power was a function of impact velocity. This function had to be chosen so that it was positive for a 6.5 km/s impact (which would result in decreasing hole diameters and crack lengths with increasing obliquity) and negative for a 11.3 km/s impact (which would result in increasing hole diameters and crack lengths with increasing obliquities).

The form of $f(\theta_p)$ given by equation (H.4) for the BLC and BJC wall systems satisfies the

requirements put forth in the preceding paragraph provided that the curve fitting parameter V_c was found to be between 6.5 and 11.3 km/s. This indeed was the case as Table 8 of Reference [13] indicates. In this table, V_c is seen to lie between 8.1 and 9.6 for the four equations in which it appears. Since only two of the six wall systems tested at 6.5 and at 11.3 km/s exhibited this unexpected response characteristic, the discussion in Reference [13] regarding this matter ended with a statement of the need to explore whether any of the remaining seven wall systems would exhibit similar behavior when tested at 11.3 km/s.

An explanation of the unexpected response for the BLC and JLC wall systems was presented and discussed in Reference [12], where Williamsen, *et al* hypothesized that the response of the BLC and JLC wall configuration is not unusual in any way, but is to be expected considering the differences in the shapes of the projectiles fired at 6.5 km/s and at 11.3 km/s. However, by simply using projectile mass equation (H.1) ignored the effects of projectile shape or aspect ratio on impact response. Moreover, Williamsen, et al. postulated that if the effects of the *effective* aspect ratio of the projectile were include in equation (H.1), then equation (H.3) would apply to the BLC and JLC wall systems as well.

The effective aspect ratio of a cylindrical projectile is based on the projected vertical and horizontal dimensions of the projectile, rather than on the absolute projectile length and diameter. Specifically, effective projectile aspect ratio is defined to be the ratio of the projectile dimension measured along the outer bumper normal (L_e in Figure H.1 below) divided by the projectile dimension measured along the bumper surface (D_e in Figure H.1):

$$\rho_{eff} = \frac{L_e}{D_e} \tag{H.5}$$

Figure H.1 below presents a sketch of an obliquely incident projectile and a summary of

the length quantities necessary for calculating the effective aspect ratio of a projectile. Figures H.2a-c shows how the shape and orientation of a projectile can have a strong effect on the pressure wall hole diameter and crack length.

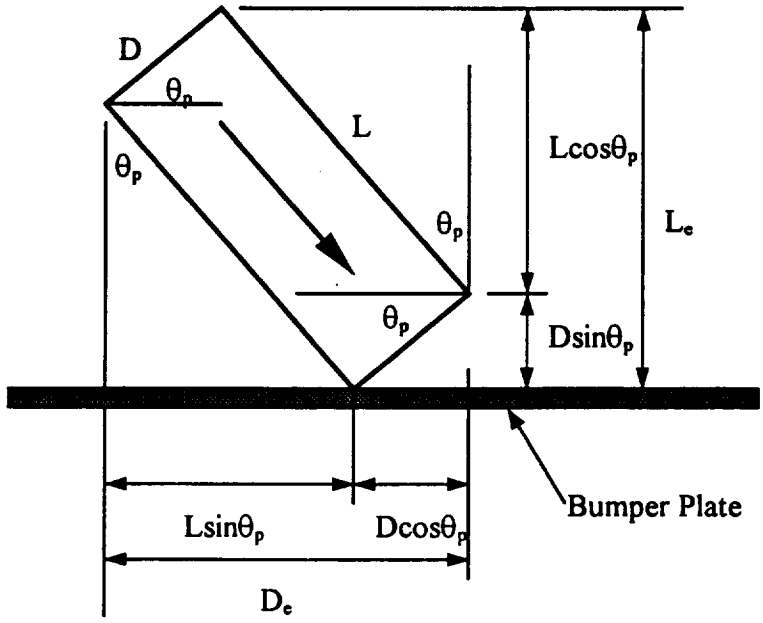

Figure H.1 Definition of Effective Projectile Aspect Ratio

Whereas spherical projectiles break up into small fragments due to the action and interaction of shock waves in the projectile and bumper materials (Figure H.2a), long cylindrical projectiles impacting normally often experience incomplete breakup. Thus, in the case of normal cylindrical impact, there is a lack of significant particle dispersion, which results in a smaller pressure wall hole (Figure H.2b). However, at oblique impact angles, the effective aspect ratio of the same cylindrical projectile is reduced compared to its value in a normal impact, and a more uniform breakup of the cylindrical projectile is likely to occur (Figure H.2c). This results in an increased dispersion of the debris cloud particles and in larger pressure wall hole diameters and crack lengths.

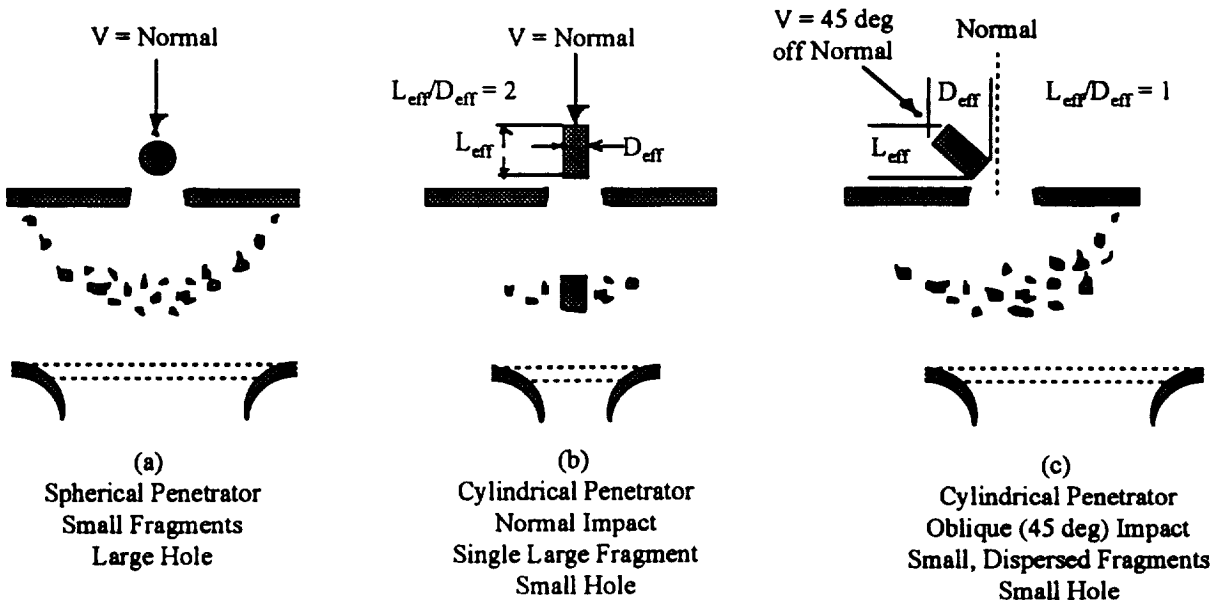

Figure H.2 Effect of Projectile Shape and Orientation on Pressure Wall Hole Diameter

Based on the encouraging results presented in Reference [12], equation (H.1) was modified to account for the effects of effective projectile aspect ratio. In order to have a large pool of data containing information at both ends of the impact velocity spectrum (i.e. at 6.5 km/s and 11.3 km/s), the data for the BLC, ELC, and LEC wall systems were combined and regressed together. Table H.1a-c presents a summary of the impact conditions, the geometric parameters, and the experimental hole diameter and crack length values for the ELC, BLC, and LEC wall systems, respectively.

Since the three wall systems being considered had different geometric parameters as well as different inner bumpers, additional terms were added to equation (H.1) to account for these differences. The final form of the equation was as follows:

$$X = A\cos^{B}\theta_{p}\left[1 - e^{-C(M_{p}/M_{BL}-1)}\right](V_{p}/6.5)^{D}\rho_{eff}^{E}(t_{b}/t_{w})^{F}(t_{w}/S)^{G}(S_{2}/S)^{H}(\lambda_{ib}/\lambda_{b})^{J} \qquad (H.6)$$

Table H.1a Pressure Wall Hole Diameter and Crack Length Data for Enhanced Lab Cylinder (ELC)

Shot No.	V_p (km/s)	θ_p (deg)	D_p (cm)	M_p (gms)	D_{BL} (cm)	M_{BL} (gms)	ρ (---)	ρ_{eff} (---)	t_b (cm)	λ_{tb} (gm/cm^2)	t_w (cm)	S (cm)	S_2 (cm)	D_h (cm)	L_{tt} (cm)
UAH-PT1	6.00	0.00	1.43	4.15	1.29	3.02	1.00	1.00	0.16	1.17	0.48	11.43	5.72	2.34	18.80
UAH-5	6.58	0.00	1.59	5.68	1.38	3.73	1.00	1.00	0.16	1.17	0.48	11.43	5.72	13.41	24.89
UAH-9	6.21	0.00	1.59	5.68	1.33	3.33	1.00	1.00	0.16	1.17	0.48	11.43	5.72	8.26	22.61
UAH-13	6.52	0.00	1.59	5.68	1.37	3.67	1.00	1.00	0.16	1.17	0.48	11.43	5.72	7.11	25.15
WS-44	6.58	0.00	1.59	5.68	1.38	3.73	1.00	1.00	0.18	0.80	0.48	11.43	5.72	16.94	25.40
WS-47	6.65	0.00	1.59	5.68	1.37	3.69	1.00	1.00	0.18	0.80	0.48	11.43	5.72	16.10	25.40
WS-63	6.61	45.00	1.75	7.58	1.49	4.66	1.00	1.00	0.18	0.80	0.48	11.43	5.72	10.95	30.48
WS-64	6.58	0.00	1.75	7.58	1.38	3.73	1.00	1.00	0.18	0.80	0.48	11.43	5.72	18.11	24.13
WS-77	6.47	45.00	1.59	5.68	1.47	4.50	1.00	1.00	0.18	0.80	0.48	11.43	5.72	6.30	22.86
WS-78	6.47	45.00	1.59	5.68	1.47	4.50	1.00	1.00	0.18	0.80	0.48	11.43	5.72	7.09	19.05
1722	6.78	0.00	1.43	4.14	1.36	3.58	1.00	1.00	0.20	0.80	0.48	11.43	5.72	11.20	32.39
1782	6.49	0.00	1.67	6.60	1.37	3.67	1.00	1.00	0.20	0.80	0.48	11.43	5.72	18.48	34.67
1783	6.65	45.00	1.67	6.60	1.49	4.73	1.00	1.00	0.20	0.80	0.48	11.43	5.72	10.33	24.00
7139-9	11.00	0.00	xxx	2.97	1.16	2.22	1.66	1.66	0.20	0.80	0.48	11.43	5.72	20.80	41.91
7139-10	11.19	0.00	xxx	8.00	1.16	2.19	0.97	0.97	0.20	0.80	0.48	11.43	5.72	44.25	58.42
7139-15	11.01	45.00	xxx	7.60	1.38	3.75	3.50	1.00	0.20	0.80	0.48	11.43	5.72	26.47	71.12
7698-3	11.64	0.00	xxx	3.34	1.11	1.94	2.29	2.29	0.20	0.80	0.48	11.43	5.72	22.17	41.91
7698-21	11.30	0.00	xxx	2.54	1.15	2.16	1.54	1.54	0.20	0.80	0.48	11.43	5.72	7.62	22.23

Table H.1b Pressure Wall Hole Diameter and Crack Length Data for Baseline Lab Cylinder (BLC)

Shot No.	V_p (km/s)	θ_p (deg)	D_p (cm)	M_p (gms)	D_{BL} (cm)	M_{BL} (gms)	ρ (---)	ρ_{eff} (---)	t_b (cm)	λ_{tb} (gm/cm^2)	t_w (cm)	S (cm)	S_2 (cm)	D_h (cm)	L_{tt} (cm)
HS-10	6.40	0.00	0.80	0.71	0.79	0.69	1.00	1.00	0.13	0.033	0.48	11.43	5.72	0.23	1.65
HS-11	6.41	0.00	0.95	1.23	0.79	0.69	1.00	1.00	0.13	0.033	0.48	11.43	5.72	3.25	5.66
HS-12	6.32	0.00	1.11	1.96	0.78	0.67	1.00	1.00	0.13	0.033	0.48	11.43	5.72	5.11	5.99
HS-13	6.40	45.00	0.80	0.71	0.64	0.36	1.00	1.00	0.13	0.033	0.48	11.43	5.72	0.91	1.37
HS-14	6.35	45.00	0.95	1.23	0.63	0.36	1.00	1.00	0.13	0.033	0.48	11.43	5.72	2.39	3.18
HS-15	6.40	45.00	1.11	1.96	0.64	0.36	1.00	1.00	0.13	0.033	0.48	11.43	5.72	2.74	3.63
7139-1	11.30	0.00	xxx	1.24	0.64	0.36	1.27	1.27	0.13	0.033	0.48	11.43	5.72	2.87	5.84
7139-13	10.70	45.00	xxx	1.42	0.82	0.78	1.07	1.00	0.13	0.033	0.48	11.43	5.72	1.27	1.27
7698-1	11.70	0.00	xxx	4.56	0.62	0.34	1.41	1.41	0.13	0.033	0.48	11.43	5.72	3.96	10.29
7698-4	11.40	45.00	xxx	3.17	0.78	0.69	1.97	1.00	0.13	0.033	0.48	11.43	5.72	6.55	28.58
7698-13	11.50	45.00	xxx	1.04	0.78	0.67	1.34	1.00	0.13	0.033	0.48	11.43	5.72	1.42	1.78
7698-19	11.30	45.00	xxx	1.92	0.79	0.70	1.97	1.00	0.13	0.033	0.48	11.43	5.72	3.24	15.08
7698-20	11.40	45.00	xxx	2.90	0.78	0.69	0.86	1.00	0.13	0.033	0.48	11.43	5.72	8.76	20.96
UAH-1	6.70	0.00	1.27	2.91	0.83	0.80	1.00	1.00	0.16	0.033	0.48	11.43	5.72	5.84	15.24
UAH-3	6.42	0.00	1.59	5.68	0.79	0.70	1.00	1.00	0.16	0.033	0.48	11.43	5.72	6.10	8.64
UAH-6	6.50	0.00	1.59	5.68	0.80	0.73	1.00	1.00	0.16	0.033	0.48	11.43	5.72	6.35	14.22
UAH-10	6.63	0.00	1.59	5.68	0.82	0.77	1.00	1.00	0.16	0.033	0.48	11.43	5.72	6.60	9.65
UAH-11	6.46	0.00	1.27	2.91	0.79	0.71	1.00	1.00	0.16	0.033	0.48	11.43	5.72	6.10	7.87
WS-34	6.72	0.00	0.95	1.23	0.83	0.81	1.00	1.00	0.13	0.033	0.48	11.43	8.89	2.06	2.54
WS-76	6.63	0.00	1.27	2.91	0.81	0.76	1.00	1.00	0.13	0.033	0.48	11.43	8.89	4.90	5.33

Table H.1c Pressure Wall Hole Diameter and Crack Length Data for Lab End Cone (LEC)

Shot No.	V_p (km/s)	θ_p (deg)	D_p (cm)	M_p (gms)	D_{BL} (cm)	M_{BL} (gms)	ρ (---)	ρ_{eff} (---)	t_b (cm)	λ_{tb} (gm/cm^2)	t_w (cm)	S (cm)	S_2 (cm)	D_h (cm)	L_{tt} (cm)
1691	6.62	0.00	1.19	2.41	1.01	1.46	1.00	1.00	0.19	0.033	0.48	22.15	18.34	1.22	9.91
1699	6.67	0.00	1.43	4.14	1.02	1.52	1.00	1.00	0.19	0.033	0.48	22.15	18.34	7.12	18.67
1792	6.41	0.00	1.67	6.60	0.97	1.31	1.00	1.00	0.19	0.033	0.48	22.15	18.34	9.03	25.91
1711	6.65	45.00	1.19	2.41	0.77	0.65	1.00	1.00	0.19	0.033	0.48	22.15	18.34	3.01	5.72
1727	6.59	45.00	1.43	4.14	0.76	0.63	1.00	1.00	0.19	0.033	0.48	22.15	18.34	4.19	6.48
1769	6.51	45.00	1.67	6.60	0.75	0.60	1.00	1.00	0.19	0.033	0.48	22.15	18.34	6.36	8.76
7698-2	11.38	0.00	xxx	3.78	0.78	0.67	1.09	1.09	0.19	0.033	0.48	22.15	18.34	6.78	22.02
7698-7	11.37	45.00	xxx	3.34	0.98	1.34	1.14	1.00	0.19	0.033	0.48	22.15	18.34	6.25	13.72
7698-11	11.47	0.00	xxx	1.28	0.77	0.65	3.41	3.41	0.19	0.033	0.48	22.15	18.34	1.52	0.79

Based on equation (H.5) and the information in Figure (H.1) , the term ρ_{eff} in equation (H.6) is given by the following expression:

$$\rho_{eff} = \frac{\rho \cos\theta_p + \sin\theta_p}{\cos\theta_p + \rho \sin\theta_p} \tag{H.7}$$

where ρ is the actual aspect ratio of the impacting projectile (i.e. L/D). We note that for spherical projectiles, ρ_{eff} was taken to have a value of unity.

As in Reference [12], three different sets of the exponents A through J were obtained using the information in the combined BLC-ELC-LEC database. The first set of exponents was obtained using only impact tests performed at a 6.5 km/s impact velocity. The second set was obtained using all of the tests in the combined database, that is, the tests considered were performed at 6.5 km/s and at 11.3 km/s. The third and final set was obtained by forcing all but one of the exponents in equation (H.6) to take on predetermined values, and the solving for the remaining unknown exponent. Specifically, except for the effective aspect ratio and velocity terms, the exponents were all taken to have the values obtained from the regression using only data at 6.5 km/s. The velocity exponent was assigned the value obtained in the regression of the complete data set, while the ρ_{eff} exponent was kept as the sole unknown value. The value of the ρ_{eff} exponent was then obtained from a regression of the data in the entire combined data set.

The primary purpose of obtaining these three sets of exponents is to provide a means of determining whether or not the exponents obtained from a regression of only the 6.5 km/s data, when used in conjunction with the velocity term exponent obtained from a regression of the full data set, could accurately predict pressure wall hole diameters and crack lengths at impact velocities beyond 6.5 km/s. The level of agreement between the values of the two calculated ρ_{eff} term exponents would determine the extent to which such an extrapolation would be possible.

Table H.2 below presents the results of the three regression analyses performed. Also presented in the last row of the Table are the correlation coefficients for the various equations obtained. Examination of the information in this Table reveals several interesting features.

- First, all the correlation coefficients are above 0.9. This indicates that the equations derived are an excellent fit to the empirical data.
- Second, the velocity term exponent (i.e. constant 'D') is nearly 1.0 for hole diameter and crack length in the regression of the full combined data set (i.e. Regression No. 2). This implies that pressure wall hole diameters and crack lengths are directly related to projectile momentum, not kinetic energy. A value exactly equal to unity was used in Regression No. 3 for convenience.
- Third, the negative values of the ρ_{eff} exponent (i.e. the constant 'E') indicate that normal impacts of longer projectiles will result in smaller hole diameters and crack lengths as theorized in Figure H.2. This correlation between projectile momentum and pressure wall response is consistent with the observations made by Burch following a regression of different hole diameter data [3].

- Finally, the exponents of the ρ_{eff} terms in Regression Nos. 1 and 2, while not identical, are fairly close. This lends further weight to the validity of the claim originally made in Reference [12] that the coefficients obtained from a regression of 6.5 km/s data could be used in an equation with a first order velocity term to predict pressure wall hole diameter and crack length at impact velocities beyond 6.5 km/s.

Table H.2 Regression Results for Equation (H.6)

	Regression No. 1[a]		**Regression No. 2[b]**		**Regression No. 3[c]**	
	D_{eq}	L_{tt}	D_{eq}	L_{tt}	D_{eq}	L_{tt}
A (cm)	2211.47	9.2352	53103.78	30.809	*2211.47*	*9.2352*
B	1.0354	0.8127	1.0052	-0.0853	*1.0354*	*0.8127*
C	3.0738	16.1926	2.4037	5.1041	*3.0738*	*16.1926*
D	-----	-----	0.9488	1.0943	*1.0*	*1.0*
E	-----	-----	-0.6211	-0.6132	-0.7684	-0.8988
F	3.1451	2.3611	3.1619	2.1707	*3.1451*	*2.3611*
G	0.6484	-0.8046	1.4683	-0.3599	*0.6484*	*-0.8046*
H	-0.2311	-1.0764	0.4686	-1.1315	*-0.2311*	*-1.0764*
J	0.1722	0.2206	0.2042	0.2417	*0.1722*	*0.2206*
R^2	0.924	0.948	0.969	0.939	0.966	0.907

[a]Using only 6.5 km/s data [b]Using full combined data set
[c]Using full combined data set but with some exponent values equal to those from Regression No. 1 (in italics) and with the velocity term exponent set equal to 1.0